Turquoise Exchange and Procurement in the Chacoan World

by

Sharon Kaye Hull

A thesis submitted to the Faculty of Graduate Studies of

The University of Manitoba

In partial fulfilment of the requirements of the degree of

Doctor of Philosophy

Department of Anthropology

University of Manitoba

Winnipeg

Abstract

The large amount of turquoise artifacts recovered from archaeological sites in the American Southwest and Mesoamerica suggests that turquoise was an important commodity in pre-Columbian trade networks. However, the spatial and temporal patterns of turquoise exchange networks and the provenance regions of the turquoise in the southwestern United States and Mesoamerica are poorly understood. Turquoise ($CuAl_6(PO_4)_4(OH)_8{\bullet}4(H_2O)$) is a supergene mineral that forms from meteoric water along fractures that are often associated with copper porphyry deposits. This copper-rich mineral can range in color and chemistry within a single sample or deposit. The ability to identify the turquoise resource areas of turquoise artifacts using the stable isotopes of hydrogen ($^{2}H/^{1}H$) and copper ($^{65}Cu/^{63}Cu$) has overcome many of the limitations of trace element analyses of complex minerals such as turquoise. The geography and geology of turquoise deposits dictate the isotopic composition of turquoise.

Employing the Secondary Ion Mass Spectrometry (SIMS) technique to measure the hydrogen and copper stable isotope ratios in turquoise samples, a comparative reference database consisting of 876 analyses from 21 turquoise resource areas in the western United States was established. Sixty-two turquoise artifacts recovered from Aztec Ruin, Salmon Ruin, and nine sites in Chaco Canyon were analyzed and their isotopic signatures were compared to the reference database identifying the turquoise resource areas of 35 artifacts. These results were compared to pre-existing models of trade and exchange in the American Southwest and models that explain the complex culture history of the inhabitants of these sites. The results showed that turquoise was obtained from several different turquoise provenance regions across the western United States and there are notable differences in the turquoise procurement patterns between the

three major great houses and between Pueblo Bonito and the small sites within Chaco Canyon.

The results from this study improved the understanding of turquoise trade and relationships among the occupants of important Ancestral Puebloan sites in northwestern New Mexico. The development of the turquoise comparative reference database established the foundation of future research for reconstruction of ancient turquoise trade networks and investigation of turquoise procurement strategies in the American Southwest and Mesoamerica.

Acknowledgments

I convey my most sincere appreciation to my advisor, Professor Mostafa Fayek of the Department of Geological Sciences at the University of Manitoba, and Dr. Frances Joan Mathien for funding and making this interdisciplinary project possible. I thank Dean Norman Halden and Assistant Professor Brooke Milne who participated on my advisory committee and Dr. Linda Cordell for participating as my external examiner. I also thank the many people who guided and allowed me access to turquoise resource areas and collections: Homer Milford, Bill Baxter, Doug Magnus, and Todd Brown (Cerrillos Hills), Ken Frye (BLM) and Anne Horton (King Manassa), Mary Hughes (Villa Grove), Marty Colbaugh (Mineral Park), Robert Reynolds, Robert Hilburn, Ed Nazelrod, and Jim Sherer (Halloran Springs), Bill Crank (Crescent Peak), Bruce Woods (Godber), Dean and Donna Otteson (Royston Mine area), Chris Lott (Lone Mountain), Phil Weigand (Museum of Northern Arizona), and Virgil W. Lueth (New Mexico Bureau of Mines and Mineral Resources), and Dan Courvoisier who sent samples from Sleeping Beauty Mine. For the artifacts, I thank Nancy Sweet Espinosa, Larry Baker, and Paul Reed (Salmon Ruins Museum), Wendy Bustard (Chaco Culture National Historical Park Museum), and David Hurst Thomas, Kristen Marble, and Anibal Rodriquez (American Museum of Natural History).

This work was funded by Canada Research Chairs in Environmental and Isotope Geochemistry, a Major Facilities Access Grant, Research Tools and Equipment, and Discovery Grant from the Natural Sciences and Engineering Research Council of Canada, a Canada Foundation for Innovation Grant under professor Mostafa Fayek, and by the National Science Foundation under Grant No. 0609638 to Professor Mostafa Fayek (principle investigator) and Dr. Frances Joan Mathien (co-principle investigator).

Table of Contents

List of Tables

List of Figures

Chapter 1: Introduction

"*Thousands of years ago this region was the home of the Desert Mojave. Among them appeared a strange tribe from the south, searching for precious stone [turquoise]…*"

(Desert Piute legend recounted by Indian Johnny; Berkholz 1960:10-11).

Pre-Colombian turquoise mining and long-distance exchange has been an enduring research topic among American Southwestern and Mesoamerican archaeologists for over a century. Although over one million turquoise artifacts were recovered from archaeological sites throughout the southwestern United States and the Valley of Mexico (Harbottle and Weigand 1992), the spatial and temporal patterns of turquoise exchange networks and the provenance regions of the turquoise are poorly understood. The ability to link archaeologically recovered turquoise to specific turquoise resource areas significantly improves our understanding of pre-contact trade systems and turquoise procurement strategies, offering important insights into cultural intensification of social systems in Greater Southwest. The Greater Southwest is a term used to describe a culture area that encompasses the American Southwest and northern Mexico; Las Vegas, Nevada to Las Vegas, New Mexico and Durango, Colorado to Durango, Mexico (Reed 1964).

In northwestern New Mexico, Chaco Canyon (Fig. 1.1) was one of the most significant Ancestral Puebloan regional centers. The amount of turquoise recovered throughout Chaco Canyon, over 200,000 pieces (Harbottle and Weigand 1992; Mathien 1981a; Pepper 1996), is extraordinary when compared with other archaeological sites located in the American Southwest suggesting that turquoise was a highly prized mineral and considered an exotic commodity in the economic and religious structures of the inhabitants of this ancient culture. Communities began to aggregate in Chaco Canyon around A.D. 400; however, by late A.D. 800 the inhabitants of the canyon began to build the large multistoried Pueblo Bonito (Windes and Ford 1992), the largest great house in the canyon. Great houses were massive, multistoried, masonry structures with many

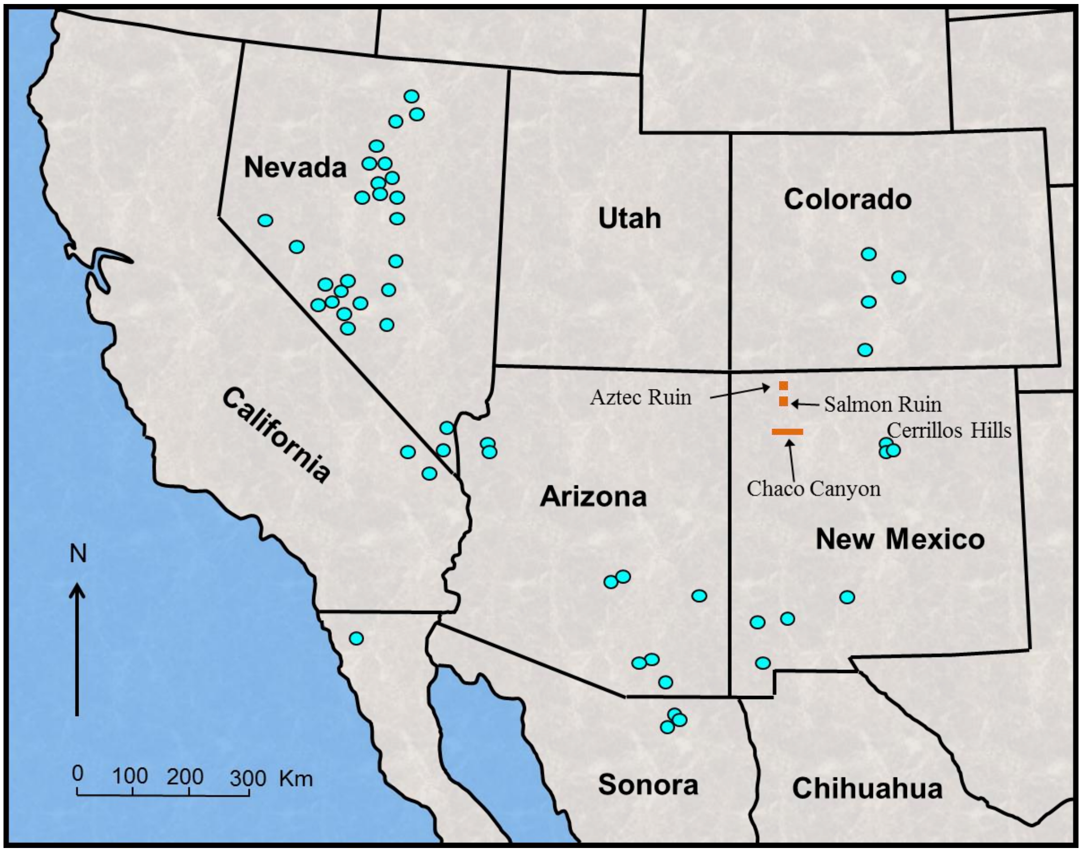

Fig. 1.1. Locations mentioned in the text: Chaco Canyon, Aztec Ruin, Salmon Ruin (represented by a brown rectangle for Chaco Canyon and brown squares for Aztec and Salmon Ruins), and the turquoise resource areas (represented by blue circles).

rooms, much larger than the surrounding structures, and typically included kivas; round rooms built within rectangular or square rooms (Lekson 1986, 1991:32-36). Chaco Canyon contains a large collection of archaeological sites throughout Chaco Wash (Fig. 1.2) where twelve of these great houses are surrounded by hundreds of smaller habitation sites (Lekson 2006:13). Although turquoise was recovered in many sites throughout the Canyon, thousands of turquoise beads and many of the most elaborate turquoise artifacts were recovered from Pueblo Bonito (Judd 1954; Pepper 1996). Turquoise artifacts were also recovered from small sites in the Canyon. At one site in particular, the Spadefoot Toad site located in Marcia's Rincon (Fig. 1.2), turquoise debris was recovered suggesting the manufacture of turquoise ornaments (Mathien 1984, 1993, 2001; Windes 1993). The number of turquoise artifacts recovered in Chaco Canyon is remarkable because the nearest known source of turquoise is over 200 kilometers in the Cerrillos Hills Mining District (Fig. 1.1), near present-day Santa Fe, New Mexico (Mathien 1986; Weigand and Harbottle 1993). Ever since George F. Pepper first reported on the thousands of turquoise artifacts recovered from Pueblo Bonito in 1920 (Pepper 1996), and William P. Blake (1858) recorded evidence of pre-Columbian mining and the enormous excavated pit at Mt. Chalchihuitl in the Cerrillos Hills, archaeologists have suggested this resource area as the nearest and most probable source of turquoise for Chaco Canyon. Turquoise deposits are also located in other parts of the western United States (New Mexico, Colorado, Arizona, Nevada, southeastern California) and northern Mexico, and some researchers (e.g., Harbottle and Weigand 1992; Hull 2006, Hull et al. 2008; Weigand and Harbottle 1993) have proposed that turquoise was not only acquired from Cerrillos Hills, but from several locations (Fig 1.1). The resource areas of the turquoise recovered from Chacoan sites and the role of the Chacoans in turquoise

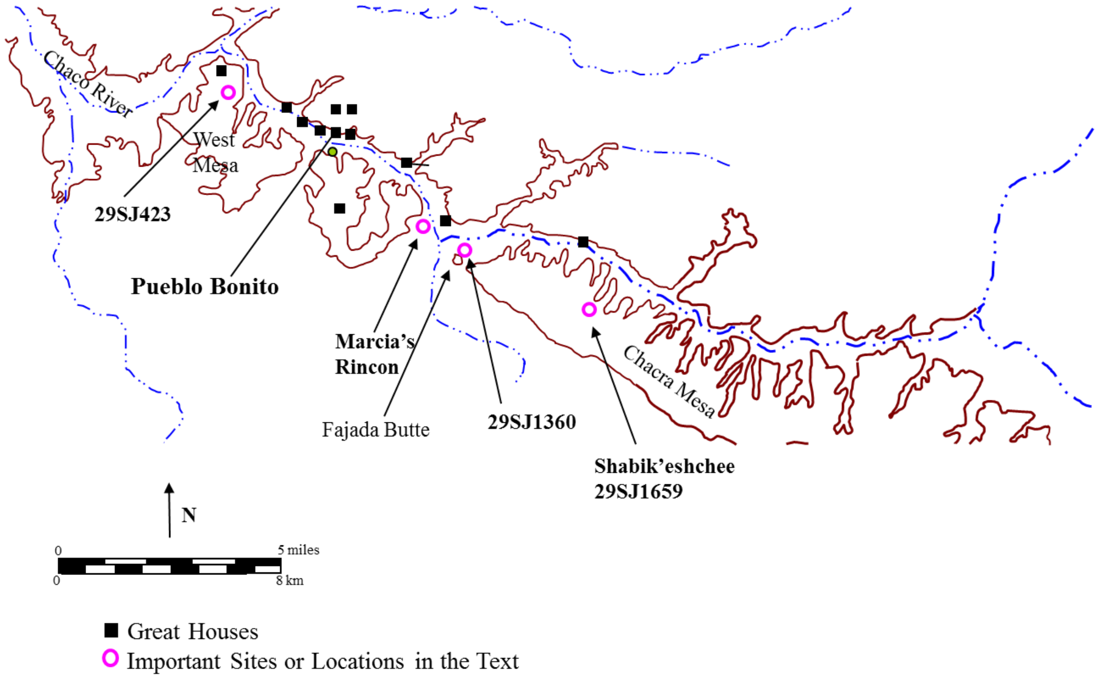

Fig. 1.2. Location of the sites within Chaco Canyon mentioned in the text: Marcia's Rincon contains the sites 29SJ625 Three C site, 29SJ627, 29SJ628, 29SJ629 Spadefoot Toad, and 29SJ633 Eleventh Hour.

procurement and exchange networks continue to be enduring themes in Southwestern archaeology.

Chaco Canyon fluoresced into what was known as the Chaco Phenomenon, A.D. 850 to A.D. 1150 (Cameron 2009:1). Chacoan influence was observed across the San Juan Basin as many communities constructed great houses, one of the most obvious identifying attributes of the Chacoan culture. Other types of material culture with Chacoan attributes (e.g., ceramics) were also recovered from other sites in the San Juan Basin that suggested strong ties with the canyon. As construction declined in the Canyon, two great house communities, Aztec and Salmon Ruins, developed to the north of Chaco Canyon, near the San Juan River. Aztec and Salmon Ruins (Fig. 1.1) were the two largest great house communities constructed outside of the canyon. Some archaeologists proposed that the great house communities of Aztec and Salmon were Chacoan settlements that grew as the inhabitants of Chaco Canyon migrated and colonized the northern San Juan Basin (e.g., Irwin-Williams and Shelley 1980; Lipe 2006; Morris 1915), possibly due to a period of regional drought between A.D. 1080 and A.D. 1100 (Reed 2006c). Stephen H. Lekson (1999, 2006) suggested that the central power of the Chacoan world was deliberately moved to the Aztec community as the Chacoans struggled to maintain their influence across the San Juan Basin in the 12th century. Ruth M. Van Dyke (2008:335) proposed that the Aztec complex was built emulating Chacoan attributes, becoming a regional center that was in competition with Chaco Canyon. Turquoise artifacts and other exotic trade commodities were recovered at all of the three great house communities suggesting that they were all connected to extensive trade networks. Although there have been attempts to understand the relationship between the three large great house communities of Pueblo Bonito, Aztec

Ruin, and Salmon Ruin (e.g., Durand et al. 2010; Reed 2006c, 2008) and their role as participants in turquoise procurement and exchange, these relationships still remain elusive.

Turquoise ($CuAl_6(PO_4)_4(OH)_8 \cdot 4(H_2O)$) is a supergene mineral that forms along fractures and is generally associated with copper porphyry deposits (Arrowsmith 1974; Pogue 1974). Supergene minerals, or secondary minerals, mineralize from oxidation or weathering within an ore deposit. For decades, archaeologists have sought to develop a technique that could identify the resource areas of turquoise artifacts using a variety of methods including trace and rare earth element concentration patterns (Bishop 1979; Harbottle and Weigand 1992; Judd 1954; Kim et al. 2003; Mathien and Olinger 1992; Ronzio and Salmon 1967; Ruppert 1982, 1983; Sigleo 1970, 1975; Weigand et al. 1977; Weigand and Harbottle 1993; Welch and Triadan 1991; Zedeño et al. 2005). However, these studies met with limited success due to the intrinsic limitations of trace element or chemical analysis of complex minerals such as turquoise, which can range in color and chemistry within a single sample or deposit. To overcome these limitations, Sharon Hull and colleagues (Hull 2006; Hull et al. 2008) developed a method to identify the origin of turquoise artifacts using hydrogen ($^2H/^1H$) and copper ($^{65}Cu/^{63}Cu$) stable isotopes. This method was successful because the geography and geology of turquoise deposits dictate the isotopic signature of turquoise. The hydrogen and copper isotope ratios were measured by a Secondary Ion Mass Spectrometer (SIMS). The SIMS is capable of *in situ* (solid sample) microanalytical analyses and is relatively non-destructive when compared to other isotopic analytical techniques that require complete destruction and consumption of the samples (e.g., powdering). The SIMS method developed by Hull et al. (2008) allows artifacts to be returned to their original collections.

Employing the turquoise sourcing technique using hydrogen and copper isotope ratios, the objectives of my dissertation are: 1) establish a comparative reference database by the characterization of turquoise resource areas in the western United States, 2) analyze turquoise artifacts recovered from Aztec Ruin, Salmon Ruin, Pueblo Bonito, and eight small sites in Chaco Canyon, 29SJ1360, 29SJ1659 Shabik'eshchee, 29SJ423, 29SJ625 Three C site, 29SJ627, 29SJ628, 29SJ629 Spadefoot Toad, and 29SJ633 Eleventh Hour, and 3) compare the results to existing models of trade and exchange in the American Southwest and models that explain the complex culture history of the inhabitants of these sites.

This dissertation is organized into nine chapters. Chapter 1 is an introduction to the dissertation. Chapter 2 discusses turquoise formation, the geology and locations of all known turquoise resource areas in the western United States and northern Mexico, and ancient turquoise mining. Chapter 3 provides a background of turquoise provenance techniques, the use and methods to measure isotope ratios in archaeology, and a discussion on why hydrogen and copper isotope ratios are successful discriminators for identifying the resource areas for turquoise artifacts. Chapter 4 provides the background for existing turquoise exchange models for the Greater Southwest and Chapter 5 discusses the culture history of the Chacoan World. Chapter 6 details the methods used to obtain the data and Chapter 7 provides the results. Chapter 8 compares the results to the existing models of trade and culture history for the Chacoan World and Chapter nine presents the conclusions of this dissertation research.

Chapter 2: Turquoise Resource Areas

"*In every important place where modern man has mined turquoise, aborigines have mined it before him*."
(Johnston 1964:76)

To develop a successful technique to identify resource areas of turquoise artifacts and establish a comparative database, it is essential to understand the mineral turquoise and its formation processes. Also, all known turquoise resource areas in the region that may have been used by the inhabitants of the archaeological sites that are included in the study need to be identified, examined, sampled, and geochemically characterized. This chapter presents general information of the turquoise mineral group and the geology of turquoise formation. All known turquoise resource areas are discussed and grouped together by region with details of the location and geology of each area. The description for each turquoise resource area also includes information for the turquoise provenance samples used to establish the comparative database. This chapter concludes with general information on ancient turquoise mining.

2.1. The Mineral Turquoise and Turquoise Formation

The turquoise mineral group consists of at least six end members: aheylite ($Fe^{2+}Al_6(PO_4)_4(OH)_8 \cdot 4(H_2O)$), chalcosiderite ($CuFe^{3+}{}_6(PO_4)_4(OH)_8 \cdot 4(H_2O)$), faustite ($(Zn,Cu)Al_6(PO_4)_4(OH)_8 \cdot 4(H_2O)$), planerite ($Al_6(PO_4)_2(PO_3OH)_2(OH)_8 \cdot 4(H_2O)$), turquoise ($CuAl_6(PO_4)_4(OH)_8 \cdot 4(H_2O)$), and an unnamed iron-rich end member ($Fe^{2+}Fe^{3+}{}_6(PO_4)_4(OH)_8 \cdot 4(H_2O)$) (Cid-Dresdner 1965; Foord and Taggart 1998). Turquoise is generally massive and occurs as thin veins or disseminated grains. The texture of turquoise is fibrous or spherulitic, consisting of triclinic crystals (Cid-Dresdner 1965; Foord and Taggart 1998). Forming in the fractures of igneous, sedimentary, and metamorphic rocks throughout the western United States, this secondary mineral draws its elemental constituents from the surrounding host rock (Fig. 2.1) (Morrissey 1968; Northrop 1975; Pogue 1974). The majority of turquoise deposits are associated with copper porphyry intrusive bodies including many of the key economic copper deposits in

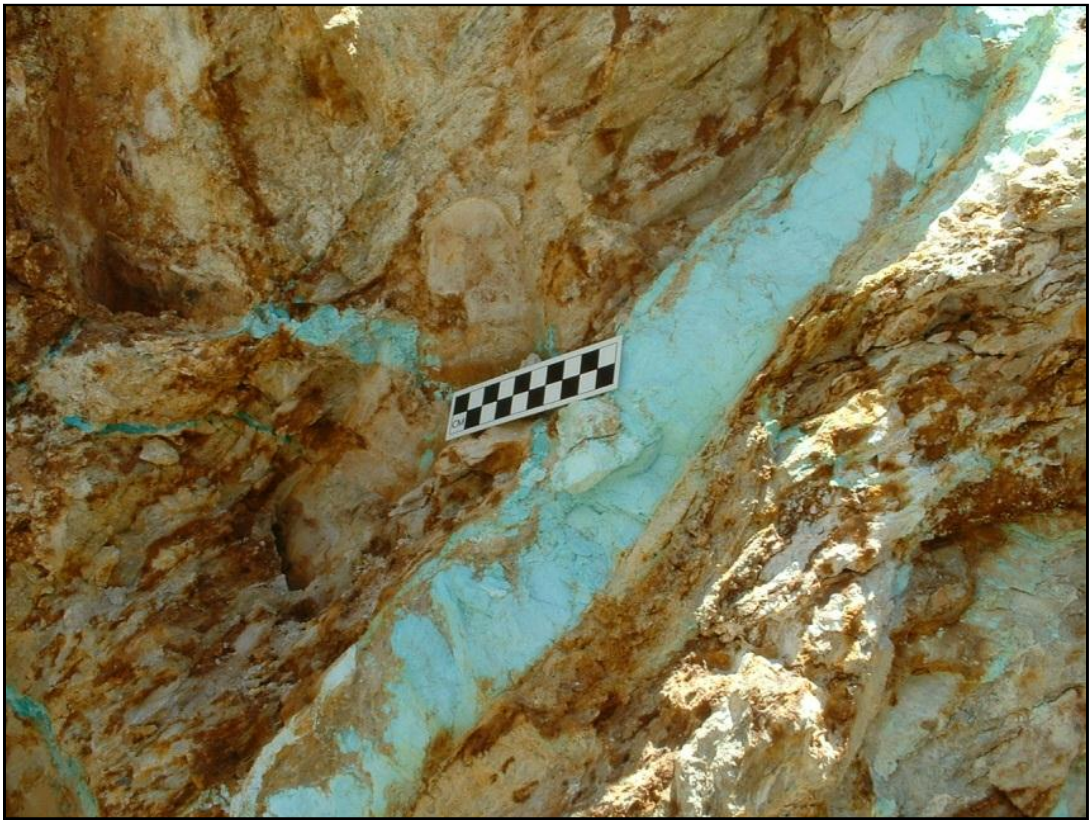

Fig. 2.1. A large vein of turquoise that formed in the fracture of copper porphyry at Mineral Park, Arizona.

the American Southwest and the Great Basin region of Nevada (Anthony et al. 1977; Arrowsmith 1974; Morrissey 1968; Sigleo 1970).

Much of the current topography of the American Southwest that is important to turquoise formation resulted from tectonic processes within the last 100 million years. Periods of intense magmatism, mountain building, and large areas of crustal extension developed when the Farallon plate was subducted beneath the North American plate (Baldridge 2004). During the upper Eocene and Oligocene periods, large volcanic events helped shape the topography from central Mexico to central New Mexico with periods of magmatism continuing into the mid-Tertiary. Intense magmatism and volcanism throughout the Basin and Range province occurred between 43 million years ago in northern Nevada to 21 million years ago in southern Nevada, southeastern California, and western Arizona. Central Colorado, southwestern New Mexico, and southeastern Arizona show evidence of magmatism 43 million years ago with younger dates further west across southern Arizona. Large eroded calderas in southwestern New Mexico, ranging in age from about 35 to 27 million years ago, suggest intense explosive volcanism in this region (Baldridge 2004).

It was during this time, about 30 million years ago, that the crustal extension formed a graben known as the Rio Grande Rift. Extending from central Colorado south into Mexico, the Rio Grande Rift sank between two sets of major faults causing many fractures and faults in the stressed rocks. Increasing pressure in the earth's crust and the movement of other faults helped shape the Colorado Plateau. Extensional events from 20 to 30 million years ago along with major uplift episodes about 10 million years ago were a significant factor in shaping the north-south trending fault-block mountain ranges of the Basin and Range province exposing many of the intrusive rocks to supergene processes

(Kues 1992). It is in the thinner extension crust of the Basin and Range province and along the Rio Grande Rift that turquoise occurs in shallow igneous intrusions at the intersection of several fault zones (Bergen et al. 2007).

Although most researchers will readily agree that turquoise occurs in association with copper porphyry intrusive bodies (Anthony et al. 1977; Arrowsmith 1974; Morrissey 1968; Sigleo 1970), the geologic origin of turquoise has long been debated. Some researchers (e.g., Clarke and Diller 1887; Johnson 1903; Pogue 1974; Weber 1979) suggest that turquoise is a hydrothermal mineral, precipitating from hot fluids or vapors that flowed upward through fractures, whereas others believe it forms as a result of supergene processes where the host rock is weathered by descending rain (meteoric) water through fractures and faults (Bergen et al. 2007; Gustafson 1965; Lueth 1998; Paige 1912; Sterrett 1909). Copper porphyry deposits in the American Southwest show a complex history of repeated oxidation events and supergene effects that are deep in some of the ore bodies (Titley 1982). The extent of weathering of these intrusive bodies depended on the chemistry and permeability of the host rocks (Anthony et al. 1977:12-13).

Based on observations of turquoise in the field while obtaining turquoise provenance samples (Bergen et al. 2007), as well as the work of others (e.g., Lueth 1998; Paige 1912), the supergene model (weathering of the host rock) best explains the features of most turquoise deposits. Acidic solutions, produced from the near-surface oxidation, leach elements such as iron and copper as the fluids descend through the host rock (Anthony et al. 1977). The descending fluids encounter progressively more reducing conditions, either as a function of the neutralization of acidic solutions by the host rock or at the water table (Robb 2005:239). Copper and iron form various secondary supergene minerals such as azurite/malachite or turquoise depending on the fluid chemistry, the pH, and the depth relative to the water table (e.g., reduction-oxidation zone). For example, the Morenci copper deposits in Arizona are much more financially viable because of the supergene enrichment process and the precipitation of secondary copper minerals such as chalcocite (Cu_2S) (Anthony et al. 1977). The supergene enrichment model for the formation of turquoise presents a similar process, which suggests that many of the elemental constituents of turquoise were leached by cool descending surface waters. Although, most turquoise deposits occur within 70 meters of the surface, other turquoise deposits that are reported at much greater depth (e.g., ~360 meters at Bisbee - Anthony et al. 1977; ~1365 meters at Morenci - Sigleo 1970) can be explained by changes in the water table level and the location of the reduction-oxidation zone.

2.2. Turquoise Resource Areas and Provenance Samples

Turquoise was heavily mined long before Europeans reached the North American continent. In the early 1980s, Phil C. Weigand (1982) began surveying, sampling, and documenting evidence of prehistoric mining concluding that 16 of the areas had definite evidence of ancient mining and four were inconclusive. Garman Harbottle and Phil C. Weigand (1992) continued the survey and identified 120 individual turquoise deposits that displayed evidence of prehistoric mining in 28 provenance areas. Documented evidence of the ancient extraction of turquoise included the presence of stone tools, ceramics, and the actual mines and quarries. Ceramics may have been left behind as trash and, in some cases, were used to link the ancient miners to specific culture groups by the style of the ceramics. Many of these deposits have been mined historically or are still in operation obliterating any evidence of pre-Columbian exploitation of turquoise (Fig. 2.2).

Fig. 2.2. Modern-day copper mining at Mineral Park, Arizona.

Most turquoise deposits are located in the semiarid regions of the Basin and Range province and along the Rio Grande rift (Fig. 1.1). Appendix 1 contains a full listing of turquoise resource areas discussed in this chapter that was compiled from many literature sources (e.g., Anthony et al. 1977; Arrowsmith 1974; Morrissey 1968; Northrop 1959; Pearl 1941; Pogue 1974; Ransome 1913). Table 2.1 list information on the 21 turquoise provenance samples used to establish the comparative database. Eleven of the turquoise provenance samples were collected directly from the turquoise deposits. However, due to modern-day copper mining where many of the deposits were either destroyed or inaccessible, eight of the samples were obtained from Phil C. Weigand's collection of turquoise provenance samples at the Museum of Northern Arizona, one sample was supplied directly from the mine (Sleeping Beauty), and one sample (Cripple Creek) was obtained from Dough Magnus (owner of the Castillian and Tiffany mines at Cerrillos Hills Mining District). Viable turquoise provenance samples for analyses were not available for all of the provenance regions. Many of the turquoise deposits in Grant, Hidalgo, and Otero counties in New Mexico have long closed down their operations and the Sullivan deposit in Nevada became a parking lot for a casino. With the exception of the sample from Baja California, provenance samples from Mexico were severely weathered or not turquoise. However, the turquoise comparative reference database currently contains a representative sample of turquoise resource areas throughout the western United States and will be updated as more provenance samples become available.

Table 2.1. Turquoise Provenance Samples that were Isotopically Characterized.

Name	Area/District	State	Evidence of Prehistoric Mining	Where Sample was Obtained
Sleeping Beauty	Globe District	Arizona	Yes	Received directly from the mine
Kingman	Mineral Park	Arizona	Extensive	Collected directly from the deposit
Morenci Mine	Clifton District	Arizona	Yes	Weigand's collection
Bisbee Mine	Bisbee	Arizona	Yes	Weigand's collection
East Camp/Middle Camp	Halloran Springs	California	Extensive	East Camp collected by author directly from the deposit; Middle Camp – contributed by Ed Nazelrod
Evans Turquoise	El Rosario	Baja California	Not reported	Weigand's collection
King's Manassa	San Luis Valley	Colorado	Extensive	Collected directly from the deposit
Villa Grove Mine	San Luis Valley	Colorado	Inconclusive	Collected directly from the deposit
Leadville	St. Kelvin Mining District	Colorado	Inconclusive	Weigand's collection
Cripple Creek	Cripple Creek	Colorado	Not reported	Received from Douglas Magnus (Cerrillos Hills)
Aztec Mountain/Blue Point/Locality #7	Crescent Peak	Nevada	Yes	Aztec Mountain and Blue Point collected directly from the deposit; Locality #7 – Weigand's collection
Royal Blue	Royston District	Nevada	Yes	Collected directly from the deposit
Lone Mountain	Paymaster Canyon	Nevada	Not reported	Collected directly from the deposit
Blue Gem	Bullion District	Nevada	Not reported	Weigand's collection
Green Tree	Cortez	Nevada	Not reported	Weigand's collection

Name	Area/District	State	Evidence of Prehistoric Mining	Where Sample was Obtained
Godber	Austin	Nevada	Not reported	Collected directly from the deposit
Black Hills	Royston District	Nevada	Not Reported	Collected directly from the deposit
Verde Blue	Royston District	Nevada	Not reported	Collected directly from the deposit
Fox Mine	Cortez	Nevada	Not reported	Weigand's collection
Old Hachita	Little Hachita Mountains	New Mexico	Yes	Weigand's collection
Castillian Mine	Cerrillos Hills District	New Mexico	Extensive	Collected directly from the deposit

2.2.1. Rio Grande Rift

The Cerrillos Hills Mining District in Santa Fe County, New Mexico has been exploited for its natural resources for over a millennium (Fig. 2.3). It is one of the best surveyed and documented turquoise provenance regions, with some of the most compelling evidence of pre-Columbian turquoise mining. These turquoise deposits have produced high-quality turquoise and other economic ores for centuries. Some of the earliest documentation of the turquoise mine at Mount Chalchihuitl describes evidence of massive ancient turquoise extraction, archaeological artifacts scattered throughout the area, and Native Americans from the Rio Grande pueblos obtaining turquoise out of the extensive tailings pile more than a century ago (Blake 1858). The presence of huge sledges and hafted hammers were reported in proximity to where turquoise occurs in fractures and nodules in the 120 meter thick porphyry (Silliman 1881). Much of Mount Chalchihuitl (Fig. 2.4) has been chiseled away with ancient stone tools with century old trees reported growing in the bottom of the ancient quarry in the 1800s (Pogue 1974). Weigand and Harbottle (1993) and Weigand (1982) also reported evidence of prehistoric mining. Helene A. Warren and Frances Joan Mathien (1985) documented the quarries and underground mines at Mount Chalchihuitl, and the mining debris and archaeological sites that cover over a 20 acre area around this important turquoise resource area. The amount of evidence of prehistoric workings has led to many hypotheses on the origin of the ancient miners such as ties with Chaco Canyon (Judd 1954; Pepper 1996).

Fig. 2.3. Location of Cerrillos Hills Mining District, near Santa Fe, New Mexico (Google Earth 2012).

Fig. 2.4. Extensive turquoise extraction at Mount Chalchihuitl, Cerrillos Hills Mining District, New Mexico.

The once highly productive Tiffany (Fig. 2.5) and Castillian mines (Fig. 2.6) are located on Turquoise Hill about five kilometers to the north and ten kilometers northeast of the town of Cerrillos. Samples were collected on several visits to Cerrillos Hills Mining District. The turquoise provenance sample included in this study from the Castillian Mine was collected by Professor Mostafa Fayek directly from the mine, as well as many other samples that were collected from this area during several tours provided by Homer Milford, Bill Baxter, Joan Mathien, Douglas Magnus, and Todd Brown over a ten year period. Other mining claims in this area include the Blue Bell, Consul Mahoney, Morning Star, Sky Blue and the Gem. The entire area is scattered with ancient quarries, sherds, scrapers, hammerstones, and mauls (Weigand 1982) providing conclusive evidence of prehistoric turquoise extraction (Weigand and Harbottle 1993).

The Cerrillos Hills region, situated on the eastern margin of the Rio Grande Rift, is deformed and highly fractured, and is intruded by a series of monzonite stocks, plugs, laccoliths, sills, and dikes (Disbrow and Stoll 1957). The monzonite porphyry intrusive is exposed because the overlying Cretaceous sediments have long been eroded away (Pogue 1974). Turquoise occurs in the sericitized igneous rocks (Disbrow and Stoll 1957) at shallow depths (Gustafson 1965).

Following the Rio Grande Rift northward into Colorado, there are four known sources of turquoise along or very near to the margins of the rift (Fig. 2.7). The most southern turquoise deposit in Colorado is the King Manassa mine, also known as the King or La Jara mine; which is located in Conejos County in the southern part of the San Luis Valley, about 14 kilometers east of Manassa and 30 kilometers west of the town of San Luis (Fig. 2.8). The King Manassa deposit is associated with Tertiary age felsic igneous rocks (Fig. 2.9). Richard M. Pearl (1941) reported prehistoric implements and


Fig. 2.5. Tiffany Mine, Cerrillos Hills Mining District, New Mexico.

Fig. 2.6. Castillian Mine, Cerrillos Hills Mining District, New Mexico.

Fig. 2.7. Location of the four principle turquoise resource areas in Colorado: King Manassa, Villa Grove, Cripple Creek, and Leadville (Google Earth 2012).

Fig. 2.8. Location of the King Manassa mine, near Manassa, Colorado (Google Earth 2012).

Fig. 2.9. The King Manassa mine, as seen from the road.

bone tools present at the site and Weigand (1982) documented ancient stone tools during his survey. The turquoise provenance samples for this study were collected in 2006 during a tour of the mine provided by the granddaughter of the current owners, the King family, and accompanied by Ken Frye (United States Forest Service). Turquoise occurs in veinlets and nodules in the fractures and voids of felsic porphyry (Pearl 1941). The highly altered volcanic host rock is possibly part of the Conejos Foundation that is Oligocene in age (Modreski and Murphy 2002). The porphyry, where turquoise occurs, is cut by a ridge of fine-grained extrusive rock and capped with a six meter outcrop of chert (Arrowsmith 1974; Pogue 1974).

Tucked away in the far northern corner of the San Luis Valley in Saguache County is the Villa Grove or Hall mine. This deposit is situated at the head of the Turquoise Gulch drainage about eight kilometers east of the Bonanza Mining District in the Cochetopa Hills (Fig. 2.10). Located on the edge of the Bonanza caldera, the porphyry is part of a large area of volcanic formations that exists over most of the Bonanza District. Turquoise occurs in veinlets and nodules in highly fractured felsic porphyry of Tertiary age (Modreski and Murphy 2002; Pearl 1941). The Villa Grove mine is located in rugged mountainous terrain at an altitude of over 3,000 meters above sea level and the whole region is heavily faulted and fractured due to mountain building events (Fig. 2.11). More than a century ago, the Villa Grove mine was mined for its copper until good quality turquoise was discovered. Weigand and Harbottle (1993) report inconclusive evidence of prehistoric mining which would be difficult to identify due to the extensive historical turquoise and copper mining (Fig. 2.12). The provenance sample used in this study was collected in 2006 during a tour provided by Mary Hughes of Villa Grove.

Fig. 2.10. Location of the Hall Mine, near Villa Grove, Colorado (Google Earth 2012).


Fig. 2.11. The Hall Mine, as seen from above.

Fig. 2.12. Extensive historical copper mining at the Hall Mine.

Turquoise occurs in association with Tertiary felsic igneous rocks, which intrude Precambrian granites in the La Plata Mountains near Cripple Creek in Teller County, Colorado (Fig. 2.13). The La Plata Mountains consist of Paleozoic and Mesozoic sedimentary rock intruded by monzonite porphyry. Located on the northwest edge of the Cripple Creek volcanic center, the main turquoise deposit is the Florence mine on the south side of Mineral Hill, which is hosted by moderately altered granite, possibly part of the Pikes Peak Granite (Modreski and Murphy 2002). Permission was not granted to visit the Cripple Creek mine; however, a provenance sample was provided by Douglas Magnus of Cerrillos Hills.

The most northern turquoise deposits in Colorado are located in St. Kelvin and Sugarloaf Mining District in Lake County. One of the principle deposits, the Turquoise Chief, is located a few kilometers north of the center of Turquoise Lake about eleven kilometers northwest of the town of Leadville (Fig. 2.14). In this high alpine setting, turquoise occurs in veinlets and nodules in Tertiary felsic igneous rocks that intrude Precambrian granite (Modreski and Murphy 2002). The Leadville area is part of the Central Colorado Mineral Belt. Lake County's rugged topography is a result of many mountain building events. Evidence of prehistoric mining is inconclusive (Weigand and Harbottle 1993).

Fig. 2.13. Location of the mining area near Cripple Creek, Colorado (Google Earth 2012).

Fig. 2.14. Location of a turquoise deposit north of Turquoise Lake near Leadville, Colorado (Google Earth 2012).

2.2.2. South Central and Southwestern New Mexico

Turquoise occurs in several areas of the Jarilla Mountains in Otero County (Fig. 2.15). The Jarilla Mountains are a small range of hills located in the Tularosa Basin, about 80 kilometers north-northeast of El Paso, Texas (Pogue 1974:58). The limestone, sandstone, and shale of the region are intruded by Tertiary igneous stocks, dikes and sills that are highly fractured (Schmidt and Craddock 1964). The Providence, also known as DeMeules, Garnet, Nannie Baird, Lucky, I, and Three Bears mines (Pogue 1974:58), is situated in altered quartz monzonite host rock (Lueth 1998). Turquoise also occurs in the Orogrande Mining District at the Iron Mask mine that is situated in a shale unit (Lueth 1998) on the margin of a porphyry copper deposit (Crook 2001). Sherds, stone tools, and other evidence of prehistoric mining were reported in the Orogrande area (Mathien 1995; Weigand 1982; Weigand and Harbottle 1993).

The Burro Mountains of Grant County, in southwestern New Mexico, contain some of the most productive turquoise deposits in the state and displays evidence of heavy exploitation (Fig. 2.16) (Arrowsmith 1974; Pogue 1974). The heavily faulted region consists of the Little Burro Mountain range and the Big Burro Mountains separated by the Magnas Valley. On the southwestern side of the Magnas Valley, the Big Burro Mountains are dominated by Precambrian granite, except in the northeastern region of where quartz monzonite porphyry (Tyrone laccolith), intrudes the country rock (Gillerman 1964; Kolessar 1982). This area has experienced several igneous intrusive events evident by the documentation of five different types of porphyry. Turquoise occurs in fractures, seams, and nodules in the altered granite and intruding porphyry dikes (Pogue 1974:55).

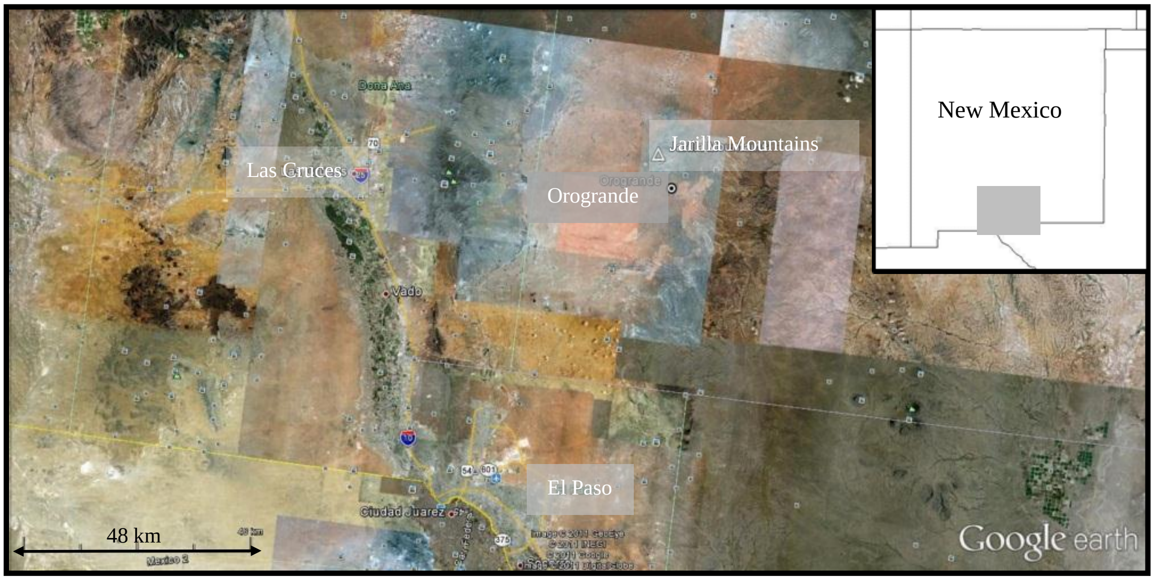

Fig. 2.15. Location of Orogrande and other locations mentioned in the text (Google Earth 2012).

Fig. 2.16. Location of the Old Hachita turquoise deposit and other locations referenced in the text (Google Earth 2012).

Most of the turquoise deposits in the region are located in the Tyrone District in the Burro Mountains. One of the most commercially successful deposits was the Azure mine, about 16 kilometers southwest of Silver City and about two kilometers north of the town of Leopold (Northrop 1959:523). Turquoise occurs in the fractures and voids of an altered medium-grained porphyritic rock. In 1893, the discovery of the *Elizabeth pocket* set this mine apart from the others and is one of the single most economical pockets ever recorded (Arrowsmith 1974; Pogue 1974:55-56). The pocket contained exceptionally pure turquoise and was 30 meters long, 12 meters wide, and 12 to 15 meters high. The Azure deposit was most likely a valuable economic source of turquoise for pre-Columbian miners as evidenced by the presence of ancient quarries, stone tools, and ceramic sherds (Weigand 1982; Weigand and Harbottle 1993). Other major turquoise deposits with similar geological settings are in the same vicinity, including the New Azure, Burro Chief, and Parker mines. The Tyrone copper deposit is also located in the Tyrone District where turquoise occurs in veins and nodules of the highly altered quartz monzonite porphyry (Gillerman 1964). Evidence of prehistoric extraction of turquoise is evident with the presence of ancient quarries, sherds, hammerstones, and mauls throughout the region (Weigand 1982; Weigand and Harbottle 1993).

Turquoise also occurs in the White Signal District on the southeastern part of the Burro Mountains. This district is riddled with rhyolite plugs of different compositions and ages that crosscut the Precambrian granite country rock. The Precambrian granite is part of the Burro Mountain batholith. Dikes of quartz monzonite porphyry are common in the northern area of the district, one dike in particular was reported as 15 meters wide, and about two kilometers long (Gillerman 1964:81). Although Weigand (1982) reports the presence of scrapers, sherds, stone tools, and a possible ancient quarry, Weigand and

Harbottle (1993) report evidence of prehistoric mining at the White Signal as inconclusive. Turquoise occurs along porphyritic dikes cutting through granite at the Chapman Turquoise mine on the southeast side of Saddle Mountain (Arrowsmith 1974) and at the Red Hill mine, about three kilometers northwest of White Signal. In the Red Hill mine, turquoise occurs in veinlets and small seams in a fractured and altered monzonite dike along with talc, clay and quartz (Gillerman 1964:81).

In the past 30 million years, the early intrusive Precambrian granite of the Little Hachita Mountains was exposed to episodes of mountain building, faulting and thrusting, and igneous intrusions and volcanic activity. This area is geologically similar to the areas of the Burro Mountains. Turquoise occurs in and around two altered monzonite intrusions, one west of Old Hachita (Fig. 2.16) and the other situated on the north slope of Howells Ridge near Smugglers Pass (Zeller 1970:19). The Old Hachita mine is reported to have definite evidence of ancient turquoise extraction with the presence of prehistoric quarries, sherds, scrapers, mauls, and hammerstones (Weigand 1982; Weigand and Harbottle 1993). A sample included in this study from these turquoise resource areas is the only unaltered provenance sample that was available to represent this region and was obtained from Weigand's collection.

About ten kilometers west of Hachita, several turquoise deposits cluster in an area known as Turquoise Mountain; including the Robinson and Porterfield mines and the Azure, Cameo, Galilee, and Aztec claims. West of the Old Hachita, turquoise occurs in and along the contact of the monzonitic porphyry (Pogue 1974:57) where a monzonite intrusion along with dikes and sills dominate the area (Zeller 1970:13). Turquoise has been reported from the Chino mine in the Santa Rita District, located about 20 kilometers east of Silver City where turquoise occurs as veinlets and nodules in altered quartz diorite porphyry in the open-pit copper mine (Sigleo 1970:33).

Small amounts of turquoise have been reported at the Torpedo mine in the Organ Mountains in Doña Ana County (Northrop 1959:522). The Torpedo mine is located in an area of kaolinized and brecciated porphyry intruding Paleozoic sedimentary rock and the Organ batholith. The highly altered porphyry that hosts the turquoise contains other minerals, including pyrite, chalcopyrite, and quartz (Ludington et al. 1988).

2.2.3. Arizona Turquoise Provenance Regions

In Arizona, most of the turquoise deposits occur in the Basin and Range province, including Bisbee, the Courtland area, the Pima and Silver Bell districts in Pima County, and Mineral Park in the Wallapai district near Kingman. Turquoise is not reported in the Colorado Plateau province to the north, although turquoise is found in the Globe and Miami Districts south of the Mogollon Rim in the Central Highlands province. This province is a transitional area in between the larger area of the Colorado Plateau province to the north and the Basin and Range province to the south. Much of the turquoise in Arizona is found in some of the many copper open-pit mines around Bisbee and Morenci in the southern desert, and in Globe and Miami in the Central Highland province (Fig. 2.17). The Mineral Park District clusters with the group of turquoise deposits in southeastern California and the Crescent Peak area of southern Nevada and is discussed under the next sub-section, Mineral Park, Halloran Springs, and Crescent Peak.

Turquoise occurs in the Globe and Miami Mining Districts in the Central Highland province in Gila County. In the Globe District, some of the purest high-quality blue turquoise is recovered from the Sleeping Beauty mine (Fig. 2.18). This mine is also known as the Copper Cities mine. It is located a little over five kilometers north of the

Fig. 2.17. Location of the principal turquoise provenance regions in Arizona and other locations mentioned in the text (Google Earth 2012).

Fig. 2.18. Location of the Sleeping Beauty mining area (Google Earth 2012).

city of Miami on the south side of Sleeping Beauty Peak where turquoise occurs in the oxidized area of the open-pit copper mine (Arrowsmith 1974). The host rock for the turquoise at the Sleeping Beauty mine has been reported as a quartz monzonite containing intrusive dikes of fine-grained diorite and granite porphyry (Simmons and Fowells 1966). Permission to visit and sample the mine was not granted due to the current copper mining. However, the provenance sample included in this study was supplied by the current owners. Weigand (1982) and Weigand and Harbottle (1993) reported the presence of ancient quarries, hammerstones, and mauls that provide conclusive evidence of turquoise extraction by prehistoric miners. Located in the Tonto National Forest not far from the Sleeping Beauty mine, the Castle Dome mine consists of a quartz monzonite and turquoise occurs in association with the supergene enrichment area in the leached capping and chalcocite zones (Peterson 1947).

The Canyon Creek Mine is located on the Grasshopper Plateau on the Fort Apache Reservation (Welch and Triadan 1991). The deposit is on the east side of Canyon Creek about two kilometers northeast of the confluence of Canyon Creek with the Salt River (Fig. 2.17). Emil W. Haury (1934:15-16) reported the presence of stone tools described by early visitors.

South of Tombstone, turquoise occurs in the Lavender Pit at the Bisbee copper mine (Fig. 2.19). The Bisbee mine is well known for its economic copper deposits that formed in 180 million year quartz monzonite porphyry. Many of the original silicate minerals from this quartz monzonite porphyry have been weathered and have recrystallized. Consisting largely of quartz, sericite, and disseminated pyrite, the strongly altered quartzite country rock and the quartz monzonite porphyry are visually very

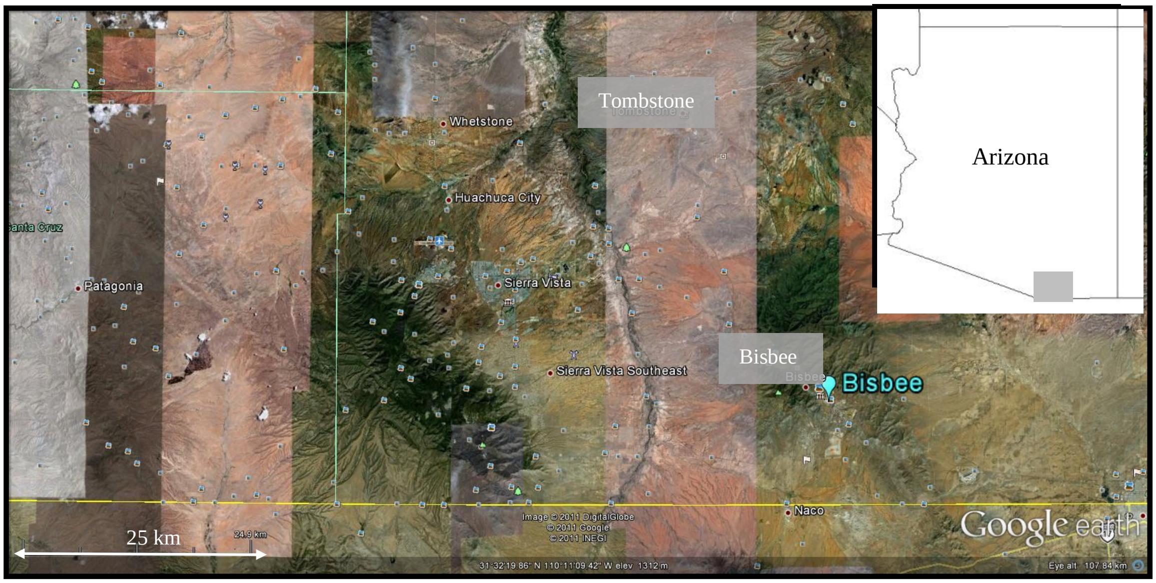

Fig. 2.19. Location of the Bisbee copper and turquoise deposit, near the town of Bisbee (Google Earth 2012).

similar (Anthony et al. 1977:18). Turquoise occurs as veinlets, stringers, and nuggets in the large open-pit area of the Lavender Pit in the surrounding granite and quartzite (Arrowsmith 1974) along with other oxidation products such as jarosite (Anthony et al. 1977:20-21). Turquoise was also reported in the Cole Shaft from a depth of 360 meters (Arrowsmith 1974). Weigand and Harbottle (1993) reported inconclusive evidence of prehistoric mining and Weigand (1982) documented the presence of hammerstones and mauls. The sample included in this study from Bisbee was obtained from Weigand's collection.

In the Clifton District of Greenlee County, turquoise occurs in a 30 meter dike that runs northwest across the Morenci open-pit copper mine (Fig. 2.20). Large quantities of turquoise are found in altered intrusive rocks and in the contact zone of a monzonite that is about 58 million years old. Turquoise deposits are also reported at some of the deepest areas of the mine, around 1365 meters below the surface (Sigleo 1970). The turquoise provenance sample from Morenci was obtained from Weigand's collection. Weigand (1982) reported the presence of stone tools during his survey.

Large amounts of high-quality turquoise have been historically mined from the Courtland area in Cochise County. The presence of prehistoric quarries, stone tools, and sherds suggest that the area was also exploited by ancient turquoise miners (Weigand 1982; Weigand and Harbottle 1993). This area is also known as the Turquoise District, Avalon Group, and Turquoise Mountain. Some of the mines in this area are the Avalon, Brown's Peak, Courtland, Herget, and the Tiffany and two claims, the Avalon Azul and the Nightingale (Anthony et al. 1977; Arrowsmith 1974; Crawford and Johnson 1937; Ransome 1913). Turquoise deposits cluster around the western side of Turquoise Ridge (Crawford and Johnson 1937), also referred to as Turquoise Mountain, about a kilometer

Fig. 2.20. Location of the Morenci copper mines (Google Earth 2012).

west of Courtland, and the eastern edge of Dragoon Mountain (Fig. 2.17), located about 29 kilometers northeast of Bisbee and 22 kilometers east of Tombstone (Ransome 1913).

Situated deep within the Basin and Range province, the region's topography was heavily influenced by periods of normal and thrust faulting. The host rocks of the Turquoise Ridge turquoise deposits consist of Cambrian age quartzite and Tertiary granite with some outcrops occurring in intrusive dikes. Forming as stringers and nuggets, turquoise is commonly associated with sericite and kaolin (Crawford and Johnson 1937). On the eastern side of Dragoon Mountain, Paleozoic rocks are cut by a large mass of coarse-grained granite along with other types of igneous intrusions. Between Dragoon Range and the Turquoise Hills, the low ground and some of the low foothills are composed of highly altered and decomposed fine-grained granite (Ransome 1913). The quartzite of the surrounding mountains is similar and probably part of the same middle Cambrian Bolsa quartzite found in the Bisbee District (Crawford and Johnson 1937; Ransome 1913). There appear to be two separate intrusive events: older porphyry consisting of irregular dikes that are light colored and extremely decomposed and a second event where the porphyry is much darker in color (Ransome 1913).

Turquoise occurs at several locations in Pima County, primarily associated with the Silver Bell and Esperanza copper mines. Turquoise occurs in the Oxide Pit of the Silver Bell mine (Anthony et al. 1977). The Silver Bell District is located on the south side of Silver Bell Mountain about 56 kilometers northwest of Tucson (Fig. 2.17). This mining district is heavily faulted, containing rocks of varying ages from Precambrian to recent. The district is riddled with dikes and pipes of quartz monzonite porphyry intruding into Cambrian age quartzite (Graybeal 1982), generally referred to as a vein complex.

Turquoise has been reported in the oxidized zone at the Safford porphyry copper deposit in the Lone Star District in the Gila Mountains (Fig. 2.17) of Graham County (Anthony et al 1977:194), 19 kilometers east of Morristown in Maricopa County (Arrowsmith 1974), and near Kelvin in the Mineral Creek District of Pinal County (Anthony et al. 1977:194; Arrowsmith 1974). Turquoise occurs in shallow deposits in several locations in Yavapai County, one in Chino Valley southwest of Prescott (Arrowsmith 1974) and another located northeast of Wittmann (Anthony et al. 1977:194; Arrowsmith 1974), and in the Castle Dome Mountains in Yuma County (Arrowsmith 1974).

2.2.4. Mineral Park, Halloran Springs, and Crescent Peak

This turquoise provenance region encompasses portions of three states; northwestern Arizona, southeastern California, and the southern tip of Nevada (Fig. 2.21) and may contain some of the best documented turquoise resource areas other than the Cerrillos Hills. These areas are well known for heavy evidence of pre-Columbian turquoise mining and one area in particular, Halloran Springs, has been the focus of previous turquoise provenance studies and excavations (Leonard and Drover 1980; Sigleo 1975). Because of its proximity to Kingman and association with large economic copper mines in the Cerbat Mountains, Mineral Park is probably one of the most well-known present-day turquoise mineral source areas.

Mineral Park is situated on the eastern edge of the Basin and Range province near the Colorado Plateau (Thomas 1950) about 24 kilometers northwest of Kingman, Arizona (Fig. 2.22). Turquoise occurs in seams, fractures and cavities in the highly altered and shattered areas of the host rocks consisting of Precambrian metamorphic rocks intruded by granite and quartz monzonite porphyry and rhyolite dikes (Fig. 2.23) (Pogue 1974:45-

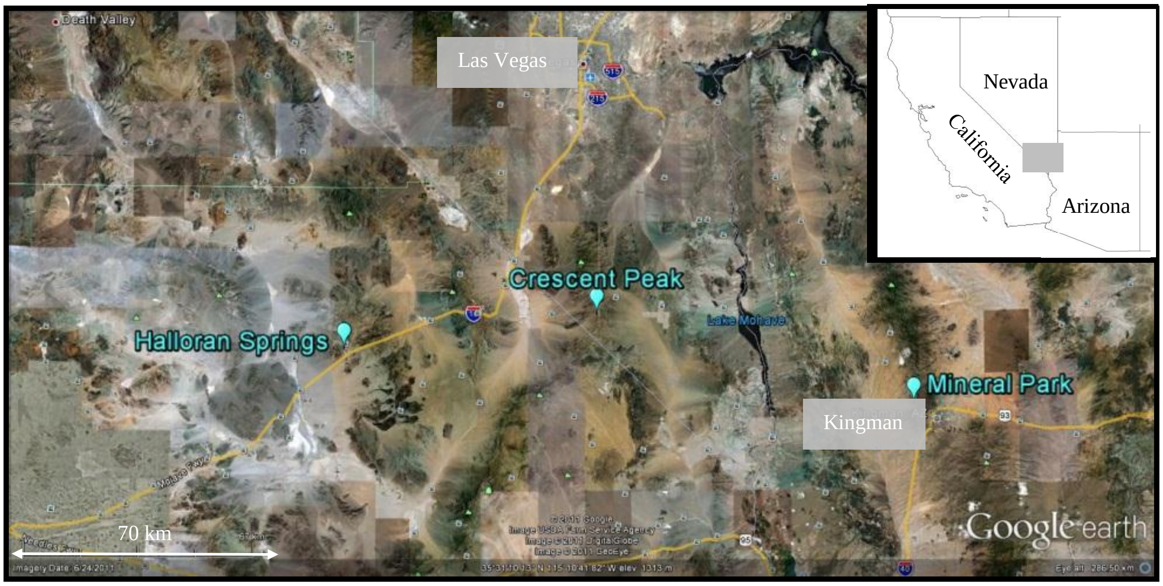

Fig. 2.21. Location of the turquoise provenance region that encompasses turquoise resource areas in western Arizona, southern Nevada, and southeastern California (Google Earth 2012).

Fig. 2.22. Location of the Mineral Park Mining District, near Kingman, Arizona (Google Earth 2012).

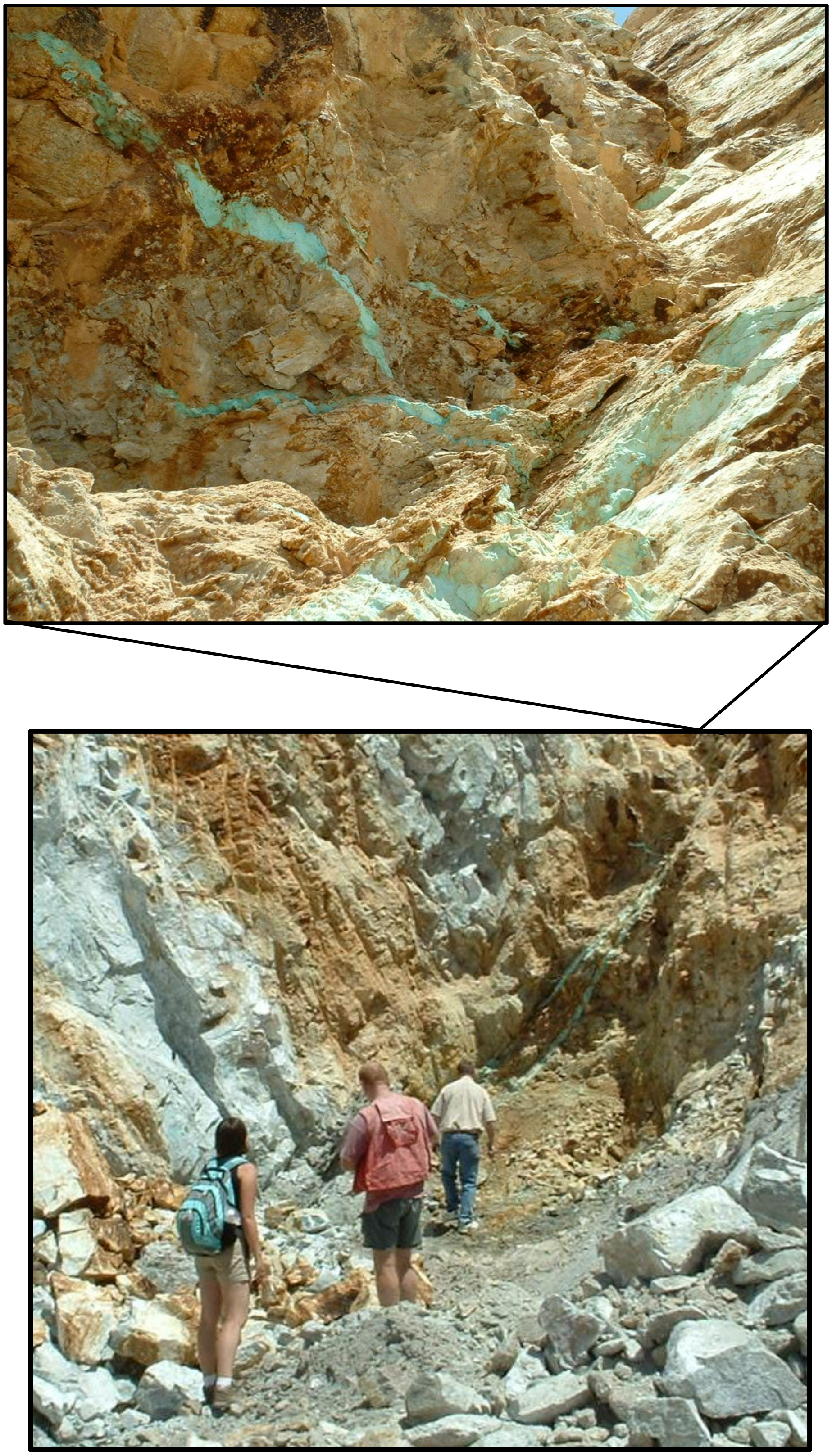

Fig. 2.23. Large turquoise veins and sample collection at Mineral Park near Kingman, Arizona.

46; Thomas 1950; Wilkinson et al. 1982). Many large rhyolite dikes cut through the region, some as long as 150 meters (Wilkinson et al. 1982). Along with the long, thick dikes, large areas of white pegmatite can be found between layers of metamorphic rock (Thomas 1950:666). Although most of the turquoise has been found in the central copper porphyries, it also occurs in the radiating dikes and in the sheets of white pegmatite.

Many of the turquoise mines, including the Monte Cristo, Turquoise King, Queen, Peacock, Ithaca Peak, the Metallic, and the Accident mines, produced large quantities of turquoise. Most of these turquoise deposits have been obliterated by modern-day copper mining (Fig. 2.2). Although much of the evidence of pre-Columbian mining activities has been destroyed, some evidence was documented in early accounts of the area (e.g., Pogue 1974). Also, artifacts that were recovered during modern-day turquoise mining by Mr. Colbaugh were given to museum collections (Johnston 1964). Conclusive evidence of prehistoric mining includes the presence of ancient quarries and stone tools (Weigand 1982; Weigand and Harbottle 1993). Prehistoric tunnels, some as long as seven meters, have also been reported that contained ancient stone tools, charcoal, and animal skin water containers (Johnston 1964; Pogue 1974). Samples used in this study were collected from several areas in Mineral Park during a visit provided by Mr. Colbaugh (Colbaugh Processing, Inc.).

In San Bernardino County, there are three groups of turquoise claims, East Camp, Middle Camp, and West Camp, all located near Halloran Springs along Highway 40 (Fig. 2.24). The Halloran Springs region is a continuation of the Great Basin region where playas sit at the bottom of closed basins among north-south trending mountain ranges and desert plains. Dominated by Cretaceous thrust faulting and igneous intrusive rocks, the

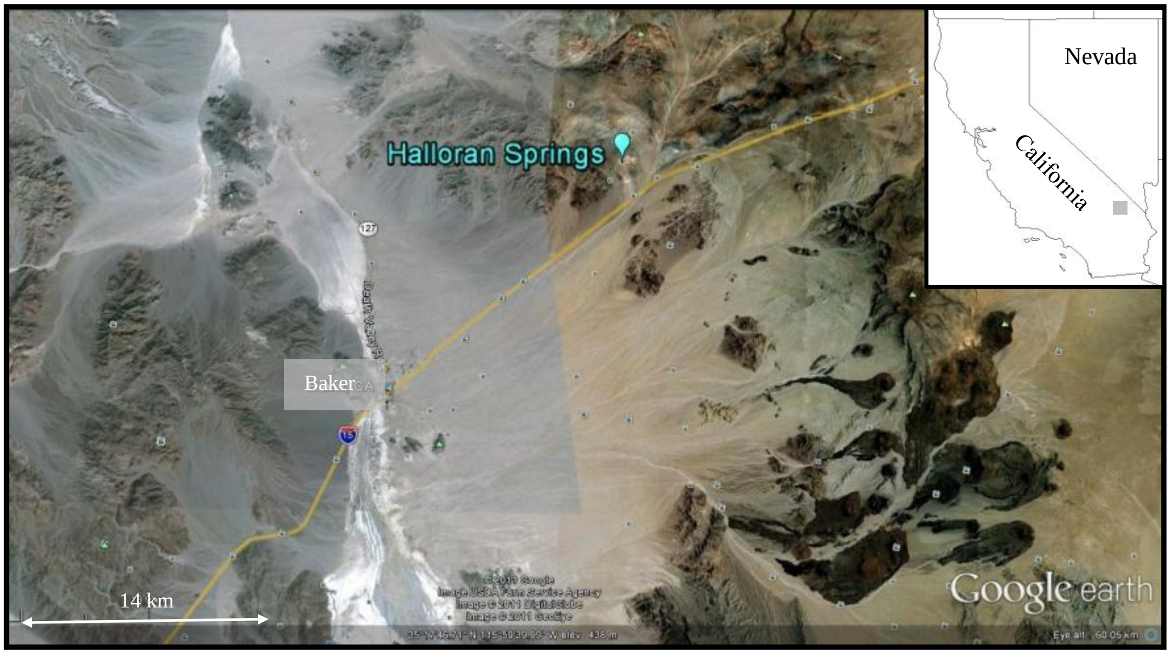

Fig. 2.24. Location of the Halloran Springs turquoise resource area near Baker, California (Google Earth 2012).

regional geology is characterized by the typical fault-block mountains: steeply tilted on one side and sloping on the other (Cloudman et al. 1917; Hall 1972). Some of the earliest intrusive rocks in this region date as far back as 190 to 200 million years ago (Sutter 1968), while the dominant quartz monzonite intrusive is probably a result of Late Cretaceous thermal events. Many of the extrusive rhyolite, basalts, and intrusive stocks date to the mid Tertiary (Hall 1972). Turquoise occurs in the area of altered copper porphyry and sandstones, and has been reported in basaltic dikes radiating in all directions from extinct craters (Kunz 1905). At the Himalaya mine, turquoise fills joint planes and fracture zones in the intrusive and country rock as well as along some of the many quartz veins that cut throughout the region (Pogue 1974).

The turquoise deposits around Halloran Springs display evidence of heavy exploitation of ancient miners with many prehistoric quarries, hammerstones, scrapers, ceramic sherds, camps, and petroglyphs (Jenson 1985; Leonard and Drover 1980; Rogers 1929; Weigand 1982; Weigand and Harbottle 1993). Many of these prehistoric tunnels have been *mucked-out* (Fig. 2.25) where an individual or small group of historical miners remove the softer sediments of ancient adits and tunnels that were filled when they were abandoned (Nazelrod 1977). Hammerstones and other stone tools were recovered scattered throughout the soft sediments (Fig. 2.26). The largest incident of an area that was mucked-out was reported to Malcolm J. Rogers (1929) where workers cleared out a prehistoric quarry that was nine meters long, and over three meters wide and deep. Native tortoise shells and an elk scapula were recovered in the debris as well as many stone tools. William A. Jenson (1985) provides an excellent recap of information including descriptions of artifacts, ceramics, excavations, turquoise deposits, and field

Fig. 2.25. A modern-day turquoise deposit where a prehistoric tunnel has been *mucked-out* at Halloran Springs, California.

Fig. 2.26. Stone tools recovered in the soft sediments of an ancient tunnel near Halloran Springs, California.

notes of early surveys. Samples included in this study from this area were collected on several visits to the area in 2007 and 2008 arranged and guided by Robert Reynolds, Robert Hilburn (Mojave River Valley Museum), Ed Nazelrod (Apache Mining Company), and Jim Sherer (Bureau of Land Management). The provenance sample from Middle Camp was provided by Ed Nazelrod.

The Grove Turquoise mine is located in the Mohave Desert about three kilometers west of Cottonwood Siding on the Santa Fe Railroad. Turquoise occurs in seams and nuggets in and along the contact zone of highly altered porphyry that cuts through fine-grained biotite gneiss (Pogue 1974:47).

A large turquoise mining area is found near Crescent Peak in Clark County about 19 kilometers west of the town of Searchlight (Fig. 2.27). This area of claims is known as Crescent Peak, Simmons, Aztec, Right Blue, and the Turquoise mines (Fig. 2.28). The turquoise is found in quartz monzonite and altered granite. The presence of stone tools and possible ancient quarries provided evidence of prehistoric exploration by ancient miners (Weigand 1982; Weigand and Harbottle 1993). The pre-Columbian mine was discovered by George Simmons in the late 1800s. He mucked-out the ancient mine and reported the presence of stone tools. Simmons also reported a level terrace nearby that was used for a habitation area and a workshop. Wood recovered from the site suggests that the area was abandoned in the late A.D. 1200s (Morrissey 1968). The area is now part of a gravel pit owned and operated by Bill Crank (Crescent Mineral Resources), who gave permission to obtain provenance samples and provided a tour of the area in 2007. The one other turquoise provenance sample (Locality #7) used in this study was obtained from Weigand's collection.

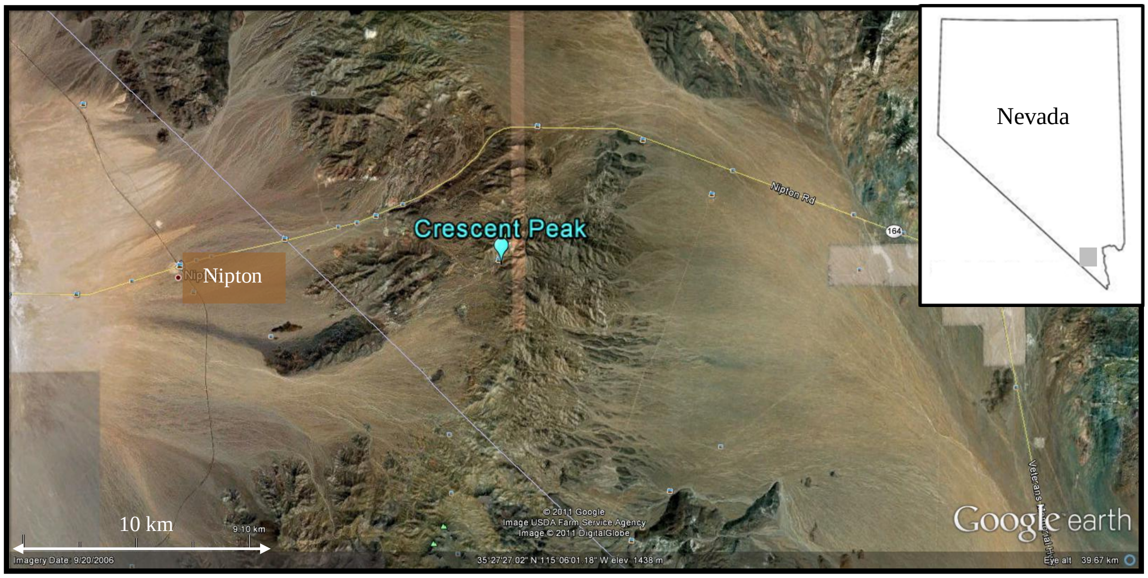

Fig. 2.27. Location of the Crescent Peak mining area near the town of Searchlight, Nevada (Google Earth 2012).

Fig. 2.28. Prehistoric and historic turquoise mines near Crescent Peak, Nevada.

The Sullivan Mine is located near Boulder City, Nevada and the site was visited in 2007. Unfortunately, the site has been developed and the collection of any provenance samples from the surrounding area was not allowed.

2.2.5. Nevada Turquoise Provenance Regions

The most northern known turquoise deposits in the United States are found in the Basin and Range province in Nevada including the Carlin Black Matrix and Stampede mines in Elko County and the August Berning and Number Eight mines in the Lynn District of Eureka County. Turquoise occurs in brecciated chert and quartzite, and in seams along bedding planes at the Stampede mine. The August Berning and Number Eight mines are located within 300 meters of each other on the west side of the Tuscarora Range (Fig. 2.29) where turquoise occurs in the highly altered and fractured monzonite intrusive rock. Turquoise occurs 210 meters below and about 300 meters southwest of the Number Eight mine; along bedding planes and in the contact zones between the country and intrusive rocks (Arrowsmith 1974; Morrissey 1968:12-13). The Number Eight mine consists of folded and faulted shale intruded by quartz monzonite (Morrissey 1968:12-13; Sigleo 1970:38-39) and was also reported to have produced copper and gold. In fact, this area in northeastern Nevada, known as the Carlin Trend (Fig. 2.29), is one of the largest and richest gold endowments in North America. The turquoise deposits in this region have long been obliterated by contemporary gold mining operations.

Identifying and locating specific turquoise deposits in Nevada is problematic because there are many outcrops of turquoise. Many names have been used for a single turquoise claim. Also, there are many instances were a single name, or slight variation of the name, was assigned to multiple claims. This makes it difficult to distinguish specific turquoise deposits referred to in the literature or identify the specific location of turquoise

Fig. 2.29. Locations in Nevada mentioned in the text: Blue Gem, Fox Mine, Green Tree and the Godber (Google Earth 2012).

samples that are only labeled with the name of the deposit. There has also been less survey and documentation of the evidence of prehistoric mining. Turquoise deposits occur in a belt that trends from the northeastern deposits to the southwest through the center of Nevada. There are several clusters of turquoise deposits in Lander County where two of the main areas are known as the Bullion District and Copper Basin. Turquoise deposits in the Copper Basin area, including the Myron Clark, Turquoise King, and the Blue Gem Lease, are hosted in an altered quartz monzonite occurring as seams and nodules in the intrusive rock. Many of these deposits display argillization; the replacement or alteration of feldspars forming clay minerals. This region is characterized by the repeated deformation of rocks with porphyritic intrusions during the Eocene or Oligocene (Theodore et al. 1982). The Blue Gem Lease is located within a large copper deposit and large economic copper deposits are found nearby in Copper Canyon (Morrissey 1968). On the east side of the Shoshone Range is the Bullion District near Tenabo where the most extensive historical turquoise mining in the state has occurred. This area includes the Steinich, Rufan, Little Gem, Blue Nugget, Blue Gem, Super-X, Arrowhead, Old Campground, Blue Eagle, and the Blue Matrix. Many of these deposits are found in quartzite and shale in association with highly altered intrusive dikes and sills that cut through the sedimentary rock. The sample used in this study from the Blue Gem, located near Tenabo, Nevada (Fig. 2.30), was acquired from Weigand's collection.

Further south from the Bullion District, Lone Pine, White Horse, Fox Mine, and Green Tree (Fig. 2.31) mines are located in the Cortez area. The turquoise samples used in this study from the Green Tree and the Fox mines were obtained from Weigand's collection. Both of these samples are from the same turquoise provenance region,

Fig. 2.30. Location of the Blue Gem mining area southwest of Tenabo, Nevada (Google Earth 2012).

Fig. 2.31. Location of the Fox and Green Tree turquoise resource areas (Google Earth 2012).

possibly the same deposit. The Godber, McGinness, and the Ralph King mines are located near the town of Austin. The Godber, also known as Dry Creek, is located five miles north of Hickison Summit along Highway 50 (Fig. 2.32). The sample from the Godber mine (Fig. 2.33) was obtained during a tour of the mine by the current owner Bruce Woods in 2007. Near the top of the hill above the main mining area are sediment filled prehistoric or historic mining tunnels (Fig. 2.34). These deposits are situated in a geological setting similar to the Bullion District, where turquoise occurs in fractured and brecciated quartz zones cutting through the chert and shale country rock. The Copper Blue, Zabrisky, Indian Blue, and the Tom Molly deposits located to the south in the Toquima Range in Nye County are also situated in a similar geological setting.

Further to the south, turquoise deposits cluster around Tonopah and the surrounding region (Fig. 2.35). The Royston District is a well-known area for modern-day turquoise mining. Some of the better known deposits are the Royal Blue, Bunker Hill, and the Oscar Wehrend where turquoise occurs in altered porphyritic quartz monzonite (Morrissey 1968). The Royal Blue deposit is located on the eastern side of a plateau on the western side of the Big Smokey Valley in the Royston Hills (Fig. 2.36). Weigand (1982) surveyed this area and reported evidence of prehistoric mining with the presence of hammerstones, mauls, and ceramic sherds. Samples used in this study from Royston were collected in 2007 from a tour provided by Dean and Donna Otteson (Otteson's World Famous Turquoise) allowing the investigation and sampling of several areas within the Royston District (Fig. 2.37) and several deposits to the east (Fig. 2.38), the Black Hills (Fig. 2.39) and Verde Blue (Fig. 2.40). The deposits east of the Royston District, in Mineral County, near the Esmeralda County line are located in the Pilot Mountains and near the town of Basalt. The Blue Jay Gem and the Blue Gem No. 1 are

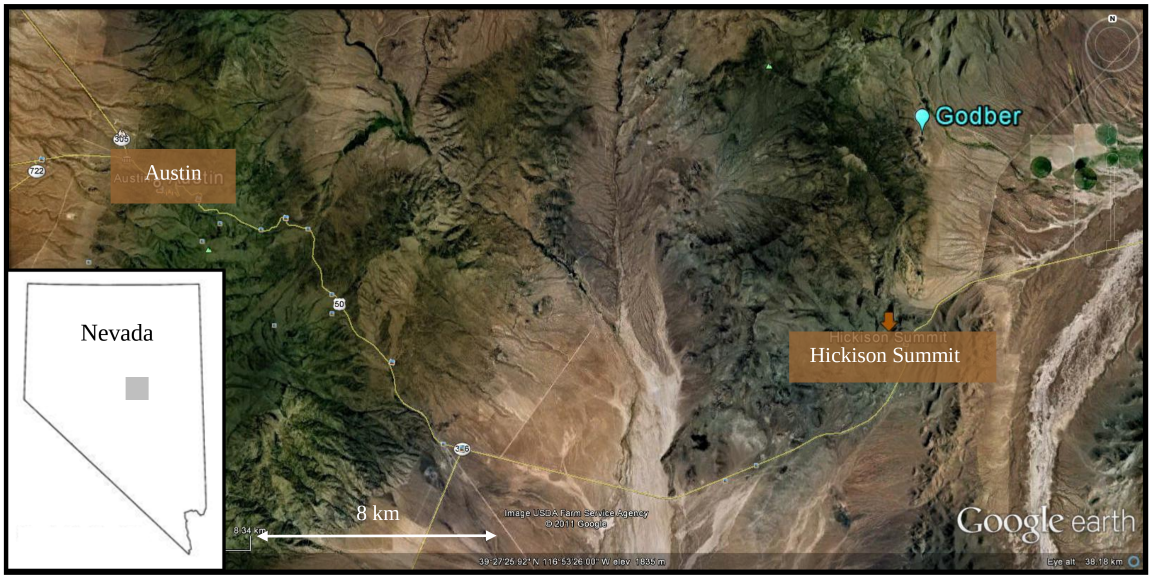

Fig. 2.32. Location of the Godber turquoise deposit near Austin, Nevada (Google Earth 2012).

Fig. 2.33. The Godber turquoise resource area, as seen from above.

Fig. 2.34. Sediment filled tunnels at the Godber Mine.

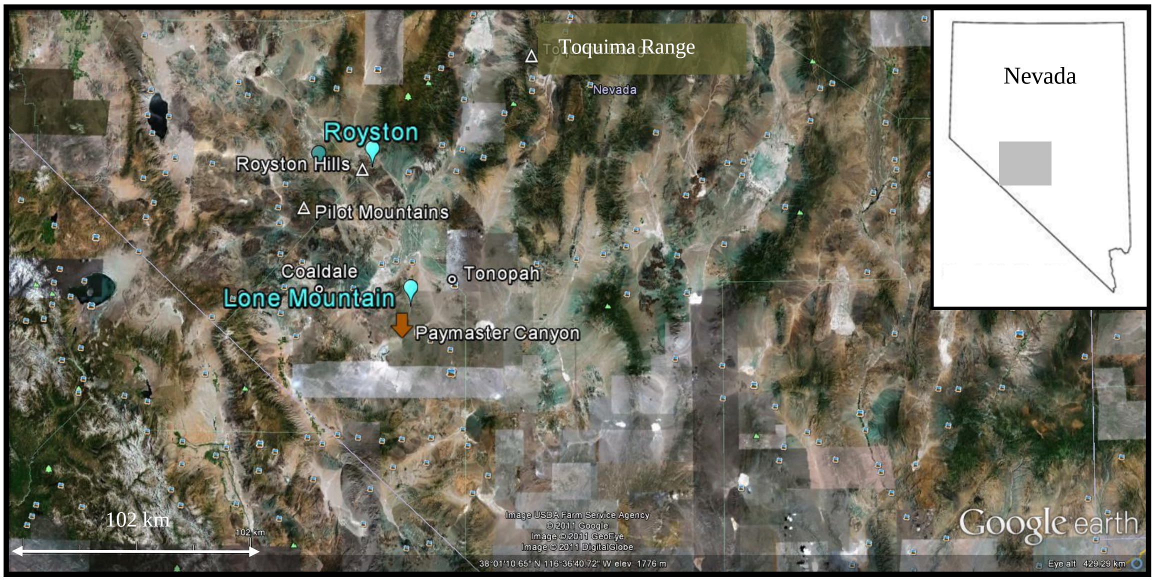

Fig. 2.35. Location of several turquoise resource areas in central Nevada along with other locations mentioned in the text (Google Earth 2012).

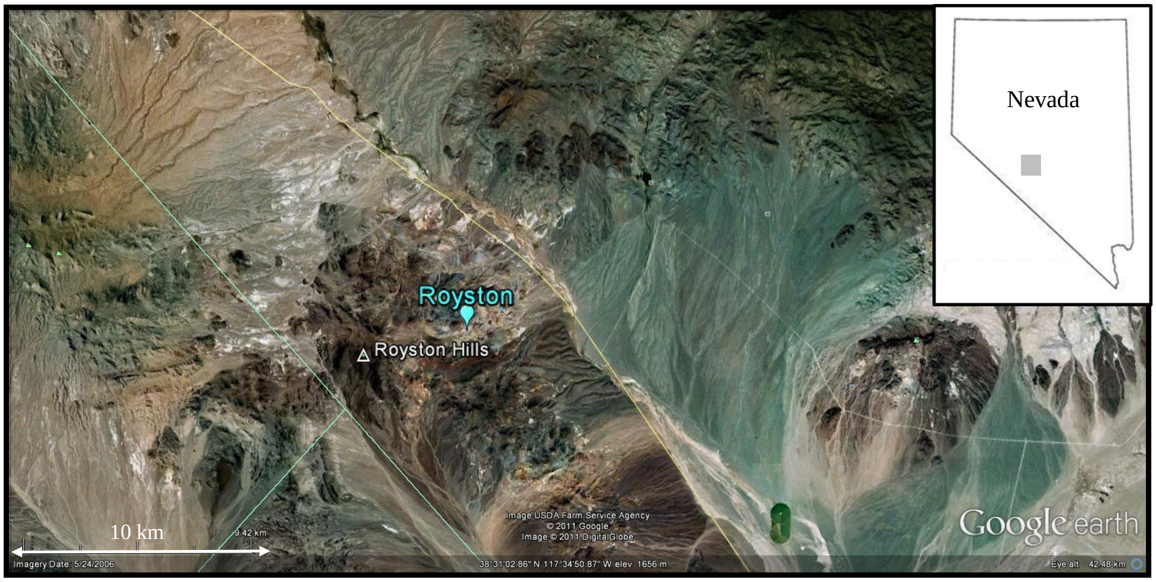

Fig. 2.36. Location of the Royston turquoise deposit in the Royston Hills, northwest of the town of Tonopah, Nevada (Google Earth 2012).


Fig. 2.37. The Big Smokey Valley, as seen from the Royston Hills, Nevada.

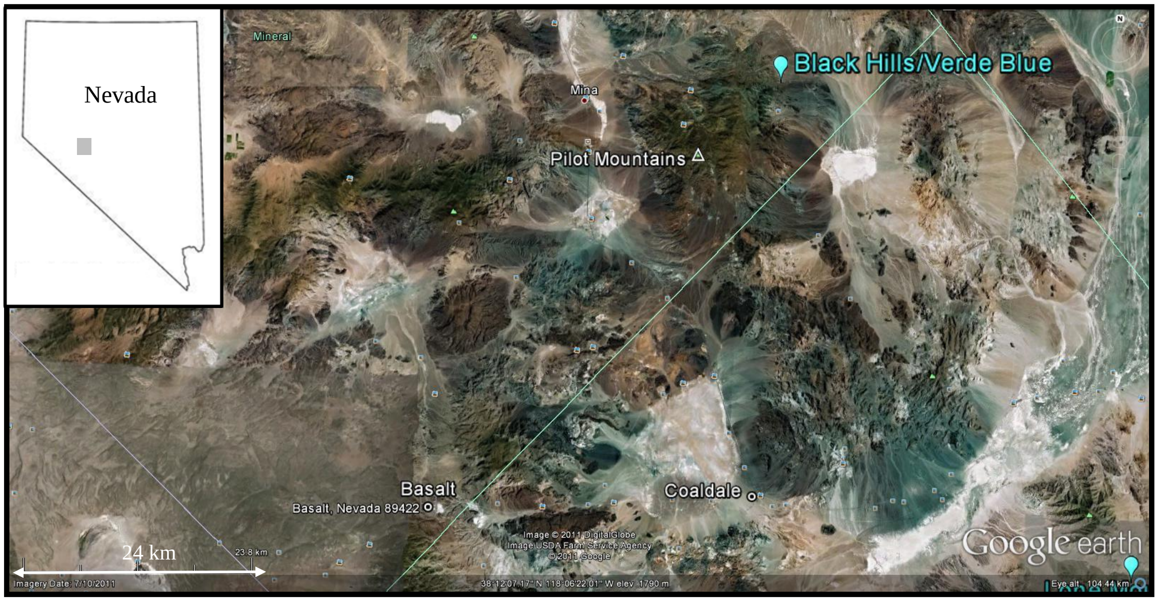

Fig. 2.38. Location of the Black Hills and Verde Blue turquoise resource areas in the Pilot Mountains, Nevada (Google Earth 2012).

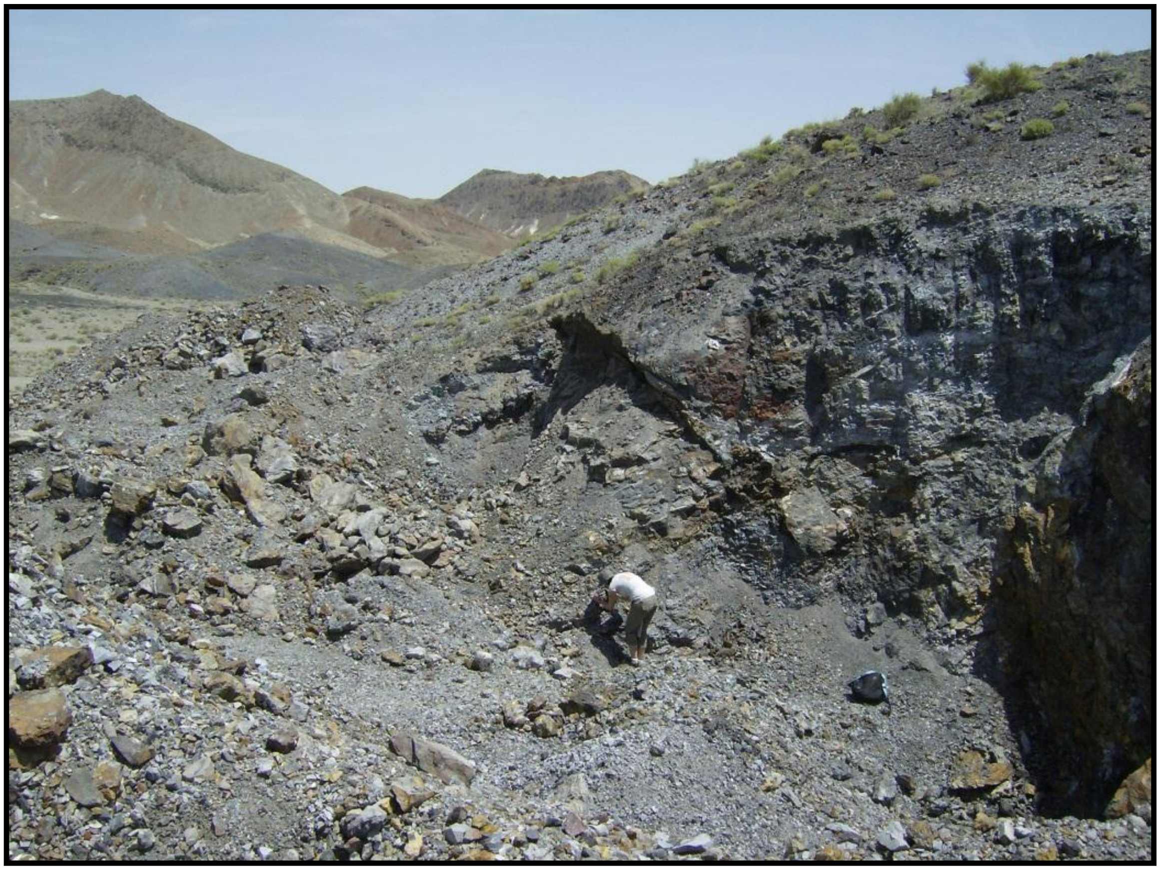

Fig. 2.39. The collection of turquoise provenance samples at the Black Hills deposit near Tonopah, Nevada.

Fig. 2.40. The Verde Blue turquoise deposit east of the Royston Hills, Nevada.

located near Basalt were nodules and veins of turquoise occur in the bedding planes and fractures of the shale and limestone country rock (Morrissey 1968).

In the Pilot Mountains, the Moqui-Aztec, Pilot Mountain, Montezuma, Troy Springs, Turquoise Bonanza and the Copper King claim are all found in association with altered quartz monzonite (Morrissey 1968; Pogue 1974). The Halley's Comet or Clara mine is found in porphyry and in rhyolite; an extrusive igneous rock (Arrowsmith 1974; Morrissey 1968; Pogue 1974). Turquoise deposits are found throughout Esmeralda County. The Carl Riek and the Miss Moffat mines, also known as the Blue Boy and Persian Blue, are located near the town of Coaldale in the foothills at the northeastern end of the Fish Lake Valley.

Near Paymaster Canyon (Fig. 2.41), several turquoise deposits, including Lone Mountain, Blue Silver, and the Livesly mine are found in association with plutonic rocks and shale. The sample from Lone Mountain (Fig. 2.42) was collected in 2007 from a visit to the deposit with the owner, Chris Lott (Lone Mountain Turquoise). Several turquoise deposits are situated in the Monte Cristo Range, including the Carrie, Carr-Lovejoy, Crow Spring, the Marguerite and the Monte Cristo, where turquoise occurs in seams, veinlets, and in the contact zones (Morrissey 1968; Pogue 1974). South of Tonopah on the Nye County Line, the Smith Black Matrix is located in a small group of hills about a kilometer east of Klondyke Peak (Morrissey 1968). Turquoise occurs in veinlets, joints, fractures, and seams in limestone and shale (Morrissey 1968; Pogue 1974).

Fig. 2.41. Location of Paymaster Canyon; the area of the Lone Mountain turquoise deposit in Nevada (Google Earth 2012).


Fig. 2.42. Lone Mountain turquoise mine in Paymaster Canyon, near Tonopah, Nevada.

2.2.6. Turquoise Provenance Regions of Mexico

Investigating turquoise resource areas in Mexico is more complicated as there is less documentation and opportunity to visit and obtain sample from the mines south of the international border. Weigand and Harbottle (1993) surveyed and sampled several of the areas and documented evidence of prehistoric mining activities. The geochemical fingerprinting of these turquoise provenance regions will be crucial when analyzing Mesoamerican turquoise artifacts. As with turquoise deposits in the western United State, the turquoise deposits in Mexico are associated with copper mines.

There are several occurrences of turquoise reported in the Baja California peninsula (Arrowsmith 1974; Panczner 1987). Turquoise deposits are located in the El Aguajito Mining District including the Vincent, Hermonsa, Preciosa, and the La Reina also known as the La Turquesa. East of Ensenada in the El Rosario area is the Evans Turquoise, also known as the Mexico Turquoise mine and the American Hole (Fig. 2.43). The turquoise sample used in this study from the Evans Mine was obtained from Weigand's collection.

In the state of Coahuila there are two turquoise deposits documented, the Beta Perez mine and a deposit in the area of Santa Rosa (Fig. 2.44). Weigand and Harbottle (1993) report inconclusive evidence of prehistoric mining at Beta Perez and conclusive evidence in Santa Rosa. Turquoise has been reported at the Mipimi mine in Chihuahua as well as three different areas in Sonora: Cananea, La Carida, and the La Barranca Copper District near Copper Canyon (Arrowsmith 1974; Panczner 1987; Pogue 1974; Weigand and Harbottle 1993). Weigand and Harbottle (1993) report evidence of ancient mining at Cananea and considerable evidence at La Carida. In the Santa Rosa District in Zacatecas, turquoise is reported near the town of Bonanza at the Concepción del Oro,

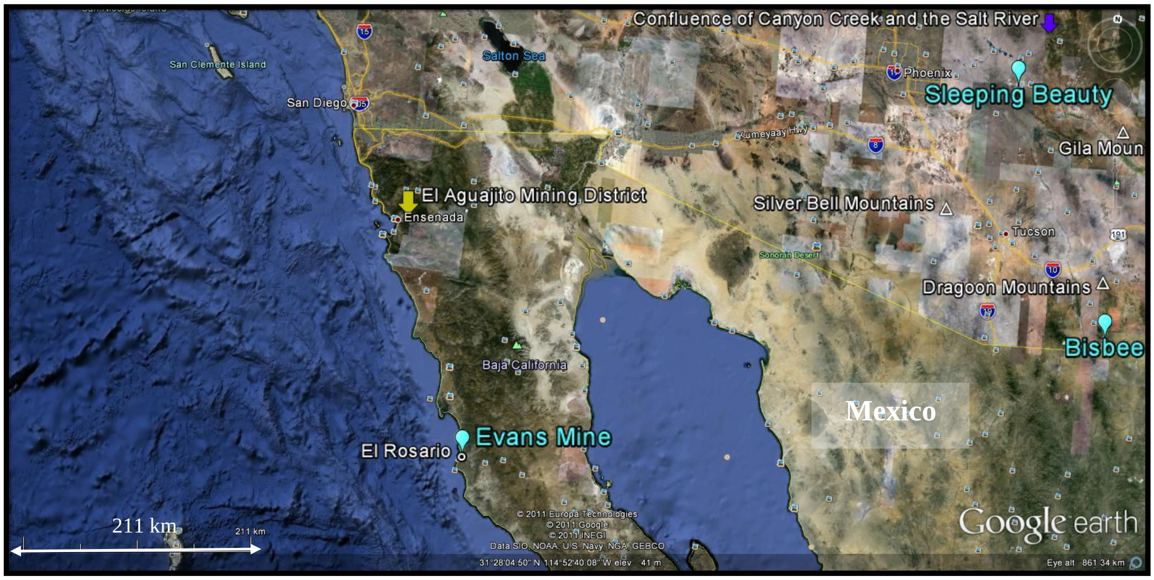

Fig. 2.43. Location of the Evans Mine in Baja California, Mexico and other locations mentioned in the text (Google Earth 2012).

Fig. 2.44. Location of areas in Mexico mentioned in the text (Google Earth 2012).

Mazapil, Todos Santos, and the Socovánn de las Turquesas mines (Arrowsmith 1974; Panczner 1987; Pogue 1974) and in the Aranzazu Mining District located southwest of Saltillo (Arrowsmith 1974).

2.3. Ancient Turquoise Mining

Considering the abundant evidence of prehistoric turquoise mining and, in some cases, the extent of the mining, it is clear that there was a lot of planning, organization, and vested labor for the extraction of turquoise. These pre-Columbian miners had a good knowledge of the location of turquoise deposits (e.g., Arrowsmith 1974; Harbottle Weigand 1992; Pogue 1974; Weigand 1982; Weigand and Harbottle 1993); however without modern-day technology, the extraction of turquoise was difficult. Evidence supports that turquoise was normally extracted by the use of stone tools as well as fire and water (Pogue 1974). Fires were built to heat the surrounding rock and then water was poured over the area to quickly cool it causing the rock to crack and split.

Many of the turquoise resource areas are located in hot arid regions (Fig. 2.45) far from the support of their communities (Weigand and Harbottle 1993). Not only were the ancient miners challenged by working in difficult climatic conditions (Fig. 2.46), they had to transport the turquoise and their supplies without the help of the wheel or large domesticated pack animals. Turquoise must have been as important a resource and display of status and wealth for the prehistoric cultures of the American Southwest as is gold and diamonds in current western cultures.

In this chapter, turquoise mineralogy, formation processes, locations of turquoise resource areas, and evidence of ancient mining were discussed. It was shown that turquoise is a complex mineral and is formed by supergene enrichment processes on exposed copper porphyry intrusive bodies. All known turquoise resource areas were

Fig. 2.45. A view of the hot and arid region near Crescent Peak, Nevada.

Fig. 2.46. Water would have been an essential resource in the landscape around Halloran Springs, California.

listed in Appendix 1 and the turquoise provenance samples used to establish the comparative database are presented in Table 2.1. Clearly, it is essential to have a good understanding of the mineral of interest and how it was formed for the development of a successful and robust technique to identify the origin of archaeological materials. A comparative database needs to be established for the comparison of unknown samples (in this case, the artifacts). And as stated in the beginning of the chapter, all known turquoise resource areas need to be identified, examined, sampled, and geochemically characterized to develop an effective comparative database.

Chapter 3: Turquoise Provenance Techniques

Bernard of Chartres said we are like dwarfs sitting on the shoulders of giants. We see more, and things that are more distant, than they did, not because our sight is superior or because we are taller than they, but because they raise us up, and by their great stature add to ours (John of Salisbury, Metalogicon, 1159).

In this chapter, a brief history of the techniques developed to identify the resource areas of turquoise artifacts is presented as well the limitations of trace element concentration studies. Isotopes, their use in archaeological research, and analytical methods used to measure isotope ratios are discussed. The chapter then focuses on the use of hydrogen and copper isotope ratios to identify the origin of turquoise artifacts and why they are successful discriminators.

3.1. Turquoise Provenance Research

Early attempts to characterize and/or identify turquoise provenance regions relied on comparisons of color and other visual similarities between archaeologically recovered turquoise and turquoise from specific mines. However, each turquoise deposit does not have a unique color or visible characteristic that can support a visual method. For example, the color of turquoise can range from light blue to green within a few centimeters in a single sample (Fig. 3.1). Therefore, researchers investigated the use of techniques similar to those used to characterize other archaeological materials, such as obsidian (e.g., Shackley 2005). Sourcing techniques for obsidian artifacts include the measurement of minor and trace elements (e.g., rubidium, strontium, and zirconium) by instruments such as X-ray fluorescence (XRF) and instrumental neutron activation analysis (INAA). In addition, the measurements of rare earth elements (e.g., lanthanum and lutetium) have been quite useful in further defining obsidian sources (e.g., Glascock and Neff 2003; Glascock et al. 2007). Once chemical profiles, or source groups, are established for geologic sources, it is then possible to match data from artifacts against these reference groups to identify the geologic origin of the artifacts. The supposition here is that chemical variation within discrete compositional groups is less than variation between compositional groups. This approach, also known as the *provenance postulate*

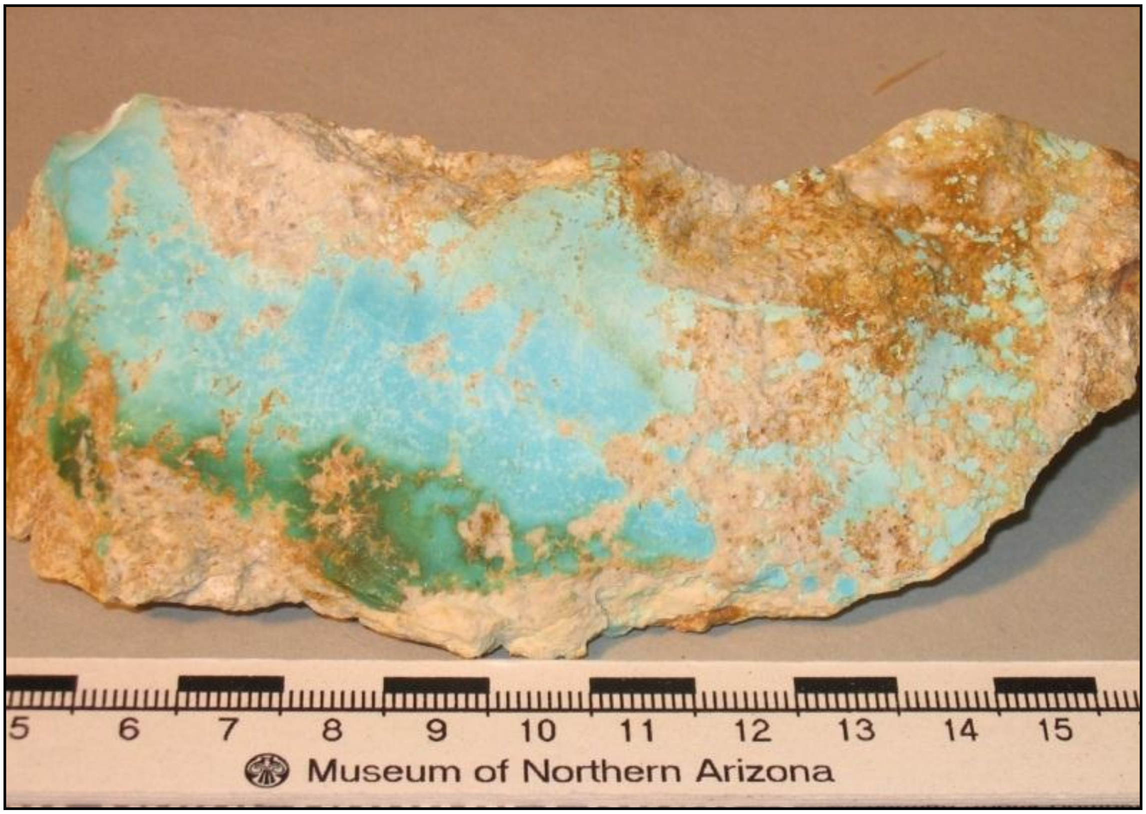

Fig. 3.1. Turquoise sample from Nevada that shows the range in color in a single vein that would cause variation in trace element composition patterns from multiple samples analyzed from this one rock.

(Weigand et al. 1977), is the underlying basis for provenance-based studies of archaeological materials and allows researchers to examine relationships and connections between the known provenance area and the unknown artifact sample.

Studies attempting to define trace element composition *fingerprints* for turquoise provenance regions spans four decades utilizing different instruments including XRF (Judd 1954; Mathien and Olinger 1992; Ronzio and Salmon 1967), INAA (Bishop 1979;Harbottle and Weigand 1992; Sigleo 1975; Weigand et al. 1977; Weigand and Harbottle 1993), electron microprobe analyses (EMPA) (Ruppert 1982, 1983), atomic emission spectroscopy (AES) (Sigleo 1970), proton induced X-ray emission (PIXE) (Kim et al. 2003), laser ablation-inductively coupled plasma-mass spectrometry (LA-ICP-MS) (Zedeño et al. 2005), and the mineralogy of turquoise using X-ray diffraction (XRD) (Welch and Triadan 1991).

As early as 1954, archaeologists began to experiment with the concept of trace element composition patterns to define turquoise provenance regions. One of the first attempts to link turquoise artifacts from Chaco Canyon to known turquoise provenance areas was unsuccessful (Judd 1954). In the late 1960s, A. R. Ronzio and M. L. Salmon (1967) analyzed 15 turquoise samples from eleven different provenance regions including the King Manassa, Hall Mine (Villa Grove), and Cripple Creek mines in Colorado and several deposits from Arizona, Arkansas, Nevada, and Mexico. Their trace element data obtained by XRF were also inconclusive.

A few years later, Anne Marguerite Colberg Sigleo (1970) used AES to compare the trace element composition of 80 samples from 25 turquoise mines to test for variation within and between mines. In her study, she also included turquoise artifacts from eight archaeological sites in New Mexico. Four of the artifacts were from Chaco Canyon, two from Site-is-i-isa near Zia Pueblo, and one each from Casamero and Red Mesa. Sigleo (1970) measured lead, zinc, barium, cobalt, chromium, iron, magnesium, manganese, nickel, strontium, and vanadium. Although the results showed significant variation in the trace element composition of the samples from these mines, Sigleo (1970) was able to identify trends in the element concentration ratios; especially the element concentration ratios of barium, cobalt, magnesium, and strontium. However, she does not clarify which combination of element concentration ratios showed the significant trends. Sigleo (1970) attributed the variation of element concentrations within the turquoise sources to different events of turquoise mineralization and the possible effects of weathering or leaching. Because the chemical variation within the mines was so extensive, there was a considerable amount of overlap between the mines and, therefore, her data had limited interpretative value.

In 1975, Sigleo reported on the use of INAA to analyze turquoise; this analytical approach increased the number of elements measured from 11 to 30. She used antimony, cobalt, chromium, europium, scandium, and tantalum concentrations to match 13 turquoise beads from Snaketown, a large Hohokam site in Arizona, to the Himalaya turquoise mine near Halloran Springs, California. Other element concentrations, such as gold, barium, lanthanum, lutetium, and iron, exhibited too much variation within each turquoise mine to be useful (Sigleo 1975).

In the early 1980s, Hans Ruppert (1982, 1983) analyzed roughly fifteen hundred turquoise artifacts and geological samples from both North and South America by EMPA. He measured the element concentrations of aluminum, arsenic, barium, calcium, chlorine, chromium, cobalt, copper, iron, nickel, potassium, magnesium, manganese, phosphorus, scandium, sodium, silicon, sulfur, titanium, vanadium, and zinc. Although he used cluster analyses to process the data, he was unsuccessful at fingerprinting the provenance regions in the American Southwest.

A decade later, Frances Joan Mathien and Bart Olinger (1992) used XRF to measure the trace element composition of turquoise from several locations within the Cerrillos Hills Mining District and 24 other turquoise deposits including localities in Arizona, Colorado, Nevada, New Mexico, and northern Mexico. They measured arsenic, chromium, cobalt, iron, lead, manganese, molybdenum, nickel, niobium, rubidium, strontium, yttrium, zinc, and zirconium. Once again, unique chemical fingerprints could not be defined.

John R. Welch and Daniela Triadan (1991) attempted a new approach using XRD to focus more on the mineralogy of turquoise and any associated minerals. Their XRD patterns indicated the presence of turquoise and metatorbernite ($Cu(UO_2)_2(PO_4)_2 \cdot 8(H_2O)$), a rare uranium mineral, in both their turquoise mine and artifact samples. Because both samples contained this rare mineral, they were able to tie the artifacts recovered in the Grasshopper Ruin in Arizona to the Canyon Creek Mine. Although the authors noted that XRD was not the best method for turquoise provenance studies (XRD results show the mineral structure of a sample) they were able to conclude, in this particular case, that the artifacts were from that particular source.

Weigand et al. (1977) began working on characterizing turquoise provenance regions over 25 years ago and conducted one of the most comprehensive turquoise provenance studies. Weigand (1982) and Weigand and Harbottle (1993) surveyed and sampled over 41 turquoise deposits. The main strength of the Weigand (1982) study is the thorough investigation of the turquoise provenance regions. He documented evidence of prehistoric turquoise extraction from the chambered mines of Old Hachita of New

Mexico to the turquoise pits of northern Nevada and throughout most of the western United States and northern Mexico. The evidence was based on the presence of ancient mines, quarries, hammerstones, mauls, scrapers, and pottery sherds. The pottery sherds were examined and identified to associate any affiliation with cultural groups and to help suggest possible time periods. The turquoise samples are now located at the Museum of Northern Arizona. The collection is an important asset for sampling by current turquoise researchers and, as noted in Chapter 2, many of the turquoise provenance samples used in this research were obtained from this collection.

In the 1970s, Weigand et al. (1977) used INAA to measure the element concentrations in turquoise samples to investigate the relationships between Mesoamerican turquoise artifacts and turquoise provenance regions across the western United States and northern Mexico. Although they measured the elemental contents of antimony, arsenic, cesium, cobalt, copper, europium, iron, lanthanum, manganese, potassium, rubidium, scandium, sodium, thorium, and zinc, the results of the INAA analyses were inconclusive (Weigand et al. 1977). Additional samples from the Cerrillos Hills Mining District and turquoise artifacts from Chaco Canyon were sent to the Brookhaven National Laboratory (BNL) for analyses. The results showed that the turquoise artifacts had consistent copper values, but specific provenance regions lacked unique chemical signatures (Bishop 1979; Mathien 1981b). Despite these findings, Weigand and Harbottle (1993) continued their research with the analysis of additional mine samples and artifacts from more than one hundred archaeological sites. As part of their ongoing research, they analyzed over 2,000 samples resulting in the creation of a large composition database for turquoise. Measuring more than twenty elements in each sample, Weigand and Harbottle (1993) used many statistical techniques, such as multivariate manipulations and cluster analysis, to sort the results. Examination of the data suggested that the most important elements for sourcing turquoise were antimony, arsenic, barium, chromium, cobalt, copper, iron, lanthanum, manganese, potassium, scandium, sodium, and zinc (Weigand and Harbottle 1993). Despite their efforts, many of the turquoise provenance regions could not be uniquely fingerprinted and some artifacts did not plot within the trace element distribution pattern of a specific provenance region. Weigand and Harbottle (1993) suggested that these artifacts originated from an unidentified Rio Grande source that was possibly completely mined out by prehistoric miners. Although they were unsuccessful in identifying unique trace element signatures for each turquoise provenance region, their data were used to support trade models that encompassed most of Mexico and many of the turquoise mines in the western United States (Harbottle and Weigand 1992).

On a much smaller scale, Jangsuk Kim and colleagues (Kim et al. 2003) used PIXE to investigate turquoise artifacts recovered from two communities in the Salado Platform Mound area located in the Tonto Basin in central Arizona. PIXE was chosen because of its non-destructive capability. Their main objective was to document variation in chemistry between artifacts within a single site and between sites to examine differences in access to turquoise provenance areas. A large range in chemistry was assumed to represent multiple sources, whereas a homogenous chemistry for the group was assumed to represent few sources or even a single source. Kim et al. (2003) measured aluminum, calcium, copper, iron, manganese, phosphorus, silicon, sulfur, titanium, and zinc concentrations from 50 turquoise artifacts; 23 from Cline Terrace Mound and 27 from Schoolhouse Point Mound. They were able to show that there was greater trace element variation among the artifacts at Cline Terrace Mound compared to

Schoolhouse Point Mound. Therefore, they concluded that the inhabitants of Cline Terrace Mound had access to multiple sources of turquoise whereas the artifacts from Schoolhouse Point Mound likely originated from a single source. While Kim et al. (2003) were not focused on identifying the resource areas of the turquoise artifacts; their research showed that not all the blue-green artifacts were turquoise.

Inorganic elemental-based approaches have largely been unsuccessful for identifying turquoise provenance, primarily due to significant chemical variation within individual turquoise deposits. This variation has repeatedly masked the ability to identify specific provenance regions regardless of the analytical approach used to measure the chemistry of the turquoise (Harbottle and Weigand 1992; Mathien 1981b; Mathien and Olinger 1992; Ruppert 1982, 1983; Sigleo 1970, 1975; Weigand et al. 1977; Weigand and Harbottle 1993). At least four reasons exist as to why elemental analysis of turquoise cannot be used to source turquoise artifacts and/or identify their provenance regions.

3.2. Limitations of Trace Element Concentration Studies

The first two problems that plague turquoise provenance research using trace element analysis are: 1) many blue-green minerals are mistaken for turquoise, and 2) the complex mineralogy of turquoise affects the trace element composition within a single locale. The latter issue is further compounded when bulk analytical (e.g., INAA and XRF) approaches are used to analyze turquoise. Azurite ($Cu_3(OH)_2(CO_3)_2$), malachite ($Cu_2(OH)_2CO_3$), and chrysocolla ($(Cu, Al)_2H_2SiO_5(OH)_4 \cdot nH_2O$) are common blue-green minerals and have been used by Native Americans in the same context as turquoise and, in some instances, were misidentified as turquoise artifacts by modern researchers (Kim et al. 2003; Weigand et al. 1977). Weigand et al. (1977) coined the term *cultural turquoise* for any blue-green mineral versus *chemical turquoise*, which has the general formula $A_{0\text{-}1}B_6(PO_4)_4(OH)_8{\cdot}4H_2O$ with copper (Cu^{2+}) or ferrous iron (Fe^{2+}) as the most common substitutions for the A site and aluminum (Al^{3+}) and ferric iron (Fe^{3+}) for the B site. However, calcium (Ca^{2+}) or zinc (Zn^{2+}) can occupy the A site in some of the more rare members of the turquoise family. Therefore, trace element analysis of other blue-green minerals that may be mistaken for turquoise would result in large variation in trace element compositions and mask the provenance regions of the cultural turquoise artifacts.

The mineralogy of chemical turquoise is complicated, because it consists of at least six end members (see Chapter 2) (Foord and Taggart 1998). These end members that have different chemical compositions, but the same mineral structure. Kim et al. (2003) selected twelve artifacts for mineralogical analyses by XRD. They found that only three of the samples were actually chemical turquoise. One sample was identified as planerite, which is one of the turquoise group end members, and the other samples were identified as other blue-green minerals including azurite and malachite. One sample of particular interest contained several mixed phases including turquoise, chrysocolla, and ferrian turquoise. Mixed phases of turquoise and planerite have been observed at the Verde Blue source in Nevada (Fig. 3.2). In addition to the complex mineralogy of chemical turquoise, a study showed that turquoise samples can consist of numerous mineral inclusions at the micrometer scale (Hull et al. 2008) (Fig. 3.3).

Eugene E. Foord and Joseph E. Taggart (1998) suggested that differences in the copper and iron ratio are responsible for the differences in color of the samples. Normally, blue turquoise will have copper occupying the A site and aluminum occupying the B site, and green turquoise (chalcosiderite) largely contains ferric iron in the B site. The weight percent content of the elements occupying the A and B sites will vary in samples of different colors and shades, including samples collected within the same

Fig. 3.2. The mixed phases of turquoise and planerite at the Verde Blue turquoise deposit in Nevada.

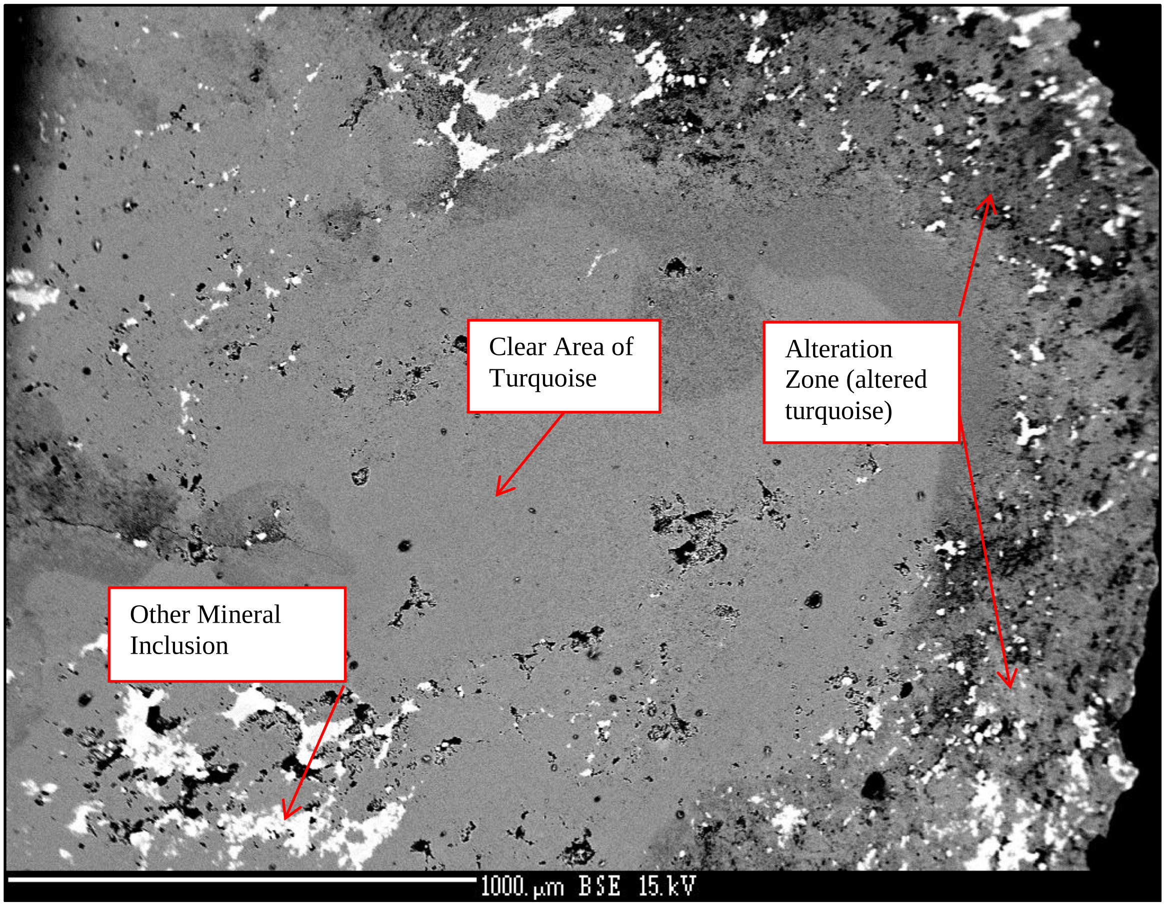

Fig. 3.3. Multiple mineral phases shown in this back scatter electron image of a turquoise artifact sample.

turquoise provenance area (Fig. 3.1). The other members of the turquoise group (faustite, aheylite, planerite, and the iron-rich end member), can contain many possible combinations including a member where the A site is mostly occupied by ferrous iron, with ferric iron occupying the B site (Foord and Taggart 1998). Trace and rare earth elements can occupy several different sites within the turquoise structure, including the A and B sites, which results in turquoise with a wide range in color and chemistry from a single deposit.

Two other issues related to turquoise sourcing using trace and rare earth element concentrations are: 1) the geology and formation processes of turquoise deposits are similar between provenance regions (Chapter 2), which produce similar trace and rare earth element patterns, and 2) the weathering of turquoise can cause variation in trace and rare earth element concentrations.

Trace and rare earth element composition patterns are largely controlled by the structure of the host mineral. For example, some minerals can accommodate higher concentrations of trace and rare earth elements or heavy versus light rare earth elements. Therefore, these elements or elemental patterns can be used to distinguish between mineral phases (e.g., garnet vs. apatite) or rocks that contain an abundance of one phase relative to other phases (e.g., garnet-rich metamorphic rocks vs. apatite-rich granitic rocks) (Grauch 1989; McLennan 1989). However, they cannot be used to distinguish between samples of single mineral phase from different localities. For example, apatite from a variety of igneous and metamorphic rocks generally will have similar rare earth patterns and concentrations (Puchelt and Emmermann 1976). The dominant source for trace and rare earth elements in turquoise deposits is the host rock because the rainwater that precipitates turquoise has very low trace and rare earth concentrations (Michard

1989; Michard et al. 1987). In the southwestern United States, turquoise deposits are generally hosted by very similar rock types (e.g., apatite-rich monzonites/granites), that have relatively similar trace and rare earth element concentrations (Longstaffe et al. 1982). Turquoise from different provenance regions should have indistinguishable trace and rare earth element composition patterns. Therefore, it is not surprising that trace and rare earth element studies have been largely unsuccessful at distinguishing between turquoise provenance regions.

The majority of turquoise deposits occur in similar geological environments across the western United States. The mid-Tertiary events that helped form the Basin and Range province and areas such as the Rio Grande Rift played an important part in setting the stage for the formation of this rare mineral. Highly altered and fractured copper porphyries that experienced erosion and exposure to long periods of supergene enrichment were an important dynamic in setting the discrete physical conditions for turquoise to form. Therefore, turquoise is stable in very specific geological environments and conditions and will weather or alter to other minerals when removed from these conditions (Abdu et al. 2011; Bergen et al. 2007; Hull 2006; Hull et al. 2005). Extended exposure of turquoise to surface conditions will eventually leach important elements (e.g., phosphorous) from turquoise and alter turquoise to clay minerals (Fig. 3.4). When turquoise fully alters to clay, the clay minerals are white. However, partially altered turquoise commonly observed in turquoise mines can be a faint blue or green color. The alteration of turquoise will cause extensive chemical and mineralogical changes (Abdu et al. 2011; Hull 2006; Hull et al. 2005) that cause variation in the trace and rare earth element concentrations of turquoise.

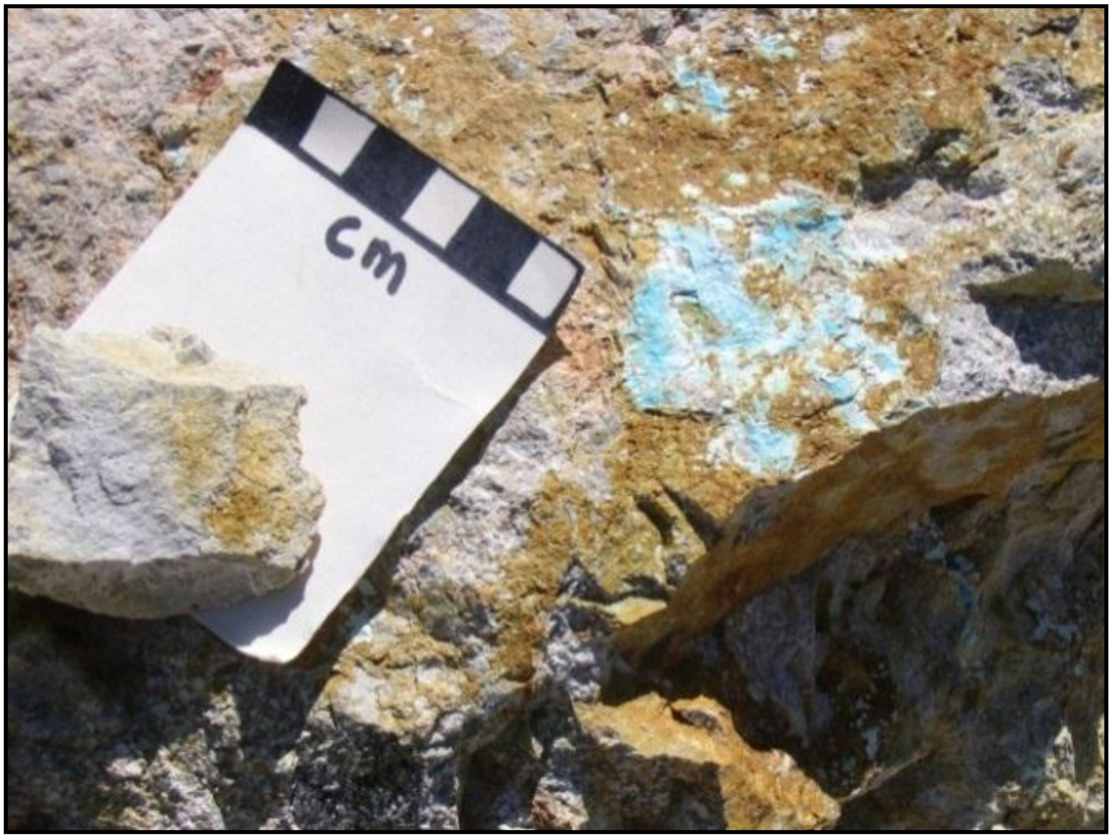

Fig. 3.4. Turquoise weathering to clay minerals at the Tiffany Mine, New Mexico.

The trace and rare earth element concentrations in turquoise are largely governed by the geology of turquoise deposits, the chemistry of the supergene fluids, and the weathering of turquoise. Therefore, it is clear why trace element analysis of turquoise has not satisfactorily differentiated between all of the turquoise provenance regions. As a result, several researchers are now working with isotope ratios to fingerprint turquoise and their provenance regions (Fayek et al. 2002; Hull et al. 2008; Thibodeau et al. 2007; Young et al. 1994).

3.3. Isotope Research in Archaeology

Some of the earliest applications of isotopes in archaeology were the non-stable or radiogenic isotopes of carbon used in ^{14}C dating of organic archaeological artifacts (Libby 1962). The isotopic values of oxygen (Dupras and Schwarcz 2001; White et al. 2004; White et al. 2000), strontium (Hodell et al. 2004; Price et al. 1994; Price et al. 2000; Schweissing and Grupe 2003), and the combination of both oxygen and strontium of human or faunal tooth and bone have been used to investigate patterns of ancient migration in many different parts of the world (e.g., Britton et al. 2009; Turner et al. 2009) and past environmental conditions (e.g., Emery and Thornton 2008). Lead was used to isotopically trace prehistoric Rio Grande glaze-paint production and trade (Habicht-Mauche et al. 2000) in the American Southwest. Suszanne M. M. Young and colleagues (Young et al. 1994) were the first to apply the use of lead isotope ratios to turquoise provenance studies when they attempted to distinguish between 26 samples of turquoise from seven mining districts in the southwestern United States and northern New Mexico. The ratios of lead isotopes were later paired with strontium isotope ratios to source turquoise (Thibodeau et al. 2007). Ben Stern and colleagues (Stern et al. 2008) applied the so called *traditional* stable isotopes such as hydrogen, carbon, and oxygen isotope ratios to detect the transport of resins in antiquity, and *non-traditional* stable isotopes such as copper have been used in conjunction with the more traditional isotope, hydrogen, to geochemically fingerprint turquoise provenance regions (Hull et al. 2008).

Isotopes are nuclear configurations of atoms with a specific number of neutrons. Isotopes of the same element differ in the atomic mass, the total of protons and neutrons in the nucleus, but never in the atomic number, the total number of protons which define the element. For example, the oxygen atom has eight protons, whereas the hydrogen atom has only one proton. Atoms can gain neutrons and mass; however, there is a limit to the number of neutrons that can fit into a nucleus of an atom. If there are too many neutrons in a nucleus, the atom begins to breakdown and emits radiation or particles until it reaches a steady or stable state, which could transform that atom into a completely different element if protons are lost during the break down of the atom. These types of isotopes are non-stable and are radiogenic isotopes (e.g., ^{14}C, ^{87}Rb, and ^{234}U).

Hydrogen has an atomic number of 1 (^{1}H), consisting of one proton and zero neutrons in its nucleus (Fig. 3.5). There are two other isotopes of hydrogen, deuterium (^{2}H or D) and tritium (^{3}H). Deuterium is a stable isotope, whereas tritium is an unstable isotope (radioactive). Hydrogen is the only element that has designated names for its isotopes. The isotopes of oxygen are designated by the atomic mass, the superscript preceding the element character, which is the number of protons plus neutrons found in its nucleus. Oxygen has three key stable isotopes, ^{16}O, ^{17}O, and ^{18}O. Sourcing techniques use the most abundant isotopes, ^{16}O and ^{18}O.

Because isotopes of a given element (e.g., oxygen or hydrogen) have different atomic masses, they behave or are affected differently by geological and biological processes, which will cause isotopes of different masses to separate or fractionate.

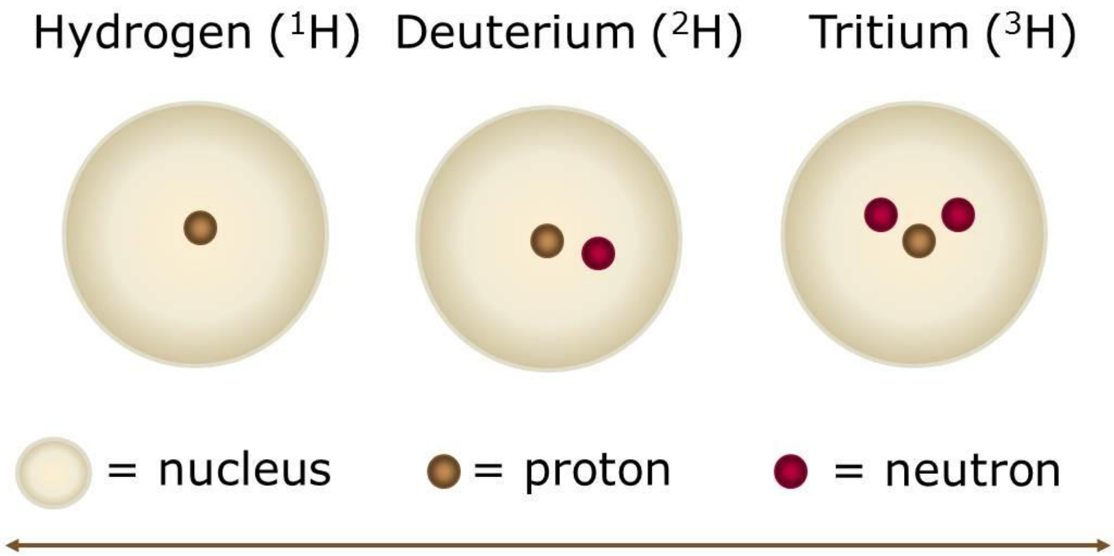

Fig. 3.5. The three isotopes of hydrogen showing that all three isotopes have one proton; however the number of neutrons is different defining the isotope.

Isotopic fractionation is the partitioning of isotopes of the same element between two or more phases (solid, liquid, gas), and it is produced through isotope exchange reactions and kinetic processes. These processes depend on differences in reaction rates between molecules containing the heavy isotopes and those containing the light isotopes of the same element (Hoefs 2004).

3.4. Analytical Methods for Measuring Stable Isotopes

There are several types of mass spectrometers that are used to measure stable isotope ratios; sample preparation (e.g., destructive analysis), precision required to distinguish between provenance regions, cost, and availability of equipment dictate the type of instrument and isotope system that can be used by researchers. Some of these techniques are destructive and require extensive sample processing prior to analysis. For example, Thermal Ionization Mass spectrometry (TIMS) (Faure 1986), has superior precision (0.001‰, parts per thousand), but requires samples to be completely digested and processed through a lengthy wet chemical process, requiring days to process a handful of samples (e.g., Maréchal et al. 1999; Maréchal and Albarède 2002). Other techniques, such as the Secondary Ion Mass Spectrometer (SIMS), are less destructive, have adequate precision (0.1 to 1‰), and can analyze solid samples at the micrometer-scale (Fayek 2009; Stern 2009).

There are two other mass spectrometers commonly used to measure isotopes; the gas source mass spectrometer and the Inductively Coupled Plasma Mass Spectrometer (ICP-MS). The gas source mass spectrometer is the principle instrument for measuring the light stable isotopes of hydrogen, oxygen, carbon, nitrogen, and sulfur. Although precision is good (0.05‰), this technique is destructive because samples need to be powdered and combusted (de Groot 2009). ICP-MS is mostly used to measure metals, alkali earths, alkaline earths, and rare earths (e.g., zinc, copper, iron, and chromium) that are then expressed as abundance data (e.g., ppm, wt%) (Speakman et al. 2007). However, some ICP mass spectrometers are equipped with multiple detectors (MC) that allow simultaneous measurement of multiple isotopes of the same element. Although the precision can be excellent (0.1‰), samples need to be powdered or dissolved into solution. Laser ablation ICP-MS (LA-ICP-MS) can be used to analyze solid samples (e.g., thin sections) or as pressed powders. However, external calibration standards are necessary and the precision is generally lower than traditional solution-based MC-ICP-MS (0.1 to 1‰) (e.g., Iñañez et al. 2010).

For turquoise provenance studies, SIMS (Fig. 3.6) has shown to be the least destructive technique. The microanalytical capabilities of SIMS allow analyses of solid samples and the ability to focus the primary ion beam on clear turquoise grains with a spatial resolution on the scale of a few micrometers (Fig. 3.7). Sample preparation is relatively simple and analysis times are short. Analyses times for hydrogen are less than 12 minutes (Liu et al. 2010). The sample preparation and SIMS analysis is relatively non-destructive to the sample - an important consideration when analyzing archaeological artifacts (Fig. 3.8). Once the artifacts are analyzed they can be returned to museum or other archaeological collections (Hull et al. 2008).

During the measurement of isotopic ratios by SIMS, a beam of primary ions (a few μm in diameter) is focused on the solid sample surface, thus obtaining a localized *in situ* analysis. *In situ* is defined as a single analysis on solid material at the micrometer-scale. Atoms, ions, and molecules are removed by the primary beam, a phenomenon referred to as *sputtering*. The ions are extracted, focused, and accelerated by a *secondary*

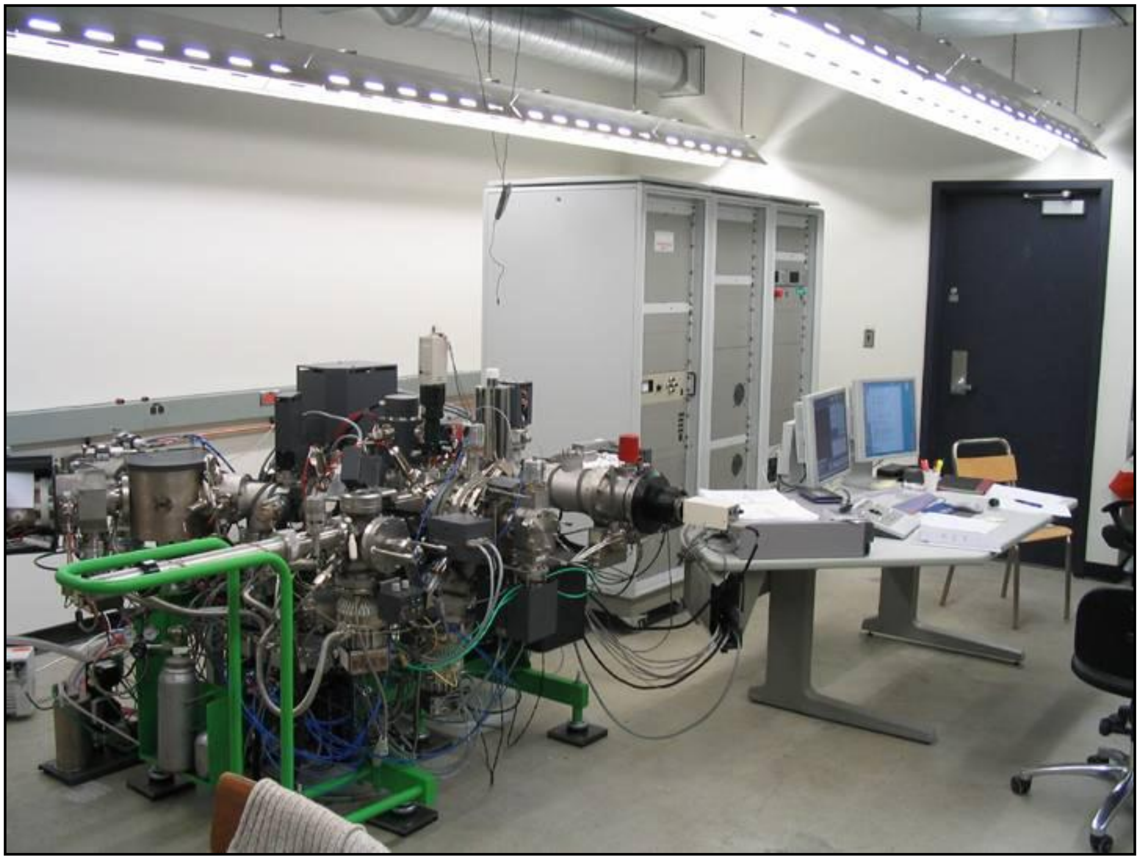

Fig. 3.6. The Secondary Ion Mass Spectrometer (SIMS) laboratory at the Department of Geological Sciences, University of Manitoba.

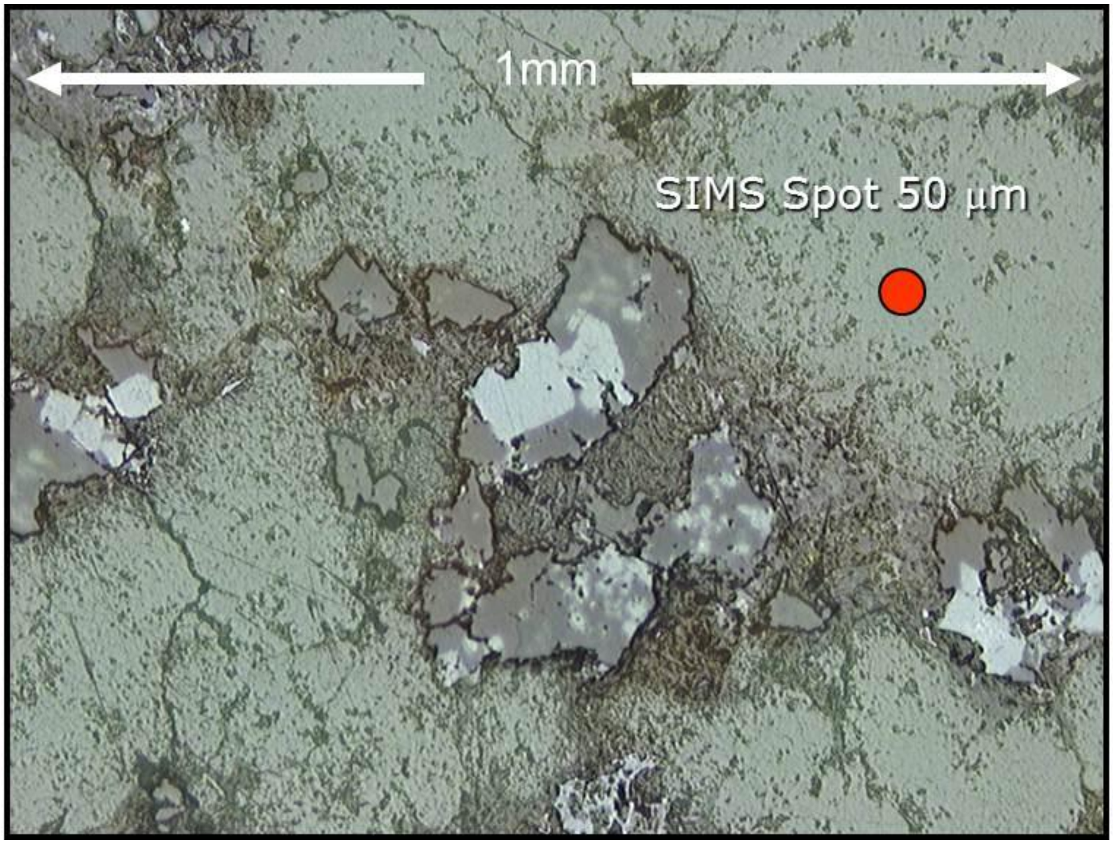

Fig. 3.7. The SIMS analysis spot on a back scatter image of a turquoise sample from the Castillian Mine, New Mexico.

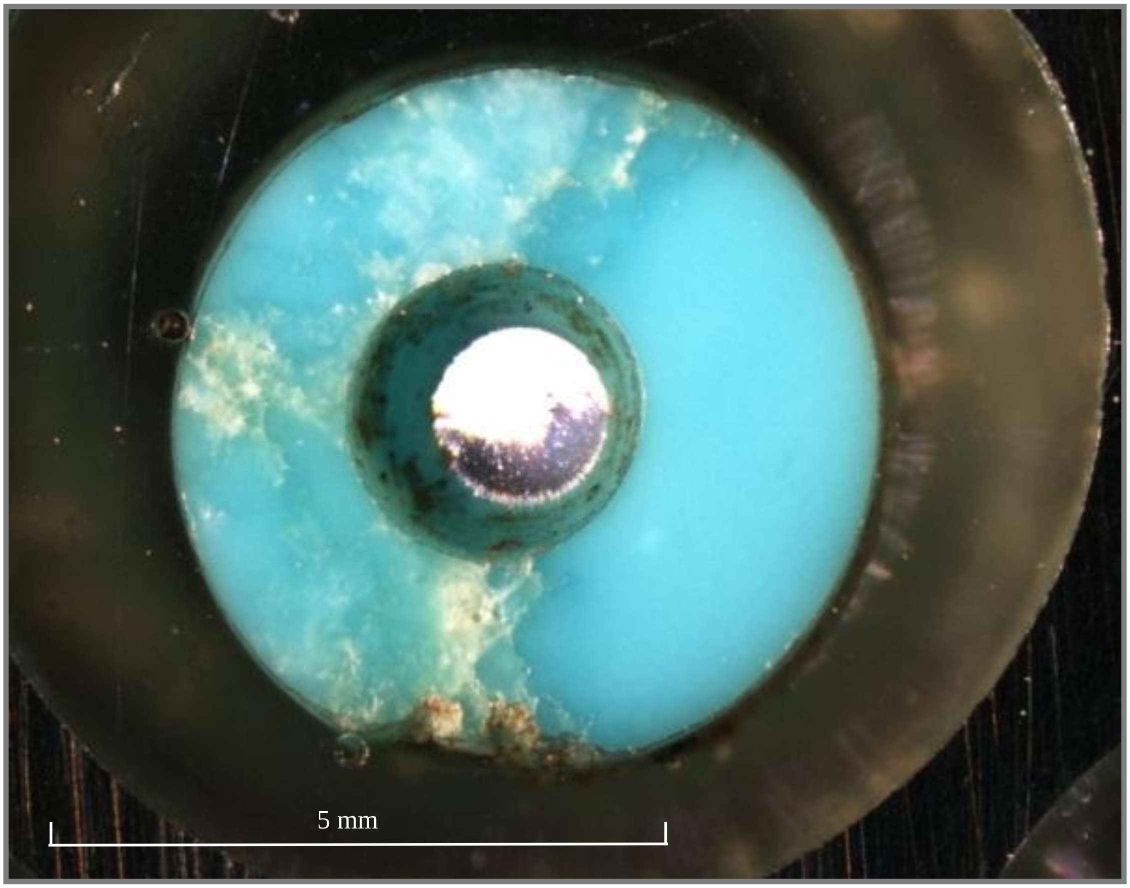

Fig. 3.8. A turquoise bead analyzed by SIMS. Alteration occurs along the fractures and mineral inclusions appear as yellow patches along the bottom and left portion of the bead. The clear blue area on the right was analyzed by SIMS and is devoid of any alteration or inclusions.

ion beam through a slit and into a mass spectrometer. During the SIMS analysis, an intrinsic mass dependent bias is introduced (similar to LA-ICP-MS), which is referred to as *instrumental mass fractionation* (IMF) and typically favors the low mass isotope. The greatest contributor to the IMF is the ionization process dependent upon sample characteristics such as chemical composition. This is referred to as *compositionally dependent fractionation* or *matrix effects* (Riciputi et al. 1998). Therefore, accurate isotopic SIMS analysis requires that IMF be corrected by standardizing the IMF using mineral standards that are compositionally similar to the unknown samples. SIMS results from the standard are compared to its accepted isotopic composition in order to compute a correction factor that is applied to the unknown samples measured during the same analysis session (Riciputi et al. 1998).

Hydrogen and copper isotope ratios have been successfully obtained by SIMS. Before accurate data can be generated by SIMS, the development of standards that are isotopically and chemically homogenous is important (Hull et al. 2008). The instrument used to measure isotope ratios is an important consideration in provenance studies. MC-ICP-MS and SIMS are the instruments used in the most current isotope studies of turquoise provenance.

3.5. Lead and Strontium Isotope Analyses

One of the first attempts using isotopic ratios to identify turquoise provenance regions was by Young et al. (1994). They measured lead isotope ratios by ICP-MS on several turquoise deposits within the Cerrillos Hills Mining District and other turquoise provenance regions including the Manassa and Leadville mines in Colorado, Bisbee in Arizona, Hachita in New Mexico, the Blue Gem and Lone Mountain in Nevada, and the Chrysacolla Cusi in northern Mexico. There are four stable isotope of lead (^{204}Pb, ^{206}Pb,

^{207}Pb, and ^{208}Pb); however, Young et al. (1994) reported that the isotopic ratios of ^{208}Pb/^{207}Pb displayed the best variation between the mines. Unfortunately, as more turquoise localities were analyzed, the distribution patterns of the turquoise provenance regions began to overlap. Although lead isotope ratios showed only limited success, Young et al. (1994) suggested that lead isotope ratios may prove more successful when paired with a second discriminator.

Alyson M. Thibodeau and colleagues (Thibodeau et al. 2007) paired lead isotope ratios with those of strontium (^{87}Sr/^{86}Sr) measured by MC-ICP-MS. They analyzed 17 turquoise samples from five different localities, including Cerrillos Hills, Old Hachita, and the Tyrone mines in New Mexico and the Sleeping Beauty and Gleeson mines in Arizona. Their pilot study shows meaningful separation of the five provenance regions. Thibodeau et al. (2009) reported that they are continuing their research by obtaining lead and strontium isotope ratios of more turquoise provenance regions and turquoise artifacts from archaeological sites in the Tucson Basin and along the Rio Grande Valley.

3.6. Hydrogen, Oxygen, and Copper Isotopes

Fingerprinting the origin of minerals using the isotopic ratios of hydrogen (^{1}H, ^{2}H) and oxygen (^{16}O, ^{18}O) is an established technique in geochemistry (Sheppard 1986). Isotope fractionation of hydrogen and oxygen in meteoric water is affected by latitude (distance from the equator), longitude (distance inland from the ocean), and altitude, where the heavier deuterium (^{2}H) is depleted as rain clouds move towards the poles, further inland, and higher in altitude (Albarède 2003). For example, ocean water contains both deuterium and hydrogen. As the evaporation process begins, the water vapor will contain more hydrogen than deuterium relative to sea water. The heavier isotopes do not partition into the vapor phase as readily as the lighter isotopes. In this respect, the heavier isotopes will partition into the liquid phase (rainwater) causing variation of isotope ratios in different geographical locations (Hoefs 2004). Therefore, rainwater will have less of the heavier isotopes as the clouds move from the equator to the poles and as they move from the ocean inward into the continent. Consequently, the hydrogen and oxygen isotopic composition of meteoric water varies as a function of geography.

As mentioned before, turquoise is a supergene mineral that forms from meteoric water. The meteoric water is bound in the turquoise mineral structure (Gustafson 1965). Therefore, the hydrogen and oxygen isotopic composition of minerals, such as turquoise, which precipitate from rainwater, will also reflect these temporal and geographic variations in their hydrogen isotopic composition (Craig 1961; Dansgaard 1964; Epstein and Mayeda 1953; Friedman 1953; Friedman et al. 1964; Sheppard 1986; Yurtsever and Gat 1981). The hydrogen isotopic composition of turquoise can be particularly diagnostic because once turquoise forms, it retains water at the molecular level, making it very difficult to alter the hydrogen isotopic composition of turquoise (Anderson et al. 1962; Manley 1950).

A survey of published data on the hydrogen isotopic composition of meteoric fluids (rainwater) from the turquoise source localities show that they are distinct and have remained constant over the past 100 million years (Sheppard 1986; Taylor 1979). Theoretically, turquoise from each of these localities can have a distinct hydrogen isotopic composition. A preliminary study using gas source mass spectrometry showed variation in the hydrogen and oxygen isotopic compositions of several turquoise deposits located in Arizona, Colorado, New Mexico, and Nevada (Fayek et al. 2002).

Transition metal stable isotopes (e.g., iron, copper, zinc, and chromium) offer a second potential avenue for isotopic fingerprinting of turquoise. Natural variations in transition metal stable isotopes are now known to occur in a wide variety of minerals and these variations may be produced by either abiotic or biotic processes (Bullen et al. 2001). As with hydrogen isotopes, abiotic fractionation is produced through isotope exchange reactions and kinetic processes. Biotic (or microbial) fractionation is produced because microbes, which may use transition metals from minerals as part of their metabolic processes, selectively use lighter isotopes because this maximizes the free energy obtained from the reaction (Bullen et al. 2001).

Copper has two stable isotopes: ^{63}Cu and ^{65}Cu. Although copper isotope geochemistry is still in its formative stage, a relatively abundant data set exists for the isotopic compositions of copper minerals which show that natural variations in $\delta^{65}Cu$ values vary by 34‰ (Klein et al. 2010; Larson et al. 2003; Mason et al. 1997; Mathur et al. 2009a,b; Palacios et al. 2011). Therefore, variations in the copper isotope ratios of turquoise samples are large enough that when used in conjunction with hydrogen, are a successful discriminator. Fractionation of hydrogen and copper isotopes are driven by different geological processes, thus potentially displaying more variation between turquoise source regions than using the isotopic compositions of hydrogen and oxygen, which are governed by similar geological processes.

3.7. Using Hydrogen and Copper Isotopes to Source Turquoise

Geochemical provenance studies are becoming more common in archaeology. It is essential to have accurate knowledge of the mineral of interest and the provenance regions. For example, it is important to know the geologic context of the mineral (e.g., magma or supergene) and understand the mineralogy and the processes that may alter the mineral. The depositional environment and post depositional modification of the mineral of interest can influence the choice of geochemical method. Protocols also need to be established (e.g., petrography) that can be used to exclude altered or impure samples. The use of the *in situ* stable isotopic analysis of hydrogen and copper by SIMS has been successful in defining turquoise provenance regions (Hull et al. 2008). The advantages of this technique are: 1) isotope ratios of turquoise are geographically distinct thus overcome the limitations of trace element analyses; 2) *in situ* micro analysis avoids inclusions of other minerals, which could profoundly affect the trace element and isotopic composition of turquoise; 3) except for minor polishing of the surface of artifacts and 50 micrometer pits that are created during analysis, turquoise artifacts are relatively undamaged; and 4) the technique is relatively inexpensive and capable of rapid analyses.

The major disadvantage of this technique is that the provenance regions of altered turquoise artifacts cannot be identified because alteration of turquoise variably affects the hydrogen and copper isotopic composition. Although the technique that uses lead and strontium isotopic ratios measured by MC-ICP-MS may be destructive, preliminary results show that this technique is not affected by turquoise alteration (Thibodeau et al. 2007) and the process of isolating the specific elements in turquoise would avoid any instrumental matrix effect. Therefore, the lead and strontium isotope method may be appropriate for provenance studies of altered turquoise artifacts. An additional discriminator, such as oxygen, or another combination of the discriminators may prove successful in overcoming any limitations of current turquoise provenance research (e.g., alteration or destructive sample preparation).

The use of element concentration patterns to identify the resource areas of turquoise artifacts was not successful due to significant variation within deposits. Any provenance fingerprinting technique, regardless of instruments or discriminators used requires less geochemical variation within discrete compositional groups than between compositional groups. There were four main factors affecting the results of previous turquoise provenance studies: 1) other blue-green misidentified as turquoise; 2) the complicated mineralogy of turquoise, 3) similar geology and formation of turquoise provenance regions, and 4) the weathering of exposed turquoise. As trace element concentration studies were problematic for turquoise provenance studies, archaeologists turned to the use of isotope ratios to fingerprint turquoise resource areas. Hydrogen and copper isotope ratios have proven to be successful discriminators for fingerprinting turquoise resource areas because the isotope ratios are dictated by the geology and geography of the turquoise deposits, overcoming the many limitations of trace element concentration studies.

There are two essential points to consider in regards to provenance studies of any archaeological material: 1) the research will always be a work-in-progress, and 2) the data obtained from unknown samples will only be as good as the reference database of resource areas used for comparison. As more data are obtained it is critical that the comparison database is maintained and made available for archaeologists to examine turquoise procurement and exchange on many scales throughout time and space.

Chapter 4: Culture History and Exchange Models of the Greater Southwest

"*Trade studies … may be understood in the plural, illustrating that the macro-scale models so thoroughly developed in the 1970s and 1980s and newer concepts such as agency are not so much contradictory as complementary*." (Bauer and Agbe-Davies 2010:41)

Geochemical turquoise provenance techniques, especially those that use isotope ratios, are an excellent tool to identify the provenance region *where* a natural resource was originally obtained. The provenance data are important for the reconstruction of ancient trade routes and supporting existing trade/exchange models or the development of new models. Also following the supposition put forth by Greg Urban (2010:208) that trade routes were avenues of migration and diffusion of culture, the data can be used to support existing culture history models. However, these data must be used in conjunction with other archaeological evidence and the context of the sites under consideration to understand *how* turquoise was moved to the archaeological site (e.g., exchange, trade, or direct acquisition) and what was the meaning to the end user of the natural resource under study. Although this research is focused on establishing a turquoise comparative database and identifying the origin of turquoise artifacts, it is important to consider not just the movement of the mineral turquoise, but also the social dimensions of the trade or exchange (Agbe-Davis and Bauer 2010:13); it was humans that mined, transported, and utilized this precious blue-green stone. Anna S. Agbe-Davis and Alexander A. Bauer (2010:15) defined the terms *trade* and *exchange* suggesting that they are not necessarily interchangeable. A trade is a business-like transaction and would occur at a market or more formal setting, whereas the transfer of goods is an exchange that can occur as a gift, negotiation, coercion, or dowry.

In this chapter, a brief background of the culture history of the Greater Southwest is presented, along with existing trade/exchange models of the Greater Southwest and how they were influenced by archaeological theory. Although the focus of this research is to investigate the trade and exchange networks and patterns of turquoise procurement of Aztec Ruin, Salmon Ruin, and several sites within Chaco Canyon, most exchange and procurement models of the Greater Southwest incorporate regions far beyond the scope of this study. Many of these models include the development, growth, and abandonment of the Greater Southwest and the impact that Mesoamerica may have had on this region through diffusion of ideas, direct migration, or the exploitation of natural resources along its northern frontier; especially turquoise.

4.1. Culture History of the Greater Southwest

There are three main culture areas defined for the puebloan settlements across the American Southwest and northern Mexico; the Ancestral Puebloan, Hohokam, and Mogollon. Evidence suggest that they shifted from hunting and gathering lifeway patterns to more sedentary and horticulture subsistence strategies around A.D. 200/500 to A.D. 750/800. As they became more sedentary, they left larger areas of accumulated artifacts and structures across the landscape that showed more distinctive patterns such as ceramic styles, architecture styles, and the design and layout of their communities. For example, the Ancestral Pueblo people built great kivas in contrast to Hohokam ball courts. Pithouses and ceramics were commonly found throughout the Colorado Plateau (Cordell and Gumerman 1989:6-10) and other areas of the Greater Southwest. Typical early Ancestral Puebloan sites included less than a dozen pithouse structures (Cordell 1997:190) along with slab-line cysts that were most likely used for storage of surplus resources. At the same time, the inhabitants of the Hohokam region occupied small hamlets across the landscape (Cordell 1997) and used water control features, such as canals, to complement their agriculture practices. Large quantities of shell artifacts suggested that the Hohokam participated in a large trade network (Fish 1989:28-29) that probably extended to the Gulf of California and the Pacific Coast.

Population densities increased and communities expanded across the landscape around A.D. 700/800 to A.D. 1000/1050 depending on each culture area. Each culture group became more distinct as their material culture (e.g., ceramics) displayed more individual attributes. As the inhabitants of the Mogollon culture area continued to build subsurface pithouses, the Hohokam and Ancestral Puebloans began building residential and storage rooms on the surface. In Chaco Canyon, the Ancestral Puebloan shifted from building jacal and adobe style structures to masonry structures, which were constructed from sandstone slabs (Cordell 1997). The inhabitants of the Hohokam culture area became more distinctive from their Ancestral Puebloan neighbors as they built ball courts and platform mounds (Cordell and Gumerman 1989:6-10). As the size of large communities in the Hohokam area increased, there was also an increase in trade and craft specialization (Fish 1989:29).

Around A.D 1000/1050 to A.D 1130/1150, the social complexity of the Hohokam and Ancestral Puebloan culture areas increased. There was also an increase in the exchange of ceramics, and the procurement and distribution of more exotic items such as shell and turquoise (Cordell and Gumerman 1989:6-10). The Ancestral Puebloans built extensively in Chaco Canyon with a marked increase in its population. The Hohokam culture area reached its maximum expansion and the center of Snaketown reached its greatest size. Between A.D. 950 and A.D. 1150, the Mogollon experienced an increase in population and expanded across the landscape reflecting the beginning of a strong relationship with the Ancestral Puebloan by building above ground structures and adopting similar ceramic styles (Cordell 1997:207-208).

Between A.D 1130/1150 and A.D 1275/1300 there was a shift in cultural and political centers along with the abandonment of some areas. Based on tree-rings, this time period coincides with drought conditions. In Chaco Canyon, construction ceased and it was once thought that the canyon was abandoned. Recently, it has been suggested that the centers of power and authority may have moved to the north and Chaco Canyon was not necessarily abandoned but experienced a period of reorganization (see Lekson and Cameron 1995; Lekson et al. 2006). The Hohokam cultural area showed a period of change as ball courts were no longer built and the use of platform mounds shifted to a more residential and common ritual use (Fish 1989:31). Both the Ancestral Puebloan and the Hohokam experienced changes in their styles of architecture and the use of space. In the Hohokam region, old trade networks appeared to have been disrupted as new trade networks were established (Cordell and Gumerman 1989:11-12). For example, there was an increase in shell objects and trade items became more widespread (Fish 1989:33). Sometime between A.D. 1150 and A.D. 1350 in the Mogollon area, populations shifted to the south and Paquimé became a large regional center.

The period, A.D 1275/1300 to A.D 1540, is often associated with the *Great Drought* where tree-ring evidence suggested a time of low moisture and low water tables and many large areas were completely abandoned. The San Juan Basin and the Mesa Verde region were no longer inhabited as the great cities were left to decay. As the older established communities were abandoned, populations shifted to much larger settlements with hundreds of rooms; such as those in the northern Rio Grande River drainage, Hopi Mesa, Cibola, and Tsigi Canyon. By the time Europeans made contact, only a few of these communities were occupied (Cordell and Gumerman 1989:12-13). After A.D. 1450, the patterns that archaeologists used to define the Ancestral Puebloan, Hohokam, and Mogollon cultural entities did not persists in the Greater Southwest.

4.2. The Greater Southwest and Mesoamerican Connection

One of the most contested debates in Southwestern archaeology surrounds pre-contact trade and the extent of diffusional influence or even migration of Mesoamericans into the Greater Southwest culture area. The current literature is rather polarized on this issue. On one end of the spectrum are the researchers whose paradigm was based on a very large regional scale and argued that the Greater Southwestern cultures were directly influenced by the more highly complex societies in Mesoamerica (e.g., Di Peso 1968, 1974; Kelley and Kelley 1975; Lister 1978; Rafferty 1990; Washburn 1980; Weigand et al. 1977; Weigand and Harbottle 1993; Weigand 1994). With a far more focused regional perspective, other researchers argued that the development of complexity in American Southwestern cultures was independent of outside influences and there was little if any contact with Mesoamerica (e.g., Cordell and Plog 1979; Judge 1989; Mathien and McGuire 1986; Martin and Plog 1973; Vivian 1970; Whalen and Minnis 2001).

Early archaeologists reported on the similarities of the communities of the Greater Southwest and Mesoamerican cultures. While there were unique aspects of the northern communities, diffusion or even possible migration from the Valley of Mexico was a common theme (Riley 1978:4). Although there were distinct opinions on pre-Columbian contact, there was a general consensus that a shift in archaeological theory was largely responsible for the rift (see Kelley and Kelley 1975; Mathien and McGuire 1986:2). Culture history concepts, such as *diffusion* and *migration* that were considered archaic by some researchers, were soon rejected and replaced by *New Archaeology* that was more focused on human ecology. Cultural systems and their interaction and adaptation strategies with the environment became the new focal point. Changes in the local ecology or environmental stress were the basis of explanatory models for cultural change.

Establishment of communities, population growth, and eventual abandonments in the Greater Southwest were dependent on the local environment and independent of any connection to diffusion or migration from the complex societies in Mesoamerica. In the processual paradigm, pre-contact trade was often investigated on a much smaller regional scale such as between local communities (e.g., Chaco Canyon and Aztec Ruin) or between the Ancestral Puebloan, Hohokam, or Mogollon.

The early development of culture history in the 1930s and 1940s was greatly influenced by the early excavations of Nels C. Nelson (1916), Alfred V. Kidder (1916, 1917; Kidder and Kidder 1917), and Alfred L. Kroeber (1919). The culture history approach dominated archaeological theory in the 1930s and 1940s and was central in the development of local typological classifications. The main goal of the culture historians was to develop a formal set of procedures to *document* and interpret the development of ancient cultures. Using stratigraphy and artifact classification, the focus was defining cultural areas and their chronology; grouping by similar attributes. With the development of dendrochronology and ^{14}C dating, many of the cultural sequences were associated with actual time periods.

Nelson (1916) recognized the chronological relationship between stratigraphy and ceramic and began to apply relative chronological dates to his excavations at San Cristóbal in northern New Mexico. He also began looking at frequency curves of the ceramic assemblages through time. Building upon the concept of chronologies by ceramic types, Alfred L. Kroeber (1919) used surface collections at the Zuni Pueblo in New Mexico to establish cultural sequences. Alfred V. Kidder (1916, 1917; Kidder and Kidder 1917) incorporated Nelson's work into his excavations at Pecos Pueblo, New Mexico where he was able to identify ceramic types from historical levels at the top to the earliest ceramic types in the lower levels of the excavation. His excavations at Pecos Pueblo were performed by using stratigraphic levels versus arbitrary levels recognizing the importance of preserving cultural units and he expanded on Nelson's frequency curves by defining the popularity principle of the rise, vogue, and decline in style types of ceramic assemblages. Kidder was instrumental in the foundations of the Pecos Conference and the Pecos Classification typologies.

In the 1960s, there was a shift in archaeological theory when Lewis R. Binford (1962, 1964, 1965, 1968, 1989), a prominent figure in the *new archaeology* or processual archaeological theory movement, argued that there should be a strong focus on a scientific approach attempting to identify generalized patterns for human behavior. These patterns for human behavior are viewed as an extension of the natural sciences and these patterns could be determined by the surrounding environmental conditions. The documentation and interpretation of the development and change of ancient cultures turned to explanatory goals such as *why* cultures developed or changed, shifting the focus of *documentation* to *explanation*. This change in interpretive perspective attempted to go beyond historical typologies in order to interpret actual meaning as it is represented in patterned variability within the archaeological record. During this time, there was a strong focus on human ecology and paleoenvironmental studies in the American Southwest interpreting cultural changes as adaptation to environmental stress or changes in the physical surroundings (e.g., Dean 1988; Gumerman 1988; Plog et al. 1988).

The processual paradigm dominated the archeological community for many decades, however some researchers argued that there was a fatal flaw in processual theory and social cultural concepts needed to be incorporated in interpretive models (e.g., Hodder 1995, 1999, 2000; Hodder and Hutson 2003; Shanks 1995; Shanks and Hodder

1995; Trigger 2006). Human behavior is unpredictable and generalized models cannot determine the course of human action. Humans could make reasonable and knowledgeable decisions and take action as their behavior is not a set of predetermined patterns.

During the 1960s and 1970s, the most popular explanation for cultural change in the Greater Southwest was human adaptation to environmental fluctuations (Fish 1989:43). Influenced by cultural ecology, cultural change of the Ancestral Puebloan, Hohokam, and Mogollon was perceived as predominantly stimulated by ecological factors. Suggesting that fluctuation in climate and the limitations of the local environment were fundamental mechanisms in understanding cultural changes, Linda S. Cordell and George J. Gumerman (1989) proposed that the shift from a hunting and gathering way of life to a more sedentary and horticulture subsistence strategy resulted from an episode of decreased precipitation and lower water tables. Shifting their subsistence strategies, the local populations became more dependent on agriculture and food storage. With unpredictable rainfall and intervals of depleted moisture, many of the culture areas in the Greater Southwest expanded their agriculture and food storage strategies. Communities spread across the landscape and each culture area became more distinct. Social complexity increased and there was an increase in procurement and distribution of more long-distant commodities, such as shell and turquoise (Cordell and Gumerman 1989:10). Experiencing relatively good environment conditions, many of the communities flourished and there was expansion of building in Chaco Canyon.

As environmental conditions worsened, the cultural areas appeared to experience a period of reorganization. Local populations attempted to adapt by changing their strategies and reforming their communities. There was a final period of aggregation that coincided with a period of complete environmental deterioration (Cordell and Gumerman 1989:6-13). Some areas were completely abandoned while large aggregated communities appeared in other areas. There was evidence of fluctuations in the climate and environmental conditions, although there was not enough variation to explain the changes in the material culture and social organization. This was especially apparent in southwestern Colorado where there was evidence of cultural change, but the environmental record did not reflect the same fluctuations as seen in other areas across the American Southwest (Rohn 1989:152-153). The concept of direct influence from Mesoamerica disrupted many of the suggested sequences of internal cultural developments and the perception that the expansion of the important communities in the Greater Southwest was a result of long-distance Mesoamerican traders building northern frontier towns was not well received. Especially in the case of Chaco Canyon, where researchers were accused of ignoring Mesoamerican similarities and suggested that obvious imported items (e.g., macaws) were unimportant and negligible (Kelley and Kelley 1975:479-180).

Based more in culture history (e.g., diffusion and migration), the perception of direct Mesoamerican influence was of a much larger macroregional scale that included the landscape encompassing Mesoamerica, the Greater Southwest, and the vast area between the two culture areas in northern Mexico. Many of the arguments supporting a Mesoamerican connection are based on similarities that existed between Mesoamerica and the cultures in the Greater Southwest. Some of the most compelling evidence were the exotic trade items found in archaeological sites in the Greater Southwest that were obviously from a Mesoamerican origin (e.g., macaws) and the amount of turquoise recovered from Mesoamerican archaeological sites that was presumably from turquoise deposits located in the western United States. In principle, the further a commodity was moved from its geological provenance, the more it was considered an *exotic* or *luxury* item. Many of the exotic items were recovered in core regional centers (e.g., Chaco Canyon, Paquimé, Teotihuacán, Tula, and Tenochtitlan). Although these core centers would change through time, there was a continual commonality for the quest of exotic items, such as turquoise, that was a chief component in the validation of prestige and status within their social organization (Weigand 1994). Over one million pieces of turquoise were recovered in American Southwestern and Mesoamerican archaeological sites (Harbottle and Weigand 1992; Weigand et al. 1977). Considering the amount of turquoise recovered, the hardships of ancient mining, and the distance between the turquoise deposits and home communities, turquoise must have been a significant status symbol and an important commodity of pre-Columbian trade structures.

Although there is much debate over diffusion and trade contact between the Greater Southwest and Mesoamerica, most researchers acknowledge that the concept of agriculture and many of the cultigens originated in Mesoamerica (Riley 1978:5). Many agree that ceramics, or at least the concept of making pottery, was also a relic originating from Mesoamerica.

4.3. Exchange Models for the Greater Southwest

There are many explanatory models for the movement of goods between these two cultural areas and these models differ greatly in their interpretations. The prospective that includes direct influence from Mesoamerica proposed that long-distance trade items, along with other similarities between the Valley of Mexico and the Greater Southwest (e.g., architecture), were evidence of a well-organized trade structure that was a strong determinant in the establishment, growth, and the eventual abandonment of the larger settlements of the Greater Southwest (e.g., Di Peso 1968, 1974; Kelley and Kelley 1975; Weigand et al. 1977; Weigand and Harbottle 1993; Weigand 1994). The perspective that rejects direct involvement from the Valley of Mexico argued that the number of long-distance trade items that passed between Mesoamerica and the Greater Southwest were far too few to be significant and may have been moved through a very fluid type of down-the-line trade network (e.g., Mathien 1999), and any other similarities were insufficient to support direct influence from Mesoamerica. Although most of the models focused on the relationship between the Greater Southwest and Mesoamerica (e.g., world systems model - Wallerstein 1974), other models incorporated the Greater Southwest with other areas of the western United States (e.g., trade festival model - Janetski 2002). In this section I describe the key exchange models for the Greater Southwest.

4.3.1. World Systems Model

The world systems model (Wallerstein 1974) was originally developed as an explanatory model for the emergence and expanse of modern capitalism in Europe. Integrating historical theory and the modern capitalistic system, the world systems model included sociopolitical interaction on an economic basis laying the foundation for a model that included long-distance trade systems. Immanuel Wallerstein's (1974:348) model included concepts of *mini-systems* and *world systems*. Mini-systems were a more local and short lived exchange network relative to the much larger world system. The world systems model contained components of a core, semi-periphery, and periphery. The core was the center of technology with advantages that included diversified production, high profits, and high wages compared to the less advantaged peripheries. Surrounding the core region were peripheral regions, such as the neighboring agricultural areas or subsystems of the core region. The wages and profits of the semi-peripheries advantages were more equal with the core and served as a buffer for the unbalanced relationship between the core and the exploited peripheries. The external areas, which were located beyond the peripheries, were seldom interacted with or included in the world system (Wallerstein 1974:347-348).

There were two important considerations in regards to the application of Wallerstein's (1974) world systems model to the economic relationship between the Greater Southwest and Mesoamerica: 1) this model downplayed the importance of luxury items in the economic and political positioning in society, and 2) the problem of the vast distance without the aid of domesticated pack animals for transport. The world systems model was developed for modeling exchange and networks that were involved in the movement of necessary items and not for luxury commodities (Wilcox 1986:32), such as turquoise. There are several thousand kilometers between the Valley of Mexico and the communities of the Ancestral Puebloan, Hohokam, and Mogollon. However, some of the exotic commodities (e.g., turquoise and macaws) may have been such an intricate part of the ritual and ceremony or important status markers in some of the communities that consumers may have been willing to pay a hefty price for these items. Non-perishable luxury items may have been transported over long distances and would have been worth the travel and hardships as many merchants may have become rich or gained higher status in their homeland communities through these journeys.

Another important critique for the world systems model was the assumption that the peripheries were the suppliers and the resources were only transported in one direction; to the dominant core that had control over the periphery diminishing the role of the periphery (Stein 2002:904). It is important to consider how much control, dominance, or influence core regional centers had over the periphery. The further the distance from the core center, the more difficult it would have been to have maintained any type of control over the resource areas. This is a significant dynamic considering the distances that trade items were transported over rough terrain.

The world systems model perceived the Greater Southwest as a northern periphery of Mesoamerica. Although there was a lot of criticism of this model, it was instrumental in changing perceptions from *diffusion* and *adaptation* to *interaction* and *dependency,* and recognizing the core and periphery as interactive social relationships and not just designations on a map (McGuire et al. 1994:241). It also laid the foundation for the concept of an economic system that could be independent of any political systems or empire that it serviced; an economic system that included merchants and trade routes that were structured but could become more fluid as core regions shifted.

The *core-periphery* concept (Palerm and Wolf 1957) was used to model long-distance exchange of luxury items on a smallar regional scale. An explanatory model using the concepts of regional core and periphery areas was applied to changing structures within Mesoamerica (Palerm and Wolf 1957) several decades before the application of the world systems model (Wallerstein 1974). Angel Palerm and Eric Wolf (1957) proposed the concept of core regions described as centers of innovative change and economic networks. The core contained the cultural centers, redistribution hub, and the political and religious authorities. The development and subsistence of the peripheral regions had a symbiotic relationship with the core region with a constant exchange of items and ideas. The peripheral regions that had the maximum access and communication with the core regions and contained the greatest areas of ecological diversity experienced the more privileged symbiotic relationships with the core region

(Palerm and Wolf 1957:31-32). Peripheral regions were incorporated into the economic networks of the core region by a mutual agreement, military force, or possibly by direct colonization.

4.3.2. Pochteca-like Trade Models

There were variations of the world systems model and how these models were applied to the Greater Southwest. Building on the concept of an exploited northern frontier, Charles C. Di Peso (1974) argued that the sudden growth of Paquimé as a central trade center was tied to long-distance traders from Tula, a large Toltec center in the Valley of Mexico. Overseeing the extensive excavations at Paquimé between 1958 and 1961, Di Peso was central in the interpretation of the cultural dynamics of the Gran Chichimeca; an area in northern Mexico encompassing over 170,521,470 km^2 (Di Peso 1974:1:48-55). Now considered by many archaeologists as the successor of the Mogollon, Paquimé is located in northern Mexico along the Rio Casas Grandes (Di Peso 1974). Expanding between A.D. 1200 and 1450, this community was considered an important center of trade and culture. Incorporated into Paquimé's Puebloan architectural design was masonry style buildings, Mesoamerican style platform mounds, and ball courts which were identifiable structures built for a game that was deeply rooted in Mesoamerican culture. Defining the period of Paquimé's fluorescence between A.D. 1060 and A.D. 1340, Di Peso (1974) argued that Paquimé was a trading outpost built by Toltec long-distance traders for the purpose of exploiting the region's resources. These long-distance merchants may have brought along their own warriors and priests so they could control all aspects of trade, religion, and political administration in the surrounding region.

Other regions in the Greater Southwest besides Paquimé were incorporated into Di Peso's model of direct influence from Mesoamerica. Di Peso (1968:52) proposed that the Hohokam settlement of Snaketown may have been a key element in the transport of turquoise from mines such as Sleeping Beauty in Arizona and the Himalaya (Halloran Springs) in southeastern California to Mesoamerica through the actions of pochteca-like traders. Other commodities probably existed in the trade structures; such as slaves, cotton, peyote, shell, and salt. Relative to the Ancestral Puebloan communities, there was stronger evidence of Mesoamerican and Greater Southwestern interaction in the Hohokam (Wilcox and Sternberg 1983) and Paquimé (Di Peso 1974) regions, especially with the presence of platform mounds and ball courts.

Disputing Paquimé's chronology established by Di Peso (1974), some archaeologists argued against the pochteca-like trade models. Dates, derived from dendrochronology using trees that were trimmed and missing some of their outside rings, were reassessed and the dates for pre-contact periods were revised (Dean and Ravesloot 1993; Foster 1992; Ravesloot et al. 1995). Most archaeologists agree on the revisions that placed the fluorescence of Paquimé (A.D. 1200 to A.D. 1450) somewhat later than Di Peso had proposed (A.D. 1060 to A.D. 1340). Once the dates of Paquimé were revised, the importance of its expansion as a trade center was not contemporaneous with the rise and expansion of the Toltec or Chaco Canyon.

Although Paquimé's importance as a trade center was dated later than the proposed Toltec pochteca-like traders, other archaeologists (see Foster 1986, 1999; Kelley 1986, 1993, 1995) argued that there still was a great Mesoamerican influence stemming from the Aztatlán tradition that was from the same time period. The Aztatlán culture was located along the coast of west Mexico extending from southern Sinaloa to the south of Jalisco, and east into the state of Durango existing from as early as A.D. 750 and into the A.D. 1300s (Foster 1999:157-158). Trading in items such as cotton, textiles, obsidian, ocean shell, and copper bells, the Aztatlán trade routes covered an area from central Mexico, along the western coast and into central Durango. Michael S. Foster (1986, 1999) and Charles J. Kelley (1986, 1993, 1995) suggested that the trade routes of the Aztatlán merchants extended into Paquimé serving as an economic bridge to the communities in the north.

For over a decade, Kelly (1986, 1993, 1995) developed his proposal of the expansion of the Aztatlán culture group along the highlands and coastal lowlands of northwestern México and the establishment and incorporation of Paquimé into the sphere of the Aztatlán tradition. Charles J. Kelley and Ellen Abbott Kelley (1975) first published a version of the pochteca-like trade model recognizing that the settlements of the Greater Southwest were conditioned by the local environment and affected by ecological factors; however, the main basis of cultural change was connected to the *cultural evolution* of Mesoamerica (Kelley and Kelley 1975:179). Arguing that the Ancestral Puebloans did not evolve within an *isolated cultural universe*, Kelley and Kelley (1975:179) proposed that they were directly affected by Mesoamerican influences. Focusing on the relationship between Mesoamerica and the Ancestral Puebloans, they argued that there were too many similarities between these cultures. These influences not only include similar physical traits (e.g. architecture), but direct reactions to specific events and cultural dynamics in Mesoamerica.

Kelley and Kelley (1975:178) also proposed that the principal casual factor for the exploitation of the American Southwest was specifically turquoise. During the fluorescence of Teotihuacán (A.D. 400 to A.D. 600), the Ancestral Puebloans were shifting from hunter and gatherer subsistence patterns to a more sedentary and horticulture existence. It was also during this time period that a small amount of turquoise fragments were present in Teotihuacán (Linné 2003:132). Kelley and Kelley (1975:203) suggested that travelers from Teotihuacán may have had scheduled contacts with the Ancestral Puebloans. Sometime after A.D. 650, Teotihuacán fell and the Toltec became the dominant culture in the Valley of Mexico (A.D. 800-925). Kelley and Kelley (1975:203) proposed that a hiatus occurred between Mesoamerica and Ancestral Puebloan communities at this time. As the Toltec empire rose and the city of Tula developed into a large regional center, Chaco Canyon experienced expansion and growth spreading its influence across the San Juan Basin. As well as when the Tula and the Toltec empire began to decline, the Greater Southwest fell into a period of reorganization and shifts in population centers. By A.D. 1300, the Toltec were replaced by the rise and spread of the Aztec. Also by A.D. 1300, the culture group defined as the Ancestral Puebloan was no longer present in the San Juan Basin. The Greater Southwest was in the mist of its aggregation period with profound changes in how people organized their communities.

Investigating evidence in support of Mesoamerican influence, Robert H. Lister (1978) identified features and items in Chaco Canyon that could be considered to have Mesoamerican attributes. He recorded architectural features that were similar to those found in the Valley of Mexico, such as rubble core masonry, square columns, circular structures, platform mounds, and T-shaped doorways. Presence of ceramic cylinder jars, copper bells, iron pyrite mirrors, conch shells, and macaw bones were just a few examples of Mesoamerican objects recovered in Chacoan archaeological sites (Lister 1978:236-237).

A few researchers (Frisbie 1978; Reyman 1978) in support of the pochteca-like trader models suggested that the *high-status* burials recovered in the Greater Southwest were evidence of actual long-distance merchants from Mesoamerica; especially those burials found in Pueblo Bonito and Aztec Ruin in New Mexico, and the *magician* burial in at Ridge Ruin in Arizona. These burials were found with grave goods that were associated with exotic trade items such as turquoise, macaws, and shell.

Opponents to the concept of the Greater Southwest as a frontier of Mesoamerica argued that the distance between the two cultural groups was too far for direct trade, especially without the aid of domesticated pack animals. This vast area, sometimes called a cultural hiatus, between the complex societies in the Valley of Mexico and the communities in the Greater Southwest is part of the Basin and Range physiographic province consisting of large areas of arid deserts. The pre-Columbian culture and communities of this region have not been well studied or represented in the literature. This has been changing in the past few decades as surveys and excavations were increased in northern Mexico and more information was published about these desert communities (e.g., Antillón and Maxwell 1999; Brooks 1978; Pailes 1978; Palma 1982) and their possible economic relationships with Mesoamerica and the Greater Southwest (e.g., Kelley 1993, 1995).

Proposing the concept of interaction spheres, Steven A. LeBlanc (1986:106) divided the Greater Southwest into three major cultural divisions or *cultural phenomena*: the Ancestral Puebloan, Hohokam, and the Mogollon. The interaction spheres of these cultural phenomena, especially their large regional centers (e.g., Chaco, Snaketown, and Paquimé), may have been dependent on trade and exchange that originated out of Mesoamerica. Although they were in different geographical locations and were culturally distinct from each other, LeBlanc (1986:129) suggested that each interaction sphere would have a profound effect on the others. For example, Paquimé expansion soon after the demise of Chaco's interaction sphere, or perhaps Chaco lost its position as a large regional trade center with the establishment and growth of Paquimé's interaction sphere (LeBlanc 1989:195-196).

New models begin to emerge from the concepts of interaction spheres (LeBlanc 1986:106) and *empty spaces*. These vast areas that were sparsely populated and far from any population centers (Upham 1992) would have been populated by roaming hunter and gatherer groups and small hamlets of *rural folk* (McGuire et al. 1994). These groups, that inhabited these regions, may have varied between hunter and gatherer lifeway patterns with occasional periods of sedentary horticulture, such as the Jornada Mogollon of south central New Mexico (Upham 1992) or the Chichimeca of the Chihuahua desert (Wilcox 1986:35). They would not have left much of a footprint in the archaeological record; however, they may have played an important role as middle-men in trade and the flow of ideas.

4.3.3. Prestige Goods Model

Building on these concepts, Nelson (1986) proposed the prestige goods model that included concepts of exchange with Mesoamerica but without direct influence or colonization. For example, merchants from the south may have established alliances through the exchange of socially valuable goods or through marriage forming a group of elites (McGuire 1980). This could help explain sudden changes in the stratification of social ranking in some communities. The prestige goods model is built on power, and the power was maintained by the elite control of valuable goods and sacred knowledge that, in turn, validated their positions as leaders (McGuire 1989:49). The control and circulation of sacred items was crucial for establishment and growth of regional political and economic networks (Hirth 1996:208). The significance of sacred items, such as turquoise, was assigned by the ideology and/or religion of the communities allowing the objects to be associated with great power of those individuals that maintained the control of these items. In turn, the exchange and circulation of these items maintained the ideology (McGuire 1989:50) and perpetuated social cohesion. Participating as a member of the ideology was an important factor in the social identity of the individual (Stein 2002:907). Therefore, prestige economies are supported by the presence of an elite or elder group, accumulation and exchange of controlled items that had a scared value (Bradley 2000:173; Hirth 1996:216), and the distribution of valued items to the community through feasting or organized ceremonies (Hirth 1996:216).

Focusing on the Hohokam area, Richard S. Nelson (1986) modeled interregional relationships through the concept of spheres of exchange. It was through these spheres of exchange that Mesoamerican items (e.g. copper bells) and similar structures (e.g. ball courts and platform mounds) may have spread throughout the Greater Southwest (Nelson 1986:155). Assuming that Hohokam elites were responsible for exchange with Mesoamerica, long-distance trade items would cluster in areas such as elaborate burials, ceremonial structures, or ball courts. These exotic items would also be found clustered in the larger centers rather than in smaller sites, even those in closer proximity to the source region (Nelson 1986:157). Supporting this assumption, David R. Wilcox and Charles Sternberg (1983) found that sites with ball courts typically had more exotic trade items. The control of the exotic items and the association of political power was the basis of a prestige goods economy. Typically, the elites were older males who obtained power and authority through the control of goods (McGuire 1986:251). Although the objects were not necessary for the physical welfare of any individual, they were meaningful social items. The elites who controlled the foreign exchange would use this power to extract surplus or labor from subordinates within their group and build political bonds and exchange alliances with other communities (Saitta 2000:152-153).

4.3.4. Peer Polity Interactions

Colin Renfrew (1986) proposed the peer polity interaction model for the movement of trade goods throughout areas consisting of states and chiefdoms where neither was dominant. A polity is described as a politically organized unit. Exchange and economic relationships only existed between communities that were located beside or nearby, within a single geographical area (Renfrew 1986:1). One assumption of this model was that culture change was more affected by interactions on a local level rather than those through external relationships. Several expectations were defined for the peer polity interaction model. The first expectation was that as one polity was defined in a region, others nearby would be recognized by similarities in size and organization. Some of these polities would experience similar and contemporaneous cultural changes resulting from a range of events (e.g., warfare, changes in ideas, or the flow of goods) and did not manifest out of a single innovative event (Renfrew 1986:7-8).

Recognizing problems with unbalanced relationships between core and periphery elements of an intergraded world system, Paul E. Minnis (1989:299) focused on the concepts of interaction versus integration. Working in northern Mexico, Minnis (1989) applied the polity interaction model to Paquimé and its surrounding area. Archaeological excavations at Paquimé revealed an abundance of elite goods, including shell, turquoise, macaws, and copper bells. Minnis (1989:294-296) proposed that most of the luxury goods recovered from Paquimé were found in specific areas or clusters of rooms suggesting that the exotic goods were controlled by an elite group and only they had access to them. Almost four million shell artifacts were recovered among three rooms (Di Peso 1974:500-505). Michael E. Whalen and Paul E. Minnis (2003) argued that the fluorescence of Paquimé was consistent with previous growth in the surrounding area and did not manifest as the result of the exploitation from a more complex regional core center. Although there were some traits that were similar with those in groups in western Mexico, they were probably willingly adopted. Similarities with Mesoamerica were perceived as an interaction and not integration (Minnis 1989:300). Paquimé was not considered as an important center of trade and that peer polity interaction could account for all of the long-distance trade items.

4.3.5. Trade Festival Model

Focusing on the western United States, Joel C. Janetski (2002) proposed the trade festival model to account for trade between the Fremont, Ancestral Puebloan, and other cultural groups in the American Southwest and the Great Basin. Long-distance trade items such as turquoise, shell, and Ancestral Puebloan ceramics have been recovered in Fremont archaeological sites suggesting that they participated in some of the same exchange networks or interacted directly with the Ancestral Puebloan. Trade festivals were pre-scheduled and organized events that included feasting, gaming, bartering, social interaction, and rituals between the participants. Drawing from ethnographic studies in the Great Basin (Hughes and Bennyhoff 1986) and the American Southwest (Ford 1983), Janetski (2002:347) suggested that there were similarities and that trade festivals could explain pre-Columbian trade and exchange. Richard E. Hughes and James A. Bennyhoff (1986) proposed that although a simple down-the-line trade occurred between individuals or small groups in the Great Basin, most trade occurred at organized trade festivals.

Those held at Taos and Pecos included the Puebloan peoples and other nomadic groups including the Comanche and Apache. Richard I. Ford (1983) expounded on the different scales of trade suggesting that different variations of trade models applied to trade between individuals, within a cultural group, or between cultural groups.

The world systems model may not be the best model for the Greater Southwest and its possible ties to Mesoamerica; however this model enhanced the perceptions of the communities of the American Southwest and northern Mexico as *dynamic entities,* and they were not just restricted and bound by their surrounding environmental conditions. These communities were perceived of and defined as part of the peripheral frontier in an unequal relationship with a much larger core region in Mesoamerica (McGuire 1986:244). All of these models have significant aspects that should be investigated on different regional scales. For example, the concepts of core/periphery applied on a smaller regional scale, such as the perception of Chaco Canyon as a core and the turquoise resource areas as external areas beyond the periphery, is an excellent tool to investigate the movement of goods into a regional center. The prestige model can be applied to the mini-systems, such as turquoise trade among communities (e.g., Chaco Canyon and Aztec Ruin), and the trade festival model can be functional in linking trade among the communities at the focus of this study and the hunter and gatherer groups that inhabited many of the turquoise resource areas.

Chapter 5: The Chacoan World

"*The abundance of turquoise found in Chaco, as well as the positive archaeological evidence of bead manufacture there, strongly suggests its use as a medium of exchange …*"

(Judge 1976:5).

The terms *Chacoan World* and *Chacoan* have many definitions in the archaeological literature. The term *Chacoan* has been used to describe a specific suite of attributes that is contrasted with the *Chaco Core*, the sites in Chaco Wash (Kintigh 2003:94). *Chacoan archaeology* is described as the archaeology that dates to the *Chaco era* and has distinctive *Chacoan attributes* (Kintigh 2003:95; Reed 2008:7). Not all researchers agree on the definition of Chacoan attributes and the dates of the Chaco era. Paul F. Reed (2008:7, 2011:13) defined the term *Chacoan* as those attributes that belonged to a distinct social identity or set of traits rather than a distinct biological population or ethnic group. For example, the set of attributes can include the type and layout of communities that were similar to what was found in Chaco Canyon (e.g., great houses) and how the occupants used their space (e.g., large rooms). These traits also include material culture that had similar styles (e.g. ceramics, lithics, textiles, and basketry) and the presence of long-distance trade goods such as turquoise, copper bells, and macaws. For the purpose of this research, the term *Chacoan World* is used to include Chaco Canyon and those populations that have similar attributes. In this chapter, the Chacoan World is presented along with descriptions of the archaeological sites and turquoise artifacts used in this study. There is also a brief discussion of the turquoise resource areas and the culture groups that occupied these regions.

One of the problems with using similar attributes of material culture to define a culture area is that, especially in the case of the Ancestral Puebloan, more than one entity or tribe may occupy that culture area (Fowler and Cordell 2005:8) or local groups may emulate certain styles to enhance their prestige (Reed 2011). However, similar material culture can be useful in tracing prehistoric peoples associated with clans and religious cults (Ferguson 2003:141-142) as long as concepts, such as emulation, are considered.

Urban (2010:208) proposed that exchange relationships were social avenues for the flow of culture and the physical objects of these exchanges were a conduit for the diffusion of culture. Trade and exchange interactions suggest cultural interaction (Bauer 2008). Therefore, to investigate diffusion and possible migration of a culture group the material culture (turquoise in this study) needs to be linked to it geological provenance region. To investigate the relationship of subgroups within a culture area, examining patterns of turquoise procurement strategies would help in identifying variation between these subgroups. Shared materials and trade/exchange interactions may suggest social relationships and social cohesion along with shared practices and ideas (Bauer and Agbe-Davis 2010:29). Therefore, similar patterns of turquoise procurement strategies between communities would support shared practices, ideologies, and knowledge suggesting strong social relations between these communities; whereas different patterns of turquoise procurement would suggest differences in knowledge and practices.

5.1. The Archaeological Sites

The inhabitants of Chaco Canyon, Aztec Ruin, and Salmon Ruin lived in the San Juan Basin, one of the main regions where the Ancestral Puebloan culture developed. Chaco Canyon is located in the approximate center of the basin (Fig. 5.1). Although the main arroyo and its tributaries flow only during periods of rainfall, it has higher potential for agricultural production than the areas that immediately surround it. Aztec and Salmon ruins are located further north on Animas and San Juan rivers respectively (Fig. 5.1). The San Juan Basin covers an area of approximately 12,000 square kilometers with elevations ranging from 1,500 meters in the south and 2,500 meters in the north. The high desert environment consists of broad plains cut by arroyos and canyons surrounded by low mesas and buttes (Vivian et al. 2006). Temperatures in the San Juan Basin range

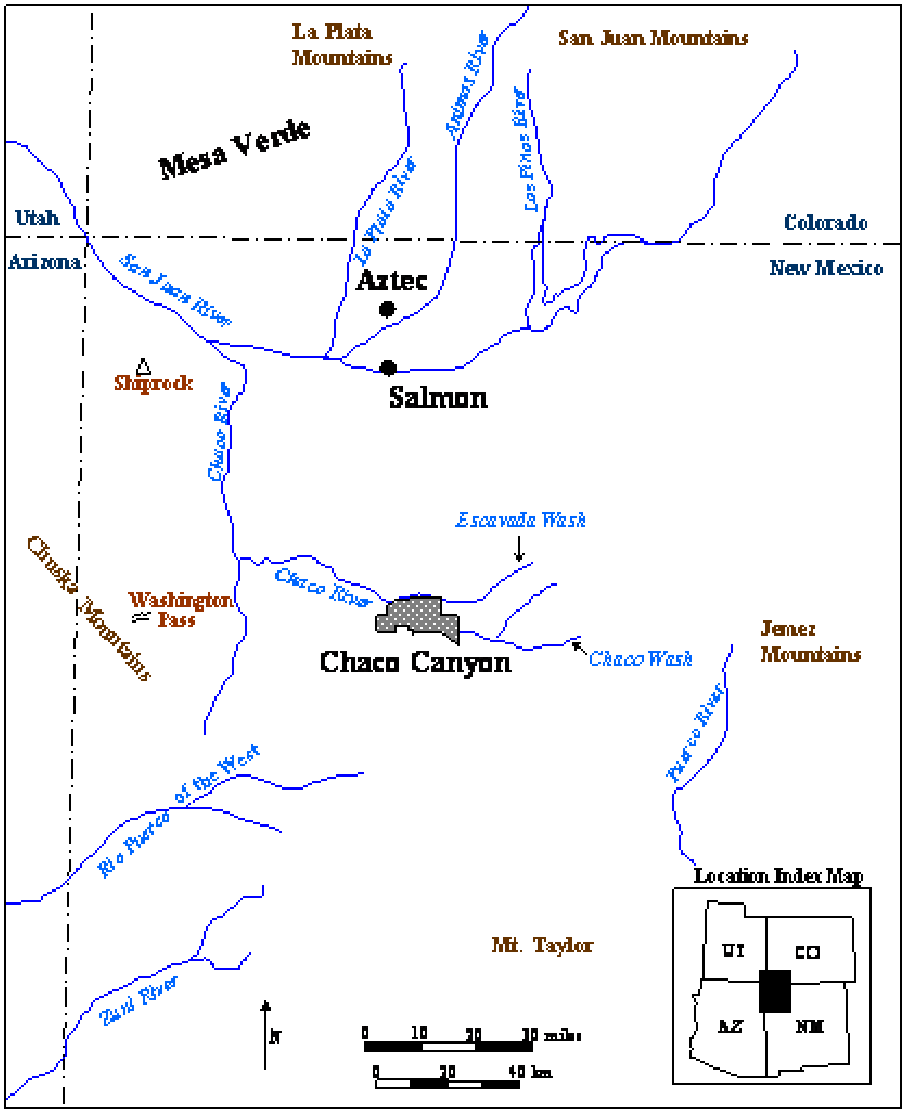

Fig. 5.1. Locations in northwestern New Mexico mentioned in the text: Chaco Canyon, Aztec Ruin, and Salmon Ruin.

from -38°F (-38°C) in the winter to 102°F (39°C) in the summer, with an average annual moisture of 22 centimeters (Vivian 1991). During the period of the Chacoan expansion throughout the San Juan Basin, many communities constructed great houses. These great houses contained Chacoan features, such as the design and masonry style, suggesting that Chacoan influence was evident far beyond the canyon boundaries.

5.1.1. Chaco Canyon

In Chaco Canyon, there is evidence that the local population aggregated into small communities around A.D. 400 (a period which is characterized by pithouses and rainfall dependent horticulture), followed by the building of monumental architecture and the use of water control systems that started around A.D. 900 and continued to about A.D. 1140 (Lekson 1986). The fluorescence of Chaco Canyon is unique in the prehistory of the southwestern United States. During this period, there is no other area in the American Southwest that rivaled the monumental architecture and evidence of long-distance trade goods that were documented in Chaco Canyon. Imports of ceramics, wood, and lithic items were recovered during excavations as well as exotic imports including shell, macaws, parrots, copper bells, and turquoise. Several Chacoan sites were interpreted as turquoise workshops with evidence of the production of jewelry and other ornaments (Mathien 1981a; Windes 1993). Recovered turquoise artifacts included elaborate zoomorphs, jewelry, and other ornamental objects. Over one thousand pieces of turquoise were placed in structures during construction episodes in Chaco Canyon (Mathien 2001), suggesting that turquoise was a highly prized mineral and considered an exotic commodity in the economic and religious structures of this ancient culture. Judge (1976; 1989) argued that turquoise became so important in the exchange system that it may have developed into currency.

Chaco Canyon contains twelve great houses surrounded by hundreds of smaller habitation sites (Lekson 2006). Most of the great houses are located on the north side of Chaco Wash and the small sites are mostly located on the southern side. Although the purpose of the great houses is still disputed (e.g., ritual center, military, or homes of the elites); the small sites were clearly habitation sites. The great houses were larger and contained the bulk of exotic goods (Mathien 1981a; Toll 1991). The burials in the great houses also contained far more burial goods than those in the small sites leading some researchers to suggest that elite families lived (or at least were buried) in the great houses, while the small sites in Chaco Canyon were occupied by the common population (Akins 1986; Akins and Schelberg 1984). Not only were variations noted between the great house communities and small site communities, but also between the small communities (e.g., Judge and Cordell 2006:195; Lekson et al. 2006:96; Vivian 1990:196-197) and studies on skeletal remains showed several diverse biological populations (Akins 1986; Schillaci 2003; Schillaci and Stojanowski 2002). The relationships between the communities within Chaco Canyon are still unclear.

Although turquoise was recovered in many sites throughout the canyon, thousands of turquoise beads and most of the elaborate turquoise artifacts were recovered from Pueblo Bonito (Mathien 1981a; Pepper 1996). Located on the north side of the Canyon, Pueblo Bonito (Fig. 5.2) is the largest great house in the Canyon and is arguably the most extensively studied site in Chaco Canyon. Excavations at Pueblo Bonito were conducted from 1896 to 1900 by the American Museum of Natural History and 1921 to 1927 by the Smithsonian Institution and National Geographic Society (Lekson 2006).

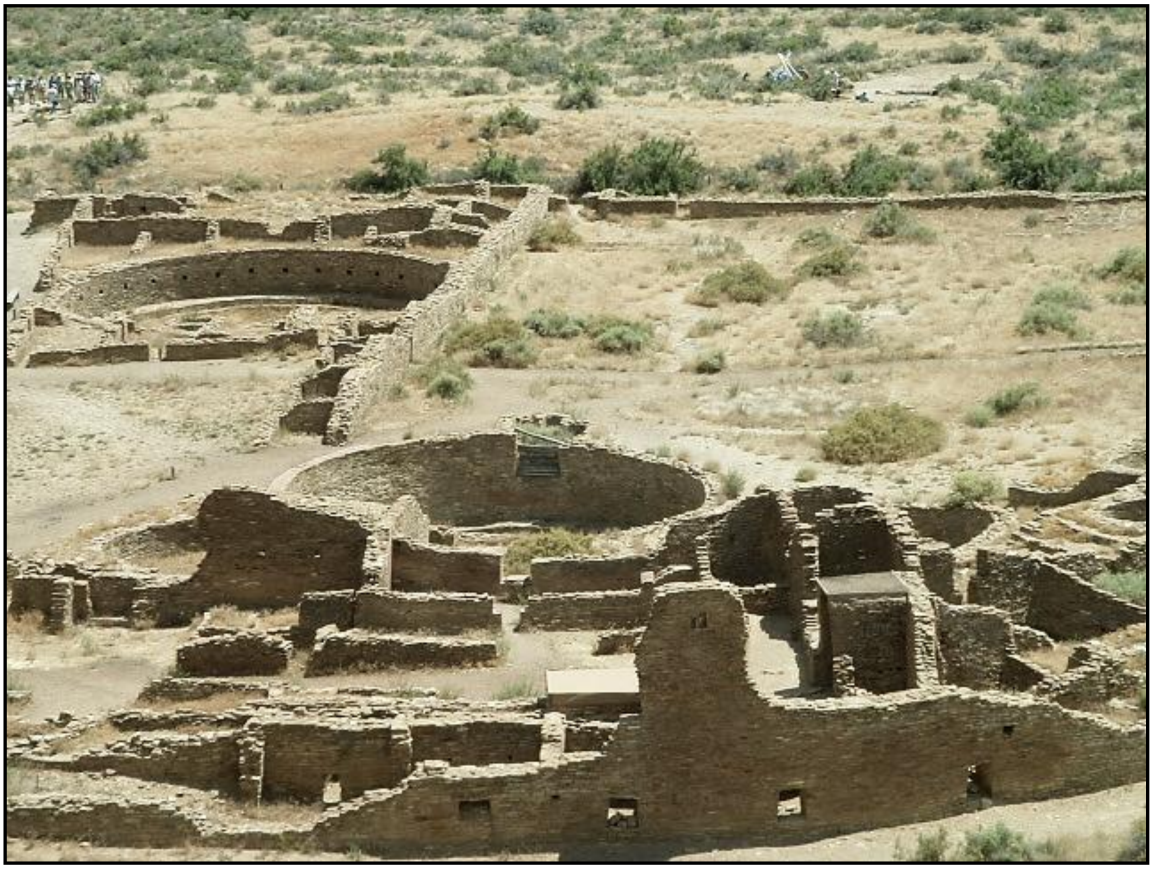

Fig. 5.2. A partial view of Pueblo Bonito, Chaco Canyon.

The Ancestral Puebloans began construction at Pueblo Bonito prior to A.D. 900 and by A.D. 1020; Pueblo Bonito was larger than any previous Puebloan structure. By A.D. 1125, it was possibly five stories encompassing almost seven hundred rooms and included at least thirty-two kivas and two great kivas. Many of these rooms were dark, with limited access yet they were much larger than most habitation rooms (Lekson 2006) which lead to numerous interpretations of what Pueblo Bonito represented. Pueblo Bonito was a proclamation of wealth and status. Not only was it the largest great house, but it contained prestige goods including pink chipped stone form the Chuska Mountains, shell from the Pacific Ocean, cooper bells from the west coast of Mexico, macaws from the Mesoamerican rainforest, and turquoise (Cameron 2009:2). While turquoise artifacts were found associated with many of the Pueblo Bonito burials that date to the Chacoan occupation, two burials recovered in Room 33 (designated as burials 13 and 14) were exceptional as they each contained thousands of turquoise pieces (Pepper 1996).

Tree-ring dates range from A.D. 828 to A.D. 1130 (Lekson 1986; Lister and Lister 1981) suggesting that there were many construction and remodeling episodes. The last tree-ring date of A.D. 1130 suggests that construction ceased and Pueblo Bonito was abandoned or was not significantly used after that date. In the late A.D. 1100s and A.D. 1200s, there is evidence of remodeling and a reoccupation or an increase in use at Pueblo Bonito (Lekson et al. 2006:100). These modifications are more conducive to habitation rather than the more ceremonial use attributed to Pueblo Bonito prior to this period (Judge and Cordell 2006:206). The material culture was also notably different and similar to the material culture of the Mesa Verde region. Therefore, this change is often referred to as the Mesa Verdean occupation (Lister and Lister 1987).

The small sites represented in this research are located throughout Chaco Wash. Site 29SJ1360 is located on a ridge north of Fajada Butte (Fig. 1.1) and was excavated by Charles R. Morrison in 1974. It was occupied A.D. 850 to A.D. 1030 (Mathien 2005) and contained at least 18 rooms and five kivas (McKenna 1984, 1986). Recovered turquoise fragments suggested that Site 29SJ1360 was a place for the production of turquoise ornaments (Mathien 1984; McKenna 1984:275). Site 29SJ1659, Shabik'eshchee, was a village located on the east end of Chaco Canyon on Chacra Mesa (Fig. 1.1). Originally it was reported that this site was built and occupied in the A.D. 500s (Robinson et al. 1974:39) and contained at least 20 pithouses, 48 storage bins, and a one great kiva (Roberts 1929). However, the dates of occupation, the expanse of the site, and models of what the site represented are currently being reevaluated and disputed (see Wills et al. 2012). Site 29SJ423 is associated with dates ranging from A.D. 1020 to A.D. 1120 and is located on near the confluence of the Chaco and Escavada wash on West Mesa (Mathien 2005). The site included cists, pithouses, and at least three kivas (McKenna 1986).

Marcia's Rincon is located on the south side of the canyon west of Fajada Butte (Fig. 1.2) and includes sites 29SJ625, 29SJ627, 29SJ628, 29SJ629, and 29SJ633. Turquoise artifacts were selected from these archaeological sites because they span a time period from A.D. 600 to the A.D. 1200s. Site 29SJ625, also known as the Three C site, was excavated by R. Gordon Vivian (1965) and re-examined, where more structures were identified suggesting that the site dates from A.D. 900s to the early A.D. 1000s (McKenna 1986). Site 29SJ627 is located in the center of an outwash plain and included a plaza, trash mound, and at least 25 rooms and seven pit structures. Occupation of the site ranged from A.D. 775 to A.D. 1150 (McKenna 1986). Unfinished turquoise ornaments and bead blanks were recovered from this site suggesting that the occupants of this site produced finished turquoise products (Mathien 1992; Truell 1976). Site 29SJ628 included a pithouse and cists that were constructed in the A.D. 700s. The site was excavated and reported by Marcia L. Truell (1976). The Spadefoot Toad site, 29SJ629, is located at the head of Marcia's Rincon. It was occupied from A.D. 900 to the mid A.D. 1000s with evidence of a reoccupation in the A.D. 1100s (McKenna 1986:65-71; Windes 1993). Unfinished turquoise objects and fragments were recovered from this site suggesting the production of turquoise ornaments (Mathien 2001; Windes 1993). Site 29SJ633, the Eleventh Hour site, was occupied from A.D. 1000 to the A.D. 1100s (Mathien 2005).

5.1.2. The Northern San Juan Basin: Aztec and Salmon Ruins

The communities of Aztec (Fig. 5.3) and Salmon (Fig. 5.4) emerged during the second half of this period and were considered part of the expansion of the Chacoan system (Cameron and Toll 2001; Lister and Lister 1987; Reed 2006a). By the early to mid A.D. 1100s, the center of the Chacoan system in Chaco Canyon (Cordell and Gumerman 1989; Lekson and Cameron 1995) was nearing its end. Across the greater San Juan Basin, the inhabitants of Aztec and Salmon Ruins continued to build with a strong Chacoan influence and a corresponding increase in population (Lekson and Cameron 1995). In the mid to late A.D. 1100s, the archaeological evidence suggested a period of reduced construction with a distinct change in the archaeological record. By the early A.D. 1200s, artifacts and masonry styles were notably different in Aztec Ruin, similar to the changes noted at Pueblo Bonito in the late A.D. 1100s and A.D. 1200s. Once again this change was referred to as the Mesa Verdean occupation (Brown et al. 2008:231; Lister and Lister 1987; Reed 2008:18).

Fig. 5.3. A partial view of Aztec Ruin in the northern San Juan Basin.

Fig. 5.4. A partial view of Salmon Ruin in the northern San Juan Basin.

Aztec Ruin is located about 60 miles north of Chaco Canyon and is on the west bank of the Animas River, which eventually merges with the San Juan River. As early as 1878, Lewis H. Morgan visited the ruins and associated Aztec Ruin with Chaco Canyon. The community consisted of several habitation complexes. Aztec West contained over 350 rooms built into three stories. Aztec East appeared to be similar to Aztec West, although most of Aztec East has not been excavated.

Excavations were conducted by Earl Morris under the direction of the American Museum of Natural History and the National Parks Service from 1916 through 1921. Almost 70 percent of Aztec West was excavated and repaired and later a great kiva was excavated and restored (Morris 1915, 1919, 1921, 1924, 1928; Reed 2006a). Morris identified two distinct occupations at Aztec West, the earliest with Chacoan attributes and the second occupation that was more similar to Mesa Verdean culture (Brown et al. 2008; Lister and Lister 1987).

Tree-ring dates suggest that building began at Aztec West as early as A.D. 1090; however the main building period was from A.D. 1110 to A.D. 1115 with some additions around A.D. 1124 (Brown et al. 2008; Lister and Lister 1987). The masonry and design style along with ceramics were very similar to the Chacoan style suggesting that the inhabitants that built Aztec were either migrants from Chaco Canyon or that the local inhabitants were strongly influenced by the Chacoan system. A second period of construction and remodeling dates between A.D. 1220 and A.D. 1260 with the difference in masonry and ceramic styles known as the Mesa Verdean occupation (Lister and Lister 1987). In the late A.D. 1200s, Aztec community was destroyed by fire and abandoned (Reed 2006b).

Salmon Ruin is located on the north bank of the San Juan River, situated roughly in a line between Chaco Canyon and the Aztec community. Salmon was intensely studied and approximately 30 percent excavated between 1970 and 1980 during the San Juan Valley Archaeological Program (Reed 2006a). The project was headed by Cynthia Irwin-Williams and encompassed many areas of research, including depositional studies, tree-ring dating, archaeomagnetic dating, archaeobotanical studies, human remains, fiber, fauna, and a complete volume on ceramics.

Although a few tree-rings date prior to A.D. 1086, the main construction dates are from A.D. 1086 to A.D. 1090. Additional rooms were added around A.D. 1118 (Reed 2006b). The construction was similar to the Bonito style masonry that was associated with the Chacoan Period. Construction of the Salmon great house was almost completed by the time the McElmo style construction and ceramics began to appear in Chaco Canyon and construction at Aztec Ruin was in its earliest stages (Reed 2006b). It is not clear if the Salmon pueblo was occupied only by the Chacoan population or if as suggested by Reed (2008:18-19), they lived contemporaneously alongside the local San Juan population within the residential core of Salmon Ruin.

Evidence suggests that the inhabitants responsible for Chacoan features at Salmon Ruin around A.D. 1120 relocated to Aztec East probably due to flooding of the San Juan River (Reed 2006c). Flood deposits were identified in a kiva at Salmon Ruin and there was an increase in construction at Aztec East, around A.D. 1120; during the proposed time period that the Chacoan population left Salmon Ruin (Reed 2006c). In addition, Salmon Ruin appeared to have been fully occupied by a local San Juan population around A.D. 1120 (Reed 2006b); much earlier than the records suggested for Chaco Canyon and Aztec Ruin. Reed (2006b) refers to population that was distinctly different than the

Chacoan population at Salmon Ruin as the San Juan population disassociating this population from the occupants of Mesa Verde arguing that the term Mesa Verdean occupation is misleading.

Exotic trade items were identified with the Chacoan population suggesting that they participated in a long-distance trade network; however this trade network diminished once the Chacoan population left. There was less evidence of exotic trade items found in association with the later population at Salmon Ruin (Reed 2006c). There was a period of remodeling, repair, and maintenance by the local San Juan population at Salmon Ruin that ranged from A.D. 1257 and A.D. 1261, with a final date of A.D. 1263 (Reed 2006b). Similar to Aztec Ruin, there was a fire in the late A.D. 1200s that destroyed most of the pueblo and Salmon Ruin was abandoned. It was during this same time period that the entire San Juan and Mesa Verde regions were abandoned by the inhabitants of the Ancestral Puebloan culture (Reed 2006b).

The relationship between the inhabitants of Chaco Canyon, Aztec Ruin, and Salmon Ruin (e.g., Brown and Paddock 2011; Lekson 1999; Reed 2006, 2008, 2011) is debated. Some archaeologists suggested that Aztec Ruin became the new regional center for the San Juan Basin (Lekson 1999; Reed 2006a). It is not clear if the Chacoans purposely moved the center of authority and migrated to the north (e.g., Irwin-Williams and Shelley 1980; Lipe 2006; Morris 1915) or if the growing Aztec center was a competitor established by a local population (Van Dyke 2008:335). Another possibility presented by Gary M. Brown and Cheryl I. Paddock (2011) was that a group of Chacoans established Aztec Ruin, utilizing a mixed labor force of Chacoan migrants and the local population. Reed (2006c) also showed evidence for a mixed population that occupied Salmon Ruin prior to A.D. 1120. Were Aztec and Salmon Ruins initially built and colonized by migrants from Chaco Canyon or were these two large communities built by local populations emulating the Chacoans? Migration or emulation is hard to identify in the archaeological records, especially when *Chacoan* is a suite of attributes pertaining to material culture versus a biological population (see Reed 2011). The local population, or a subgroup of the local population, may have adopted these attributes and their material culture would have appeared Chacoan.

The presence of turquoise and other exotic goods were one of the attributes that were associated with what is considered Chacoan. However, Reed (2011) suggested that the presence of long-distance trade items could have manifested as a local population attempted to emulate the Chacoan style. Local populations may have been encouraged to adopt the Chacoan style to become a member of the Chacoan system and gain access to the exchange networks. Acquiring exotic goods may have been one way to become Chacoan, and becoming Chacoan may have enhanced their status in their community or the prestige of the entire community (Reed 2011).

5.2. Turquoise Resource Areas

The Ancestral Puebloan, Hohokam, and Mogollon shared similar attributes as they all practiced maize agriculture, manufactured pottery, and built puebloan type structures. They also were in possession of exotic items such as turquoise. It is important to consider the occupants of the turquoise resource areas, especially if the Hohokam and Mogollon were participants in turquoise trade with the Ancestral Puebloan. The Hohokam may have obtained turquoise from nearby resource areas (e.g., Sleeping Beauty; Fig. 2.17) either by direct acquisition or trade with the occupants of the rural areas. The turquoise that originated in Arizona may have been moved to northwest New Mexico through trade networks between the Ancestral Puebloan and Hohokam. The same type of scenario may be applied to the area of the Mogollon in southern New Mexico (Fig. 2.15 and 2.16).

Although the origin of turquoise artifacts can be identified, other archaeological information is required to determine if the turquoise was procured through direct acquisition or trade networks. For example, identifying distinctive styles of ceramics can help in linking specific culture groups to turquoise resource areas, although these artifacts recovered at turquoise resource areas may be a result of trade or exchange. It is also important to consider that turquoise procurement strategies and exchange networks most likely changed through time. Opportunists who were obtaining turquoise through trade networks may have decided to locate the resource areas and mine the turquoise directly. People who desired turquoise may have had to alter their turquoise procurement strategies as old trade networks collapsed or they were denied access to this valuable resource. Turquoise procurement may have impacted (e.g., social or economic relationships or diffusion of ideas) both the inhabitants of the turquoise resource areas and the occupants of the archaeological sites where the turquoise artifacts were recovered.

The turquoise provenance region that includes Kingman, Arizona, the southern tip of Nevada, and southeastern California (Fig. 2.21) has ample evidence of heavy ancient mining activity (Jenson 1985; Leonard and Drover 1980; Rogers 1929; Weigand 1982; Weigand and Harbottle 1993). The Virgin River branch of the Ancestral Puebloan inhabited areas in southern Nevada, northern Arizona, and parts of southern Utah (Ahlstrom and Roberts 2008:130). There were several communities located in the Moapa Valley and Virgin River Valley, north and northeast of the city of Las Vegas, and possibly some small sites in the Las Vegas Valley where the present-day city of Las

Vegas is located. One of the settlements was Lost City, also known as Pueblo Grande de Nevada, and is located in the Moapa Valley. Evidence suggests that puebloan people began moving into the Moapa Valley around A.D. 1, and by A.D. 900 Lost City developed into a regional trade center that may have been an important node in a pan-Southern trade system (Rafferty 1990). On the *western frontier* of the Ancestral Puebloan cultural area, Lost City may have been responsible for the collection and transport of big trade commodities such as cotton, salt, and turquoise (Lyneis 1986).

The early inhabitants of Las Vegas Valley are not clearly defined. There was an intermixing of cultural attributes (e.g., ceramics) of the Patayan, Southern Paiute, and the occupants of the western pueblos (Ahlstrom and Roberts 2008:133). The Patayan (ancestral Mojave), whose territory was normally associated with the area around the lower Colorado River, and the Southern Paiute, whose territory traditionally included southeastern California, northwestern Arizona, southwestern Utah, and parts of southern and southeastern Nevada, were nomadic with hunter and gatherer subsistence strategies. The Southern Paiutes replaced the Patayan in the Las Vegas Valley around A.D. 1000 (Lyneis 2000), although they may have been contemporaneous for many years. Margaret Lyneis (2000) proposed that Las Vegas Valley was an interface area. It was not clear if the mixing of cultural attributes was evidence of trade, raiding, settlements, or a combination of these situations. Usable areas near vital resources (e.g., water) may have been inhabited by different cultural groups during different time periods, each leaving behind some evidence of their occupation. These cultural boundaries were likely fluid and moved through time.

The areas to the north in the Great Basin that contain many of the Nevada turquoise resource areas (e.g., Royston and Godber) were also occupied by nomadic hunter and gatherer groups referred to as the Desert Archaic or the Desert Culture. During the greatest expansion period of the western Ancestral Puebloan, ceramics from the Lost City Phase (A.D. 700 to A.D. 1150) were recovered in west central (Harrington 1926) and east central Nevada (Harrington 1928) as they most likely overlapped and were contemporaneous with the desert culture. Although there are no reported turquoise resource areas in Utah, the Fremont may have played an important role in the turquoise trade networks between the Ancestral Puebloan in northwestern New Mexico and the turquoise resource areas or the Desert Archaic in central and northern Nevada (Fig. 2.29 and 2.35). The Fremont people were similar to the Ancestral Puebloan. They practiced maize agriculture, manufactured pottery, and built adobe and masonry structures for storage. However, they were distinctive from their southern neighbors as they relied more on wild foods, produced unique clay figures, and produced different styles of basketry and pottery. They also wore moccasins that were distinctly different from the sandals of the Ancestral Puebloan (Janetski 2008:105). Trade was evident between the Fremont and their neighbors to the west and south with the recovery of turquoise and shell artifacts from Fremont archaeological sites (Janetski 2008:111).

Closer to Chaco Canyon, the areas around Cerrillos Hills in northern New Mexico, were only sparsely populated by puebloan cultures. Although the surrounding areas became the home for the major Puebloan population centers after A.D. 1300, this area was only scattered with a few clusters of pithouses that may have represented only seasonal occupation (Cordell 1997:359). Although these sites are not considered *Chacoan*, the Bronze Trail site (Wiseman and Darling 1986) exhibited similar pottery types to those found in Chaco Canyon, as well as a number of mining tools. Although southwestern Colorado was heavily populated by puebloan peoples, the inhabitants of the turquoise resource areas in Colorado (Fig. 2.7) were nomadic groups who practiced hunter and gatherer lifeways leaving only a small archaeological imprint on the landscape (Dutton 1976; Simms 2008).

5.3. Turquoise Artifacts

Sixty-two turquoise artifacts were selected for hydrogen and copper isotope analyses (Table 5.1). Thirty-seven artifacts were selected from Chaco Canyon (twenty-nine from Pueblo Bonito and a total of twelve from the eight small sites), thirteen from Aztec Ruin, and eight from Salmon Ruin. These artifacts, although low in number, allowed the: 1) testing of the hydrogen and copper sourcing technique by identifying the geological origin for these turquoise artifacts, 2) identification of the extent of turquoise procurement of the Chacoan World, and 3) comparison of turquoise procurement patterns among Aztec Ruin, Salmon Ruin, and the sites in Chaco Canyon and to current hypothesis and theories regarding exchange/trade models and the interaction of the diverse populations of Chaco Canyon and the northern San Juan Basin.

Table 5.1. Turquoise Artifacts and their Archaeological Provenience.

Archaeological Site/Room	Archaeological Provenience	Mount No.	Artifact No.	Associated Dates A.D. [a]
Pueblo Bonito				
Room 26	Kiva pilaster, top of square post	ARF7.02	AMNH 2881	1075
Room 28	Floor with vessels	ARF16.03	AMNH 12771	1100s
Room 28	Debris, floor level	ARF7.03	AMNH 4122	1100s
Room 33	Burial 13 near lower limb	ARF15.03	AMNH 3801	900s
Room 33	Burial 13 around right ankle	ARF5.02	AMNH 3847	900s
Room 33	Burial 13 around right ankle	ARF15.05	AMNH 3847	900s
Room 33	Burial 14 around left arm	ARF10.02	AMNH 9324	900s
Room 33	Burial 14 around left arm	ARF10.03	AMNH 9324	900s
Room 33	Burial 14 around left arm	ARF10.04	AMNH 9324	900s
Room 33	Burial 14 around left arm	ARF10.05	AMNH 9324	900s
Room 33	Burial 14 near wrist	ARF4.03	AMNH 3798	900s
Room 33	Burial 14 near wrist	ARF13.03	AMNH 3798	900s
Room 33	Burial 14 under Haliotus shell at right side	ARF15.01	AMNH 3849	900s
Room 33	Burial 14 under Haliotus shell at right side	ARF15.02	AMNH 3849	900s
Room 33	Burial 14 to the right	ARF5.04	AMNH 9246	900s
Room 33	Burial 14 to the right	ARF14.01	AMNH 9246	900s
Room 33	Burial 14 to the right	ARF14.02	AMNH 9246	900s
Room 33	Burial 14 to the right	ARF14.03	AMNH 9246	900s
Room 33	Burial 14 to the right	ARF14.04	AMNH 9246	900s
Room 33	SE corner, near post	ARF4.04	AMNH 3830	1000 – 1100s
Room 33	Burial 14 under Haliotus shell at right side	ARF19.02	AMNH 3769	1000 – 1100s
Room 33	Debris above floor board	ARF4.01	AMNH 3802	1000 – 1100s
Room 40	West end	ARF16.01	AMNH 5440	After 1085
Room 85	Debris	ARF19.04	AMNH 7295	After 1060
Room 85	Under Floor	ARF19.03	AMNH 7524	After 1060
Room 96	Debris	ARF6.01	AMNH 7814	After 1040
Room 127	Debris	ARF16.04	AMNH 9541	After 1075
Room 127	Debris	ARF7.01	AMNH 9541	After 1075
Room 173	Debris	ARF6.04	AMNH 10827	After 1075

Archaeological Site/Room	Archaeological Provenience	Mount No.	Artifact No.	Associated Dates A.D. [a]
29SJ1360				
Trash midden	TT 1	C2.07	CHCU 418/7276	700 - 820
29SJ1659 Shabik'eshchee				
Pithouse Y	Floor fill	C1.01	CHCU 98/18556	500 - 700
29SJ423				
Pithouse A	Stone bowl	C1.03	CHCU 59/14473	1020 - 1120
29SJ625 Three C site				
Room E	Floor, hearth	C3.10	CHCU 4/31428	900 - 1020
29SJ627				
Kiva G	Clearing plaza	C4.15	CHCU 6553/28601	1000 – 1050
Room 10	Floor 2	C3.13	CHCU 4959/28607	900 - 1000
Room 10	Level 2	C3.14	CHCU 483/28356	1000 - 1040
29SJ628				
Pithouse E		C1.04	CHCU 491/15030	600 - 820
Pithouse A	Ventilator shaft	C2.05	CHCU 98/14646	600 - 820
29SJ629 Spadefoot Toad				
Trash midden 59	Grid 59; level 2	C4.16	CHCU 1672/30310	820 - 920
29SJ633 Eleventh Hour				
Room 7	Layer 8; below floor 2	C5.22	CHCU 893/71336	1100s
Room 8	Layer 1; level 4	C5.24	CHCU 370/31371	1200s
Aztec Ruin				
N XV 2		ARF9.04	AMNH 5389	
N XV 2		ARF12.04	AMNH 5391	
N XV 2		ARF13.01	AMNH 5391	
N XV 2		ARF13.02	AMNH 5391	
N XV 2		ARF2.02	AMNH 5391	
E Room 52	Burial 14	ARF12.03	AMNH 7205	1200 - 1280
E Room 52	Burial 14	ARF2.01	AMNH 7205	1200 - 1280
N Room 65	Lower level	ARF3.02	AMNH 7476	
S Room 9		ARF2.04	AMNH 9234.01	
Wing N Room 111	Burial 25	ARF9.05	AMNH 8760	1200 - 1280
Wing N Room 111	Burial 25	ARF11.03	AMNH 8764	1200 - 1280
Wing N Room 111	Burial 25	ARF11.04	AMNH 8764	1200 - 1280

Archaeological Site/Room	Archaeological Provenience	Mount No.	Artifact No.	Associated Dates A.D. [a]
Wing N Room 111	Burial 25	ARF2.03	AMNH 8764	1200 - 1280
Salmon Ruin				
Room 51W	Secondary occupation	ARF18.02	0296	1125 - 1280
Room 51W	Secondary occupation	ARF22.01	0097	1125 - 1280
Room 62W	Secondary - redeposited	ARF21.01	0065	1125 - 1280
Room 62W		ARF18.01	FS63325 CTI	1125 - 1280
Room 91W		ARF21.02	0310	1125 - 1280
Room 98W	Secondary occupation	ARF8.02	687	1125 - 1280
Room 130W	Secondary reuse of primary feature	ARF8.03	149	1125 - 1280
Room 130W	Secondary reuse of primary feature	ARF8.01	315	1125 - 1280

[a] Dates are approximated.

Chapter 6: Methods

Each step was instrumental in obtaining the best precision and accuracy for the results, including sample preparation, technique, and interpretation.

This chapter describes the methods and procedures used to prepare turquoise provenance and artifact samples for analysis by electron microprobe (EMPA) and secondary ion mass spectrometry (SIMS). Electron microprobe analyses were done using a CAMECA SX-100 and the isotope ratios of D/H and $^{65}Cu/^{63}Cu$ were determined using the CAMECA ims 7f SIMS. Both instruments are located in the Department of Geological Sciences at the University of Manitoba, Winnipeg, Manitoba, Canada.

6.1. Sample Preparation

Turquoise provenance samples were cut into to 1 mm to 1 cm pieces and prepared in epoxy mounts. Large artifacts (>2 cm; e.g., pendants) were mounted in phenol rings, and turquoise source samples and small artifacts (<6 mm; e.g., beads) were mounted in drilled-out 25 mm diameter aluminum mounts using Buehler *Epoxide* epoxy resin. Mounts were polished using various grit (600-2400) SiC sandpaper and 1μm to15-μm-diamond polishing compounds. Polishing was the most destructive part of the procedure for the artifacts and care was taken with the positioning of the artifact in the epoxy so that any areas that were relatively flat were exposed lessening the impact of the polishing. A reflected-light photomap of each mount was made to identify the regions devoid of inclusions and alteration. The polished mounts were washed with a dilute soap solution, rinsed in deionized water and ethanol, and placed in an oven at 60°C for 20 minutes to remove absorbed water.

6.2. Electron Microprobe

Sample mounts were coated with a thin layer of carbon for conductivity. Chemical analyses were obtained using wavelength-dispersion mode with the following conditions, excitation voltage: 15 kV, specimen current: 10 nA, beam size: 10 μm. The element contents of aluminum (Al), copper (Cu), iron (Fe), phosphorus (P), silicon (Si), and sulfur (S) were analyzed with detection limits of the elements on the order of 0.1 wt%. Andalusite was used as the standard for the calibration of Al, copper sulphide ($CuFeS_2$) for Cu, fayalite for Fe, apatite for P, diopside for Si, and pyrite for S. Oxygen contents of turquoise were calculated by stochiometry and H_2O contents were calculated by difference assuming an ideal composition of turquoise [$Cu(Fe,Al)_6(PO_4)_4OH_8 \cdot 4H_2O$]. Backscatter electron images were also obtained to characterize the samples and identify homogenous regions that are devoid of inclusions or defects.

6.3. Secondary Ion Mass Spectrometer

A ~200 Å thick Au coat was sputter-deposited on the sample mount surfaces to ensure a surface conductivity of 5-10 ohms/cm. The mounts were placed in stainless steel sample holders and the entire assembly was placed in the SIMS and held at high vacuum for a minimum of eight hours prior to the start of the analysis sessions. Positive secondary ions were produced by an O^- beam with impact energy of 22.5 keV. The samples and standards were analyzed using 40 nA, -12.5 kv O^- primary beam focused on a ~50 μm spot. The largest contrast (400 μm) and field (1800 μm) apertures, in conjunction with 150 μm image field and an energy bandpass of ±25 eV, were used to maximize sensitivity. The secondary column high voltage was set to 10 kV. For $^2H/^1H$ isotopic measurements, the secondary ion mass spectrometer was operated at a mass resolution of ~800 to separate $^2H^+$ from $^1H^+$ and sample voltage offset of -50 V (e.g., 9950 V), while maintaining the electrostatic analyzer in the secondary column at 10 kV to help minimize the $2H^+$ peak. Each analysis ran for 50 to 80 cycles with a magnet settle time of 0.5 seconds between each mass and an analysis time of 1.04 seconds for ^1H and

5.04 seconds for ^{2}H. A faraday cup detector was used for ^{1}H and an electron multiplier was used for ^{2}H. The gain on the faraday cup relative to electron multiplier was calibrated before each analysis. Linear drift was corrected using mass ^{1}H.

Isobaric interferences for ^{63}Cu and ^{65}Cu isotopes were minimized by offsetting the sample high-voltage by -50 V and using a mass resolving power of ~350. Each analysis ran for 80 cycles with a magnet settle time of 0.5 seconds between mass ^{63}Cu and ^{65}Cu and analysis time of 1.04 seconds for both ^{63}Cu and ^{65}Cu. Both masses were measured using an electron multiplier with a dead time of 27 nanoseconds.

The low-iron turquoise sample from Sleeping Beauty (average Fe content of 0.52 ± 0.3 wt %; Table 6.1) was used as a standard to correct for mass bias for all of the turquoise samples (which were compositionally similar to the Sleeping Beauty sample), except for the high-iron turquoise samples from Castillian (average Fe content of 20.47 ± 1.14 wt %; Table 6.1), which were corrected using a high-iron standard from the Castillian mine. The mass bias session-to-session reproducibility for the turquoise samples from Sleeping Beauty and Castillian was relatively consistent for hydrogen (Figs. 6.1, 6.2, and Tables 6.2, 6.3) and copper isotope analyses (Figs. 6.3, 6.4 and Tables 6.4, 6.5) except for one session due to temperature fluctuations in the lab. Back scatter electron images of the Sleeping Beauty (Fig. 6.5a) and the high-iron turquoise sample from the Castillian Mine (Fig. 6.5b) standards show that the Sleeping Beauty standard is more homogenous at the micrometer-scale relative to the Castillian standard.

Table 6.1. Average Chemical Composition (wt %) Based on 24 (O,OH) and 11 Cations, for Turquoise.

Deposit	Weight% Al	P	Cu	Fe	Si	S	Ca	H	O	Elemental % Fe	Ratio Fe/Al
Sleeping Beauty											
SB-1	19.82	15.78	6.73	0.49	0.00	0.15	0.08	1.88	55.06	2.42	0.0248
SB-1	19.83	15.84	6.78	0.50	0.00	0.14	0.06	1.86	54.98	2.45	0.0251
SB-1	20.01	15.75	6.91	0.51	0.00	0.16	0.07	1.82	54.76	2.48	0.0255
SB-1	19.98	15.72	6.73	0.53	0.00	0.15	0.05	1.87	54.97	2.59	0.0266
SB-1	20.06	15.99	6.84	0.48	0.00	0.13	0.07	1.77	54.66	2.31	0.0237
SB-1	20.09	15.90	6.81	0.54	0.01	0.13	0.08	1.78	54.66	2.60	0.0267
SB-1	19.91	15.86	6.79	0.51	0.01	0.14	0.06	1.84	54.89	2.48	0.0255
SB-1	20.11	16.09	6.95	0.55	0.00	0.14	0.08	1.71	54.37	2.67	0.0275
SB-1	19.94	15.82	6.88	0.54	0.01	0.15	0.06	1.82	54.77	2.66	0.0273
SB-1	19.90	15.89	6.84	0.54	0.00	0.15	0.06	1.82	54.79	2.66	0.0273
Avg	19.97	15.86	6.83	0.52	0.00	0.14	0.07	1.82	54.79	2.53	0.03
Std	0.10	0.11	0.07	0.03	0.00	0.01	0.01	0.05	0.20	0.12	0.00
Castillian Mine											
CAS-1	7.90	14.00	4.62	21.88	0.01	0.33	0.03	1.70	49.53	73.48	2.7710
CAS-1	9.35	14.23	5.22	19.75	0.01	0.30	0.02	1.60	49.52	67.86	2.1114
CAS-1	8.60	14.09	4.99	21.11	0.01	0.34	0.03	1.60	49.24	71.04	2.4533
CAS-1	8.51	13.95	5.00	21.05	0.01	0.34	0.03	1.66	49.45	71.21	2.4736
CAS-1	7.93	13.99	4.45	22.17	0.01	0.34	0.04	1.67	49.40	73.66	2.7965
CAS-1	9.11	14.17	5.23	20.04	0.01	0.31	0.05	1.61	49.46	68.75	2.1999
CAS-1	8.69	14.17	4.96	20.88	0.01	0.31	0.03	1.61	49.34	70.61	2.4023
CAS-1	9.56	14.40	5.29	19.18	-0.01	0.29	0.03	1.60	49.63	66.74	2.0064
CAS-1	9.83	14.27	5.44	18.68	0.01	0.29	0.03	1.63	49.82	65.53	1.9007
CAS-1	9.18	14.28	5.30	19.94	0.00	0.31	0.03	1.58	49.37	68.48	2.1725
Avg	8.87	14.16	5.05	20.47	0.01	0.32	0.03	1.63	49.48	69.74	2.33
Std	0.65	0.15	0.32	1.14	0.01	0.02	0.01	0.04	0.16	2.73	0.30

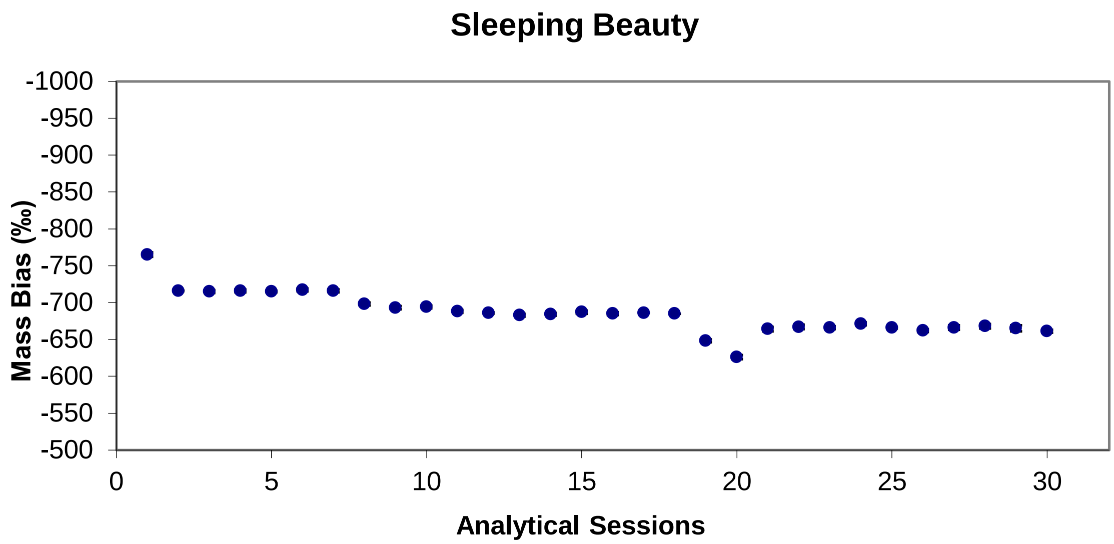

Fig. 6.1. Mass bias verses analytical sessions for hydrogen isotope analyses for the low-iron turquoise standard (average Fe content of 0.52 ± 0.3 wt %; Table 6.1) from Sleeping Beauty (Table 6.2). These 30 analytical sessions were run from March 3, 2009 through August 10, 2010 showing consistent values over time.

Table 6.2. Hydrogen Isotope Fractionation Factor and Mass Bias Data for the Turquoise Standard from Sleeping Beauty.

Analytical Session	Number of Analyses	Fractionation Factor	Mass Bias	1σ	Date
1	6	0.2348	-765	3	Mar 3 2009
2	5	0.2837	-716	1	Apr 10 2009
3	5	0.2851	-715	2	Apr 11 2009
4	5	0.2838	-716	2	Apr 12 2009
5	4	0.2852	-715	1	Apr 13 2009
6	6	0.2830	-717	2	Apr 14 2009
7	6	0.2836	-716	2	Apr 15 2009
8	4	0.3024	-698	2	Sep 9 2009
9	4	0.3068	-693	2	Sep 10 2009
10	5	0.3062	-694	2	Sep 11 2009
11	4	0.3115	-688	2	Sep 13 2009
12	4	0.3137	-686	1	Sep 14 2009
13	4	0.3175	-683	2	Sep 16 2009
14	3	0.3164	-684	2	Sep 17 2009
15	3	0.3132	-687	2	Sep 18 2009
16	3	0.3145	-685	2	Sep 19 2009
17	4	0.3141	-686	0	Sep 20 2009
18	2	0.3148	-685	0	Sep 21 2009
19	4	0.3520	-648	2	Feb 26 2010
20	6	0.3736	-626	3	Mar 2 2010
21	4	0.3359	-664	3	Jul 30 2010
22	3	0.3334	-667	3	Aug 1 2010
23	4	0.3338	-666	2	Aug 2 2010
24	5	0.3286	-671	2	Aug 3 2010
25	4	0.3335	-666	1	Aug 5 2010
26	6	0.3377	-662	2	Aug 6 2010
27	6	0.3340	-666	3	Aug 7 2010
28	6	0.3323	-668	3	Aug 8 2010
29	4	0.3354	-665	4	Aug 9 2010
30	4	0.3385	-661	2	Aug 10 2010

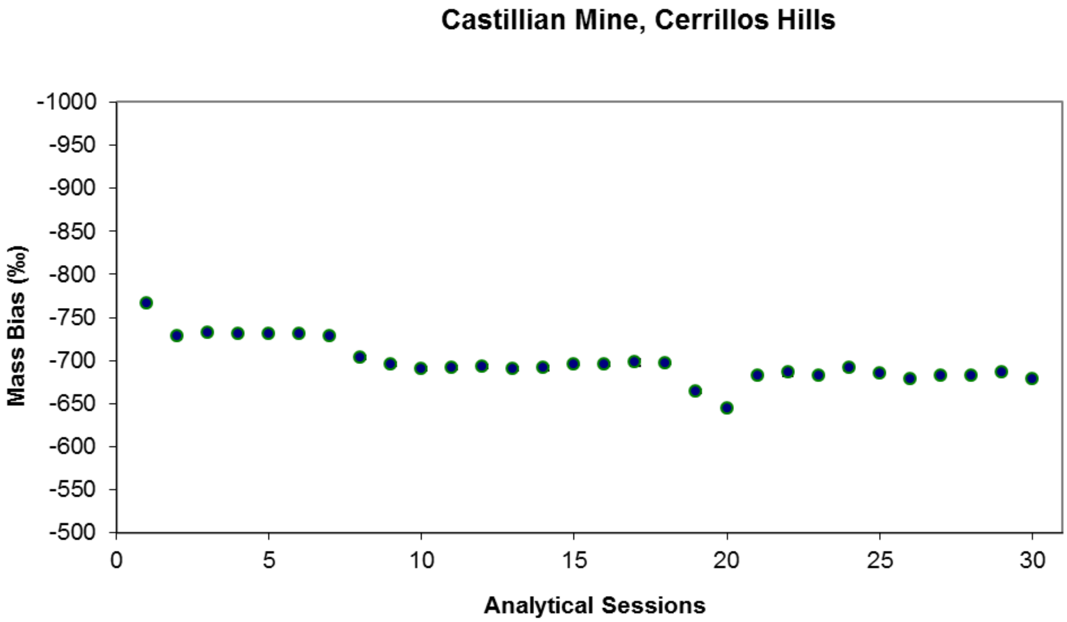

Fig. 6.2. Mass bias verses analytical sessions for hydrogen isotope analyses for the high-iron turquoise standard (average Fe content of 20.47 ± 1.14 wt %; Table 6.1) from Castillian Mine (Table 6.3). These data were collected during the same analytical sessions as the low-iron turquoise standard from Sleeping Beauty, showing similar consistent trends.

Table 6.3. Hydrogen Isotope Fractionation Factor and Mass Bias Data for the Turquoise Standard from Castillian Mine.

Analytical Session	Number of Analyses	Fractionation Factor	Mass Bias	1σ	Date
1	6	0.2330	-767	1	Mar 3 2009
2	6	0.2716	-728	3	Apr 10 2009
3	4	0.2678	-732	2	Apr 11 2009
4	5	0.2687	-731	1	Apr 12 2009
5	4	0.2689	-731	2	Apr 13 2009
6	4	0.2688	-731	1	Apr 14 2009
7	8	0.2709	-729	2	Apr 15 2009
8	4	0.2963	-704	2	Sep 9 2009
9	3	0.3047	-695	2	Sep 10 2009
10	4	0.3098	-690	2	Sep 11 2009
11	4	0.3079	-692	2	Sep 13 2009
12	4	0.3070	-693	2	Sep 14 2009
13	4	0.3099	-690	2	Sep 16 2009
14	3	0.3094	-691	2	Sep 17 2009
15	3	0.3054	-695	0	Sep 18 2009
16	4	0.3038	-696	2	Sep 19 2009
17	4	0.3021	-698	4	Sep 20 2009
18	3	0.3028	-697	1	Sep 21 2009
19	5	0.3359	-664	2	Feb 26 2010
20	7	0.3552	-645	2	Mar 2 2010
21	5	0.3184	-682	2	Jul 30 2010
22	6	0.3145	-686	4	Aug 1 2010
23	4	0.3166	-683	2	Aug 2 2010
24	5	0.3094	-691	3	Aug 3 2010
25	3	0.3147	-685	1	Aug 5 2010
26	4	0.3205	-679	1	Aug 6 2010
27	7	0.3172	-683	3	Aug 7 2010
28	5	0.3168	-683	2	Aug 8 2010
29	4	0.3141	-686	1	Aug 9 2010
30	5	0.3207	-679	3	Aug 10 2010

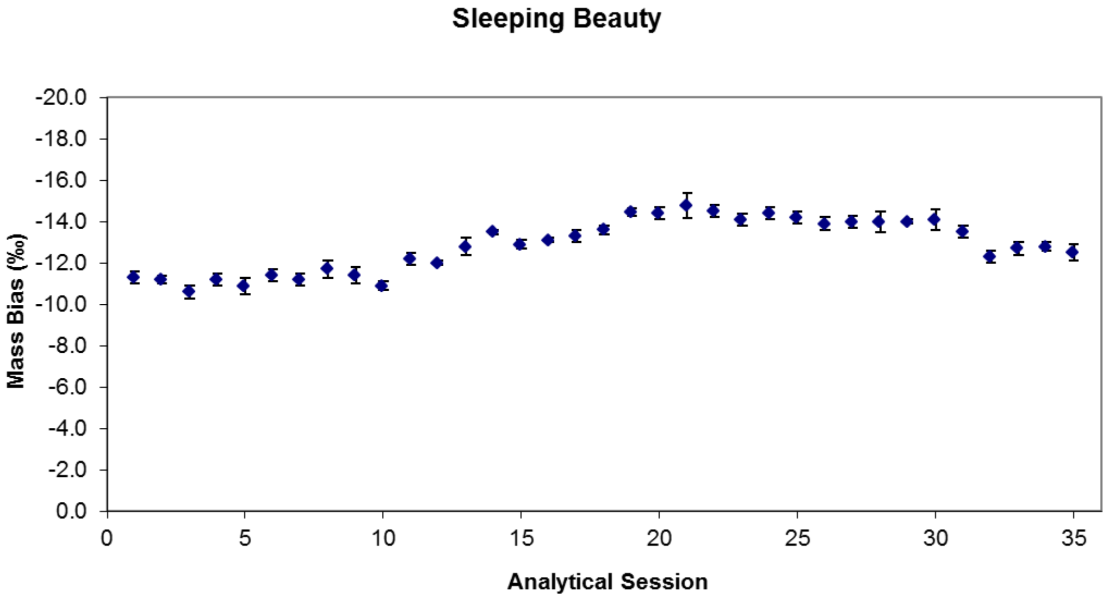

Fig. 6.3. Mass bias verses analytical sessions for copper isotope analyses for the low-iron turquoise standard (average Fe content of 0.52 ± 0.3 wt %; Table 6.1) from Sleeping Beauty (Table 6.4). These 35 analytical sessions were run from March 18, 2009 through September 4, 2010 showing consistent values over time.

Table 6.4. Copper Isotope Fractionation Factor and Mass Bias Data for the Turquoise Standard from Sleeping Beauty.

Analytical Session	Number of Analyses	Fractionation Factor	Mass Bias	1σ	Date
1	5	0.9887	-11.3	0.3	Mar 18 2009
2	6	0.9888	-11.2	0.2	Mar 19 2009
3	4	0.9894	-10.6	0.3	Mar 20 2009
4	4	0.9888	-11.2	0.3	Mar 21 2009
5	6	0.9891	-10.9	0.4	Mar 22 2009
6	4	0.9886	-11.4	0.3	Mar 23 2009
7	4	0.9888	-11.2	0.3	Apr 2 2009
8	5	0.9883	-11.7	0.4	Apr 3 2009
9	7	0.9886	-11.4	0.4	Apr 4 2009
10	5	0.9891	-10.9	0.2	Apr 6 2009
11	5	0.9878	-12.2	0.3	Jun 6 2009
12	5	0.9880	-12.0	0.1	Jun 7 2009
13	5	0.9872	-12.8	0.4	Jun 9 2009
14	4	0.9865	-13.5	0.1	Jun 10 2009
15	4	0.9871	-12.9	0.2	Jun 11 2009
16	3	0.9869	-13.1	0.1	Jun 13 2009
17	5	0.9867	-13.3	0.3	Jan 11 2010
18	5	0.9864	-13.6	0.2	Jan 12 2010
19	4	0.9855	-14.5	0.2	Jan 28 2010
20	5	0.9856	-14.4	0.3	Jan 29 2010
21	4	0.9852	-14.8	0.6	Jan 30 2010
22	4	0.9855	-14.5	0.3	Feb 22 2010
23	6	0.9859	-14.1	0.3	Feb 23 2010
24	5	0.9856	-14.4	0.3	Feb 24 2010
25	5	0.9858	-14.2	0.3	Feb 25 2010
26	5	0.9861	-13.9	0.3	Aug 10 2010
27	5	0.9860	-14.0	0.3	Aug 11 2010
28	5	0.9860	-14.0	0.5	Aug 12 2010
29	5	0.9860	-14.0	0.1	Aug 13 2010
30	4	0.9859	-14.1	0.5	Aug 15 2010
31	4	0.9865	-13.5	0.3	Aug 16 2010
32	7	0.9877	-12.3	0.3	Aug 30 2010
33	6	0.9873	-12.7	0.3	Aug 31 2010
34	4	0.9872	-12.8	0.2	Sep 3 2010
35	4	0.9875	-12.5	0.4	Sep 4 2010

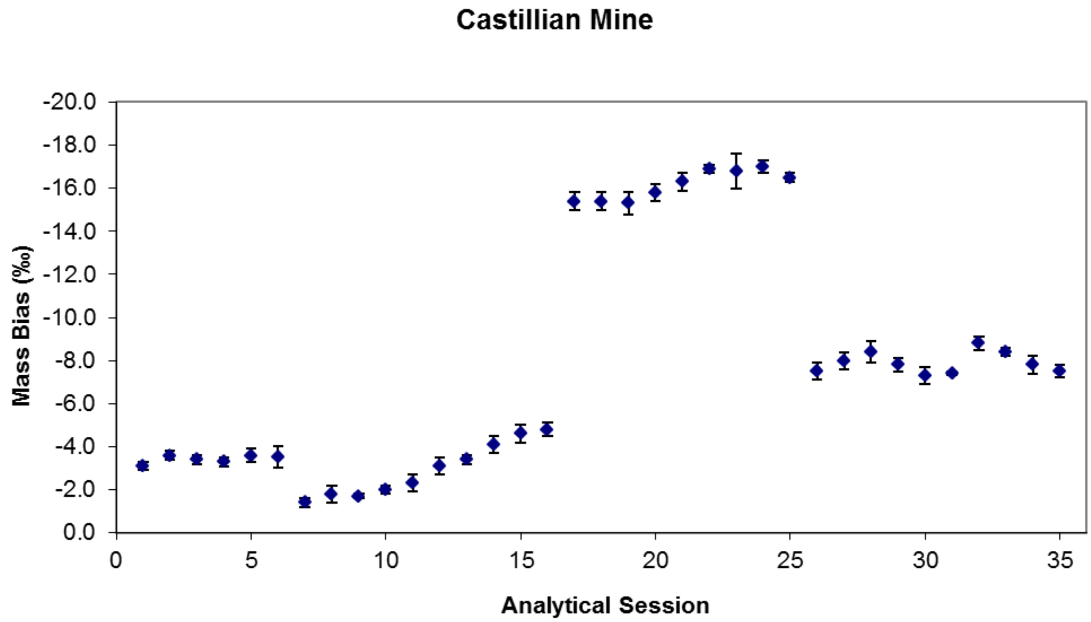

Fig. 6.4. Mass bias verses analytical sessions for copper isotope analyses for the high-iron turquoise standard (average Fe content of 20.47 ± 1.14 wt %; Table 6.1) from the Castillian Mine (Table 6.5). These data were collected during the same analytical sessions as the low-iron turquoise standard from Sleeping Beauty. These data show a heterogeneous mass bias over time.

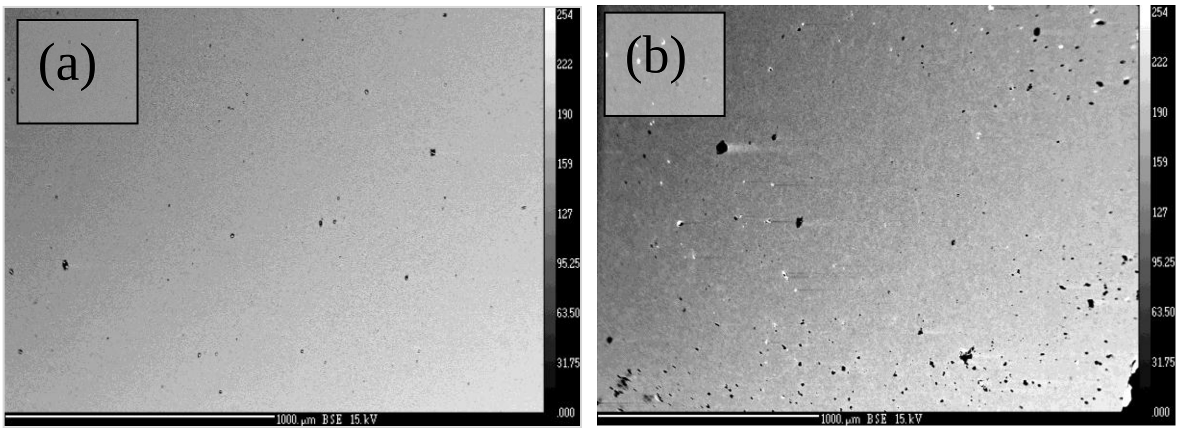

Fig. 6.5. Back scatter electron microprobe images showing (a) the homogenous low-iron turquoise sample from Sleeping Beauty and (b) the heterogeneous high-iron turquoise sample from the Castillian Mine.

Table 6.5. Copper Isotope Fractionation Factor and Mass Bias Data for the Turquoise Standard from Castillian Mine.

Analytical Session	Number of Analyses	Fractionation Factor	Mass Bias	1σ	Date
1	3	0.9969	-3.1	0.2	Mar 18 2009
2	5	0.9964	-3.6	0.2	Mar 19 2009
3	6	0.9966	-3.4	0.2	Mar 20 2009
4	5	0.9967	-3.3	0.2	Mar 21 2009
5	4	0.9964	-3.6	0.3	Mar 22 2009
6	4	0.9965	-3.5	0.5	Mar 23 2009
7	5	0.9886	-1.4	0.2	Apr 2 2009
8	6	0.9982	-1.8	0.4	Apr 3 2009
9	6	0.9983	-1.7	0.1	Apr 4 2009
10	5	0.9980	-2.0	0.2	Apr 6 2009
11	6	0.9977	-2.3	0.4	Jun 6 2009
12	8	0.9969	-3.1	0.4	Jun 7 2009
13	5	0.9966	-3.4	0.2	Jun 9 2009
14	5	0.9959	-4.1	0.4	Jun 10 2009
15	5	0.9954	-4.6	0.4	Jun 11 2009
16	4	0.9952	-4.8	0.3	Jun 13 2009
17	5	0.9846	-15.4	0.4	Jan 11 2010
18	5	0.9846	-15.4	0.4	Jan 12 2010
19	5	0.9847	-15.3	0.5	Jan 28 2010
20	5	0.9842	-15.8	0.4	Jan 29 2010
21	6	0.9837	-16.3	0.4	Jan 30 2010
22	3	0.9831	-16.9	0.2	Feb 22 2010
23	5	0.9832	-16.8	0.8	Feb 23 2010
24	5	0.9830	-17.0	0.3	Feb 24 2010
25	5	0.9835	-16.5	0.2	Feb 25 2010
26	4	0.9825	-7.5	0.4	Aug 10 2010
27	6	0.9920	-8.0	0.4	Aug 11 2010
28	5	0.9916	-8.4	0.5	Aug 12 2010
29	6	0.9922	-7.8	0.3	Aug 13 2010
30	4	0.9927	-7.3	0.4	Aug 15 2010
31	4	0.9926	-7.4	0.1	Aug 16 2010
32	7	0.9912	-8.8	0.3	Aug 30 2010
33	4	0.9916	-8.4	0.2	Aug 31 2010
34	5	0.9922	-7.8	0.4	Sep 3 2010
35	4	0.9925	-7.5	0.3	Sep 4 2010

Hydrogen and copper isotopic compositions were reported as delta (δ) values in units of per mil (parts per thousand (‰)) relative to the standard, Vienna Standard Mean Ocean Water (V-SMOW) for hydrogen and NIST976 for copper such that:

$\delta_A=[(R_A-R_{STD})/\ R_{STD}]x10^3$

where R_A and R_{STD} were the absolute ratios of $^2H/^1H$ (D/H; D=deuterium) or $^{65}Cu/^{63}Cu$ in the sample (turquoise) and the standard (V-SMOW or NIST976), respectively. The absolute $^2H/^1H$ ratio of V-SMOW is $155.76x10^{-6}$ (Hagemann et al. 1970) and the absolute $^{65}Cu/^{63}Cu$ ratio of NIST976 is defined as 4.4563×10^{-1}. Also, see Chapter 2 for discussion of IMF and the measurement of isotope ratios by SIMS.

The results for turquoise provenance and artifact samples were presented as average δ values at 2σ (95% confidence) calculated as:

((x) ^2+(y) ^2) ^0.5

where x was the error associated with the spot to spot reproducibility (listed in appendixes 2, 3, 5, and 6) and y equaled the counting statistical error for each spot. Statistical errors ranged from 4 to 6 ‰ for D/H and 0.4 to 0.5‰ for $^{65}Cu/^{63}Cu$ isotope ratios.

Turquoise artifacts that plotted in overlapping distribution patterns of turquoise provenance regions were assigned a region by measuring the distance of the centroid of the turquoise artifact and the centroid of the turquoise provenance regions and selecting the shortest distance.

Chapter 7: Results

"*Any sort of 'fingerprint' geological or otherwise, is only as good as the data base within which you can compare it*." (Lee 2004:302)

This chapter presents the results of the isotope ratios obtained for the turquoise comparative database and the artifacts. As noted in Chapter 6, the hydrogen and copper isotopic compositions are reported as delta (δ) values in units of per mil (parts per thousand (‰)). For the comparative data base, the average values of the δD_{VSMOW} and $\delta^{65}Cu_{NIST976}$ results are presented in plots in the first section of this chapter; seven of the plotted δD_{VSMOW} and $\delta^{65}Cu_{NIST976}$ results are shown with maps to compare the relationship of the hydrogen and copper isotopic values with the geographic locations. In the second section of this chapter, the δD_{VSMOW} and $\delta^{65}Cu_{NIST976}$ results for the archaeological sites are presented in four separate plots; one each for Pueblo Bonito, the small sites in Chaco Canyon, Aztec Ruin, and Salmon Ruin.

7.1. Turquoise Provenance Regions

Twenty-one turquoise resource areas were geochemically characterized and comprised the comparative reference database. Figure 7.1 displays a map of the western United States and the geographical location of the turquoise resource areas in this study. A recap of the average values of the δD_{VSMOW} and $\delta^{65}Cu_{NIST976}$ results of the turquoise resource areas and the standard deviation (2σ) are listed in Table 7.1. These results are plotted and displayed in Figure 7.2 showing δD_{VSMOW} versus $\delta^{65}Cu_{NIST976}$ with color boxes representing the 2σ range. The hydrogen isotopic analyses data of turquoise provenance samples are listed in Appendix 2 and the copper isotopic analyses data are listed in Appendix 3. Sleeping Beauty and Castillian were used as standards and their δD_{VSMOW} and $\delta^{65}Cu_{NIST976}$ measurements were collected during each analytical session. A plot of δD_{VSMOW} versus $\delta^{65}Cu_{NIST976}$ (Fig. 7.2) showed good separation among the mines although there was some overlap. The majority, but not all, of the overlapping

Fig. 7.1. Location of the 21 turquoise resource areas that were isotopically characterized (turquoise resource areas are represented by the blue circles).

Table 7.1. Recap of SIMS Analyses of Hydrogen and Copper Isotope Ratios of Turquoise Provenance Regions.

Turquoise Deposits	Average δD_{VSMOW} (‰)	STD 2σ δD_{VSMOW} (‰)	Average $\delta^{65}Cu_{NIST976}$ (‰)	STD 2σ $\delta^{65}Cu_{NIST976}$ (‰)
Sleeping Beauty, Arizona	-76	7	7.3	0.5
Mineral Park, Arizona	-90	7	4.9	0.6
Morenci, Arizona	-114	6	1.8	0.6
Bisbee, Arizona	-61	8	2.6	0.5
Halloran Springs, California	-98	7	6.8	0.8
Evans Mine, Baja California	-118	6	9.9	0.5
King Manassa, Colorado	-77	7	3.7	0.6
Villa Grove, Colorado	-99	6	2.2	0.7
Leadville, Colorado	-78	6	12.6	0.6
Cripple Creek, Colorado	-87	5	6.7	0.7
Crescent Peak, Nevada	-85	8	4.8	0.6
Royston, Nevada	-114	7	3.6	0.5
Lone Mountain, Nevada	-133	8	6.4	0.6
Blue Gem, Nevada	-136	6	6.9	0.8
Green Tree, Nevada	-119	7	15.0	0.5
Godber Mine, Nevada	-139	7	1.3	0.7
Black Hills, Nevada	-122	5	-0.7	0.7
Verde Blue, Nevada	-123	4	-0.3	0.7
Fox Mine, Nevada	-112	8	14.8	0.5
Old Hachita, New Mexico	-107	5	2.4	0.5
Cerrillos Hills, New Mexico	-95	8	1.1	0.5

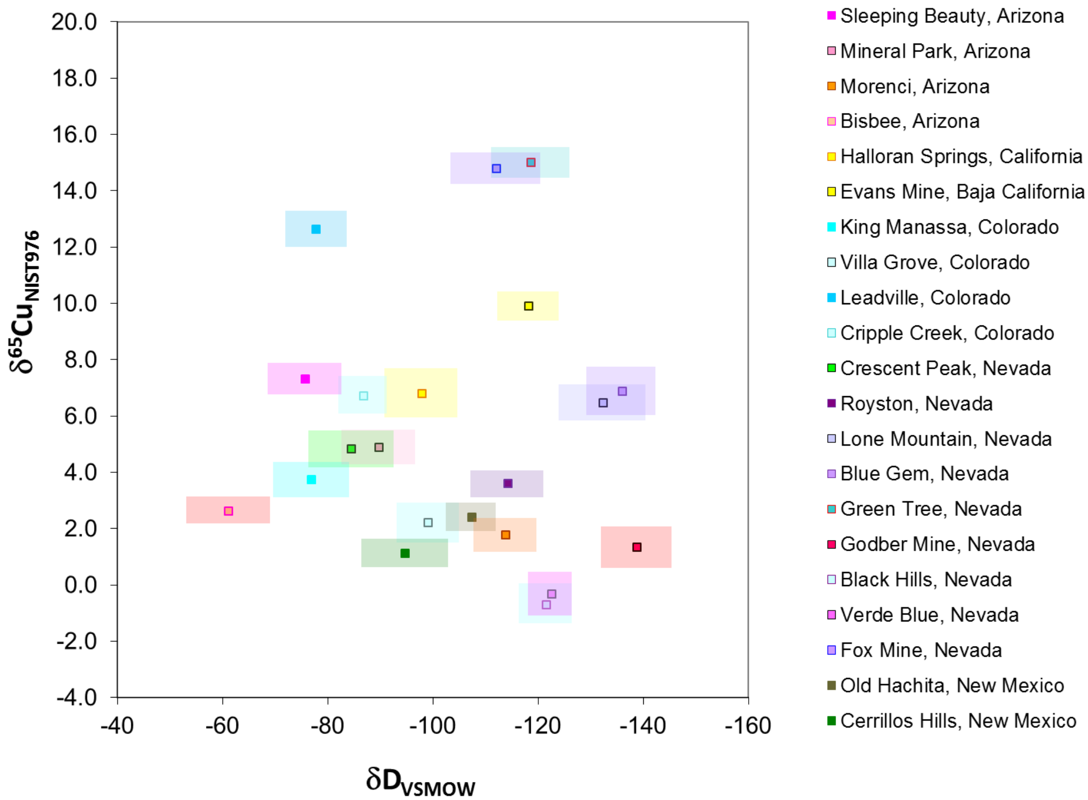

Fig. 7.2. The δD_{VSMOW} and $\delta^{65}Cu_{NIST976}$ values (Table 7.1; 2σ error bars represented by the colored boxes) of the 21 turquoise resource areas represented in this study.

distribution patterns belonged to samples that were from turquoise deposits from the same turquoise provenance region.

For example, the turquoise mines that are located along the Rio Grande Rift and the Rocky Mountains in southern Colorado displayed a 22‰ difference in their average δD values, ranging from King Manassa with an average δD value of -77‰ to Villa Grove with an average δD value of -99‰ (Fig. 7.3a; Table 7.1; Fig 7.3b). However, there was a much larger difference in the range of average δ^{65}Cu values (11.5‰), ranging from an average δ^{65}Cu value of 1.1‰ in the Cerrillos Hills to the average δ^{65}Cu value of 12.6‰ at Leadville (Table 7.1). The average δ^{65}Cu value collected from the Leadville sample was among the highest values obtained; surpassed only by the two deposits in northern Nevada (e.g., the Fox Mine with an average δ^{65}Cu value of 14.8‰ and Green Tree with an average value of 15.0‰; Fig. 7.2; Table 7.1). The distribution patterns of Cerrillos Hills (average δD value of -95‰ and average δ^{65}Cu value of 1.1‰; Table 7.1) and Villa Grove (average δD value at -99‰ and average δ^{65}Cu value of 2.2‰; Table 7.1) showed similar average δD values, but distinct average δ^{65}Cu values. Two of these deposits are located in the San Luis Valley; the Hall Mine located near the town of Villa Grove in the northern end of the valley and the King Manassa (average δD value of -77‰ and average δ^{65}Cu value of 3.7‰; Table 7.1) near La Junta in the southern end of the valley. The Cripple Creek deposit is located further north and on the eastern front of the Rocky Mountains in Colorado. Turquoise from this deposit had an average δD value of -87‰ and an average δ^{65}Cu value of 6.7‰ (Table 7.1). The most northern Colorado turquoise deposit near the town of Leadville, gave an average δD value of -78‰ and an average δ^{65}Cu value of 12.6‰ (Table 7.1).

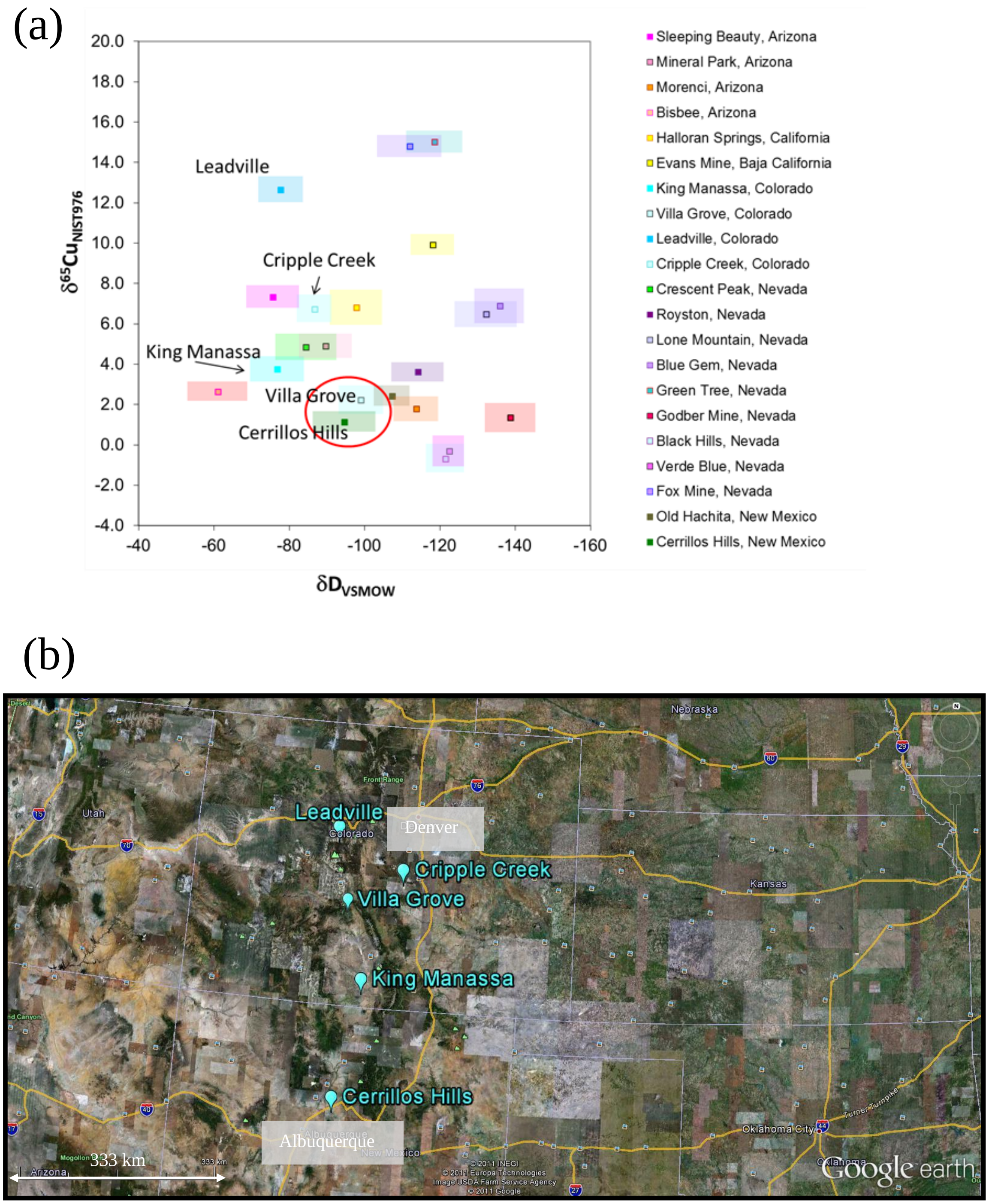

Fig. 7.3. The four principle Colorado turquoise mines and the Cerrillos Hills Mining District in New Mexico (a) labeled in the δD_{VSMOW} and $\delta^{65}Cu_{NIST976}$ plot (Table 7.1) and (b) their geographical locations (Google Earth 2012).

The distribution pattern of the Old Hachita deposit (New Mexico) overlapped with the patterns of the Villa Grove and Morenci (Arizona) deposits (Fig. 7.4a). Old Hachita was the only turquoise deposit represented in this study from southwestern New Mexico and is geographically close to Bisbee and Morenci in Arizona (Fig. 7.4b). The average δ^{65}Cu values clustered with average values of 1.8‰ for the Morenci deposit, 2.6‰ for Bisbee and 2.4‰ for Old Hachita. Morenci and Old Hachita's overlapping average δD values were -114‰ and -107‰ respectively (Table 7.1). The average δD value reported from Bisbee was -61‰ (the highest average δD of all of the turquoise resource areas) and was more similar to the average δD value of the Sleeping Beauty mine, -76‰, located further north of Bisbee (Fig. 7.4b). Turquoise from the Sleeping Beauty mine showed an average δ^{65}Cu value of 7.3‰, which was higher than the average δ^{65}Cu values displayed by the Bisbee, Morenci, and Old Hachita deposits.

The δD and δ^{65}Cu distribution patterns of Mineral Park, near Kingman, Arizona, and the Crescent Peak deposit in southern Nevada (Fig. 7.5a) were similar to each other. Although their locations are divided by state boundaries, they are in the same geographical region (Fig. 7.5b). Turquoise from the Mineral Park deposit had an average δD value of -90‰ and an average δ^{65}Cu value of 4.9‰, whereas Crescent Peak turquoise had average δD and δ^{65}Cu values of -85‰ and 4.8‰, respectively. To the west, in California, Halloran Springs turquoise (Fig. 7.5b) showed an average δD value of -98‰ and average δ^{65}Cu value of 6.8‰ (Fig. 7.5a; Table 7.1).

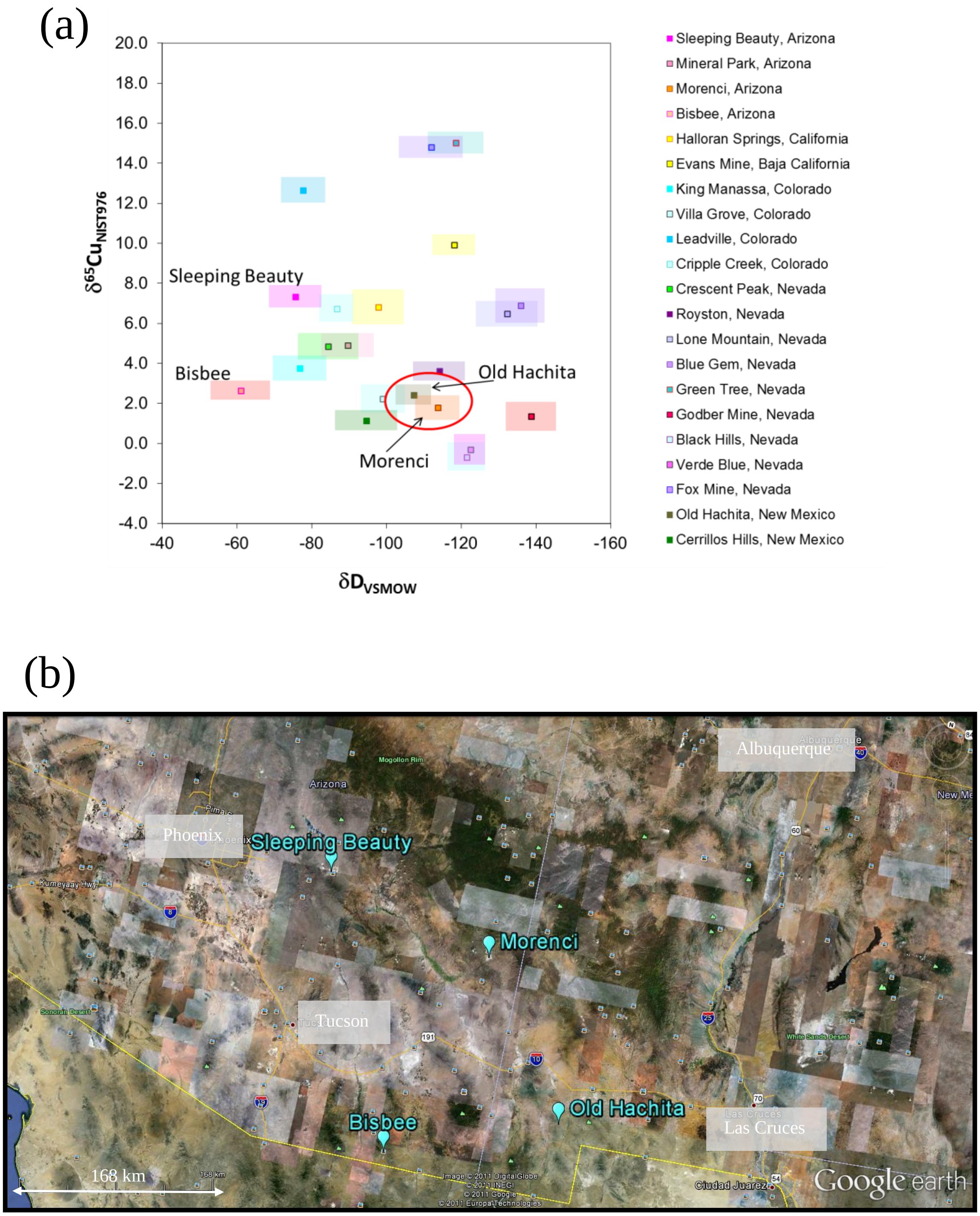

Fig. 7.4. Old Hachita, Bisbee, Morenci, and Sleeping Beauty turquoise resource areas (a) labeled in the δD_{VSMOW} and $\delta^{65}Cu_{NIST976}$ plot (Table 7.1) and (b) their geographical locations (Google Earth 2012).

(a)

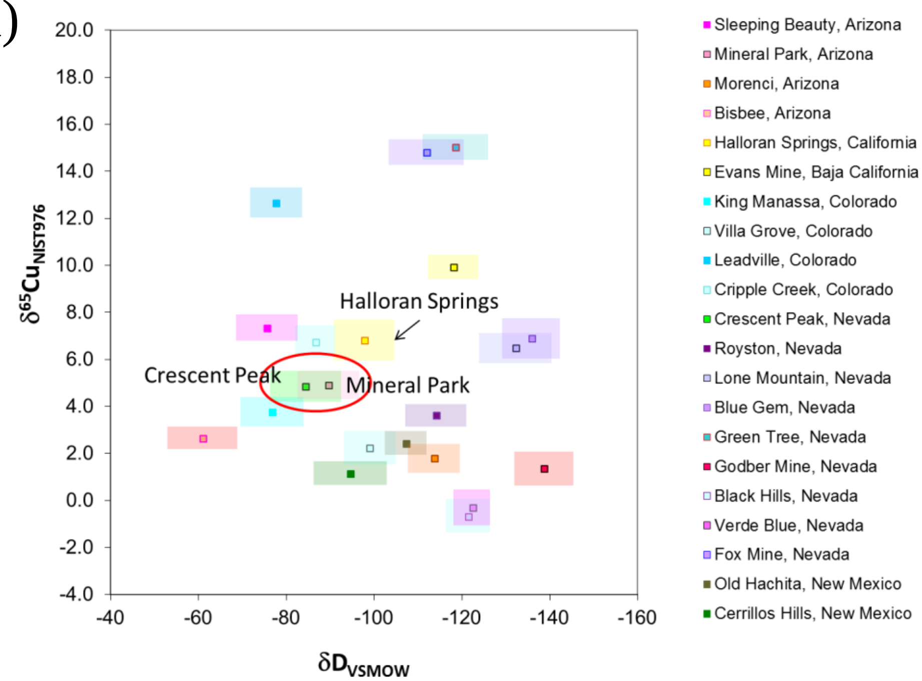

(b)

Fig. 7.5. Halloran Springs, Crescent Peak, and Mineral Park (a) labeled in the δD_{VSMOW} and $\delta^{65}Cu_{NIST976}$ plot (Table 7.1) and (b) their geographical locations (Google Earth 2012).

Although turquoise samples from the Fox Mine and Green Tree turquoise deposits (same turquoise provenance regions) in northern Nevada (Fig. 7.6b) were different in color (Fig. 7.7) they had overlapping distribution patterns (Fig. 7.6a). Both of these turquoise provenance samples were obtained from Weigand's collection at the Museum of Northern Arizona consequently specific location information (e.g., longitude and latitude) was not available. Fox Mine turquoise had an average δD value of -112‰ whereas the average δ^{65}Cu value is 14.8‰. Turquoise from the Green Tree deposit had similar average stable isotopic values, average δD value of -119‰ and average δ^{65}Cu value of 15.0‰ (Table 7.1).

Further to the southwest in Nevada, the Verde Blue and the Black Hills deposits from the same turquoise provenance region also displayed overlapping average δD and average δ^{65}Cu values (Fig. 7.8a, 7.8b). Verde Blue showed an average δD value of -123‰ and an average δ^{65}Cu value of -0.3‰ and the Black Hills turquoise displayed an average δD value of -122‰ and an average δ^{65}Cu value of -0.7‰ (Fig. 7.8a; Table 7.1).

The lowest average δD value reported from the turquoise provenance samples was -139‰ (Fig. 7.9a; Table 7.1) from the Godber deposit in Nevada (Fig. 7.9b). The Godber deposit reported an average δ^{65}Cu value of 1.3‰ (Fig. 7.9a; Table 7.1). Turquoise from the Lone Mountain deposit had an average δD value of -133‰ and an average δ^{65}Cu value of 6.4‰ which overlapped with the average δD value of -136‰ and average δ^{65}Cu value of 6.9‰ of turquoise from the Blue Gem deposit (Fig. 7.9a; Table 7.1). The Royston deposit (Fig. 7.9b), showed an average δD value of -114‰ and an average δ^{65}Cu value of 3.6 ‰ (Fig. 7.9a; Table 7.1).

(a)

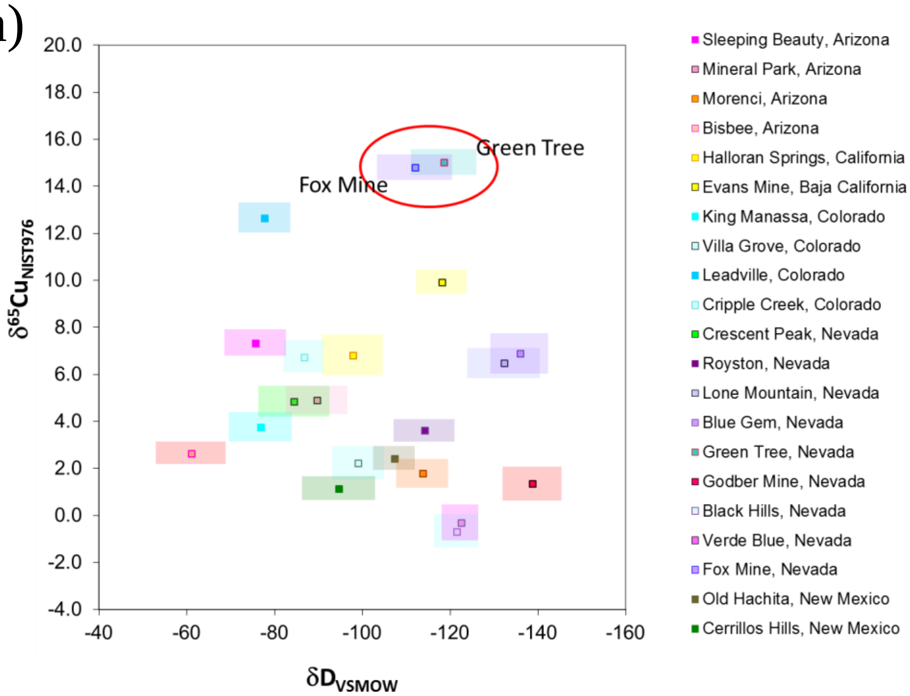

(b)

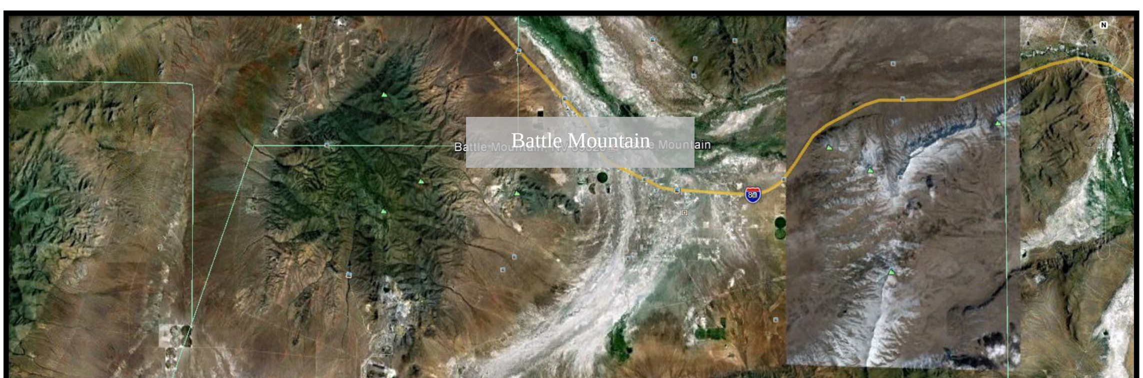

Fig. 7.6. The Fox Mine and Green Tree turquoise resource areas (a) labeled in the δD_{VSMOW} and $\delta^{65}Cu_{NIST976}$ plot (Table 7.1) and (b) their geographical locations (Google Earth 2012).

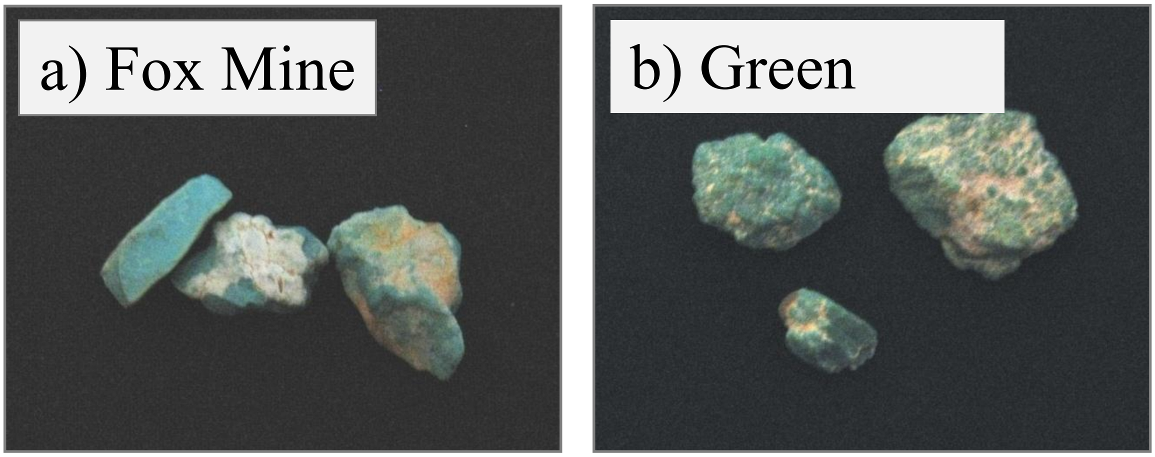

Fig. 7.7. Although very different in appearance, these turquoise provenance samples, (a) the Fox Mine and (b) Green Tree, have overlapping average δD and $\delta^{65}Cu$ values.

(a)

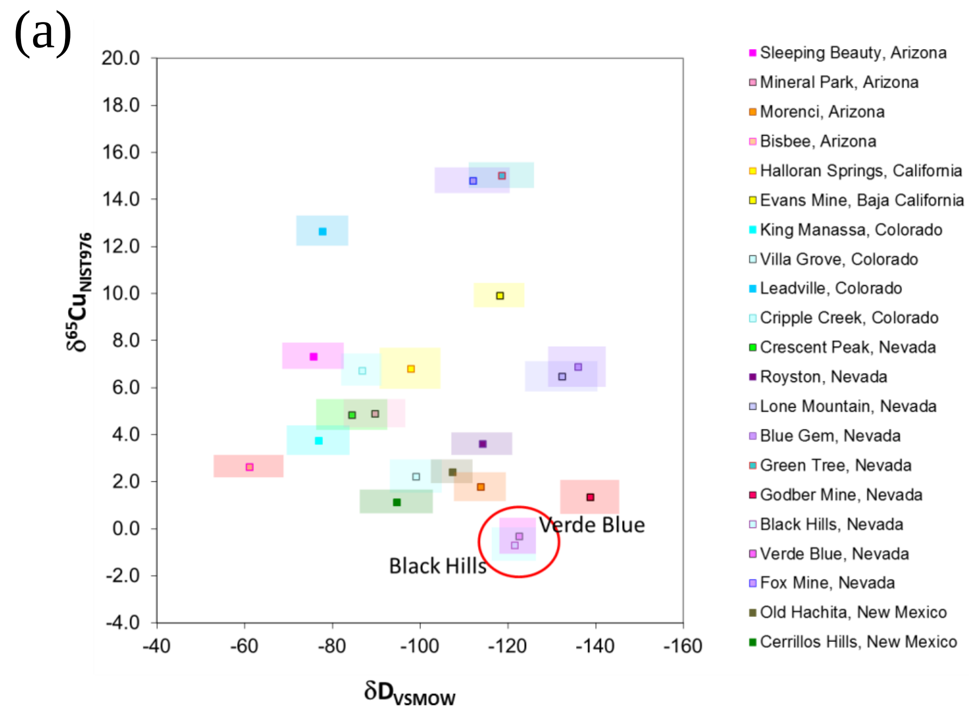

(b)

Fig. 7.8. Black Hills and Verde Blue turquoise resource areas (a) labeled in the δD_{VSMOW} and $\delta^{65}Cu_{NIST976}$ plot (Table 7.1) and (b) their geographical locations (Google Earth 2012).

(a)

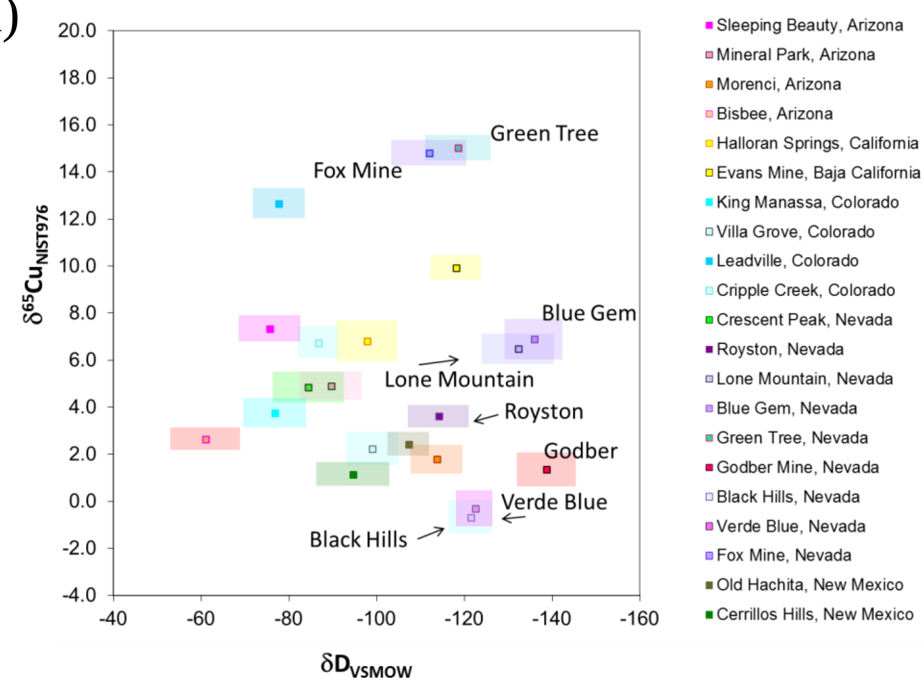

(b)

Fig. 7.9. Nevada turquoise resource areas (a) labeled in the δD_{VSMOW} and $\delta^{65}Cu_{NIST976}$ plot (Table 7.1) and (b) their geographical locations (Google Earth 2012).

Turquoise from the Evans Mine, Baja California, showed an average δD value of -118‰ and an average δ^{65}Cu value of 9.9‰ (Fig. 7.10a; Table 7.1). The Evans Mine (Fig. 7.10b) was the most southern source of turquoise in this study and is located in present-day Mexico.

The average δD and δ^{65}Cu values of the turquoise resource areas (Fig. 7.2; Table 7.1) avails the provenance postulate presented in Chapter 3, that chemical variation within discrete compositional groups is less than variation between compositional groups (Weigand et al. 1977). It was also demonstrated that most of the overlapping distribution patterns of turquoise resource areas tend to group by geographical locations (e.g., Crescent Peak and Mineral Park, Verde Blue and Black Hills). The average δD and δ^{65}Cu values of the 21 turquoise resource areas included in the reference database are sufficiently different to use as an initial database with which to compare the results of artifacts analyses from archaeological sites included in this research.

(a)

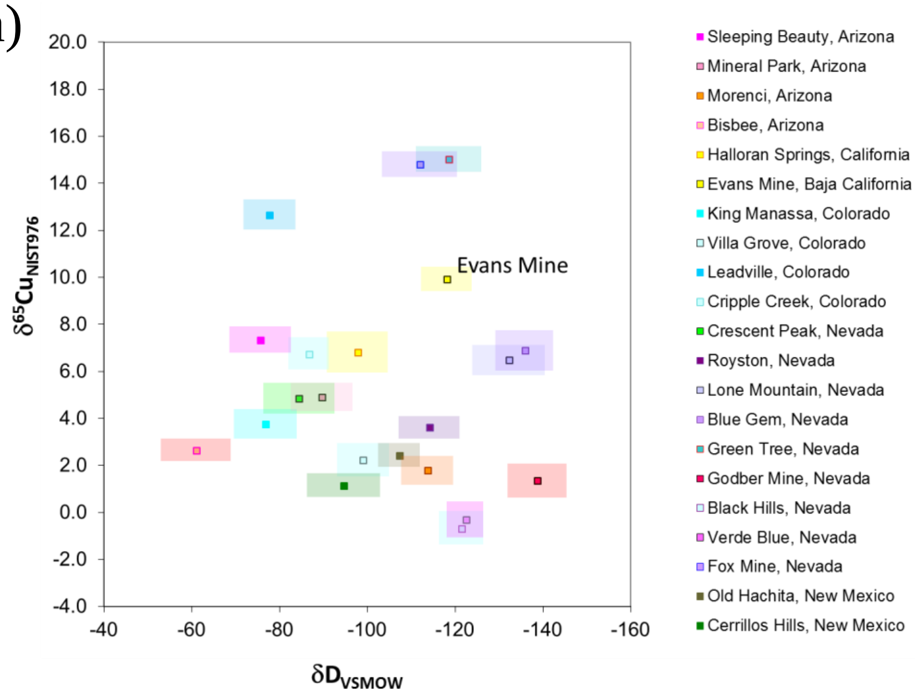

(b)

Fig. 7.10. The Evans Mine (a) labeled in the δD_{VSMOW} and $\delta^{65}Cu_{NIST976}$ plot (Table 7.1) and (b) its geographical location (Google Earth 2012).

7.2 Turquoise Artifacts

Sixty-two turquoise artifacts from the three Ancestral Puebloan great houses and eight small sites in Chaco Canyon were isotopically characterized and compared to the turquoise reference database. Twenty-nine turquoise artifact samples were analyzed from Pueblo Bonito, along with twelve turquoise artifacts samples from the small sites in Chaco Canyon, thirteen turquoise artifact samples from Aztec Ruin, and eight turquoise artifact samples from Salmon Ruin. A recap of the average δD and $\delta^{65}Cu$ values of turquoise artifacts and the standard deviation (2 σ) are listed in Appendix 4. Table 7.2 shows the archaeological sites and the number of turquoise artifacts that were obtained from the associated turquoise resource areas. The hydrogen copper isotopic composition of the turquoise artifacts are listed in Appendix 5 and Appendix 6, respectively. The δD_{VSMOW} and $\delta^{65}Cu_{NIST976}$ of the turquoise artifacts (Appendix 4) from Pueblo Bonito were plotted in Figure 7.11.

The turquoise procurement and exchange pattern from Pueblo Bonito showed a strong representation from the turquoise resource areas that are located along the Rio Grande Rift (Fig. 7.3). Cerrillos Hills is the closest turquoise resource area to Chaco Canyon (~ 200 kilometers) and it was fully expected that much of the turquoise would have been obtained from this region. However, only seven turquoise artifacts plotted within the distribution pattern of Cerrillos Hills whereas eight samples plotted with the distribution pattern of the other mines located along the Rio Grande Rift including King Manassa and Villa Grove (Fig. 7.3). The provenance regions for two turquoise artifacts were Lone Mountain (Fig. 7.9) and Crescent Peak (Fig. 7.5), both in Nevada. The origin of twelve turquoise artifacts was not identified.

Table 7.2. Archaeological Sites and their Associated Turquoise Provenance Regions.

Turquoise Provenance Regions	Pueblo Bonito	Chaco Canyon-Other	Aztec Ruin	Salmon Ruin
Cerrillos Hills, NM	7		1	
King Manassa, CO	2		2	
Villa Grove, CO	6		2	
Cripple Creek, CO			1	
Royston, NV		5		
Lone Mountain, NV	1	1		1
Crescent Peak, NV	1			1
Halloran Springs, CA			1	
Mineral Park, AZ				1
Sleeping Beauty, AZ		1		
Morenci, AZ		1		
Unknown	12	4	6	5
Total Sample	29	12	13	8

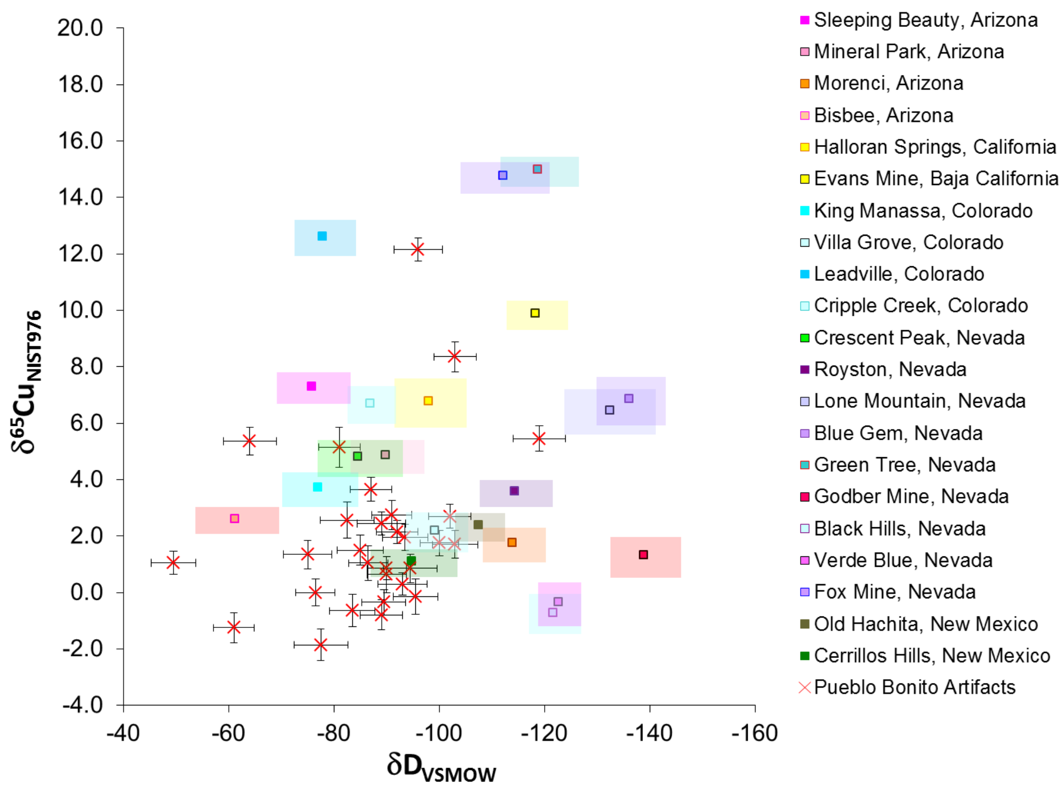

Fig. 7.11. The average δD_{VSMOW} and $\delta^{65}Cu_{NIST976}$ values (2σ error bars represented by the colored boxes) of the 21 turquoise resource areas represented in this study (Fig. 7.2; Table 7.1) with the average δD_{VSMOW} and $\delta^{65}Cu_{NIST976}$ values of the turquoise artifacts from Pueblo Bonito (Appendix 4; 2σ error bars).

There were a total of twelve turquoise artifacts from small sites throughout Chaco Canyon (Fig. 7.12; Appendix 4). Nine turquoise artifacts were from the five archaeological sites that cluster in Marcia's Rincon (29SJ625, 29SJ627, 29SJ628, 29SJ629, and 29SJ633). Five of the these turquoise artifacts originated from Royston, one originated from Lone Mountain (Fig. 7.9), and three of the turquoise artifacts have no known origin (Fig. 7.12). The one turquoise artifact from the Shabik'eshchee site (29SJ1659) plotted in the distribution pattern of Sleeping Beauty (Fig. 7.4) and the one turquoise artifact from site 29SJ423 near Peñasco Blanco plotted in the distribution pattern of Morenci (Fig. 7.4). The turquoise artifact from site 29SJ1360 near Fajada Butte was from an unknown origin. There was a strong difference in the turquoise provenance and exchange patterns of these small sites compared to the pattern from Pueblo Bonito. For example, small sites did not procure turquoise from regions located in present-day Colorado and New Mexico.

The thirteen turquoise artifacts from Aztec Ruin were plotted in Fig. 7.13 (Appendix 4). There were some similarities in the turquoise procurement and exchange pattern of Aztec Ruin and Pueblo Bonito (Fig. 7.11; Appendix 4). One of the turquoise artifacts originated from Cerrillos Hills whereas five others came from the Colorado deposits (Fig. 7.3). Four turquoise artifacts originated from King Manassa (2 artifacts) and Villa Grove (2 artifacts), whereas Cripple Creek was the origin of one turquoise artifact. Halloran Springs (Fig. 7.5) was identified as the turquoise resource area for one of the turquoise artifacts and six were from unknown origins. The major difference among the turquoise provenance and exchange patterns of Aztec Ruin and those patterns

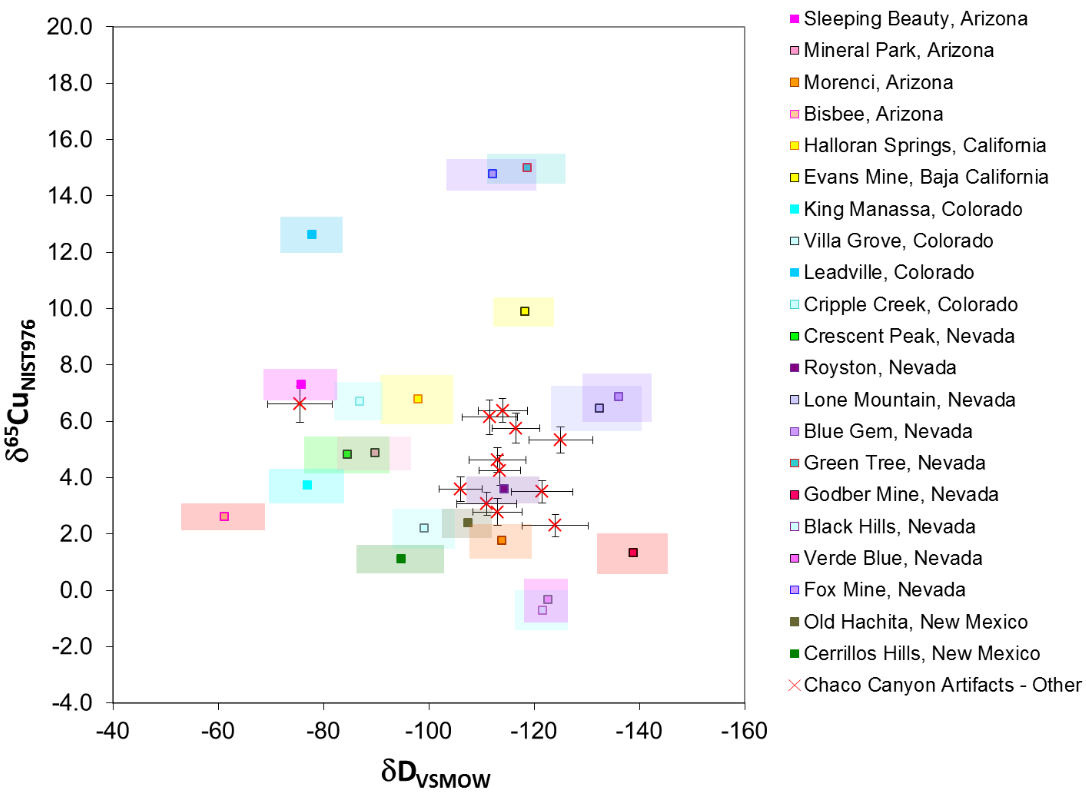

Fig. 7.12. The average δD_{VSMOW} and $\delta^{65}Cu_{NIST976}$ values (2σ error bars represented by the colored boxes) of the 21 turquoise resource areas represented in this study (Fig. 7.2; Table 7.1) with the average δD_{VSMOW} and $\delta^{65}Cu_{NIST976}$ values of the turquoise artifacts from the eight small sites in Chaco Canyon (Appendix 4; 2σ error bars).

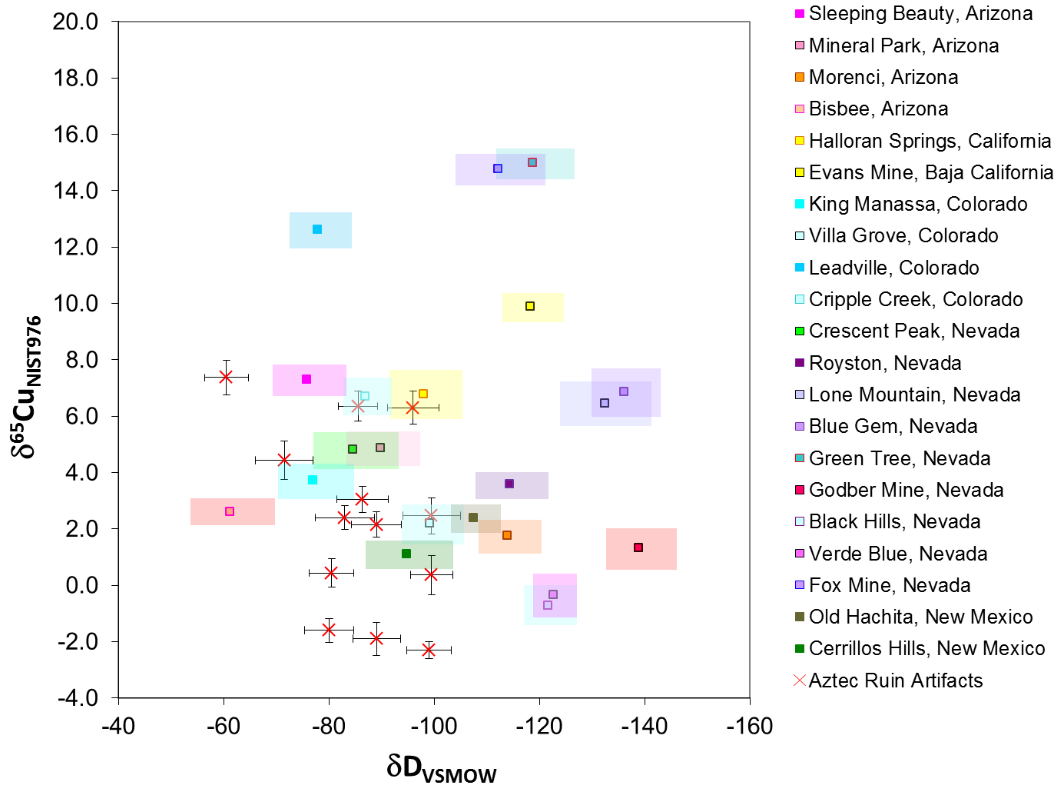

Fig. 7.13. The average δD_{VSMOW} and $\delta^{65}Cu_{NIST976}$ values (2σ error bars represented by the colored boxes) of the 21 turquoise resource areas represented in this study (Fig. 7.2; Table 7.1) with the average δD_{VSMOW} and $\delta^{65}Cu_{NIST976}$ values of the turquoise artifacts from Aztec Ruin (Appendix 4; 2σ error bars).

of the small sites in Chaco Canyon is that Aztec Ruin did not procure turquoise from any turquoise resource areas located in Arizona or Nevada (Fig. 7.12; Appendix 4).

There were eight turquoise artifacts samples analyzed from Salmon Ruin (Fig. 7.14; Appendix 4). The turquoise resource areas identified for three of the turquoise artifacts were all from the west including Lone Mountain (Fig. 7.9), Crescent Peak, and Mineral Park (Fig. 7.5). The only common source of turquoise for Salmon Ruin and Pueblo Bonito were the Nevada turquoise resource areas (Fig. 7.11; Appendix 4).

Although the turquoise procurement and exchange patterns among Pueblo Bonito and the small sites in Chaco Canyon were not similar, similarities were recognized among the patterns of Pueblo Bonito and Aztec Ruin, and among the patterns of Salmon Ruin and the small sites that cluster in Marcia's Rincon. Cerrillos Hills and turquoise resources areas located in Colorado were identified as the origin of a high percentage of the turquoise artifacts from Pueblo Bonito (51%) and Aztec Ruin (46%), especially when considering that the origin of 57% of the artifacts from Pueblo Bonito and 46% of the artifacts from Aztec Ruin were not identified. The identified provenance of the turquoise from the sites in Marcia's Rincon and Salmon Ruin tend to originate from turquoise resource areas located in Nevada western Arizona (Mineral Park). There were 27 turquoise artifacts that did not plot within the distribution pattern of any of the isotopically characterized turquoise resource areas. As more turquoise provenance samples are isotopically characterized, the origin of these turquoise artifacts may be identified. Some of the artifacts with unknown origins did cluster in groups, which implies that there may be a unique source for each group. For example, in Figures 7.11 and 7.13 there were groups of artifacts that plotted in the range of average δD values between -77‰ and -99‰ and average $\delta^{65}Cu$ values between -2.3‰ and 0.0‰.

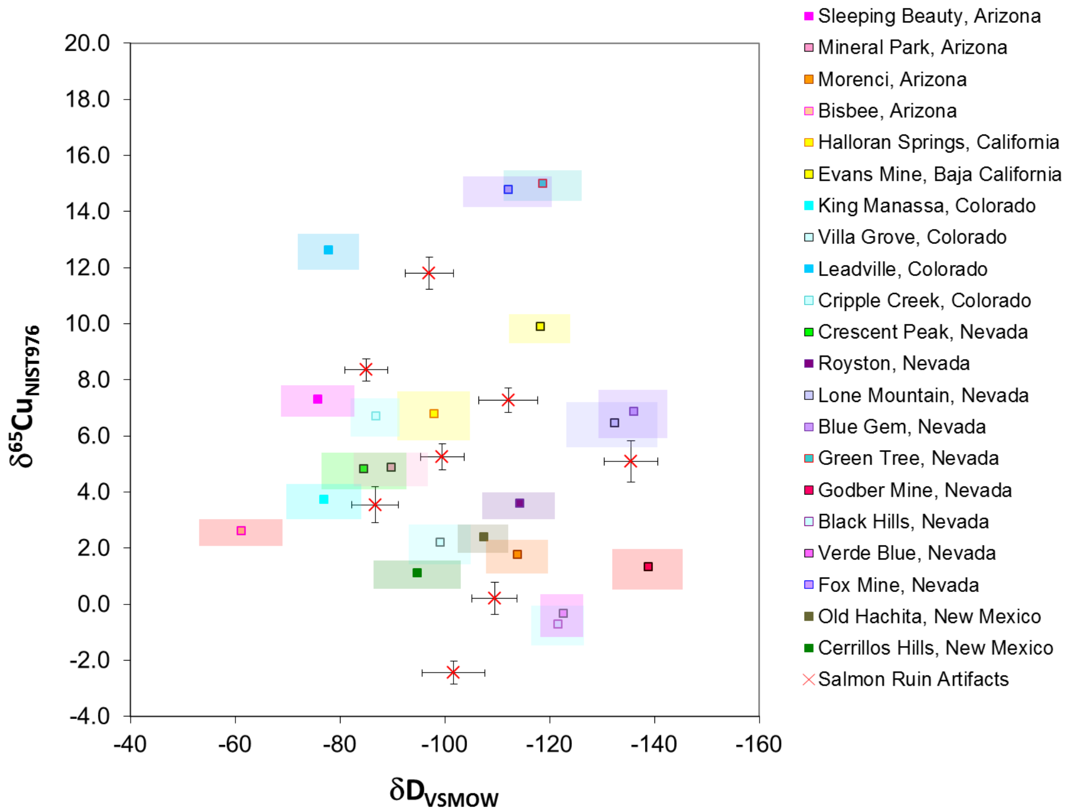

Fig. 7.14. The average δD_{VSMOW} and $\delta^{65}Cu_{NIST976}$ values (2σ error bars represented by the colored boxes) of the 21 turquoise resource areas represented in this study (Fig. 7.2; Table 7.1) with the average δD_{VSMOW} and $\delta^{65}Cu_{NIST976}$ values of the turquoise artifacts from Salmon Ruin (Appendix 4; 2σ error bars).

Chapter 8: Discussion: Turquoise Procurement Strategies in the Chacoan World

"*Explorers to the Southwest were impressed by the amount of trade they witnessed and the distances walked by Indian traders*." (Ford 1983:712)

There are several hypotheses (see Chapter 4) that have been proposed to model exchange/trade networks and relationships in the Greater Southwest (e.g., Di Peso 1974; Ford 1983; Foster 1986, 1999; Frisbie 1978; Janetski 2002; Kelley 1986, 1993, 1995; LeBlanc 1986; Nelson 1986; Renfrew 1986; Reyman 1978; Weigand and Harbottle 1993; Weigand et al. 1977). However, beyond ceramics (e.g., Habicht-Mauche et al. 2000; Neitzel and Bishop 1990) and obsidian (e.g., Shackley 1998, 1995), there are few geochemical studies that have been developed to support these exchange models (e.g., Harbottle and Weigand 1992; Hull et al. 2008; Thibodeau et al. 2007; Weigand and Harbottle 1993; Weigand et al. 1977). In an effort to overcome the paucity of geochemical data, a regional comparative database based on 21 turquoise resource areas was developed and 62 artifacts from three great house communities and eight small sites within Chaco Canyon were analyzed. The data from this study are compared to various culture history models and three of the exchange/trade models, and are discussed in this chapter.

Applying the concepts of the core-periphery model to the Chaco World as a cohesive unit with Chaco Canyon as the core regional center is a useful tool to link the turquoise resource areas with the center of the Ancestral Puebloan culture group. A core–periphery model has the following attributes: 1) commodities moved into the core regional center from several peripheral locales, 2) the presence of an elite group, and 3) the core regional center shows dominance over peripheral locales and long-distance traders. The prestige goods model is used to investigate the relationship and turquoise procurement strategies among the people who inhabited Chaco Canyon, Aztec Ruin, and Salomon Ruin. The prestige goods model is based on the alliance of an elite group through exchange of valuable goods. The elite are associated with political power and are in control of exotic items, such as turquoise. The exotic items are usually found to cluster in the larger center rather than small sites (Nelson 1986). The trade festival model is applied to investigate the social and exchange relationships, and the diverse turquoise procurement and exchange patterns among the sites within Chaco Canyon. This model is based on ethnographic accounts of historic trade festivals held at Taos and Pecos Pueblos (e.g., Ford 1983) and is applicable to sites where the presence of organized and prescheduled gathering of multiethnic groups for trade and other festivities is proposed (e.g., Bernardini 1999).

8.1 The Core-Periphery Model

The data show that Chaco Canyon fits the definition of a core regional center, described as centers of culture, innovation, technology, politics, religion, and redistribution (Palerm and Wolf 1957). The movement of turquoise into Chaco Canyon was from multiple resource areas, some hundreds of kilometers from the Canyon (Fig. 8.1; Table 7.2; Appendix 4). For example, Cerrillos Hills was an important turquoise resource area. Turquoise originating from Cerrillos Hills was not unexpected due to its relative proximity to Chaco Canyon (almost 200 kilometers) and evidence of heavy prehistoric mining (Blake 1858; Judd 1954; Pepper 1996; Pogue 1974; Silliman 1881; Warren and Mathien 1985; Weigand 1982; Weigand and Harbottle 1993). However, the data from this study show that the turquoise resource areas in the San Luis Valley in Colorado were also heavily exploited by the occupants of Chaco Canyon. The turquoise resource areas in Nevada, especially those in the Tonopah area north of Las Vegas, and the region that encompasses Mineral Park, Arizona, Crescent Peak, Nevada, and Halloran Springs, California were also identified as important turquoise resource areas for the

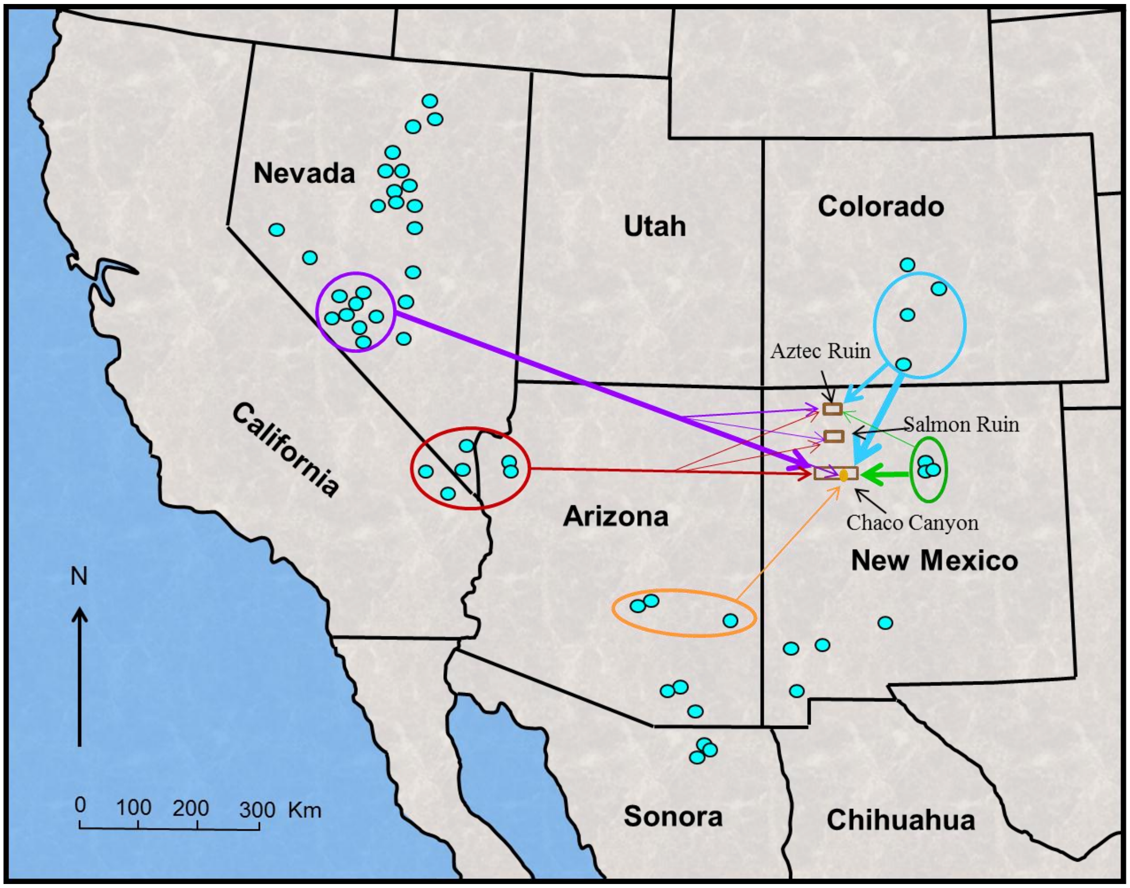

Fig. 8.1. The directionality of the movement of turquoise from turquoise provenance regions (turquoise resource areas are represented by blue circles) to the archaeological sites (represented by a brown rectangles).

Ancestral Puebloans of Chaco Canyon. Although not largely represented, other areas in Arizona (Sleeping Beauty and Morenci) were recognized as sources of turquoise. Other studies that show that there were many commodities other than turquoise that were transported into Chaco Canyon, including chert (Cameron 2001), obsidian (Cameron and Sappington 1984; Duff et al. 2012), ceramics (Toll 1991), timber (English et al. 2001), and maize (Benson et al. 2003), as well as the exotic goods such as shell, copper bells, macaws (Toll 1991), and cacao (Crown et al. 2009). Several studies also show evidence of an elite group that occupied Pueblo Bonito (e.g., Akins 1986; Akins and Schelberg 1984) as well as diverse populations throughout Chaco Canyon (e.g., Akins 1986; Judge and Cordell 2006:195; Lekson et al. 2006:96; Schillaci 2003; Schillaci and Stojanowski; Vivian 1990:196-197).

It is more problematic to identify how much control, dominance, or influence the elite of Chaco Canyon had over the turquoise resource areas. The further the distance from the core center, the more difficult it would have been to maintain any type of control over the resource areas. That is a significant dynamic considering that turquoise was transported to Chaco Canyon over 800 kilometers from Crescent Peak and over a thousand kilometers from the turquoise resource areas located in the Tonopah region. Turquoise resource areas that were closer in proximity to the core (e.g., Cerrillos Hills and deposits in Colorado) were good candidates for control and/or direct acquisition. Deposits located in Nevada, Arizona, and California (e.g., Royston, Kingman, and Halloran Springs) that were used by the Ancestral Puebloans of Chaco Canyon may have *developed* into a core-periphery system at the height of the Chacoan expansion. These significant commodities may have been obtained for the use by the elite inhabitants of Chaco Canyon and transported through long-distance traders.

The turquoise obtained from Cerrillos Hills and the turquoise provenance regions in Colorado may have been procured through direct acquisition. It is difficult to identify evidence of any type of control of the turquoise resource area; especially if that control only included withholding the knowledge of the locations of the turquoise resource areas from the general population. Although Cerrillos Hills was almost 200 kilometers from Chaco Canyon, organized mining expeditions may have been feasible because of the location of other Ancestral Puebloan settlements between them. For example, Guadalupe Ruin, a great house community on the eastern edge of the Chacoan World, may have been used to support mining expeditions and the transport of turquoise between Cerrillos Hills and Chaco Canyon (Judge 1989). Prior to A.D. 1300, there is evidence of small pithouse communities in the Rio Grande Valley suggesting seasonal occupation; however there were no known Chacoan outliers in the area (Cordell 1997:359). These small pithouse communities may have assisted in the support of Chacoan miners.

Although the southwestern region of Colorado contained many puebloan communities, the turquoise resource areas in Colorado were occupied by nomadic hunter and gatherer groups (Dutton 1976; Simms 2008). They may have been responsible for some trade or exchange of turquoise with the Ancestral Puebloan. However, once Chacoan miners were established at Cerrillos Hills, following the Rio Grande Rift into the San Luis Valley would have been much less difficult when compared to sponsoring and organizing mining expeditions across the hot arid landscape to the far west (e.g., Royston and Halloran Springs). Another possible route to the turquoise provenance regions in Colorado may have been through the mountains into the San Luis Valley from one of the many puebloan communities in the northern San Juan Basin or southwestern

Colorado. At the entrance of one of the mountain passes that is known as an old Ute trail are pictographs of flute players that are known as a puebloan symbol (Fig. 8.2).

This study also shows geochemical evidence of turquoise that was obtained by the Ancestral Puebloans of Chaco Canyon from the western turquoise provenance regions in Nevada, Arizona, and southeastern California. Evidence of heavy prehistoric exploitation of turquoise from various western turquoise resource areas (Halloran Springs - Jenson 1985; Leonard and Drover 1980; Rogers 1929; Weigand 1982; Weigand and Harbottle 1993; Mineral Park - Pogue 1974; Weigand 1982; Weigand and Harbottle 1993; Crescent Peak - Weigand 1982; Weigand and Harbottle 1993) suggest a large labor investment for obtaining turquoise from this region. The presence of the Virgin branch of the Ancestral Puebloan, who occupied areas in southern Nevada, northern Arizona, and parts of southern Utah (Ahlstrom and Roberts 2008:130), suggest they may have been responsible for some of the extraction of turquoise in the far western mines. However, it is important to consider that the turquoise resource areas may have been exploited by other culture groups as well as the Ancestral Puebloan (e.g., the Hohokam – see Sigleo 1975). The settlement of Lost City, located in the Moapa Valley (Fig. 8.3), may have been an important hub in pan-southwestern trade and may have sponsored mining expeditions that ventured to western turquoise resource areas (Rafferty 1990).

Kevin Rafferty (1990) suggested that the inhabitants of Lost City were exploiting turquoise from Halloran Springs, Crescent Peak, and the Sullivan mine near Boulder City, Nevada. There was also an ancient legend of the Desert Mojave, told by the Desert Paiute, of a tribe that came to the Mojave for turquoise (Berkholz 1960:10-11). Lost City phase ceramics have been identified in west central Nevada (Harrington 1926), east

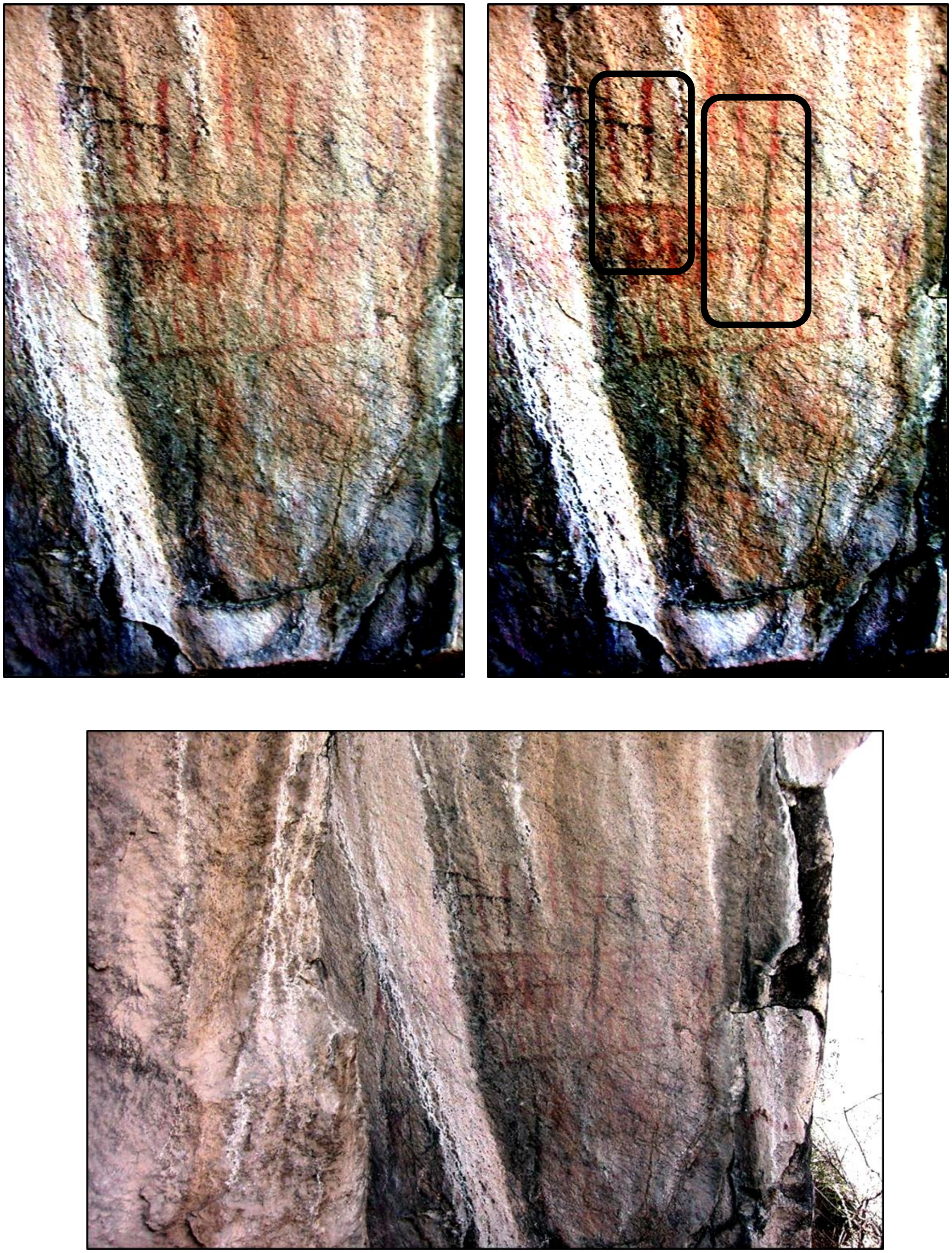

Fig. 8.2. The flute player pictographs in the San Luis Valley: a) an image of the flute players drawn over previous red pictographs, b) the same image with enhanced contrast and a border around two of the flute players, and c) the same pictograph from a different perspective. Pictures were provided by Ken Frye and used with his permission.

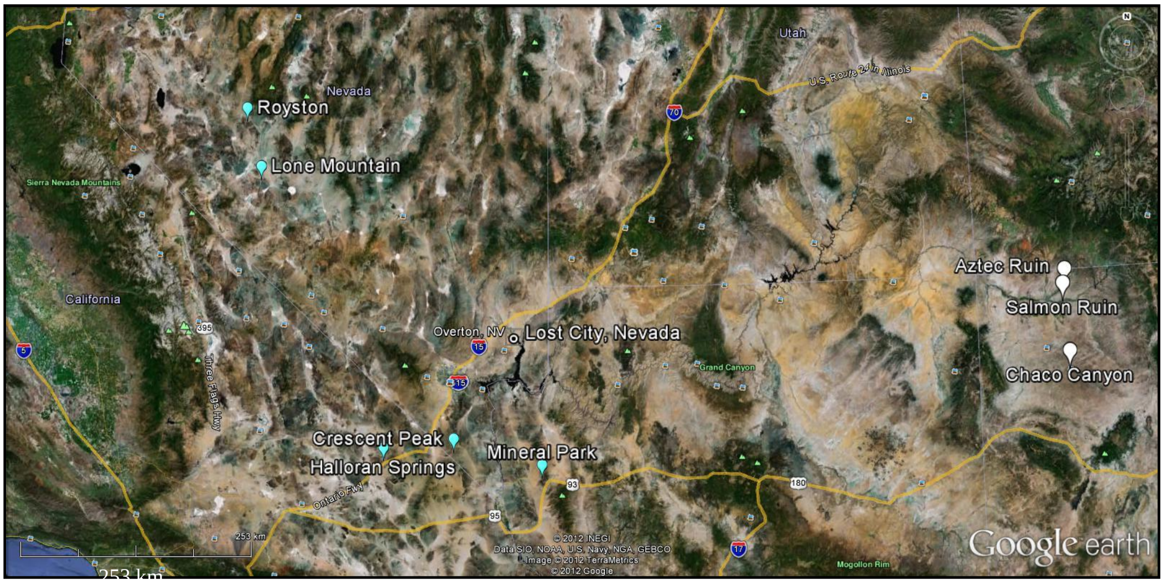

Fig. 8.3. Locations mentioned in the text: Chaco Canyon, Aztec Ruin, and Salmon Ruin in northwestern New Mexico, and Lost City, Nevada in reference to its geographical relationship with five of the western turquoise resource areas where turquoise from the San Juan Basin originated (Google Earth 2012).

central Nevada (Harrington 1928), Las Vegas Valley (Lyneis 2000), and the Halloran Springs area (Leonard and Drover 1980; Rogers 1929) suggesting that they may have expanded into or were trading with the inhabitants of turquoise resource areas. The transport of turquoise, along with shell from the Pacific Coast and the Gulf of California and salt from the lower Virgin River (Harrington 1925), would have been a lucrative business for any traders willing to transport these commodities over the hundreds of kilometers to the San Juan Basin. Although the distances were still long, the location of Lost City was central to many of the western turquoise deposits because it was within a few hundred kilometers to five major turquoise resource areas that are represented in this study (Fig. 8.3). Therefore, based on this study showing that turquoise artifacts that originated from the Lost City Region and previous studies by Rafferty (1990) and Lyneis (1986), the Lost City areas can be interpreted to be a periphery of the Chacoan world.

Although turquoise was transported to Chaco Canyon from several sources *how* the turquoise was transported over 100s of kilometers is still not clear. In general, the world systems models included a group of middle-men or a group of long-distance traders that were responsible for the transport of the commodities from the peripheries to the core regional centers. Some researchers (e.g., Frisbie 1978; Kelley and Kelley 1975; Reyman 1978) suggested that organized trade ventures of long-distance traders account for trade items between the Greater Southwest and Mesoamerica. In this model, which includes a core-periphery system, a subgroup within the Ancestral Puebloan may have filled this niche within the Chacoan world. Steadman Upham (1982) proposed that long-distance trade was controlled and conducted by the elite suggesting that long-distance traders were either controlled by or were members of the upper echelon of the Ancestral Puebloan hierarchy. In exchange for luxury items, the occupants of the western frontier may have received non-material resources such as ideology and religious concepts to reaffirm their status from the elite in Chaco Canyon (Rafferty 1990:13).

Turquoise originating from Sleeping Beauty and Morenci, Arizona may have been obtained through an exchange network because Chaco Canyon and the Hohokam were contemporaneous regional systems in the eleventh and early twelfth centuries (Duff and Lekson 2006:332). The archaeological sites for both cultures contain exotic goods suggesting that they both were participants in long-distance trade. The recovery of shell jewelry and pyrite mirrors (associated with the Hohokam) in Chacoan sites (Bradley 2000; Crown 1991) suggest that there was exchange between the two cultures either through direct exchange or through a down-the-line network. In view of the luxury items that were traded between the two cultural centers, the type of exchange between can be explained by the prestige goods model that is discussed in the next section.

8.2. The Prestige Good Exchange Model

A prestige good exchange model is a valuable tool to explain the exchange relationship between the three great houses (Pueblo Bonito, Aztec Ruin, and Salmon Ruin) and small sites of Chaco Canyon (29SJ1360, 29SJ1659 Shabik'eshchee, 29SJ423, 29SJ625 Three C site, 29SJ627, 29SJ628, 29SJ629 Spadefoot Toad, and 29SJ633 Eleventh Hour). This model is supported by evidence of an elite group at Pueblo Bonito (Akins 2003; Akins and Schelberg 1984) and Aztec Ruin (Lekson 1999) where exotic items such as macaws, turquoise, and shell were recovered. The prestige goods model is built on power, and the power was maintained by the elite control of valuable goods and sacred knowledge that in turn, validated their positions as leaders (McGuire 1989:49).

Turquoise procurement and exchange patterns were identified for all of the archaeological sites. According to the results of this study, the inhabitants of Pueblo

Bonito and Aztec Ruin were obtaining the majority of their turquoise from similar locales such as Cerrillos Hills and turquoise resource areas in Colorado with a small representation from turquoise resource areas to the west including Lone Mountain, Crescent Peak, and Halloran Springs (Fig. 8.1; Table 7.2; Appendix 4). The pattern of turquoise procurement for the inhabitants of Salmon Ruin was much different than those for the other two great houses. At Salmon Ruin, the majority of turquoise was obtained from Lone Mountain, Crescent Peak, and Mineral Park (Fig. 8.1; Table 7.2; Appendix 4). Surprisingly, the turquoise procurement and exchange patterns between the sites in Marcia's Rincon and Salmon Ruin are very similar. Out of the nine turquoise artifacts analyzed from the five sites in Marcia's Rincon (Chaco Canyon), six originated from Royston and Lone Mountain. It is notable that there was a lack of turquoise obtained from the New Mexico and Colorado turquoise resource areas for the inhabitants of Salmon Ruin and the small sites in Chaco Canyon (Fig. 8.1; Table 7.2; Appendix 4). Arizona turquoise resource areas were identified for two artifacts from small sites in Chaco Canyon. Sleeping Beauty, in the Globe District, was identified for the source of an artifact from Shabik'eshchee and the Morenci mining area for an artifact from the site 29SJ423, located on the West Mesa (Fig. 8.1; Table 7.2; Appendix 4).

McGuire (1980) proposed that the accumulation of elaborate burial goods and ceremonial objects supported a prestige economy. Both Pueblo Bonito (Pepper 1996) and Aztec Ruin (Morris 1924) contained elaborate burials and clusters of ceremonial type objects. The exclusive use of the Cerrillos Hills and Colorado turquoise resource areas evident of the turquoise provenance patterns of Pueblo Bonito and Aztec Ruin suggest some type of control over these resource areas. The small sites within Chaco Canyon have been interpreted as habitation sites for the non-elite populations (Akins 1986; Akins and Schelberg 1984). The origins identified for the turquoise artifacts from the small sites are distinctive from the turquoise from Pueblo Bonito, and was transported over longer distances (e.g., Nevada and Arizona). The prestige model suggests that the elites were controlling the sacred item; therefore within the framework of the prestige model, the occupants from the small sites may have been suppliers (middle-men traders) and craftsmen of turquoise for the elites. This would account for the turquoise artifacts recovered from Pueblo Bonito that originated from Lone Mountain and Crescent Peak and the one artifact from Aztec Ruin that originated from Halloran Springs.

Considering the suppositions put forth by Bauer and Agbe-Davis (2010:29) that shared materials are associated with shared practices and ideologies, there is clearly a strong similarity between Pueblo Bonito and Aztec Ruin, and between Salmon Ruin and the small sites clustered in Marcia's Rincon suggested by the strategies/practices they used to obtain turquoise. These data suggest that the populations from Pueblo Bonito and Aztec Ruin were either the same or closely related supporting the migration model proposed by Lekson (1999) where the central power of the Chacoan world was deliberately moved to the Aztec community as the Chacoans struggled to maintain their influence across the San Juan Basin in the 12th century. Noting that the analyzed turquoise artifacts from Salmon Ruin were recovered in deposits associated with the local San Juan population, the turquoise procurement and exchange pattern from the San Juan population at Salmon Ruin supports Reed (2006c) suggestion that the San Juan population was distinctly different from the Chacoan population. The results from the study of discrete dental traits by Kathy R. Durand and colleagues (Durand et al. 2010) also suggested that the populations from Pueblo Bonito and Aztec Ruin were more closely related to each other than those of the San Juan population at Salmon Ruin.

The supply of turquoise from the western turquoise resource areas may have been brought to Chaco Canyon by the occupants of the small sites and may represent exchange, tributes, or offerings. These populations may also represent the long-distance merchants that gained social status through alliances with the exchange of the valuable goods (McGuire 1980) such as shell, salt, and turquoise from the far western peripheries. These trade connections may have eventually developed into a symbiotic core-periphery relationship on a larger regional scale.

8.3. The Trade Festival Model

The turquoise procurement and exchange patterns between Pueblo Bonito and the small sites in Chaco Canyon are distinctly different. The idea of multiple populations residing in the canyon is not a new concept and the data from this study is used to support the trade festival model. As early as 1939, Clyde Kluckhohn suggested that two different social groups lived in Chaco Canyon; those that lived in small house sites and a separate group that occupied the great houses. Not only are there noticeable difference between sites, Neil M. Judd (1964:41) suggested that there were two distinct groups occupying Pueblo Bonito. Researchers have examined other difference between sites in Chaco Canyon such as the architecture styles and layout of the sites (e.g., Vivian 1990:196-197), as well as studies on the skeletal remains (e.g., Akins 1986; Schillaci 2003; Schillaci and Stojanowski 2002).

The concept of periodic gatherings at the great houses have been the basis of pilgrimage models to help explain the diversity found in in the canyon (see Judge 1989:241-243; Neitzel 2003:145; Plog and Watson 2012; Van Dyke 2007). Organized trade festivals to Chaco Canyon may account for multiethnic populations colonizing the canyon. During times of stress, people may have decided to stay or left some members of their group in the canyon to care for the structures and prepare for future arrivals of the group. This model would account for periodic occupation and fluctuating populations.

The use of turquoise obtained from the western resource areas was consistent by the occupants of the small sites in Marcia's Rincon from A.D. 600 (29SJ628) through the A.D. 1200s (29SJ633 Eleventh Hour) as well as the occupants of Salmon Ruin (from A.D. 1125 through A.D. 1280). Turquoise procurement patterns from the sites in Marcia's Rincon and Salmon Ruin suggest close ties to the settlement of the western periphery of the Ancestral Puebloan culture area. The presence of turquoise that originated from the western most turquoise resource areas suggest that they may have been the long-distance traders or had close ties to them.

The core-periphery model showed the diversity of turquoise procurement strategies of the inhabitants of Chaco Canyon as a cohesive unit. However, these patterns showed distinct differences when the patterns were examined among the sites within Chaco Canyon (Pueblo Bonito and small sites in Chaco Canyon). In turn, there are similarities of the patterns among Pueblo Bonito and Aztec Ruin, and among Salmon Ruin and the small sites clustered in Marcia's Rincon. The aggregation of communities in Chaco Canyon may have been a result of trade festivals, gatherings of puebloan groups that represented much more than trade. These scheduled events were inundated with ritual activities and social events (Judge and Cordell 2006:194). As Chaco Canyon flourished and expanded, the framework of the prestige model is a valuable tool to explain the ideology and social structure that allowed these communities to become a cohesive unit. Once trade networks developed, down-the-line may have become more organized and developed into a core-periphery system. Exotic trade commodities, especially turquoise, were part of the material culture that supported the ideology and social structure of the Chacoan World and the Ancestral Puebloans were willing to overcome the long distance to obtain it.

Chapter 9: Conclusion

"The reason why trade has remained an important topic for archaeologists of all perspectives is that, as Malinowski and Mauss pointed out in their early anthropological studies, trade is a fundamental vehicle for establishing and maintaining social relations among individuals and groups, whether accomplished through the exchange of gifts, commodities, or kin through marriage." (Bauer and Agbe-Davies 2010:41)

This study had three objectives: 1) establish a turquoise comparative database, 2) analyze turquoise artifacts and identify their geological origin, and 3) compare the results to current models of culture history, and trade and exchange. This interdisciplinary research is significant to archaeology as it provides archaeologists with a reliable and reproducible technique for identifying the provenance regions for turquoise artifacts. The use of hydrogen and copper isotopes to source turquoise is a powerful tool for the reconstruction of pre-Columbian turquoise exchange networks and the ability to investigate the complex trade and exchange relationships of these ancient cultures.

Although geochemical provenance studies are becoming more common in archaeology, it is essential to have accurate knowledge of the mineral of interest and the provenance regions. For example, it is important to know the geologic context of the mineral (magma, supergene) and understand the mineralogy and the processes that may alter the mineral thus affecting it elemental or isotopic compositions. The depositional environment and post depositional modification of the mineral of interest can influence the choice of geochemical method.

Isotope research for archaeological provenance studies is proving to be a good method for some of the more problematic minerals (e.g., turquoise and chert). The use of the *in situ* stable isotopic analysis of hydrogen and copper by SIMS has been successful in defining turquoise provenance regions. The advantages of this technique are: 1) isotope ratios of turquoise are geographically distinct thus overcome the limitations of trace element analyses; 2) *in situ* micro analysis avoids inclusions of other minerals, which could profoundly affect the trace element and isotopic composition of turquoise; and 3) except for minor polishing of the surface of artifacts and 50 micrometer pits that are created during analysis, turquoise artifacts are relatively undamaged. The major disadvantage of this technique is that the turquoise resource areas of weathered turquoise artifacts cannot be identified because alteration of turquoise variably affects the hydrogen and copper isotopic composition (Hull 2006; Hull et al. 2005).

Based on the average δD and $\delta^{65}Cu$ values of turquoise from 21 turquoise resource areas throughout the western United States and Baja California, five turquoise provenance regions were identified (Fig. 8.1). The average δD and $\delta^{65}Cu$ values of single deposits within these regions tend to cluster together (e.g., Black Hill and the Verde Blue), as well as average δD and $\delta^{65}Cu$ values of turquoise provenance samples from different localities within a single deposit or mine (e.g., Crescent Peak). Although specific turquoise deposits often did not show a unique isotopic fingerprint and their distribution patterns overlapped, the turquoise provenance regions showed consistent distribution patterns. The development of the turquoise regional comparative database established the groundwork for the reconstruction of turquoise exchange networks and the investigation of turquoise procurement strategies in the western United States and eventually in Mesoamerica.

The identification of the geological sources of turquoise artifacts from Pueblo Bonito, Aztec Ruin, and Salmon Ruin, and the small sites in Chaco Canyon added new insight into the extent of turquoise procurement and their social and economic relationships by the comparison of their turquoise procurement and exchange patterns to current models of the culture history and exchange. Similar turquoise provenance and exchange patterns between Pueblo Bonito and Aztec Ruin and between Salmon Ruin and the small site in Marcia's Rincon in Chaco Canyon were identified. These data support the model proposed by Lekson (1999) of a migration from Pueblo Bonito to Aztec Ruin and Reed's model (2006a) suggesting that the San Juan population of Salmon Ruin was different than the Chacoan population. Just as important, the differences in patterns between Pueblo Bonito and the small sites in Chaco Canyon add more support to the hypothesis that there were diverse populations living contemporaneously in the canyon. The core-periphery model was a valuable framework for the explanation of the dynamics of turquoise procurement from the distant turquoise resource areas and the relationship between the core regional centers and the exploited peripheries. The economic relationship between the Ancestral Puebloan communities within the San Juan Basin were explained by the framework of a prestige economy with ideology and religion as the mechanisms of social cohesion that allowed these diverse communities to live and work in the same region. The trade festival model supports an explanation for the foundation of the multicultural communities within Chaco Canyon and what may have first brought them together. Prescheduled festivals with trade, ceremony, and feasting drew diverse groups into the canyon where some built seasonal structures and others decided to stay and make the canyon their permanent residence.

Ancient long-distance trade networks and trade festivals were an important avenue for the movement of goods; however they also served other purposes. Information of distant regions would have traveled along these networks providing the foundation for migration (Duff 1998:33) and the diffusion of ideas. They were also avenues of social interaction (Irwin-Williams 1977:142) and that would blend social, political, ritual, and economical aspects. Early European explorers reported an impressive amount of trade in the American Southwest and the long distances that were travel by foot (Ford 1983:712). Nomadic groups were also reported as bringing trade items to regional centers (e.g., Pecos and Taos) for trade (Ford 1983:712). Scheduled trade festivals would have been a means that brought many groups of people (e.g., sedentary agriculturalists and nomadic hunter and gatherer groups) and different trade items together. The mechanisms responsible for the movement of turquoise across the American Southwest were probably as diverse as the cultural groups that lived there.

Future consideration for this research are: 1) the expansion of the turquoise comparative database by geochemically characterizing more turquoise resource areas, 2) the continuation of testing the isotopic homogeneity of each turquoise deposit, 3) the continuation of testing the technique for limitations (e.g., weathering) and how to overcome these limitations, and 4) the analyses of more artifacts and the reconstruction of pre-Columbian turquoise trade routes. The long-term goal of this research is to map the movement of turquoise across large regions and through time to evaluate hypotheses about trade structures and networks that covered this vast expanse of territory over a period of two thousand years. In conjunction with other evidence, it will be possible to discern more about the relationships between the cultures that coveted this blue-green mineral and participated in these trade structures.

References Cited

Abdu, Yassir A., Sharon K. Hull, Mostafa Fayek, and Frank C. Hawthorn
2011 The Turquoise-chalcosiderite $Cu(Al,Fe^{3+})_6(PO_4)_4(OH)_8 \bullet 4H_2O$ Solid-Solution Series: A Mössbauer Spectroscopy, XRD, EMPA and FTIR Study. *American Mineralogist* 96:1433-1442.

Agbe-Davies, Anna S. and Alexander A. Bauer
2010 Rethinking Trade as a Social Activity: An Introduction. In *Social Archaeologies of Trade and Exchange: Exploring Relationships among People, Places, and Things*, eds., Alexander A. Bauer and Anna S. Agbe-Davies, pp. 13-28. Left Coast Press, Walnut Creek, California.

Ahlstrom, Richard V. N. and Heidi Roberts
2008 Who Lived on the Southern Edge of the Great Basin? In *The Great Basin: People and Place in Ancient Times*, eds., Catherine S. Fowler and Don D. Fowler, pp. 128-135. School for Advance Research Press, Santa Fe, New Mexico.

Akins, Nancy J.
1986 *A Bicultural Approach to Human Burials from Chaco Canyon, New Mexico*. Reports of the Chaco Center No. 9, National Parks Service, Santa Fe, New Mexico.

2003 The Burials of Pueblo Bonito. In *Pueblo Bonito: Center of the Chacoan World*, ed., Jill E. Neitzel, pp. 94-106. Smithsonian Institution Press, Washington D.C.

Akins, Nancy J. and John D. Schelberg
1984 Evidence of Organizational Complexity as Seen from the Mortuary Practices in Chaco Canyon. In *Recent Research on Chaco Prehistory*, eds., W. James Judge and John D. Schelberg, pp. 89-102. Reports of the Chaco Center No. 8, Division of Cultural Research, National Park Service, Albuquerque, New Mexico.

Albarède, Francis
2003 *Geochemistry: An Introduction.* Cambridge University Press, Cambridge.

Anderson, W. R., B. Stringham, and J. A. Welan
1962 Secondary Phosphate from Bingham, Utah. *American Mineralogist* 47:1303-1309.

Anthony, John W., Sidney A. Williams, and Richard A. Bideaux
1977 *Mineralogy of Arizona.* University of Arizona Press, Tucson, Arizona.

Antillón, Rafael Cruz and Timothy D. Maxwell
1999 The Villa Ahumada Site: Archaeological Investigations East of Paquimé. In *The Casas Grandes World*, eds., Curtis F. Schaafsma and Carroll L. Riley, pp. 43-53. University of Utah Press, Salt Lake City, Utah.

Arrowsmith, Rex
1974 Introduction. In *The Turquois. A Study of Its History, Mineralogy, Geology, Ethnology, Archaeology, Mythology, Folklore, and Technology*. Glorietta, New Mexico. Originally published 1915, Memoirs of the National Academy of Sciences Vol. XII, Part II, Washington D.C.

Baldridge, W. Scott
2004 *Geology of the American Southwest: A Journey through Two Billion Years of Plate-Tectonic History*. Cambridge University Press, Cambridge.

Bauer, Alexander A.
2008 Import, Imitation, or Communication?: Pottery Style, Technology, and Coastal Contact in the Early Bronze Age Black Sea. In *"Import" and "Imitation": Methodical and Practical Problems with an Archaeological Key Concept*, eds., P. Biehl and Y. Rassamakin, pp. 89-104. Schriften des Zentrums für Archäologie und Kulturgeschichte des Schwarzmeerraumes Band 11. Beier & Beran, Langenweiβbach.

Bauer, Alexander A. and Anna S. Agbe-Davie
2010 Trade and Interaction in Archaeology. In *Social Archaeologies of Trade and Exchange: Exploring Relationships among People, Places, and Things*, eds., Alexander A. Bauer and Anna S. Agbe-Davies, pp. 29-47. Left Coast Press, Walnut Creek, California.

Benson, Larry, Linda S. Cordell, Kirk Vincent, Howard Taylor, John Stein, G. Lang Farmer, and Kiyoto Futa
2003 Ancient Maize from Chacoan Great Houses: Where was it Grown? *Proceedings of the Academy of Sciences* 100(22)13111-13115.

Bergen, Laura L., Mostafa Fayek, and Sharon Hull
2007 *The Formation and Alteration of Turquoise Deposits in the American Southwest*. Poster presented at the Geological Society of America, Denver, Colorado.

Berkholz, Mary Frances
1960 Toltec Mojave Desert Mine of the Ancients. *Science of Man* Dec 1960:10-11.

Bernardini, W.
1999 Social Action at Pueblo Bonito, Chaco Canyon, New Mexico. *Kiva* 64(4):447-470.

Binford, Lewis R.
1962 Archaeology as Anthropology. *American Antiquity* 28:217-225.

1964 A Consideration of Archaeological Research Design. *American Antiquity* 29:425-441.

1965 Archaeological Systematics and the Study of Culture Process. *American Antiquity* 31:203-210.

1968 Archaeological Perspectives. In *New Perspectives in Archaeology*, eds., Sally R. Binford and Lewis R. Binford, pp. 5-32. Aldine, New York.

1989 The "New Archaeology," Then and Now. In *Archaeological Thought in America*, ed., C. C. Lamberg-Karlovsky, pp. 50-62. Cambridge University Press, Cambridge.

Bishop, Ronald L.
1979 *Neutron Activation Analysis of Chacoan Turquoises: An Informal Report to the Division of Chaco Research.* Report from the Department of Chemistry, Brookhaven National Laboratory, Upton, New York. MS, Division of Cultural Research, Southwest Cultural Resources Center, National Park Service, Albuquerque, New Mexico.

Blake, William P.
1858 The Chalchihuitl of the Ancient Mexicans: Its Locality and Association, and Its Identity with Turquoise. *American Journal of Science* 25:227-232.

Bradley, R. J.
2000 Networks of Shell and Ornament Exchange: A Critical Assessment of Prestige Economies in the North American Southwest. In *The Archaeology of Regional Interaction: Religion, Warfare, and Exchange across the American Southwest and Beyond*, ed., M. Hegmon, pp. 167-187. University Press of Colorado, Boulder, Colorado.

Britton, K., V. Grimes, J. Dau, and M. P. Richards
2009 Reconstructing Faunal Migrations using Intra-tooth Sampling and Strontium and Oxygen Isotope Analyses: A Case Study of Modern Caribou (Rangifer tarandus granti). *Journal of Archaeological Science* 36:1163-1172.

Brooks, Richard H.
1978 A Loma San Gabriel/Chalchihuites Cultural Manifestation in the Rio Ramos Region, Durango, Mexico. In *Across the Chichimec Sea: Papers in Honor of J. Charles Kelley*, eds., Carroll L. Riley and Basil C. Hedrick, pp. 86-95. Southern Illinois University Press, Carbondale, Illinois.

Brown, Gary M., Thomas C. Windes, and Peter J. McKenna
2008 Animas Anamnesis: Aztec Ruin or Anasazi Capital? In *Chaco's Northern Prodigies: Salmon, Aztec, and the Ascendancy of the Middle San Juan Region After AD 1100*, ed., Paul F. Reed, pp. 231-250. University of Utah Press, Salt Lake City, Utah.

Brown, Gary M. and Cheryl I. Paddock
2011 Chacoan and Vernacular Architecture at Aztec Ruins: Putting Chaco in its Place. *Kiva* 77(2):203-224.

Bullen, Thomas D., Arthur F. White, Cyril W. Childs, Davisson V. Vivit, and Marjorie S. Schultz
2001 Demonstration of Significant Abiotic Iron Isotope Fractionation in Nature. *Geology* 29:699-702.

Cameron, Catherine M.
2001 Pink Chert, Projectile Points, and the Chacoan Regional System. *American Antiquity* 66:79-102.

2009 The Chaco Phenomenon and the Bluff Great House Project. In *Chaco and After in the Northern San Juan: Excavations at the Bluff Great House*, ed., Catherine M. Cameron, pp. 1-12. University of Arizona Press, Tucson, Arizona.

Cameron, Catherine M. and H. Wolcott Toll
2001 Deciphering the Organization of Production in Chaco Canyon. *American Antiquity* 66:5-13.

Cameron, Catherine M. and R. Lee Sappington
1984 Obsidian Procurement at Chaco Canyon, A.D. 500-1200. In *Recent Research on Chaco Prehistory*, eds., W. J. Judge and J. D. Schelberg. Reports of the Chaco Center No. 8, pp. 153-73. Division of Cultural Research, National Park Service, Albuquerque, New Mexico.

Cid-Dresdner, Hilda
1965 Determination and Refinement of the Crystal Structure of Turquoise, $CuAl_6(PO_4)_4(OH)_8 \cdot 4H_2O$. *Zeitschrift für Kristallographie*, Bd. 121, S. 87-113.

Clarke, F. W. and J. S. Diller
1887 Turquoise from New Mexico. *United States Geological Survey Bulletin* No. 42:39-44.

Cloudman, H. C., Emile Huguenin, F. J. H. Merrill, and W. Burling Tucker
1917 *Mines and Mineral Resources of San Bernardino County Tulare County*. California State Mining Bureau, California State Printing Office.

Cordell, Linda S.
1997 *Archaeology of the Southwest* 2nd edition. Academic Press, San Diego.

Cordell, Linda. S. and George J. Gumerman
1989 Cultural Interaction in the Prehistoric Southwest. In *Dynamics of Southwest Prehistory*, eds., Linda S. Cordell and George J. Gumerman, pp. 1-17. Smithsonian Institution Press, Washington D.C.

Cordell, Linda S. and Fred Plog
1979 Escaping the Confines of Normative Thought: A Reevaluation of Puebloan Prehistory. *American Antiquity* 44(3):405-429.

Craig, H.
1961 Isotopic Variations in Meteoric Waters. *Science* 133:1702-1703.

Crawford, William P. and Frank Johnson
1937 Turquoise Deposits of Courtland, Arizona. *Economic Geology and the Bulletin of the Society of Economic Geologists* 32(4):511-523.

Crook, Josh C.
2001 The Origin of Turquoise at the Iron Mask Mine, Orogrande Mining District, Otero County, New Mexico. *New Mexico Geology* 23(2):54.

Crown, Patricia L.
1991 The Role of Exchange and Interaction in Salt-Gila Basin Hohokam Prehistory. In *Exploring the Hohokam: Prehistoric Desert Peoples of the American Southwest*, ed., George J. Gumerman, pp. 383-415. Amerind Foundation, Dragoon, Arizona and University of New Mexico Press, Albuquerque, New Mexico.

Crown, Patricia L., W. Jeffrey Hurst, and Bruce D. Smith
2009 Evidence of Cacao Use in the Prehistoric American Southwest. *Proceedings of the National Academy of Sciences* 106(7):2110-2113.

Dansgaard, W.
1964 Stable Isotopes in Precipitation. *Tellus* 16:436-468.

de Groot, P. A.
2009 *Handbook of Stable Isotope Analytical Techniques*, Vol. 2. Elsevier, Amsterdam.

Dean, Jeffrey S.
1988 A Model of Anasazi Behavioral Adaptation. In *The Anasazi in a Changing Environment*, ed., George J. Gumerman, pp. 25-44. Cambridge University Press, Cambridge.

Dean, Jeffrey S. and John C. Ravesloot
1993 The Chronology of Cultural Interaction in the Gran Chichimeca. In *Culture and Contact: Charles C. Di Peso's Gran Chichimeca*, eds., Anne I. Woosley and John C. Ravesloot, pp. 83-103. University of New Mexico Press, Albuquerque, New Mexico.

Di Peso, Charles
1968 Casas Grande and the Gran Chichimeca. *El Palacio* 75:47-61.

1974 *Casas Grandes: A Fallen Trading Center of the Gran Chichimeca* Vol. 1-3. The Amerind Foundation, Dragoon, Arizona.

Disbrow, Alan E. and Walter C. Stoll
1957 *Geology of the Cerrillos Area, Santa Fe County, New Mexico*. New Mexico Bureau of Mines and Mineral Resources, Bulletin 48.

Duff, Andrew I.
1998 The Process of Migration in the Late Prehistoric Southwest. In *Migration and Reorganization: The Pueblo IV Period in the American Southwest*, ed., Katherine Spielman, pp. 31-52. Anthropological Research Papers No. 51. Arizona State University, Tempe, Arizona.

Duff, Andrew I. and Stephen H. Lekson
2006 Notes from the South. In *The Archaeology of Chaco Canyon: An Eleventh-Century Pueblo Regional Center*, ed., Stephen H. Lekson, pp. 315-337. School of American Research Press, Santa Fe, New Mexico.

Duff, Andrew I., Jeremy M. Moss, Thomas C. Windes, John Kantner, and M. Steven Shackley
2012 Patterning in Procurement of Obsidian in Chaco Canyon and in Chaco-era Communities in New Mexico as Revealed by X-ray Fluorescence. *Journal of Archaeological Science* 30:2995-3007.

Dupras, T. L. and H. P. Schwarcz
2001 Strangers in a Strange Land: Stable Isotope Evidence for Human Migration in the Dakhleh Oasis, Egypt. *Journal of Archaeological Science* 28:1199-1208.

Durand, Kathy R., Meradeth Snow, David Glenn Smith, and Stephen R. Durand
2010 Discrete Dental Trait Evidence of Migration Patterns in the Northern Southwest. In *Human Variation in the Americas: The Integration of Archaeology and Biological Anthropology*, ed., Benjamin M. Auerbach, pp.113-134. Center for Archaeological Investigations, Occasional Paper No. 38. Southern Illinois University Press, Carbondale, Illinois.

Dutton, Bertha P.
1976 *The Ranchería, Ute, and Southern Paiute Peoples: Indians of the American Southwest*. Prentice-Hall, Inc., Englewood Cliffs, New Jersey.

Emery, K. F. and E. K. Thornton
2008 A Regional Perspective on Biotic Change during the Classic Maya Occupation using Zooarchaeological Isotopic Chemistry. *Quaternary International* 191:131-143.

English, Nathan B., Julio L. Betancourt, Jeffery S. Dean, and Jay Quade
2001 Strontium Isotopes Reveal Distant Sources of Architectural Timber in Chaco Canyon, New Mexico. *Proceeding of the National Academy of Sciences* 98(21):11891-11896.

Epstein, S. and T. Mayeda
1953 Variations of ^{18}O Content of Waters from Natural Sources. *Geochimica et Cosmochimica Acta* 4:213-224.

Faure, G.
1986 *Principles of Isotope Geology* 2nd Edition. Wiley, New York.

Fayek, Mostafa
2009 Hydrogen, Carbon, Nitrogen, and Sulfur Isotope Microanalysis by Secondary Ion Mass Spectrometry. In *Secondary Ion Mass Spectrometry in the Earth Sciences: Gleaning the Big Picture from a Small Spot*, ed., Mostafa Fayek, pp. 65-88. Mineralogical Association of Canada Short Course 41, Toronto, Ontario.

Fayek, Mostafa, Lee R. Riciputi, Homer Milford, and Frances Joan Mathien
2002 *Sourcing Turquoise Using Oxygen and Hydrogen Isotopes.* Paper presented at the Annual Meeting of the Geological Society of America, Denver, Colorado.

Ferguson, T. J.
2003 Anthropological Archaeology Conducted by Tribes: Traditional Cultural Properties and Cultural Affiliations. In *Archaeology is Anthropology*, eds., S. D. Gillespie and D. L. Nichols, pp. 137-144. Archaeological Papers of the American Anthropological Association No. 13.

Fish, Paul R.
1989 The Hohokam: 1,000 Years of Prehistory in the Sonoran Desert. In *Dynamics of Southwest Prehistory*, eds., Linda S. Cordell and George J. Gumerman, pp. 19-63. Smithsonian Institution Press, Washington D.C.

Foord, Eugene E. and Joseph E. Taggart, Jr.
1998 A Reexamination of the Turquoise Group: the Mineral Aheylite, Planerite (redefined), Turquoise and Coeruleolacite. *Mineralogical Magazine* 62:93-111.

Ford, Richard I.
1983 Inter-Indian Exchange in the Southwest. In *Southwest*, ed., Alfonso Ortiz, pp. 711-722. Handbook of North American Indians Vol. 10, Smithsonian Institute, Washington D. C.

Foster, Michael S.
1986 The Mesoamerican Connection: A View from the South. In *Ripples in the Chichimec Sea: New Considerations of Southwestern-Mesoamerican Interaction*, eds., Frances Joan Mathien and Randall H. McGuire, pp. 55-69. Southern Illinois University Press, Carbondale, Illinois.

1992 Arqueología del valle de Casas Grandes: Sitio Paquimé. In *Historia General de Chihuahua, Gología, Geograffa, y Arqueología*, ed., Arturo Márquez-Alameda, pp. 229-282. Universidad Autónoma de Ciudad Juárez, Chihuahua.

1999 The Aztatlán Tradition of West and Northwest Mexico and Casas Grandes: Speculations on the Medio Period Fluorescence. In *The Casas Grandes World*, eds., Curtis F. Schaafsma and Carroll L. Riley, pp. 149-163. University of Utah Press, Salt Lake City, Utah.

Fowler, Don D. and Linda S. Cordell
2005 Introduction. In *Southwest Archaeology in the Twentieth Century*, eds., Linda S. Cordell and Don D. Fowler, pp. 1-15. University of Utah Press, Salt Lake City, Utah.

Friedman, I.
1953 Deuterium Content of Natural Water and Other Substances. *Geochimica et Cosmochimica Acta* 4:89-103.

Friedman, I., A. C. Redfield, B. Schoen, and J. Harris
1964 The Variation in Deuterium Content of Natural Waters in the Hydrogenic Cycle. *Review Geophysics* 2:177-224.

Frisbie, Theodore R.
1978 High Status Burials in the Greater Southwest: An Interpretative Synthesis. In *Across the Chichimec Sea: Papers in Honor of J. Charles Kelley*, eds., Carroll L. Riley and Basil C. Hedrick, pp. 202-227. Southern Illinois University Press, Carbondale, Illinois.

Gillerman, Elliot
1964 *Mineral Deposits of Western Grant County, New Mexico*. State Bureau of Mines and Mineral Resources Bulletin 83, New Mexico Institute of Mining & Technology, Campus Station, Socorro, New Mexico.

Glascock, Michael D., Robert J. Speakman, and Hector Neff
2007 Archaeometry at the University of Missouri Research Reactor and the Provenance of Obsidian Artifacts in North America. *Archaeometry* 42(2):343-357.

Glascock, Michael D. and Hector Neff
2003 Neutron Activation Analysis and Provenance Research in Archaeology. *Measurement Science and Technology* 14:1516-1526.

Google Earth
2012 Google Earth. Electronic document, http://earth.google.com, accessed August 8, 2012.

Grauch, R. I.
1989 Rare Earth Elements in Metamorphic Rocks. In: *Geochemistry and Mineralogy of Rare Earth Elements*, pp. 147-168. MSA, Reviews in Mineralogy 21.

Graybeal, Frederick T.
1982 Geology of the El Tiro Area: Silver Bell Mining District, Pima County, Arizona. In *Advances in Geology of the Porphyry Copper Deposits: Southwestern North America*, ed., Spencer R. Titley, pp. 487-505. University of Arizona Press, Tucson, Arizona.

Gumerman, George J.
1988 A Historical Perspective on Environment and Culture in Anasazi Country. In *The Anasazi in a Changing Environment*, ed., George J. Gumerman, pp. 1-24. Cambridge University Press, Cambridge.

Gustafson, William G.
1965 *Geology of Copper-Lead-Zinc-Turquoise Deposits, Southern Part of the Cerrillos Mining District, Santa Fe County, New Mexico*. Unpublished M.A. thesis, University of New Mexico, Albuquerque, New Mexico.

Habicht-Mauche, Judith A., Stephen T. Glenn, Homer Milford, and A. Russell Flegal
2000 Isotopic Tracing of Prehistoric Rio Grande Glaze-Paint Production and Trade. *Journal of Archaeological Science* 27:709-713.

Hagemann, R., G. Nief, and E. Roth
1970 Absolute Isotopic Scale for Deuterium Analysis of Natural Waters. Absolute D/H Ratio of SMOW. *Tellus* 22:712-715.

Hall, Denis Kane
1972 *Hydrothermal Alteration and Mineralization in the East Camp of the Turquoise District, San Bernardino County, California*. Unpublished M.A. thesis, Department of Geosciences, University of Arizona, Tucson, Arizona.

Harbottle, Garman and Phil C. Weigand
1992 Turquoise in Pre-Columbian America. *Scientific American* Feb 1992:56-62.

Harrington, Mark R.
1925 An Ancient Salt Mine near St. Thomas, Nevada. *Indian Notes* 2(3):227-231. Museum of the American Indian, Heye Foundation, New York, New York.

1926 Another Ancient Salt Mine in Nevada. *Indian Notes* 3(4):221-232. Museum of the American Indian, Heye Foundation, New York, New York.

1928 Tracing the Pueblo Boundary in Nevada. *Indian Notes* 5(2):235-240. Museum of the American Indian, Heye Foundation, New York, New York.

Haury, Emil W.
1934 *The Canyon Creek Ruin and the Cliff Dwellings of the Sierra Ancha*. Medallion Papers No. 14. Gila Pueblo, Globe, Arizona.

Hirth, Kenneth G.
1996 Political Economy and Archaeology: Perspectives on Exchange and Production. *Journal of Archaeological Research* 4(3):203-239.

Hodder, Ian
1995 Material Culture in Time. In *Interpreting Archaeology: Finding Meaning in the Past*, eds., Ian Hodder, Michael Shanks, Alexandra Alexandri, Victor Buchli, John Carman, Jonathan Last, and Gavin Lucas, pp. 164-168. Routledge, London.

1999 *The Archaeological Process: An Introduction*. Blackwell Publishers, Oxford.

2000 Agency and Individuals in Long-term Processes. In *Agency in Archaeology*, eds., Marcia-Anne Dobres and John E. Robb, pp. 21-33. Routledge, London.

Hodder, Ian, and Scott Hutson
2003 *Reading the Past: Current Approaches to Interpretation in Archaeology* 3rd edition. Cambridge University Press, Cambridge.

Hodell, David A., R. L. Quinn, Mark Brenner, and G. Kamenov
2004 Spatial Variation of Strontium Isotopes ($^{87}Sr/^{86}Sr$) in the Maya Region: A Tool for Tracking Ancient Human Migration. *Journal of Archaeological Science* 31:585-604.

Hoefs, J.
2004 *Stable Isotope Geochemistry* 5th edition. Springer, Berlin.

Hughes, Richard E. and James A. Bennyhoff
1986 Early Trade. In *Great Basin*, ed., Warren L. D'Azevedo, pp. 238-255. Handbook of North American Indians Vol. 11, Smithsonian Institute, Washington D.C.

Hull, Sharon
2006 *Using Hydrogen and Copper Stable Isotopes to Source Turquoise*. Unpublished M.A. thesis, Department of Anthropology and Applied Archaeology, Eastern New Mexico University, Portales, New Mexico.

Hull, Sharon, Mostafa Fayek, Lawrence M. Anovitz, Frances Joan Mathien, and Phillip Shelley
2005 *The Effects of Alteration on Sourcing Archaeological Turquoise*. Paper presented at the Geological Society of America, Salt Lake City, Utah, Abstract 37-7.

Hull, Sharon, Mostafa Fayek, Frances Joan Mathien, Phillip Shelley, and Kathy Roler Durand
2008 A New Approach to Determining the Geological Provenance of Turquoise Artifacts Using Hydrogen and Copper Stable Isotopes. *Journal of Archaeological Science* 35:1355-1369.

Iñañez, J. G., J. J. Bellucci, E. Rodríguez-Alergía, R. Ash, W. McDonough, and R. J. Speakman
2010 Romita Pottery Revisited: A Reassessment of the Provenance of Ceramics from Colonial Mexico by LA-MC-ICP-MS. *Journal of Archaeological Science* 37:2698-2704.

Irwin-Williams, Cynthia
1977 A Network Model for the Analysis of Prehistoric Trade. In *Exchange Systems in Prehistory,* eds., Timothy K. Earle and Jonathan E. Ericson, pp. 141-151. Academic Press, New York, New York.

Irwin-Williams, Cynthia and Phillip H. Shelley
1980 *Investigations at Salmon Ruin: The Structure of Chacoan Society in the Northern Southwest. Volumes I-IV*. Eastern New Mexico University Printing Service, Portales, New Mexico.

Janetski, Joel C.
2002 Trade in Fremont Society: Contexts and Contrasts. *Journal of Anthropological Archaeology* 21:344-370.

2008 The Enigmatic Fremont. In *The Great Basin: People and Place in Ancient Times*, eds., Catherine S. Fowler and Don D. Fowler, pp. 104-115. School for Advance Research Press, Santa Fe, New Mexico.

Jenson, William A.
1985 *Prehistoric Turquoise Mining in the Turquoise Mountain Region, Northeast Mojave Desert, California*. Unpublished M.A. thesis, California State University, San Bernardino, California.

Johnson, D. W.
1903 The Geology of the Cerrillos Hills, New Mexico. *Columbia University School of Mines Quarterly* 24:493-499.

Johnston, Bernice
1964 Newly Discovered Turquoise Mine in Mohave County, Arizona. *Kiva* 29(3):76-83.

Judd, Neil M.
1954 *The Material Culture of Pueblo Bonito*. Smithsonian Miscellaneous Collections 124, Smithsonian Institution, Washington D.C.

1964 *The Architecture of Pueblo Bonito*. Smithsonian Miscellaneous Collections 147, Smithsonian Institution, Washington D.C.

Judge, W. James
1976 *The Development of a Complex Cultural Ecosystem in the Chaco Basin, New Mexico*. Chaco Center No. 21, National Park Service and University of New Mexico, Albuquerque, New Mexico.

1989 Chaco Canyon-San Juan Basin. In *Dynamics of Southwest Prehistory*, eds., Linda S. Cordell and George J. Gumerman, pp. 209-261. Smithsonian Institution Press, Washington D.C.

Judge, W. James and Linda S. Cordell
2006 Society and Polity. In *The Archaeology of Chaco Canyon: An Eleventh-Century Pueblo Regional Center*, ed., Stephen H. Lekson, pp. 189-210. School of American Research Press, Santa Fe, New Mexico.

Kelley, J. Charles
1986 The Mobile Merchants of Molino. In *Ripples in the Chichimec Sea: New Considerations of Southwestern-Mesoamerican Interaction*, eds., Frances Joan Mathien and Randall H. McGuire, pp. 81-104. Southern Illinois University Press, Carbondale, Illinois.

1993 Zenith Passage: The View from Chalchihuites. In *Culture and Contact: Charles C. Di Peso's Gran Chichimeca*, eds., Anne I. Woosley and John C. Ravesloot, pp. 227-250. University of New Mexico Press, Albuquerque, New Mexico.

1995 Trade Goods, Traders and Status in Northwestern Greater Mesoamerica. In *The Gran Chichimeca: Essays on the Archaeology and Ethnohistory of Northern Mesoamerica*, ed., Jonathan E. Reyman, pp. 102-145. Avebury, Aldershot, Great Britain.

Kelley, J. Charles and Ellen Abbott Kelley
1975 An Alternative Hypothesis for the Explanation of Anasazi Culture History. In *Collected Papers in Honor of Florence Hawley Ellis*, ed., Theodore R. Frisbie, pp. 178-223. Papers of the Archaeological Society of New Mexico 2. Hooper Publishing Company, Norman, Oklahoma.

Kidder, Alfred V.
1916 Archaeological Explorations at Pecos, New Mexico. *Proceeding of the National Academy of Sciences* 2(3):119-123.

1917 A Design-Sequence from New Mexico. *Proceeding of the National Academy of Sciences* 3(5):369-370.

Kidder, Mary A. and Alfred V. Kidder
1917 Notes on the Pottery of Pecos. *American Anthropologist* 19(3):325-360.

Kim, Jangsuk, Arleyn W. Simon, Vincent Ripoche, James W. Mayer, and Barry Wilkens
2003 Proton-induced X-ray Emission Analysis of Turquoise Artifacts from Salado Platform Mound Sites in the Tonto Basin of Central Arizona. *Measurement Science and Technology* 14:1579-1589.

Kintigh, Keith W.
2003 Coming to Terms with the Chaco World. *Kiva* 69(2):93-116.

Klein, S., P. B. Brey, S. Durali-Müller, and Y. Lahaye
2010 Characterization of the Raw Metal Sources used for the Production of Copper and Copper-based Objects with Copper Isotopes. *Archaeological and Anthropological Science* 2: 45–56.

Kluckhohn, Clyde
1939 Discussion. In *Preliminary Report on the 1937 Excavations, Bc. 50-51, Chaco Canyon, New Mexico*, eds., Clyde Kluckhohn and Paul Reiter, pp. 151-162. University of New Mexico Bulletin No. 345, Anthropological Series 3(2). University of New Mexico, Albuquerque, New Mexico.

Kolessar, Joseph
1982 The Tyrone Copper Deposit: Grant County, New Mexico. In *Advances in Geology of the Porphyry Copper Deposits: Southwestern North America*, ed., Spencer R. Titley, pp. 327-333. University of Arizona Press, Tucson, Arizona.

Kroeber, Alfred L.
1919 On the Principle of Order in Civilization as Exemplified by Changes of Fashion. *American Anthropologist* 21:235-263.

Kues, Barry S.
1992 New Mexico Geology. The Interplay of a Complex Structural History, Erosion, and Volcanism has Produced the Varied Landscapes of New Mexico. *Rocks & Minerals* 67(5)340-349.

Kunz, George F.
1905 *Gems, Jewelers' Materials, and Ornamental Stones of California*. California State Mineral Bureau Bulletin 37.

Larson, Peter B., Kierran Maher, Frank C. Ramos, Zhaoshan Chang, Miguel Gaspar, and Lawrence D. Meinert
2003 Copper Isotope Ratios in Magmatic and Hydrothermal Ore-forming Environments. *Chemical Geology* 201:337-350.

LeBlanc, Steven A.
1986 Aspects of Southwestern Prehistory: A.D. 900-1400. In *Ripples in the Chichimec Sea: New Considerations of Southwestern-Mesoamerican Interaction*, eds., Frances Joan Mathien and Randall H. McGuire, pp. 105-134. Southern Illinois University Press, Carbondale, Illinois.

1989 Cultural Dynamics in the Southern Mogollon Area. In *Dynamics of Southwest Prehistory*, eds., Linda S. Cordell and George J. Gumerman, pp. 179-207. Smithsonian Institution Press, Washington D.C.

Lee, C. W.
2004 The Nature of, and Approaches to, Teaching Forensic Geoscience on Forensic Science and Earth Science Courses. In *Forensic Geoscience: Principles, Techniques, and Applications*, eds., K. Pye and D. J. Croft, pp. 301-312. Geological Society of London, London.

Lekson, Stephen H.
1986 *Great Pueblo Architecture of Chaco Canyon, New Mexico*. University of New Mexico Press, Albuquerque. Originally published in 1984 as Publications in Archaeology No. 18B, Chaco Canyon Studies. National Park Service, Albuquerque, New Mexico.

1991 Settlement Patterns and the Chaco Region. In *Chaco and Hohokam: Prehistoric Regional Systems in the American Southwest*, eds., Patricia L. Crown and W. James Judge, pp. 31-55. School of American Research Press, Santa Fe, New Mexico.

1999 *The Chaco Meridian. Centers of Political Power in the Ancient Southwest.* Altimira Press, Walnut Creek, California.

2006 Chaco Matters. In *The Archaeology of Chaco Canyon: An Eleventh-Century Pueblo Regional Center*, ed., Stephen H. Lekson, pp. 3-44. School of American Research Press, Santa Fe, New Mexico.

Lekson, Stephen H. and Catherine M. Cameron
1995 The Abandonment of Chaco Canyon, the Mesa Verde Migrations, and the Reorganization of the Pueblo World. *Journal of Anthropological Archaeology* 14:184-202.

Lekson, Stephen H., Thomas C. Windes, and Peter J. McKenna
2006 Architecture. In *The Archaeology of Chaco Canyon: An Eleventh-Century Pueblo Regional Center*, ed., Stephen H. Lekson, pp. 67-116. School of American Research Press, Santa Fe, New Mexico.

Leonard III, N. Nelson and Christopher E. Drover
1980 Prehistoric Turquoise Mining in the Halloran Springs District, San Bernardino County, California. *Journal of California and Great Basin Anthropology* 2:245-256.

Libby, W. F.
1962 Radiocarbon: An Atomic Clock. *Annual Science and Humanity Journal*.

Linné, Sigvald
2003 *Archaeological Researchers at Teotihuacán, Mexico*. University of Alabama Press, Tuscaloosa. Originally published in 1934 by the Ethnographical Museum of Sweden Publication I, Stockholm.

Lipe, William D.
2006 Notes from the North. In *The Archaeology of Chaco Canyon: An Eleventh-Century Pueblo Regional Center*, ed., Stephen H. Lekson, pp. 261-313. School of American Research Press, Santa Fe, New Mexico.

Lister, Robert H.
1978 Mesoamerican Influence at Chaco Canyon, New Mexico. In *Across the Chichimec Sea: Papers in Honor of J. Charles Kelley*, eds., Carroll L. Riley and Basil C. Hedrick, pp. 233-241. Southern Illinois University Press, Carbondale, Illinois.

Lister, Robert H. and Florence C. Lister
1981 *Chaco Canyon: Archaeology and Archaeologists*. University of New Mexico Press, Albuquerque, New Mexico.

1987 *Aztec Ruins on the Animas: Excavated, Preserved and Interpreted*. University of New Mexico Press, Albuquerque, New Mexico.

Liu, Rong, Sharon Hull, and Mostafa Fayek
2010 A New Approach to Measuring D/H Ratios with the Cameca IMS-7F. *Journal of Surface and Interface Analysis* (www.interscience.wiley.com) DOI 10.1002/sia.3467.

Longstaffe, F. J., R. H. McNutt, and J. H. Crocket
1982 Rare-earth Element Modeling of Archean Meta-igneous and Igneous Rocks, Lake Despair Area, Northwestern Ontario. *Precambrian Research* 17:275-296.

Ludington, Steve, William F. Hanna, Robert L. Turner, and Rodney E. Jeske
1988 *Mineral Resources of the Organ Mountains Wilderness Study Area, Doña Ana County, New Mexico.* U. S. Geological Survey Bulletin 1735-D, United States Government Printing Office.

Lueth, Virgil W.
1998 Two Diverse Origins of Turquoise at the Orogrande Mining District, Otero County, New Mexico. *New Mexico Geology* 20:64-65.

Lyneis, Margaret
1986 A Spatial Analysis of Anasazi Architecture, A.D. 950-1150, Moapa Valley, Nevada. *The Kiva* 52(1): 53-74.

2000 Life at the Edge: Pueblo Settlements in Southern Nevada. In *The Archaeology of Regional Interaction: Religion, Warfare, and Exchange across the American Southwest and Beyond*, ed., Michelle Hegmon, pp. 257-274. Proceedings of the 1996 Southwest Symposium. University Press of Colorado, Boulder, Colorado.

Manley, Jr., R. L.
1950 Differential Thermal Analysis of Certain Phosphates. *American Mineralogist* 35:108-115.

Maréchal, Chloé Nadia, Philippe Télouk, and Francis Albarède
1999 Precise Analysis of Copper and Zinc Isotopic Compositions by Plasma-source Mass Spectrometry. *Chemical Geology* 156:251-273.

Maréchal, Chloé and Francis Albarède
2002 Ion-exchange Fractionation of Copper and Zinc Isotopes. *Geochimica et Cosmochimica Acta* 66(9):1499-1509.

Martin, Paul S. and Fred Plog
1973 *The Archaeology of Arizona: A Study of One Southwest Region*. Doubleday Natural History Press, New York, New York.

Mason, Thomas F. D., Dominik J. Weiss, John B. Chapman, Jamie J. Wilkinson, Svetlana G. Tessalina, Baruch Spiro, Matthew S. A. Horstwood, John Spratt, and Barry J. Coles
1997 Zn and Cu Isotopic Variability in the Alexandrinka Volcanic-hosted Massive Sulphide (VHMS) Ore Deposit, Urals, Russia. *Chemical Geology* 221:170-187.

Mathien, Frances Joan
1981a *Economic Exchange Systems in the San Juan Basin*. Unpublished dissertation, University of New Mexico, Albuquerque, New Mexico.

1981b Neutron Activation of Turquoise Artifacts from Chaco Canyon, New Mexico. *Current Anthropology* 22:293-294.

1984 Social and Economic Implications of Jewelry Items of the Chaco Anasazi. In *Recent Research on Chaco Prehistory*, eds. W. James Judge and John D. Schelberg, pp. 173-186. Reports of the Chaco Center No. 8, Division of Cultural Research, National Park Service, Albuquerque, New Mexico.

1986 External Contact and the Chaco Anasazi. In *Ripples in the Chichimec Sea: New Considerations of Southwestern-Mesoamerican Interaction*, eds., Frances Joan Mathien and Randall H. McGuire, pp. 220-242. Southern Illinois University Press, Carbondale, Illinois.

1992 Ornaments and Minerals from Site 29SJ627. In *Excavations at 29SJ 627, Chaco Canyon. New Mexico. Volume II. The Artifact Analyses*, ed., Frances Joan Mathien, pp. 265-318. Reports of the Chaco Center No. 11, Branch of Cultural Research, National Parks Service, Santa Fe, New Mexico.

1993 Ornaments and Minerals from 29SJ629. In *Investigations at 29SJ629, Chaco Canyon, New Mexico: Artifactual and Biological Analyses*. Volume II, ed., Thomas C. Windes, pp. 269-316. Reports of the Chaco Center No. 12, Branch of Cultural Research, National Park Service, Santa Fe, New Mexico.

1995 Evidence of Prehistoric Turquoise Mining at Orogrande, Jarilla Mountains, New Mexico. In *Of Pots and Rocks: Papers in Honor of A. Helene Warren*, eds., Meliha S. Duran and David T. Kirkpatrick, pp. 77-91. Archaeological Society of New Mexico 21, Albuquerque, New Mexico.

1999 Identifying Sources of Prehistoric Turquoise in North America: Problems and Implications for Interpreting Social Organization. *Beads Journal of the Society of Bead Researchers* 12-13:17-37, ed., Karlis Karklins, Society of Bead Researchers, Toronto, Ontario.

2001 The Organization of Turquoise Production and Consumption by the Prehistoric Chacoans. *American Antiquity* 66:103-118.

2005 *Culture and Ecology of Chaco Canyon and the San Juan Basin*. Publications in Archaeology 18H Chaco Canyon Studies, National Park Service, Santa Fe, New Mexico.

Mathien, Frances Joan and Randall H. McGuire
1986 Adrift in the Chichimec Sea. In *Ripples in the Chichimec Sea: New Considerations of Southwestern-Mesoamerican Interaction*, eds., Frances Joan Mathien and Randall H. McGuire, pp. 1-8. Southern Illinois University Press, Carbondale, Illinois.

Mathien, Frances Joan and Bart Olinger
1992 An Experiment with X-ray Fluorescence to Determine Trace Element Variability in Turquoise Composition. In *Archaeology, Art, and Anthropology: Papers in Honor of J.J. Brody,* eds., Meliha S. Duran and David T. Kirpatrick, pp. 123-134. The Archaeological Society of New Mexico, Albuquerque, New Mexico.

Mathur, R., S. Titley, F. Barra, S. Brantley, M. Wilson, A. Phillips, F. Munizaga, V. Maksaev, J. Vervoort, and G. Hart
2009a Exploration Potential of Cu Isotope Fractionation in Porphyry Copper Deposits. *Journal of Geochemical Exploration* 102: 1–6.

Mathur, R., S. Titley, G. Hart, M. Wilson, M. Davignon, and C. Zlatos
2009b The History of the United States Cent Revealed through Copper Isotope Fractionation. *Journal of Archaeological Science* 36: 430–433.

McGuire, Randall H.
1980 The Mesoamerican Connection in the Southwest. *The Kiva* 46:3-38.

1986 Economies and Modes of Production in the Prehistoric Southwestern Periphery. In *Ripples in the Chichimec Sea: New Considerations of Southwestern-Mesoamerican Interaction*, eds., Frances Joan Mathien and Randall H. McGuire, pp. 243-269. Southern Illinois University Press, Carbondale, Illinois.

1989 The Greater Southwest as a Periphery of Mesoamerica. In *Centre and Periphery: Comparative Studies in Archaeology*, ed., Timothy C. Champion, pp. 40-66. Unwin Hyman, London.

McGuire, Randall H., Charles Adams, Ben A. Nelson, and Katherine A. Spielmann
1994 Drawing the Southwest to Scale Perspectives on Macroregional Relations. In *Themes in Southwest Prehistory*, ed., George J. Gumerman, pp. 239-265. School of American Research Press, Santa Fe, New Mexico.

McKenna, Peter J.
1984 *The Architecture and Material Culture of 29SJ1360, Chaco Canyon, New Mexico*. Reports of the Chaco Center No. 7, Division of Cultural Research, National Park Service, Albuquerque, New Mexico.

1986 A Summary of the Chaco Center's Small Site Excavations: 1973-1978. Part I in *Small Site Architecture of Chaco Canyon, New Mexico*, by Peter J. McKenna and Marcia L. Truell, pp. 5-114. Publications in Archaeology 18D, Chaco Canyon Studies, National Park Service, Santa Fe, New Mexico.

McLennan, S. M.
1989 Rare Earth Elements in Sedimentary Rocks. Influence of Provenance and Sedimentary Processes. In: *Geochemistry and Mineralogy of Rare Earth Elements*, pp. 169-200. MSA, Reviews in Mineralogy 21.

Michard, A.
1989 Rare Earth Element Systematics in Hydrothermal Fluids. *Geochimica et Cosmochimica Acta* 53:745-750.

Michard, A., C. Beaucaire, and G. Michard
1987 Uranium and REE Contents of some CO_2-rich Waters from Vals-Les-Bains (France). *Geochimica et Cosmochimica Acta* 51:901-909.

Minnis, Paul E.
1989 The Casas Grandes Polity in the International Four Corners. In *The Sociopolitical Structure of Prehistoric Southwestern Societies*, eds., S. Upham, K. G. Lightfoot, and R. A. Jewitt, pp. 269-305. Westview Press, Boulder, Colorado.

Modreski, Peter J. and Jack A. Murphy
2002 Colorado Turquoise. *New Mexico Geology* 24(4):133.

Morris, Earl H.
1915 The Excavation of a Ruin near Aztec, San Juan County, New Mexico. *American Anthropologist* 17(4):666-684.

1919 *The Aztec Ruin*. Anthropological Papers of the American Museum of Natural History Vol. 26, part 1, pp. 1-108. The American Museum of Natural History, New York, New York.

1921 *The House of the Great Kiva at the Aztec Ruin*. Anthropological Papers of the American Museum of Natural History Vol. 26, part 2, pp. 109-138. The American Museum of Natural History, New York, New York.

1924 *Burials in the Aztec Ruin The Aztec Ruin Annex*. Anthropological Papers of the American Museum of Natural History Vol. 26, parts 3 and 4, pp. 138-257. The American Museum of Natural History, New York, New York.

1928 *Notes on Excavations in the Aztec Ruin*. Anthropological Papers of the American Museum of Natural History Vol. 26, part 5, pp. 259-420. The American Museum of Natural History, New York, New York.

Morrissey, Frank
1968 *Turquoise Deposits of Nevada*. Report 17, Mackay School of Mines, University of Nevada, Reno, Nevada.

Nazelrod, Ed
1977 Recent Developments in the Turquoise Mountains of California. *Lapidary Journal* December 1977:1982-1988.

Neitzel, Jill E.
2003 The Organization, Function, and Population of Pueblo Bonito. In *Pueblo Bonito: Center of the Pueblo World*, ed., Jill E. Neitzel, pp. 143-149. Smithsonian Press, Washington D.C.

Neitzel, Jill E. and Ronald L. Bishop
1990 Neutron Activation of Dogoszhi Style Ceramics: Production and Exchange in the Chacoan Regional System. *Kiva* 56(1):67-85.

Nelson, Nels C.
1916 Chronology of the Tano Ruins, New Mexico. *American Anthropologist* 18:159-180.

Nelson, Richard S.
1986 Pochtecas and Prestige: Mesoamerican Artifacts in Hohokam Sites. In *Ripples in the Chichimec Sea: New Considerations of Southwestern-Mesoamerican Interaction*, eds., Frances Joan Mathien and Randall H. McGuire, pp. 155-182. Southern Illinois University Press, Carbondale, Illinois.

Northrop, Stuart A.
1959 *Minerals of New Mexico*. University of New Mexico Press, Albuquerque, New Mexico.

1975 *Turquois and Spanish Mines in New Mexico*. University of New Mexico Press, Albuquerque, New Mexico.

Paige, Sidney
1912 The Origin of Turquoise in the Burro Mountains, New Mexico. *Economic Geology* 7:382-392.

Pailes, R. A.
1978 The Rio Sonora Culture in Prehistoric Trade Systems. In *Across the Chichimec Sea: Papers in Honor of J. Charles Kelley*, eds., Carroll L. Riley and Basil C. Hedrick, pp. 134-143. Southern Illinois University Press, Carbondale, Illinois.

Palacios, C., O. Rouxel, M. Reich, E. M. Cameron, and M. I. Leybourne
2011 Pleistocene Recycling of Copper at a Porphyry System, Atacama Desert, Chile: Cu Isotope Evidence. *Mineralium Deposita* 46: 1–7.

Palerm, Angel and Eric Wolf
1957 Ecological Potential and Cultural Development in Mesoamerica. In *Studies in Human Ecology*, pp. 1-37. Anthropological Society of Washington and Pan American Union Social Science Monograph No. 3.

Palma, Ana Maria Alvarez
1982 Archaeological Investigations at Huatabampo. In *Mogollon Archaeology: Proceedings of the 1980 Mogollon Conference*, ed., Patrick H. Beckett, pp. 239-250. Acoma Books, Ramona, California.

Panczner, William D.
1987 *Minerals of Mexico*. Van Nostrand Reinhold Company, New York, New York.

Pearl, Richard M.
1941 Turquoise Deposits of Colorado. *Economic Geology and the Bulletin of the Society of Economic Geologist* 36(3):335-344.

Pepper, George H.
1996 *Pueblo Bonito.* University of New Mexico Press, Albuquerque. Originally published 1920, Anthropological Papers of the American Museum of Natural History 27. New York, New York.

Peterson, N. P.
1947 Phosphate Minerals in the Castle Dome Copper Deposit, Arizona. *American Mineralogist* 32:574-582.

Plog, Fred, George J. Gumerman, Robert C. Euler, Jeffrey S. Dean, Richard H. Hevly, and Thor N. V. Karlstrom.
1988 Anasazi Adaptive Strategies: The Model, Predictions, and Results. In *The Anasazi in a Changing Environment*, ed., George J. Gumerman, pp. 230-276. Cambridge University Press, Cambridge.

Plog, Stephen and Adam S. Watson
2012 The Chaco Pilgrimage Model: Evaluating the Evidence From Pueblo Alto. *American Antiquity* 77(3):449-477.

Pogue, Joseph
1974 *The Turquois. A Study of Its History, Mineralogy, Geology, Ethnology, Archaeology, Mythology, Folklore, and Technology.* Glorietta, New Mexico. Originally published 1915, Memoirs of the National Academy of Sciences Vol. XII, Part II, Washington D.C.

Price, T. D., L. Manzanilla, and W. D. Middleton
2000 Immigration and the Ancient City of Teotihuacán in Mexico: A Study using Strontium Isotope Ratios in Human Bone and Teeth. *Journal of Archaeological Science* 27:903-913.

Price, T. D., C. M. Johnson, J. A. Ezzo, J. Ericson, and J. H. Burton
1994 Residential Mobility in the Prehistoric Southwest United States: A Preliminary Study using Strontium Isotope Analysis. *Journal of Archaeological Science* 21:315-330.

Puchelt, H. and R. Emmermann
1976 Bearing of Rare Earth Element Patterns of Apatites from Igneous and Metamorphic Rocks. *Earth and Planetary Science Letters* 31:279-286.

Rafferty, Kevin
1990 The Virgin Anasazi and the Pan-Southwestern Trade System, A.D. 900-1150. *Kiva* 56:3-24.

Ransome, Frederick Leslie
1913 *The Turquoise Copper-Mining District, Arizona*. Contributions to Economic Geology (Short Papers and Preliminary Reports) 1911. Part 1: Metals and Nonmetals except Fuel, U. S. Geological Survey Bulletin No. 530, pp. 125-134.

Ravesloot, John C., Jeffrey S. Dean, and Michael S. Foster
1995 A New Perspective on the Casas Grandes Tree-Ring Dates. In *The Gran Chichimeca: Essays on the Archaeology and Ethnohistory of Northern Mesoamerica*, ed., Jonathan E. Reyman, pp. 240-251. Avebury, Aldershot, Great Britain.

Reed, Erik K.
1964 The Greater Southwest. In *Prehistoric Man in the New World*, eds., Jesse D. Jennings and Edward Norbeck, pp. 175-193. University of Chicago Press, Chicago.

Reed, Paul F.
2006a The Center for Desert Archaeology's Salmon Reinvestment Program and New Research at Salmon Ruins. In *Thirty-five years of Archaeological Research at Salmon Ruins, New Mexico*, ed., Paul F. Reed, pp. 1-15. Center for Desert Archaeology, Tucson, Arizona and Salmon Ruins Museum, Bloomfield, New Mexico.

2006b The Ruins of Salmon Pueblo in Historic Context. In *Thirty-five years of Archaeological Research at Salmon Ruins, New Mexico*, ed., Paul F. Reed, pp. 41-55. Center for Desert Archaeology, Tucson, Arizona and Salmon Ruins Museum, Bloomfield, New Mexico.

2006c Salmon Pueblo: Chacoan Outlier and Thirteenth-Century Middle San Juan Community Center. In *Thirty-five years of Archaeological Research at Salmon Ruins, New Mexico*, ed., Paul F. Reed, pp. 367-376. Center for Desert Archaeology, Tucson, Arizona and Salmon Ruins Museum, Bloomfield, New Mexico.

2008 Setting the Stage: A Reconsideration of Salmon, Aztec, and the Middle San Juan Region. In *Chaco's Northern Prodigies: Salmon, Aztec, and the Ascendancy of the Middle San Juan Region After AD 1100*, ed., Paul F. Reed, pp. 3-28. University of Utah Press, Salt Lake City, Utah.

2011 Chacoan Immigration or Local Emulation of the Chacoan System? The Emergence of Aztec, Salmon, and Other Great House Communities in the Middle San Juan. *Kiva* 77(2):119-138.

Renfrew, Colin
1986 Introduction: Peer Polity Interaction and Socio-Political Change. *In Peer Polity Interaction and Socio-Political Change*, eds., Colin Renfrew and J. F. Cherry, pp. 1-18. Cambridge University Press, Cambridge.

Reyman, Jonathan E.
1978 Pochteca Burials at Anasazi Sites? In *Across the Chichimec Sea: Papers in Honor of J. Charles Kelley*, eds., Carroll L. Riley and Basil C. Hedrick, pp. 242-259. Southern Illinois University Press, Carbondale, Illinois.

Riciputi, Lee R., Bruce A. Paterson, and Robert L. Ripperdan
1998 Measurement of Light Stable Isotope Ratios by SIMS: Matrix Effects for Oxygen, Carbon, and Sulfur Isotopes in Minerals. *International Journal of Mass Spectrometry* 178:81-112.

Riley, Carroll L.
1978 Retrospect and Prospect. In *Across the Chichimec Sea: Papers in Honor of J. Charles Kelley*, eds., Carroll L. Riley and Basil C. Hedrick, pp. 3-8. Southern Illinois University Press, Carbondale, Illinois.

Robb, L.
2005 *Introduction to Ore-forming Processes*. Blackwell Publishing, Malden, Massachusetts.

Roberts, Frank H. H., Jr.
1929 *Shabik'eshchee Village, a Late Basket Maker Site in Chaco Canyon, New Mexico*. Bureau of American Ethnology Bulletin 92, Smithsonian Institution, Washington D.C.

Robinson, William J., Bruce G. Harrell, and Richard L. Warren
1974 *Tree-Ring Dates from New Mexico B: Chaco-Gobernador Area*. The Laboratory of Tree-Ring Research, University of Arizona, Tucson, Arizona.

Rogers, Malcolm J.
1929 Report of an Archaeological Reconnaissance in the Mohave Sink Region. *The San Diego Museum Archaeology* 1(1):1-13.

Rohn, Arthur H.
1989 Northern San Juan Prehistory. In *Dynamics of Southwest Prehistory*, eds., Linda S. Cordell and George J. Gumerman, pp. 149-177. Smithsonian Institution Press, Washington D.C.

Ronzio, A. R. and M. L. Salmon
1967 Relation between Source and Composition of Turquoise. *Journal of the Colorado-Wyoming Academy of Science* 5:30-31.

Ruppert, Hans
1982 Zur verbreitung and herkunft von Türkis und Sodalith in präkolumbischen Kulturen der Kordilleren. *Baessler-Archiv* 30:69-124.

1983 Geochemische Untersuchungen an Türkis und Sodalith aus Lagerstätten und präkolumbischen Kulturen der Kordilleren. *Berliner Beiträge zur Archäometrie* 8:101-210.

Saitta, Dean J.
2000 Theorizing the Political Economy of Southwestern Exchange. In *The Archaeology of Regional Interaction: Religion, Warfare, and Exchange across the American Southwest and Beyond*, ed., Michelle Hegmon, pp. 151-166. University Press of Colorado, Boulder, Colorado.

Schillaci, Michael A.
2003 The Development of Population Diversity at Chaco Canyon. *Kiva* 68:221-246.

Schillaci, Michael A. and Christopher M. Stojanowski
2002 Investigating Social Organization at Aztec Ruins Using Determinant Ratio Analyses. In *Forward into the Past: Papers in Honor of Teddy Lou and Francis Stickney*, eds., R. N. Weisman, T. C. O'Laughlin, and C. T. Snow, pp. 93-104. Archaeological Society of New Mexico Papers 28, Albuquerque, New Mexico.

Schmidt, Paul G. and Campbell Craddock
1964 *The Geology of the Jarilla Mountains, Otero County, New Mexico*. State Bureau of Mines and Mineral Resources Bulletin 82, New Mexico Institute of Mining & Technology, Campus Station, Socorro, New Mexico.

Schweissing, M. M. and G. Grupe
2003 Stable Strontium Isotopes in Human Teeth and Bone: A Key to Migration Events of the Late Roman Period in Bavaria. *Journal of Archaeological Science* 30:1373-1383.

Shackley, M. Steven
1998 The Southwest: An Archaeological, Petrological, and Geochemical Study. *American Antiquity* 53(4):752-772.

1995 Sources of Archaeological Obsidian in the Greater American Southwest: An Update and Quantitative Analysis. *American Antiquity* 60(3):531-551.

2005 *Obsidian: Geology and Archaeology in the North American Southwest*. University of Arizona Press, Tucson, Arizona.

Shanks, Michael
1995 Archaeology and the Forms of History. In *Interpreting Archaeology: Finding Meaning in the Past*, eds., Ian Hodder, Michael Shanks, Alexandra Alexandri, Victor Buchli, John Carman, Jonathan Last, and Gavin Lucas, pp. 169-174. Routledge, London.

Shanks, Michael, and Ian Hodder
1995 Processual, Postprocessual and Interpretive Archaeologies. In *Interpreting Archaeology: Finding Meaning in the Past*, eds., Ian Hodder, Michael Shanks, Alexandra Alexandri, Victor Buchli, John Carman, Jonathan Last, and Gavin Lucas, pp. 3-29. Routledge, London.

Sheppard, Simon M. F.
1986 Characterization and Isotopic Variations in Natural Waters. In *Stable isotopes in High Temperature Geological Processes*, eds., John W. Valley, H. P. Taylor, and J. R. O'Neil, pp. 165-183. Review Mineralogy 16.

Sigleo, Anne Marguerite Colberg
1970 *Trace-element Geochemistry of Southwestern Turquoise*. Unpublished M.S. thesis, University of New Mexico, Albuquerque, New Mexico.

1975 Turquoise Mine and Artifact Correlation for Snaketown Site, Arizona. *Science* 189:459-460.

Silliman, B.
1881 Turquoise of New Mexico. *American Journal of Science* 3rd Series 122:67-71.

Simms, Steven R.
2008 *Ancient Peoples of the Great Basin and Colorado Plateau*. Left Coast Press, Walnut Creek, California.

Simmons, W. W. and J. E. Fowells
1966 Geology of the Copper Cities Mine. In *Geology of the Porphyry Copper Deposits*, eds., Spencer R. Titley and Carol Hicks, pp. 151-156. University of Arizona Press, Tucson, Arizona.

Speakman, Robert J., Michael D. Glascock, Robert H. Tykot, Christophe Descantes, Jennifer J. Thatcher, Craig E. Skinner, and Kyra M. Lienhop
2007 Selected Applications of Laser Ablation Inductively Coupled Plasma-Mass Spectrometry to Archaeological Research. In *Archaeological Chemistry: Analytical Techniques and Archaeological Interpretation*, eds., Michael D. Glascock, Robert J. Speakman, and Rachel S. Popelka-Filcoff, pp. 275-296. American Chemical Society Symposium Series 968, Washington D.C.

Stein, Gil J.
2002 From Passive Periphery to Active Agents: Emerging Perspectives in the Archaeology of Interregional Interaction. *American Anthropologist* 104(3):903-916.

Stern, B., C. D. Lampert-Moore, C. Heron, and A. M. Pollard
2008 Bulk Slight Stable Isotopic Ratios in Recent and Archaeological Resins: Towards Detecting the Transport of Resins in Antiquity. *Archaeometry* 50:351-370.

Stern, R. A.
2009 An Introduction to Secondary Ion Mass Spectrometry (SIMS) in Geology. In *Secondary Ion Mass Spectrometry in the Earth Sciences: Gleaning the Big Picture from a Small Spot*, ed., Mostafa Fayek, pp. 1-18. Short Course Series Vol. 41, Mineralogical Association of Canada, Toronto, Ontario.

Sterrett, D. B.
1909 Gems and Precious Stones. *United States Geological Survey Mineral Resources* 2:846.

Sutter, J. F.
1968 *Geochronology of Major Thrusts, Southern Great Basin, California*. Unpublished M.S. thesis. Rice University, Houston, Texas.

Taylor, H. P.
1979 Oxygen and Hydrogen Isotopic Relations in Hydrothermal Mineral Deposits. In *Geochemistry of Ore Deposits* 2nd edition, ed., H. L. Barnes, pp. 236-277. Wiley and Sons, New York, New York.

Theodore, Ted G., David W. Blake, and Edward L. Kretschmer
1982 Geology of the Copper Canyon Porphyry Copper Deposits: Lander County, Nevada. In *Advances in Geology of the Porphyry Copper Deposits: Southwestern North America,* ed., Spencer R. Titley, pp. 543-550. University of Arizona Press, Tucson, Arizona.

Thibodeau, Alyson M., Joaquin Ruiz, and John T. Chesley
2007 Lead and Strontium Isotopes as Tracers of Turquoise. *Society of Archaeological Science Bulletin* 30:10-14.

2009 *Tracing Turquoise from Site to Source using Radiogenic Isotopes*. Paper presented at the Society of American Archaeology, Atlanta, Georgia.

Thomas, Blakemore E.
1950 Ore Deposits of the Wallapai District, Arizona. *Economic Geology* 44(8):663-705.

Titley, Spencer R.
1982 Geological Setting of Porphyry Copper Deposits: Southeastern Arizona. In *Advances in Geology of the Porphyry Copper Deposits: Southwestern North America,* ed., Spencer R. Titley, pp. 37-58. University of Arizona Press, Tucson, Arizona.

Toll, H. Wolcott, III
1991 Material Distributions and Exchange in the Chaco System. In *Chaco and Hohokam Prehistoric Regional Systems in the American Southwest,* eds., Patricia L. Crown and W. James Judge, pp. 77-107. School of American Research Press, Santa Fe, New Mexico.

Trigger, Bruce. G.
2006 *A History of Archaeological Thought 2nd Edition.* Cambridge University Press, Cambridge.

Truell, Marcia L.
1976 *Site 628 Summary*. Chaco Culture NHP Museum Archive, University of New Mexico, Albuquerque, New Mexico.

Turner, B. L., G. D. Kamenov, J. D. Kingston, and G. J. Armelagos
2009 Insights into Immigration and Social Class at Machu Picchu, Peru Based on Oxygen, Strontium, and Lead Isotopic Analysis. *Journal of Archaeological Science* 36:317-332.

Upham, Steadman
1982 *Polities and Power: An Economic and Political History of the Western Pueblo*. Academic Press.

1992 Interaction and Isolation: The Empty Spaces in Panregional Political and Economic Systems. In *Resources, Power, and Interregional Interaction*, eds., Edward M. Schortman and Patricia A. Urban, pp. 139-152. Plenum Press, New York, New York.

Urban, Greg
2010 Objects, Social Relations, and Cultural Motion. In *Social Archaeologies of Trade and Exchange: Exploring Relationships among People, Places, and Things*, eds., Alexander A. Bauer and Anna S. Agbe-Davies, pp. 207-225. Left Coast Press, Walnut Creek, California.

Van Dyke, Ruth M.
2007 *The Chaco Experience: Landscape and Ideology at the Center Place*. School of American Research Press, Santa Fe, New Mexico.

2008 Sacred Landscapes: The Chaco-Totah Connection. In *Chaco's Northern Prodigies: Salmon, Aztec, and the Ascendancy of the Middle San Juan Region After AD 1100*, ed., Paul F. Reed, pp. 334-348. University of Utah Press, Salt Lake City, Utah.

Vivian, R. Gordon
1965 *The Three-C Site, and Early Pueblo II Ruin in Chaco Canyon, New Mexico*. University of New Mexico Publications in Anthropology No. 13, University of New Mexico, Albuquerque, New Mexico.

Vivian, R. Gwinn
1970 An Inquire into Prehistoric Social Organization in Chaco Canyon, New Mexico. In *Reconstructing Prehistoric Pueblo Societies*, ed., W. A. Longacre, pp. 59-83. School of American Research Press, Santa Fe, New Mexico and University of New Mexico Press, Albuquerque, New Mexico.

1990 *The Chacoan Prehistory of the San Juan Basin*. Academic Press, San Diego, California.

1991 Chacoan Subsistence. In *Chaco and Hohokam: Prehistoric Regional Systems in the American Southwest*, eds., Patricia L. Crown and W. James Judge, pp. 57-75. School of American Research Press, Santa Fe, New Mexico.

Vivian, R Gwinn, C. R. Van West, Jeffery S. Dean, Nancy J. Akins, M. S. Toll, and Thomas C. Windes
2006 Ecology and Economy. In *The Archaeology of Chaco Canyon: An Eleventh-Century Pueblo Regional Center*, ed., Stephen H. Lekson, pp. 45-65. School of American Research Press, Santa Fe, New Mexico.

Wallerstein, Immanuel
1974 *The Modern World System*. Studies in Political Discontinuity. Academic Press, New York, New York.

Warren, A. Helene and Frances Joan Mathien
1985 Prehistoric and Historic Turquoise Mining in the Cerrillos District: Time and Place. In *Southwestern Culture History: Papers in Honor of Albert H. Schroeder*. The Archaeological Society of New Mexico Vol. 10, pp. 93-127, Albuquerque, New Mexico.

Washburn, Dorothy K.
1980 The Mexican Connection: Cylinder Jars from the Valley of Oaxaca. *Transactions of the Illinois State Academy of Science* 72(4):70-85.

Weber, R. H.
1979 Turquoise in New Mexico. *New Mexico Geology* 28:39-40.

Weigand, Phil C.
1982 Sherds Associated with Turquoise Mines in the Southwest USA. *Pottery Southwest* 9(2):4-6.

1994 Observations on Ancient Mining within the Northwestern Regions of the Mesoamerican Civilization, with Emphasis on Turquoise. In *In Quest of Mineral Wealth: Aboriginal and Colonial Mining and Metallurgy in Spanish America*, eds., Alan K. Craig and Robert C. West, pp. 21-35. Geoscience and Man 33.

Weigand, Phil C. and Garman Harbottle
1993 The Role of Turquoises in the Ancient Mesoamerican Trade Structure. In *The American Southwest and Mesoamerica: Systems of Prehistoric Exchange*, eds., Jonathan E. Ericson and Timothy G. Baugh, pp. 159-177. Plenum Press, New York, New York.

Weigand, Phil C., Garman Harbottle, and Edward V. Sayre
1977 Turquoise Sources and Source Analysis: Mesoamerica and the Southwestern U.S.A. In *Exchange Systems in Prehistory*, eds., Timothy K. Earle and Jonathan E. Ericson, pp. 15-34. Academic Press, New York, New York.

Welch, John R. and Daniela Triadan
1991 Canyon Creek Turquoise Mine, Arizona. *Kiva* 56:145-164.

Whalen, Michael E. and Paul E. Minnis
2001 *Casas Grandes and its Hinterland: Prehistoric Regional Organization in Northwest Mexico*. University of Arizona Press, Tucson, Arizona.

2003 The Local and the Distant in the Origin of Casas Grandes, Chihuahua, Mexico. *American Antiquities* 68:314-332.

White, Christine, Fred J. Longstaffe, and Kimberley R. Law
2004 Exploring the Effects of Environment, Physiology and Diet on Oxygen Isotope Ratios in Ancient Nubian Bones and Teeth. *Journal of Archaeological Science* 31:233-250.

White, Christine, Fred J. Longstaffe, Michael W. Spence, and Kimberley R. Law
2000 Teotihuacán State Representation at Kaminaljuyú: Evidence from Oxygen Isotopes. *Journal of Archaeological Science* 56:535-558.

Wilcox, David R.
1986 A Historical Analysis of the Problem of Southwestern-Mesoamerican Connections. In *Ripples in the Chichimec Sea: New Considerations of Southwestern-Mesoamerican Interaction*, eds., Frances Joan Mathien and Randall H. McGuire, pp. 9-44. Southern Illinois University Press, Carbondale, Illinois.

Wilcox, David R. and Charles Sternberg
1983 *Hohokam Ballcourts and Their Interpretation*. Arizona State Museum Archaeological Series 160, Tucson, Arizona.

Wilkinson, Jr., William H., Luis A. Vega, and Spencer R. Titley
1982 Geology and Ore Deposits at Mineral Park, Mohave County, Arizona. In *Advances in Geology of the Porphyry Copper Deposits: Southwestern North America*, ed., Spencer R. Titley, pp. 523-550. University of Arizona Press, Tucson, Arizona.

Wills, W. H., F. Scott Worman, Wetherbee Dorshow, and Heather Richards-Rissetto
2012 Shabik'eschee Village in Chaco Canyon: Beyond the Archetype. *American Antiquity* 77(2):326-350.

Windes, Thomas C.
1993 *The Spadefoot Toad Site: Investigations at 29SJ 629 in Marcia's Rincon and the Fajada Gap Pueblo II Community, Chaco Canyon, New Mexico.* Chaco Center No. 13, Division of Anthropology, Branch of Cultural Research, National Park Service, Santa Fe, New Mexico.

Windes, Thomas C. and Dabney Ford
1992 The Nature of the Early Bonito Phase. In *Anasazi Regional Organization and the Chaco System*, ed., David E. Doyel, pp. 75-85. Anthropological Papers No. 5, Maxwell Museum of Anthropology, University of New Mexico, Albuquerque, New Mexico.

Wiseman, Regge N. and J. Andrew Darling
1986 The Bronze Trail Site Group: More Evidence for a Cerrillos-Chaco Turquoise Connection. In *Collected Papers in Honor of James G. Bain*, ed., Anne V. Poore, pp. 115-193. Papers of the Archaeological Society of New Mexico 12, Albuquerque, New Mexico.

Young, Suzanne M. M., Dave A. Phillips, Jr., and Frances Joan Mathien
1994 *Lead isotope analysis of turquoise in the Southwestern U.S.A. and Mesoamerica*. 29th International Symposium on Archaeometry, Ankara, Turkey.

Yurtsever, Y. and J. R. Gat
1981 Atmospheric Waters. In *Stable Isotope Hydrology: Deuterium and Oxygen-18 in the Water Cycle*, eds., J. R. Gat and R. Gonfiantini, pp. 103-142. Technical Report Series #210, International Atomic Energy Agency, Vienna.

Zedeño, Maria N., Hector Neff, and Axel Nielsen
2005 Searching for Analytical Alternatives to the Characterization of Copper Minerals. In *Laser Ablation ICP-MS in Archaeological Research*, eds., Robert J. Speakman and Hector Neff, pp. 77-84. University of New Mexico Press, Albuquerque, New Mexico.

Zeller, Jr., Robert A.
1970 *Geology of the Little Hatchet Mountains Hidalgo and Grant Counties New Mexico.* State Bureau of Mines and Mineral Resources New Mexico Bulletin 96, Institute of Mining and Technology, Socorro, New Mexico.

Appendix 1:

Turquoise Provenance Regions located in the Western United States and Northern Mexico

Appendix 1. Turquoise Provenance Regions located in the Western United States and Northern Mexico.

State	County	Area/District	Name	Evidence of Prehistoric Mining-References
Arizona	Cochise	Bisbee	Bisbee Mine (Lavender Pit)	Yes (Weigand 1982); Inconclusive (Weigand and Harbottle 1993)
Arizona	Cochise	Courtland Area; The Turquoise District; Avalon Group; Turquoise Mountain; Dragoon Mountain	Avalon; Brown's Peak; Courtland; Herget; Tiffany; Avalon Azul; Nightingale	Yes (Weigand 1982; Weigand and Harbottle 1993)
Arizona	Gila	Globe District	Sleeping Beauty (Copper Cities Mine)	Conclusive (Weigand 1982; Weigand and Harbottle 1993)
Arizona	Gila	Miami District	Castle Dome	Not reported
Arizona	Gila	Canyon Creek; Ft. Apache Reservation	Canyon Creek	Yes (Haury 1934; Weigand 1982)
Arizona	Graham	Lone Star District; Gila Mountains	Safford Porphyry Copper Deposit	Not reported
Arizona	Greenlee	Clifton District	Morenci Mine	Yes (Weigand 1982)
Arizona	Maricopa	Morristown	Name not reported	Not reported
Arizona	Mohave	Mineral Park; Kingman	Monte Cristo; Turquoise King; Queen; Peacock; Ithaca Peak; Metallic; Accident	Extensive (Johnston 1964; Pogue 1974; Weigand 1982; Weigand and Harbottle 1993)
Arizona	Pima	Pima District	Esperanza Mine	Not reported
Arizona	Pima	Silver Bell District	Silver Bell Mine	Not reported
Arizona	Pinal	Mineral Creek District; Kelvin	Name not reported	Not reported
Arizona	Yavapai	Chino Valley; Prescott;	Name not reported	Not reported

State	County	Area/District	Name	Evidence of Prehistoric Mining-References
		Whittmann		
Arizona	Yuma	Castle Dome Mountains	Name not reported	Not reported
California	San Bernardino	Halloran Springs	East Camp; Middle Camp; West Camp; Himalaya; Toltec	Extensive (Jenson 1985; Leonard and Drover 1980; Rogers 1929; Weigand 1982; Weigand and Harbottle 1993)
California	San Bernardino	Mohave Desert; Cottonwood Siding	Grove Turquoise Mine	Not reported
Colorado	Conejos	San Luis Valley; La Jara	King's Manassa Mine (King Mine; La Jara)	Extensive (Pearl 1941; Weigand 1982)
Colorado	Lake	St. Kelvin Mining District; Leadville; Turquoise Lake	Turquoise Chief; Poor Boy Lode; Iron Mask; Leadville	Inconclusive (Weigand and Harbottle 1993)
Colorado	Saguache	San Luis Valley; Villa Grove	Villa Grove Mine (Hall's Mine)	Inconclusive (Weigand and Harbottle 1993)
Colorado	Teller	Cripple Creek; Mineral Hill	Florence Mine	Not reported
Nevada	Clark	Boulder City	Sullivan	Not reported
Nevada	Clark	Crescent Peak; Searchlight	Crescent Peak; Simmons; Aztec; Right Blue; Turquoise	Yes (Weigand 1982; Weigand and Harbottle 1993)
Nevada	Elko	Lone Mountain District; Tuscarora Range	Carlin Black Matrix; Stampede	Not reported
Nevada	Esmeralda	Fish Lake Valley; Coaldale area	Carl Riek (Blue Boy); Miss Moffat (Persian Blue)	Not reported
Nevada	Esmeralda	Monte Cristo Range	Carrie; Carr-Lovejoy; Crow Spring; Marguerite; Monte Cristo	Not reported

State	County	Area/District	Name	Evidence of Prehistoric Mining-References
Nevada	Esmeralda	Paymaster Canyon	Lone Mountain; Blue Silver; Livesly	Not reported
Nevada	Eureka	Lynn District	August Berning; Number Eight	Not reported
Nevada	Lander	Copper Basin	Myron Clark; Turquoise King; Blue Gem Lease	Not reported
Nevada	Lander	Bullion District	Steinich; Rufan; Little Gem; Blue Nugget; Blue Gem; Super-X; Arrowhead; Old Campground; Blue Eagle; Blue Matrix	Not reported
Nevada	Lander	Cortez	Fox; Green Tree; Lone Pine; White Horse	Not reported
Nevada	Lander	Austin	Godber (Dry Creek); McGinness; Ralph King	Not reported
Nevada	Mineral	Pilot Mountains	Pilot Mountain; Moqui-Aztec; Montezuma; Troy Springs; Turquoise Bonanza; Copper King	Not reported
Nevada	Mineral	Pilot Mountains; Basalt	Blue Jay Gem; Blue Gem No. 1	Not reported
Nevada	Mineral	Excelsior Mountains; Sodaville	Halley's Comet; Clara	Not reported
Nevada	Nye	Nye County	Smith Black Matrix	Not reported
Nevada	Nye	Royston District; Big Smokey Valley	Royal Blue; Bunker Hill; Oscar Wehrend	Yes (Weigand 1982)
Nevada	Nye	Royston District	Black Hills; Verde Blue	Not reported
Nevada	Nye	Toquima Range	Copper Blue; Zabrisky; Indian Blue; Tom Molly	Not reported

State	County	Area/District	Name	Evidence of Prehistoric Mining-References
New Mexico	Doña Ana	Organ District	Torpedo Mine	Not reported
New Mexico	Grant	Burro Mountains; Tyrone District	Azure Mine (Elizabeth pocket); New Azure; Burro Chief; Parker	Extensive (Weigand 1982; Weigand and Harbottle 1993)
New Mexico	Grant	Burro Mountains; White Signal District	Chapman Turquoise Mine; Red Hill Mine	Yes (Weigand 1982); Inconclusive (Weigand and Harbottle 1993)
New Mexico	Grant	Little Hachita Mountains	Old Hachita	Yes (Weigand 1982; Weigand and Harbottle 1993)
New Mexico	Grant	Little Hachita Mountains; Turquoise Hill	Robinson and Porterfield mines; Azure; Cameo; Galilee; Aztec	Not reported
New Mexico	Grant	Santa Rita District	Chino Mine	Not reported
New Mexico	Otero	Jarilla District; Jarilla Mountain Area	Providence (DeMeules; Garnet; Nannie Baird; Lucky; I; Three Bears)	Yes (Weigand 1982; Weigand and Harbottle 1993)
New Mexico	Otero	Orogrande Mining District	Iron Mask	Yes (Weigand 1982; Weigand and Harbottle 1993)
New Mexico	Santa Fe	Cerrillos Hills District	Mount Chalchihuitl	Extensive (Blake 1858; Silliman 1881; Warren and Mathien 1985; Weigand 1982; Weigand and Harbottle 1992)
New Mexico	Santa Fe	Cerrillos Hills District; Turquoise Hill	Tiffany Mine; Castillian Mine; Blue Bell; Consul Mahoney; Morning Star; Sky Blue; Gem	Extensive (Weigand 1982; Weigand and Harbottle 1993)
Baja California		El Aguajito Mining District	La Reina (La Turquesa); Vincent; Hermonsa; Preciosa	Not reported
Baja		El Rosario	Evans Turquoise (Mexico Turquoise);	Not reported

State	County	Area/District	Name	Evidence of Prehistoric Mining-References
California			American Hole	
Chihuahua		Mapimi	Mapimi	Not reported
Coahuila		Santa Rosa	Name not reported	Conclusive (Weigand and Harbottle 1993)
Coahuila		Coahuila	Beta Perez	Inconclusive (Weigand and Harbottle 1993)
Sonora		Cananea	Name not reported	Yes (Weigand and Harbottle 1993)
Sonora		La Carida	Nacozari de García	Yes (Weigand and Harbottle 1993)
Sonora		La Barranca Copper District	Name not reported	Not reported
Zacatecas		Aranzazu Mining District	Name not reported	Not reported
Zacatecas		Santa Rosa District	Concepción del Oro; Mazapil; Todos Santos; Socován de las Turquesas	Not reported

Appendix 2:

Hydrogen Isotopic Analyses of Turquoise Provenance Samples by SIMS

Appendix 2. Hydrogen Isotopic Analyses of Turquoise Provenance Samples by SIMS.

Turquoise Deposit	Mount No.	Date of Analysis	δD_{VSMOW} (‰)	D/H (SIMS)	1σ (SIMS)
Sleeping Beauty, Arizona					
Sleeping Beauty	STD-X1-SB1-2	Mar 3 2009	-77	3.3771E-05	5
Sleeping Beauty	STD-X1-SB1-2	Mar 3 2009	-84	3.3496E-05	5
Sleeping Beauty	STD-X1-SB1-2	Mar 3 2009	-75	3.3818E-05	5
Sleeping Beauty	STD-X1-SB1-2	Mar 3 2009	-65	3.4217E-05	5
Sleeping Beauty	STD-X1-SB1-2	Mar 3 2009	-77	3.3765E-05	5
Sleeping Beauty	STD-X1-SB1-2	Mar 3 2009	-66	3.4179E-05	4
Sleeping Beauty	STD-X1-SB1-2	Apr 10 2009	-70	4.1099E-05	4
Sleeping Beauty	STD-X1-SB1-2	Apr 10 2009	-73	4.0967E-05	4
Sleeping Beauty	STD-X1-SB1-2	Apr 10 2009	-81	4.0602E-05	4
Sleeping Beauty	STD-X1-SB1-2	Apr 10 2009	-80	4.0663E-05	4
Sleeping Beauty	STD-X1-SB1-2	Apr 10 2009	-76	4.0822E-05	4
Sleeping Beauty	STD-X1-SB1-2	Apr 11 2009	-70	4.1294E-05	4
Sleeping Beauty	STD-X1-SB1-2	Apr 11 2009	-78	4.0931E-05	4
Sleeping Beauty	STD-X1-SB1-2	Apr 11 2009	-69	4.1328E-05	4
Sleeping Beauty	STD-X1-SB1-2	Apr 11 2009	-82	4.0763E-05	5
Sleeping Beauty	STD-X1-SB1-2	Apr 11 2009	-80	4.0859E-05	5
Sleeping Beauty	STD-X1-SB1-2	Apr 12 2009	-73	4.0995E-05	6
Sleeping Beauty	STD-X1-SB1-2	Apr 12 2009	-79	4.0692E-05	5
Sleeping Beauty	STD-X1-SB1-2	Apr 12 2009	-85	4.0470E-05	5
Sleeping Beauty	STD-X1-SB1-2	Apr 12 2009	-71	4.1070E-05	5
Sleeping Beauty	STD-X1-SB1-2	Apr 12 2009	-72	4.1005E-05	5
Sleeping Beauty	STD-X1-SB1-2	Apr 13 2009	-77	4.0983E-05	5
Sleeping Beauty	STD-X1-SB1-2	Apr 13 2009	-74	4.1153E-05	6
Sleeping Beauty	STD-X1-SB1-2	Apr 13 2009	-72	4.1224E-05	5
Sleeping Beauty	STD-X1-SB1-2	Apr 13 2009	-81	4.0811E-05	5
Sleeping Beauty	STD-X1-SB1-2	Apr 14 2009	-83	4.0435E-05	12
Sleeping Beauty	STD-X1-SB1-2	Apr 14 2009	-75	4.0793E-05	12
Sleeping Beauty	STD-X1-SB1-2	Apr 14 2009	-82	4.0471E-05	5
Sleeping Beauty	STD-X1-SB1-2	Apr 14 2009	-71	4.0960E-05	5
Sleeping Beauty	STD-X1-SB1-2	Apr 14 2009	-68	4.1084E-05	5
Sleeping Beauty	STD-X1-SB1-2	Apr 14 2009	-78	4.0633E-05	5
Sleeping Beauty	STD-X1-SB1-2	Apr 15 2009	-75	4.0855E-05	5
Sleeping Beauty	STD-X1-SB1-2	Apr 15 2009	-70	4.1097E-05	5
Sleeping Beauty	STD-X1-SB1-2	Apr 15 2009	-72	4.0997E-05	5
Sleeping Beauty	STD-X1-SB1-2	Apr 15 2009	-81	4.0602E-05	5
Sleeping Beauty	STD-X1-SB1-2	Apr 15 2009	-84	4.0471E-05	5
Sleeping Beauty	STD-X1-SB1-2	Apr 15 2009	-75	4.0855E-05	5
Sleeping Beauty	STD-X1-SB1-1	Sep 9 2009	-79	4.3372E-05	4
Sleeping Beauty	STD-X1-SB1-1	Sep 9 2009	-68	4.3893E-05	4
Sleeping Beauty	STD-X1-SB1-1	Sep 9 2009	-73	4.3681E-05	4
Sleeping Beauty	STD-X1-SB1-1	Sep 9 2009	-84	4.3139E-05	4
Sleeping Beauty	STD-X1-SB1-1	Sep 10 2009	-71	4.4406E-05	4
Sleeping Beauty	STD-X1-SB1-1	Sep 10 2009	-84	4.3795E-05	4
Sleeping Beauty	STD-X1-SB1-2	Sep 10 2009	-74	4.4263E-05	4

Turquoise Deposit	Mount No.	Date of Analysis	δD_{VSMOW} (‰)	D/H (SIMS)	1σ (SIMS)
Sleeping Beauty	STD-X1-SB1-2	Sep 10 2009	-76	4.4165E-05	4
Sleeping Beauty	STD-X1-SB1-2	Sep 11 2009	-73	4.4192E-05	4
Sleeping Beauty	STD-X1-SB1-2	Sep 11 2009	-71	4.4303E-05	4
Sleeping Beauty	STD-X1-SB1-2	Sep 11 2009	-73	4.4211E-05	4
Sleeping Beauty	STD-X1-SB1-2	Sep 11 2009	-78	4.3947E-05	4
Sleeping Beauty	STD-X1-SB1-2	Sep 11 2009	-84	4.3665E-05	4
Sleeping Beauty	STD-X1-SB1-1	Sep 13 2009	-74	4.4911E-05	4
Sleeping Beauty	STD-X1-SB1-1	Sep 13 2009	-71	4.5080E-05	4
Sleeping Beauty	STD-X1-SB1-1	Sep 13 2009	-77	4.4793E-05	4
Sleeping Beauty	STD-X1-SB1-1	Sep 13 2009	-82	4.4556E-05	4
Sleeping Beauty	STD-X1-SB1-1	Sep 14 2009	-73	4.5321E-05	4
Sleeping Beauty	STD-X1-SB1-1	Sep 14 2009	-76	4.5176E-05	4
Sleeping Beauty	STD-X1-SB1-1	Sep 14 2009	-75	4.5203E-05	4
Sleeping Beauty	STD-X1-SB1-1	Sep 14 2009	-81	4.4913E-05	4
Sleeping Beauty	STD-X1-SB1-1	Sep 16 2009	-78	4.5579E-05	4
Sleeping Beauty	STD-X1-SB1-2	Sep 16 2009	-71	4.5964E-05	4
Sleeping Beauty	STD-X1-SB1-2	Sep 16 2009	-73	4.5837E-05	4
Sleeping Beauty	STD-X1-SB1-2	Sep 16 2009	-82	4.5391E-05	4
Sleeping Beauty	STD-X1-SB1-2	Sep 17 2009	-72	4.5714E-05	4
Sleeping Beauty	STD-X1-SB1-2	Sep 17 2009	-72	4.5736E-05	4
Sleeping Beauty	STD-X1-SB1-2	Sep 17 2009	-84	4.5151E-05	4
Sleeping Beauty	STD-X1-SB1-1	Sep 18 2009	-73	4.5231E-05	4
Sleeping Beauty	STD-X1-SB1-1	Sep 18 2009	-72	4.5290E-05	4
Sleeping Beauty	STD-X1-SB1-1	Sep 18 2009	-84	4.4710E-05	4
Sleeping Beauty	STD-X2-SB1-2	Sep 19 2009	-70	4.5560E-05	4
Sleeping Beauty	STD-X2-SB1-2	Sep 19 2009	-77	4.5236E-05	4
Sleeping Beauty	STD-X2-SB1-2	Sep 19 2009	-81	4.5013E-05	4
Sleeping Beauty	STD-X2-SB1-2	Sep 20 2009	-77	4.5139E-05	4
Sleeping Beauty	STD-X2-SB1-2	Sep 20 2009	-75	4.5260E-05	4
Sleeping Beauty	STD-X2-SB1-2	Sep 20 2009	-75	4.5263E-05	5
Sleeping Beauty	STD-X2-SB1-2	Sep 20 2009	-77	4.5153E-05	4
Sleeping Beauty	STD-X2-SB1-2	Sep 21 2009	-76	4.5298E-05	4
Sleeping Beauty	STD-X2-SB1-2	Sep 21 2009	-76	4.5312E-05	4
Sleeping Beauty	STD-X1-SB1-1	Feb 26 2010	-69	5.1056E-05	4
Sleeping Beauty	STD-X1-SB1-1	Feb 26 2010	-79	5.0499E-05	4
Sleeping Beauty	STD-X1-SB1-1	Feb 26 2010	-74	5.0750E-05	4
Sleeping Beauty	STD-X1-SB1-1	Feb 26 2010	-82	5.0334E-05	4
Sleeping Beauty	STD-X1-SB1-1	Mar 2 2010	-75	5.3827E-05	4
Sleeping Beauty	STD-X1-SB1-1	Mar 2 2010	-63	5.4506E-05	4
Sleeping Beauty	STD-X1-SB1-1	Mar 2 2010	-74	5.3862E-05	4
Sleeping Beauty	STD-X1-SB1-1	Mar 2 2010	-81	5.3449E-05	4
Sleeping Beauty	STD-X1-SB1-1	Mar 2 2010	-81	5.3457E-05	4
Sleeping Beauty	STD-X1-SB1-1	Mar 2 2010	-81	5.3501E-05	4
Sleeping Beauty	STD-X2-SB1-2	Jul 30 2010	-62	4.9057E-05	4
Sleeping Beauty	STD-X2-SB1-2	Jul 30 2010	-82	4.8005E-05	4
Sleeping Beauty	STD-X2-SB1-2	Jul 30 2010	-78	4.8259E-05	4
Sleeping Beauty	STD-X2-SB1-2	Jul 30 2010	-82	4.8046E-05	4
Sleeping Beauty	STD-X2-SB1-2	Aug 1 2010	-84	4.7559E-05	4

Turquoise Deposit	Mount No.	Date of Analysis	δD_{VSMOW} (‰)	D/H (SIMS)	1σ (SIMS)
Sleeping Beauty	STD-X2-SB1-2	Aug 1 2010	-77	4.7941E-05	4
Sleeping Beauty	STD-X2-SB1-2	Aug 1 2010	-67	4.8472E-05	4
Sleeping Beauty	STD-X1-SB1-2	Aug 2 2010	-73	4.8201E-05	2
Sleeping Beauty	STD-X1-SB1-2	Aug 2 2010	-77	4.7971E-05	4
Sleeping Beauty	STD-X1-SB1-2	Aug 2 2010	-72	4.8256E-05	4
Sleeping Beauty	STD-X1-SB1-2	Aug 2 2010	-82	4.7722E-05	4
Sleeping Beauty	STD-X2-SB1-2	Aug 3 2010	-72	4.7509E-05	2
Sleeping Beauty	STD-X2-SB1-2	Aug 3 2010	-70	4.7590E-05	4
Sleeping Beauty	STD-X2-SB1-2	Aug 3 2010	-80	4.7100E-05	4
Sleeping Beauty	STD-X2-SB1-2	Aug 3 2010	-72	4.7485E-05	4
Sleeping Beauty	STD-X2-SB1-2	Aug 3 2010	-86	4.6755E-05	4
Sleeping Beauty	STD-X2-SB1-2	Aug 5 2010	-75	4.8058E-05	2
Sleeping Beauty	STD-X2-SB1-2	Aug 5 2010	-75	4.8059E-05	4
Sleeping Beauty	STD-X2-SB1-2	Aug 5 2010	-76	4.8017E-05	4
Sleeping Beauty	STD-X2-SB1-2	Aug 5 2010	-79	4.7864E-05	4
Sleeping Beauty	STD-X2-SB1-1	Aug 6 2010	-70	4.8904E-05	3
Sleeping Beauty	STD-X2-SB1-1	Aug 6 2010	-81	4.8364E-05	4
Sleeping Beauty	STD-X2-SB1-1	Aug 6 2010	-84	4.8206E-05	4
Sleeping Beauty	STD-X2-SB1-1	Aug 6 2010	-70	4.8899E-05	4
Sleeping Beauty	STD-X2-SB1-1	Aug 6 2010	-77	4.8542E-05	4
Sleeping Beauty	STD-X2-SB1-1	Aug 6 2010	-74	4.8735E-05	4
Sleeping Beauty	STD-X1-SB1-1	Aug 7 2010	-76	4.8070E-05	3
Sleeping Beauty	STD-X1-SB1-1	Aug 7 2010	-69	4.8421E-05	4
Sleeping Beauty	STD-X1-SB1-1	Aug 7 2010	-82	4.7727E-05	4
Sleeping Beauty	STD-X1-SB1-1	Aug 7 2010	-78	4.7937E-05	4
Sleeping Beauty	STD-X1-SB1-1	Aug 7 2010	-62	4.8802E-05	4
Sleeping Beauty	STD-X1-SB1-2	Aug 8 2010	-72	4.8020E-05	4
Sleeping Beauty	STD-X1-SB1-2	Aug 8 2010	-71	4.8100E-05	4
Sleeping Beauty	STD-X1-SB1-2	Aug 8 2010	-83	4.7470E-05	4
Sleeping Beauty	STD-X1-SB1-2	Aug 8 2010	-78	4.7715E-05	4
Sleeping Beauty	STD-X1-SB1-2	Aug 8 2010	-67	4.8302E-05	4
Sleeping Beauty	STD-X1-SB1-2	Aug 8 2010	-85	4.7335E-05	4
Sleeping Beauty	STD-X1-SB1-2	Aug 9 2010	-76	4.8280E-05	4
Sleeping Beauty	STD-X1-SB1-2	Aug 9 2010	-78	4.7469E-05	3
Sleeping Beauty	STD-X1-SB1-2	Aug 9 2010	-63	4.8936E-05	2
Sleeping Beauty	STD-X1-SB1-2	Aug 9 2010	-87	4.7708E-05	4
Sleeping Beauty	STD-X1-SB1-2	Aug 10 2010	-73	4.8879E-05	4
Sleeping Beauty	STD-X1-SB1-2	Aug 10 2010	-76	4.8741E-05	4
Sleeping Beauty	STD-X1-SB1-2	Aug 10 2010	-72	4.8920E-05	4
Sleeping Beauty	STD-X1-SB1-2	Aug 10 2010	-83	4.8356E-05	4
Mineral Park, Arizona					
Kingman	AZ5.02	Apr 15 2009	-95	3.9985E-05	6
Kingman	AZ5.02	Apr 15 2009	-92	4.0110E-05	5
Kingman	AZ5.02	Apr 15 2009	-100	3.9745E-05	5
Kingman	AZ5.02	Apr 15 2009	-93	4.0072E-05	5
Kingman	AZ5.02	Apr 15 2009	-89	4.0236E-05	5
Kingman	KG1.01	Jul 30 2010	-91	4.7576E-05	4
Kingman	KG1.01	Jul 30 2010	-83	4.7990E-05	4

Turquoise Deposit	Mount No.	Date of Analysis	δD_{VSMOW} (‰)	D/H (SIMS)	1σ (SIMS)
Kingman	KG1.01	Jul 30 2010	-84	4.7923E-05	4
Kingman	KG1.01	Jul 30 2010	-91	4.7532E-05	4
Kingman	KG1.01	Jul 30 2010	-83	4.7974E-05	4
Kingman	MX1.01	Aug 1 2010	-92	4.7144E-05	4
Kingman	MX1.01	Aug 1 2010	-85	4.7540E-05	4
Morenci, Arizona					
Morenci	AZ4.04	Apr 15 2009	-116	3.9063E-05	5
Morenci	AZ4.04	Apr 15 2009	-116	3.9066E-05	5
Morenci	AZ4.04	Apr 15 2009	-115	3.9082E-05	5
Morenci	AZ4.04	Apr 15 2009	-112	3.9204E-05	5
Morenci	AZ4.04	Apr 15 2009	-111	3.9279E-05	5
Bisbee, Arizona					
Lavender Pit	AZ4.02	Apr 15 2009	-66	4.1260E-05	5
Lavender Pit	AZ4.02	Apr 15 2009	-67	4.1227E-05	5
Lavender Pit	AZ4.02	Apr 15 2009	-51	4.1895E-05	5
Lavender Pit	AZ4.02	Apr 15 2009	-62	4.1420E-05	5
Lavender Pit	AZ4.02	Apr 15 2009	-63	4.1374E-05	5
Lavender Pit	AZ4.02	Apr 15 2009	-57	4.1639E-05	5
Halloran Springs, California					
Middle Camp	CA1.01	Apr 15 2009	-91	4.0153E-05	6
Middle Camp	CA1.01	Apr 15 2009	-101	3.9730E-05	6
Middle Camp	CA1.01	Apr 15 2009	-106	3.9471E-05	6
Middle Camp	CA1.01	Apr 15 2009	-104	3.9570E-05	6
Middle Camp	CA1.01	Aug 2 2010	-93	4.7166E-05	4
Middle Camp	CA1.01	Aug 2 2010	-99	4.6824E-05	4
East Camp	CA1.03	Apr 15 2009	-95	3.9970E-05	5
East Camp	CA1.03	Apr 15 2009	-100	3.9763E-05	6
East Camp	CA1.03	Apr 15 2009	-98	3.9860E-05	5
East Camp	CA1.03	Aug 2 2010	-96	4.6976E-05	4
East Camp	CA1.03	Aug 2 2010	-95	4.7055E-05	4
Baja California, Mexico					
Evans Mine	NV7.03	Aug 9 2010	-122	4.5846E-05	4
Evans Mine	NV7.03	Aug 9 2010	-114	4.6288E-05	4
Evans Mine	NV7.03	Aug 9 2010	-119	4.6044E-05	4
La Jara, Colorado					
King Manassa	CO2.04	Apr 14 2009	-73	4.0847E-05	5
King Manassa	CO2.04	Apr 14 2009	-80	4.0536E-05	6
King Manassa	CO2.04	Apr 14 2009	-86	4.0283E-05	5
King Manassa	CO2.04	Apr 14 2009	-79	4.0613E-05	5
King Manassa	CO2.04	Mar 2 2010	-75	5.3829E-05	4
King Manassa	CO2.04	Mar 2 2010	-72	5.3993E-05	4
King Manassa	CO2.04	Mar 2 2010	-68	5.4243E-05	4
King Manassa	T1.02	Aug 3 2010	-74	4.7378E-05	4
King Manassa	T1.02	Aug 3 2010	-70	4.7588E-05	4
King Manassa	CO2.04	Aug 5 2010	-84	4.7580E-05	3
King Manassa	CO4.04	Aug 8 2010	-79	4.7663E-05	4
King Manassa	CO4.04	Aug 8 2010	-82	4.7518E-05	4
Villa Grove, Colorado					

Turquoise Deposit	Mount No.	Date of Analysis	δD_{VSMOW} (‰)	D/H (SIMS)	1σ (SIMS)
Hall Mine	AZ6.04	Mar 2 2010	-95	5.2677E-05	4
Hall Mine	AZ6.04	Mar 2 2010	-103	5.2210E-05	4
Hall Mine	AZ6.04	Mar 2 2010	-105	5.2075E-05	4
Hall Mine	AZ6.04	Mar 2 2010	-98	5.2511E-05	4
Hall Mine	CO3.01	Aug 7 2010	-95	4.7091E-05	3
Hall Mine	CO3.01	Aug 7 2010	-95	4.7095E-05	3
Hall Mine	CO3.02	Aug 7 2010	-100	4.6825E-05	4
Hall Mine	CO3.02	Aug 7 2010	-104	4.6584E-05	4
Leadville, Colorado					
Turquoise Chief	CO2.02	Apr 14 2009	-78	4.0646E-05	5
Turquoise Chief	CO2.02	Apr 14 2009	-81	4.0489E-05	5
Turquoise Chief	CO2.02	Apr 14 2009	-83	4.0441E-05	5
Turquoise Chief	CO2.02	Mar 2 2010	-75	5.3833E-05	4
Turquoise Chief	CO2.02	Mar 2 2010	-77	5.3729E-05	4
Turquoise Chief	CO2.02	Mar 2 2010	-82	5.3421E-05	4
Turquoise Chief	CO2.02	Mar 2 2010	-73	5.3923E-05	4
Turquoise Chief	CO2.02	Aug 5 2010	-74	4.8078E-05	3
Cripple Creek, Colorado					
Cripple Creek	CO1.05	Aug 5 2010	-85	4.7554E-05	4
Cripple Creek	CO1.05	Aug 5 2010	-89	4.7327E-05	4
Cripple Creek	CO1.05	Aug 5 2010	-83	4.7611E-05	4
Cripple Creek	CO4.02	Aug 8 2010	-88	4.7215E-05	4
Cripple Creek	CO4.02	Aug 8 2010	-89	4.7134E-05	4
Crescent Peak, Nevada					
Aztec Mine	NV1.03	Mar 3 2009	-90	3.3277E-05	5
Aztec Mine	NV1.03	Mar 3 2009	-91	3.3248E-05	5
Aztec Mine	NV1.03	Mar 3 2009	-83	3.3541E-05	5
Aztec Mine	NV1.03	Aug 8 2010	-90	4.7103E-05	4
Aztec Mine	NV1.03	Aug 8 2010	-92	4.6974E-05	4
Blue Point	NV1.01	Aug 8 2010	-78	4.7733E-05	4
Locality #7	NV1.04	Mar 3 2009	-75	3.3830E-05	5
Locality #7	NV1.04	Mar 3 2009	-90	3.3302E-05	5
Locality #7	NV1.04	Aug 8 2010	-80	4.7591E-05	4
Locality #7	NV1.04	Aug 8 2010	-76	4.7821E-05	4
Royston, Nevada					
Royston	RY.01	Mar 3 2009	-116	3.2335E-05	5
Royston	RY.01	Mar 3 2009	-116	3.2328E-05	5
Royston	RY.01	Mar 3 2009	-119	3.2238E-05	5
Royston	RY.01	Mar 3 2009	-119	3.2241E-05	5
Royston	RY.01	Mar 3 2009	-119	3.2238E-05	5
Royston	RY.04	Mar 3 2009	-112	3.2486E-05	5
Royston	RY.04	Mar 3 2009	-108	3.2612E-05	5
Royston	NV6.01	Aug 7 2010	-106	4.6511E-05	4
Lone Mountain, Nevada					
Lone Mountain	NV2.01	Mar 3 2009	-138	3.1531E-05	5
Lone Mountain	NV2.01	Mar 3 2009	-139	3.1489E-05	5
Lone Mountain	NV2.01	Mar 3 2009	-126	3.1982E-05	5
Lone Mountain	NV2.01	Mar 3 2009	-132	3.1736E-05	5

Turquoise Deposit	Mount No.	Date of Analysis	δD_{VSMOW} (‰)	D/H (SIMS)	1σ (SIMS)
Lone Mountain	NV2.01	Mar 3 2009	-127	3.1918E-05	5
Blue Gem, Nevada					
Blue Gem	NV5.01	Apr 15 2009	-131	3.8362E-05	6
Blue Gem	NV5.01	Apr 15 2009	-133	3.8290E-05	6
Blue Gem	NV5.01	Apr 15 2009	-142	3.7903E-05	6
Blue Gem	NV5.01	Apr 15 2009	-137	3.8102E-05	6
Blue Gem	NV5.01	Apr 15 2009	-138	3.8083E-05	6
Blue Gem	NV5.01	Aug 2 2010	-138	4.4834E-05	4
Blue Gem	NV5.01	Aug 2 2010	-133	4.5078E-05	4
Green Tree, Nevada					
Green Tree	NV3.02	Mar 3 2009	-113	3.2461E-05	5
Green Tree	NV3.02	Mar 3 2009	-126	3.1981E-05	5
Green Tree	NV3.02	Mar 3 2009	-116	3.2316E-05	5
Green Tree	NV3.02	Mar 3 2009	-120	3.2179E-05	5
Godber Mine, Nevada					
Godber Mine	NV4.06	Apr 15 2009	-134	3.8237E-05	5
Godber Mine	NV4.06	Apr 15 2009	-144	3.7802E-05	6
Godber Mine	NV4.06	Apr 15 2009	-138	3.8090E-05	5
Godber Mine	NV4.06	Apr 15 2009	-138	3.8064E-05	5
Godber Mine	NV4.06	Apr 15 2009	-140	3.7988E-05	6
Black Hills, Nevada					
Black Hills	NV5.03	Aug 2 2010	-120	4.5770E-05	4
Black Hills	NV5.03	Aug 2 2010	-124	4.5567E-05	4
Verde Blue, Nevada					
Verde Blue	NV5.07	Aug 2 2010	-123	4.5619E-05	4
Verde Blue	NV5.07	Aug 2 2010	-123	4.5611E-05	4
Fox Mine, Nevada					
Fox Mine	NV7.01	Aug 9 2010	-104	4.6819E-05	4
Fox Mine	NV7.01	Aug 9 2010	-108	4.6590E-05	4
Fox Mine	NV6.03	Aug 7 2010	-119	4.5841E-05	4
Fox Mine	NV6.03	Aug 7 2010	-118	4.5864E-05	4
Old Hachita, New Mexico					
Old Hachita	NM4.04	Apr 10 2009	-107	3.9454E-05	4
Old Hachita	NM4.04	Apr 10 2009	-107	3.9453E-05	4
Old Hachita	NM4.04	Apr 10 2009	-105	3.9527E-05	4
Old Hachita	NM4.04	Apr 10 2009	-107	3.9457E-05	4
Old Hachita	NM4.04	Apr 10 2009	-110	3.9324E-05	4
Cerrillos Hills, New Mexico					
Castillian Mine	STD-X1-CAS1-3	Mar 3 2009	-87	3.3139E-05	6
Castillian Mine	STD-X1-CAS1-3	Mar 3 2009	-90	3.3022E-05	6
Castillian Mine	STD-X1-CAS1-3	Mar 3 2009	-96	3.2793E-05	6
Castillian Mine	STD-X1-CAS1-3	Mar 3 2009	-101	3.2647E-05	6
Castillian Mine	STD-X1-CAS1-3	Mar 3 2009	-98	3.2728E-05	6
Castillian Mine	STD-X1-CAS1-3	Mar 3 2009	-98	3.2753E-05	6
Castillian Mine	STD-X1-CAS1-3	Apr 10 2009	-85	3.8705E-05	6
Castillian Mine	STD-X1-CAS1-3	Apr 10 2009	-100	3.8050E-05	6
Castillian Mine	STD-X1-CAS1-3	Apr 10 2009	-85	3.8709E-05	6
Castillian Mine	STD-X1-CAS1-3	Apr 10 2009	-103	3.7930E-05	6

Turquoise Deposit	Mount No.	Date of Analysis	δD_{VSMOW} (‰)	D/H (SIMS)	1σ (SIMS)
Castillian Mine	STD-X1-CAS1-3	Apr 10 2009	-107	3.7795E-05	6
Castillian Mine	STD-X1-CAS1-3	Apr 10 2009	-90	3.8498E-05	6
Castillian Mine	STD-X1-CAS1-3	Apr 11 2009	-98	3.7642E-05	6
Castillian Mine	STD-X1-CAS1-3	Apr 11 2009	-85	3.8147E-05	6
Castillian Mine	STD-X1-CAS1-3	Apr 11 2009	-95	3.7733E-05	7
Castillian Mine	STD-X1-CAS1-3	Apr 11 2009	-102	3.7478E-05	7
Castillian Mine	STD-X1-CAS1-4	Apr 12 2009	-97	3.7766E-05	7
Castillian Mine	STD-X1-CAS1-4	Apr 12 2009	-92	3.7985E-05	7
Castillian Mine	STD-X1-CAS1-4	Apr 12 2009	-94	3.7925E-05	8
Castillian Mine	STD-X1-CAS1-4	Apr 12 2009	-102	3.7586E-05	8
Castillian Mine	STD-X1-CAS1-4	Apr 12 2009	-90	3.8088E-05	8
Castillian Mine	STD-X1-CAS1-4	Apr 13 2009	-94	3.7942E-05	7
Castillian Mine	STD-X1-CAS1-4	Apr 13 2009	-106	3.7453E-05	8
Castillian Mine	STD-X1-CAS1-4	Apr 13 2009	-91	3.8098E-05	7
Castillian Mine	STD-X1-CAS1-4	Apr 13 2009	-89	3.8153E-05	8
Castillian Mine	STD-X1-CAS1-3	Apr 14 2009	-100	3.7686E-05	7
Castillian Mine	STD-X1-CAS1-3	Apr 14 2009	-97	3.7803E-05	8
Castillian Mine	STD-X1-CAS1-3	Apr 14 2009	-90	3.8112E-05	7
Castillian Mine	STD-X1-CAS1-3	Apr 14 2009	-94	3.7941E-05	8
Castillian Mine	STD-X1-CAS1-3	Apr 15 2009	-89	3.8427E-05	7
Castillian Mine	STD-X1-CAS1-3	Apr 15 2009	-103	3.7861E-05	7
Castillian Mine	STD-X1-CAS1-3	Apr 15 2009	-91	3.8372E-05	7
Castillian Mine	STD-X1-CAS1-3	Apr 15 2009	-91	3.8371E-05	7
Castillian Mine	STD-X1-CAS1-3	Apr 15 2009	-88	3.8488E-05	7
Castillian Mine	STD-X1-CAS1-3	Apr 15 2009	-104	3.7808E-05	8
Castillian Mine	STD-X1-CAS1-3	Apr 15 2009	-93	3.8267E-05	7
Castillian Mine	STD-X1-CAS1-3	Apr 15 2009	-102	3.7890E-05	7
Castillian Mine	STD-X1-CAS1-3	Sep 9 2009	-98	4.1644E-05	5
Castillian Mine	STD-X1-CAS1-3	Sep 9 2009	-92	4.1908E-05	5
Castillian Mine	STD-X1-CAS1-3	Sep 9 2009	-87	4.2152E-05	5
Castillian Mine	STD-X1-CAS1-3	Sep 9 2009	-104	4.1353E-05	5
Castillian Mine	STD-X1-CAS1-3	Sep 10 2009	-90	4.3184E-05	5
Castillian Mine	STD-X1-CAS1-3	Sep 10 2009	-103	4.2596E-05	5
Castillian Mine	STD-X1-CAS1-3	Sep 10 2009	-92	4.3093E-05	5
Castillian Mine	STD-X1-CAS1-3	Sep 11 2009	-89	4.3976E-05	5
Castillian Mine	STD-X1-CAS1-3	Sep 11 2009	-97	4.3591E-05	5
Castillian Mine	STD-X1-CAS1-3	Sep 11 2009	-92	4.3812E-05	5
Castillian Mine	STD-X1-CAS1-3	Sep 11 2009	-102	4.3320E-05	5
Castillian Mine	STD-X1-CAS1-3	Sep 13 2009	-87	4.3791E-05	5
Castillian Mine	STD-X1-CAS1-3	Sep 13 2009	-92	4.3533E-05	5
Castillian Mine	STD-X1-CAS1-3	Sep 13 2009	-101	4.3118E-05	5
Castillian Mine	STD-X1-CAS1-3	Sep 13 2009	-100	4.3192E-05	5
Castillian Mine	STD-X1-CAS1-3	Sep 14 2009	-101	4.2976E-05	5
Castillian Mine	STD-X1-CAS1-3	Sep 14 2009	-92	4.3424E-05	5
Castillian Mine	STD-X1-CAS1-3	Sep 14 2009	-91	4.3447E-05	5
Castillian Mine	STD-X1-CAS1-3	Sep 14 2009	-95	4.3263E-05	5
Castillian Mine	STD-X1-CAS1-3	Sep 16 2009	-86	4.4091E-05	5
Castillian Mine	STD-X1-CAS1-3	Sep 16 2009	-98	4.3537E-05	5

Turquoise Deposit	Mount No.	Date of Analysis	δD_{VSMOW} (‰)	D/H (SIMS)	1σ (SIMS)
Castillian Mine	STD-X1-CAS1-3	Sep 16 2009	-100	4.3416E-05	5
Castillian Mine	STD-X1-CAS1-3	Sep 16 2009	-95	4.3672E-05	5
Castillian Mine	STD-X1-CAS1-4	Sep 17 2009	-96	4.3564E-05	5
Castillian Mine	STD-X1-CAS1-4	Sep 17 2009	-88	4.3965E-05	5
Castillian Mine	STD-X1-CAS1-4	Sep 17 2009	-101	4.3306E-05	5
Castillian Mine	STD-X1-CAS1-4	Sep 18 2009	-95	4.3068E-05	5
Castillian Mine	STD-X1-CAS1-4	Sep 18 2009	-96	4.3027E-05	5
Castillian Mine	STD-X1-CAS1-4	Sep 18 2009	-95	4.3061E-05	5
Castillian Mine	STD-X2-CAS1-4	Sep 19 2009	-97	4.2729E-05	5
Castillian Mine	STD-X2-CAS1-4	Sep 19 2009	-88	4.3165E-05	5
Castillian Mine	STD-X2-CAS1-4	Sep 19 2009	-95	4.2809E-05	5
Castillian Mine	STD-X2-CAS1-4	Sep 19 2009	-100	4.2584E-05	5
Castillian Mine	STD-X2-CAS1-4	Sep 20 2009	-87	4.2976E-05	5
Castillian Mine	STD-X2-CAS1-4	Sep 20 2009	-85	4.3071E-05	5
Castillian Mine	STD-X2-CAS1-4	Sep 20 2009	-105	4.2137E-05	5
Castillian Mine	STD-X2-CAS1-4	Sep 20 2009	-104	4.2172E-05	5
Castillian Mine	STD-X2-CAS1-3	Sep 21 2009	-93	4.2778E-05	5
Castillian Mine	STD-X2-CAS1-3	Sep 21 2009	-96	4.2628E-05	5
Castillian Mine	STD-X2-CAS1-3	Sep 21 2009	-96	4.2653E-05	5
Castillian Mine	STD-X1-CAS1-3	Feb 26 2010	-98	4.7191E-05	6
Castillian Mine	STD-X1-CAS1-3	Feb 26 2010	-92	4.7517E-05	6
Castillian Mine	STD-X1-CAS1-3	Feb 26 2010	-88	4.7738E-05	6
Castillian Mine	STD-X1-CAS1-3	Feb 26 2010	-96	4.7302E-05	6
Castillian Mine	STD-X1-CAS1-3	Feb 26 2010	-102	4.7008E-05	5
Castillian Mine	STD-X1-CAS1-3	Mar 2 2010	-89	5.0415E-05	5
Castillian Mine	STD-X1-CAS1-3	Mar 2 2010	-87	5.0511E-05	5
Castillian Mine	STD-X1-CAS1-3	Mar 2 2010	-100	4.9805E-05	5
Castillian Mine	STD-X1-CAS1-3	Mar 2 2010	-92	5.0213E-05	5
Castillian Mine	STD-X1-CAS1-3	Mar 2 2010	-96	5.0024E-05	5
Castillian Mine	STD-X1-CAS1-3	Mar 2 2010	-101	4.9739E-05	5
Castillian Mine	STD-X1-CAS1-3	Mar 2 2010	-100	4.9800E-05	5
Castillian Mine	STD-X2-CAS1-4	Jul 30 2010	-100	4.4642E-05	5
Castillian Mine	STD-X2-CAS1-4	Jul 30 2010	-104	4.4421E-05	5
Castillian Mine	STD-X2-CAS1-4	Jul 30 2010	-90	4.5109E-05	5
Castillian Mine	STD-X2-CAS1-4	Jul 30 2010	-89	4.5188E-05	5
Castillian Mine	STD-X2-CAS1-4	Jul 30 2010	-92	4.5032E-05	5
Castillian Mine	STD-X2-CAS1-4	Aug 1 2010	-88	4.4684E-05	5
Castillian Mine	STD-X2-CAS1-3	Aug 1 2010	-90	4.4593E-05	5
Castillian Mine	STD-X2-CAS1-3	Aug 1 2010	-97	4.4230E-05	5
Castillian Mine	STD-X2-CAS1-3	Aug 1 2010	-82	4.4948E-05	5
Castillian Mine	STD-X1-CAS1-3	Aug 2 2010	-90	4.4851E-05	5
Castillian Mine	STD-X1-CAS1-3	Aug 2 2010	-98	4.4460E-05	5
Castillian Mine	STD-X1-CAS1-3	Aug 2 2010	-89	4.4939E-05	5
Castillian Mine	STD-X1-CAS1-3	Aug 2 2010	-102	4.4265E-05	5
Castillian Mine	STD-X2-CAS1-4	Aug 3 2010	-99	4.3436E-05	5
Castillian Mine	STD-X2-CAS1-4	Aug 3 2010	-101	4.3324E-05	5
Castillian Mine	STD-X2-CAS1-4	Aug 3 2010	-90	4.3835E-05	5
Castillian Mine	STD-X2-CAS1-4	Aug 3 2010	-81	4.4273E-05	5

Turquoise Deposit	Mount No.	Date of Analysis	δD_{VSMOW} (‰)	D/H (SIMS)	1σ (SIMS)
Castillian Mine	STD-X2-CAS1-4	Aug 3 2010	-104	4.3196E-05	5
Castillian Mine	STD-X2-CAS1-4	Aug 5 2010	-92	4.4521E-05	5
Castillian Mine	STD-X2-CAS1-4	Aug 5 2010	-97	4.4261E-05	5
Castillian Mine	STD-X2-CAS1-4	Aug 5 2010	-96	4.4309E-05	5
Castillian Mine	STD-X2-CAS1-4	Aug 6 2010	-93	4.5294E-05	5
Castillian Mine	STD-X2-CAS1-4	Aug 6 2010	-97	4.5078E-05	5
Castillian Mine	STD-X2-CAS1-4	Aug 6 2010	-95	4.5180E-05	5
Castillian Mine	STD-X2-CAS1-4	Aug 6 2010	-95	4.5187E-05	5
Castillian Mine	STD-X1-CAS1-3	Aug 7 2010	-100	4.4453E-05	5
Castillian Mine	STD-X1-CAS1-3	Aug 7 2010	-94	4.4763E-05	5
Castillian Mine	STD-X1-CAS1-3	Aug 7 2010	-92	4.4883E-05	5
Castillian Mine	STD-X1-CAS1-3	Aug 7 2010	-89	4.4994E-05	5
Castillian Mine	STD-X1-CAS1-3	Aug 7 2010	-101	4.4392E-05	5
Castillian Mine	STD-X1-CAS1-3	Aug 7 2010	-80	4.5456E-05	5
Castillian Mine	STD-X1-CAS1-3	Aug 7 2010	-108	4.4051E-05	5
Castillian Mine	STD-X1-CAS1-3	Aug 8 2010	-93	4.4753E-05	5
Castillian Mine	STD-X1-CAS1-3	Aug 8 2010	-94	4.4697E-05	5
Castillian Mine	STD-X1-CAS1-3	Aug 8 2010	-89	4.4946E-05	5
Castillian Mine	STD-X1-CAS1-3	Aug 8 2010	-95	4.4639E-05	5
Castillian Mine	STD-X1-CAS1-3	Aug 8 2010	-103	4.4251E-05	5
Castillian Mine	STD-X1-CAS1-4	Aug 9 2010	-90	4.4503E-05	5
Castillian Mine	STD-X1-CAS1-4	Aug 9 2010	-98	4.4126E-05	5
Castillian Mine	STD-X1-CAS1-4	Aug 9 2010	-94	4.4317E-05	5
Castillian Mine	STD-X1-CAS1-4	Aug 9 2010	-97	4.4167E-05	5
Castillian Mine	STD-X1-CAS1-4	Aug 10 2010	-85	4.5687E-05	5
Castillian Mine	STD-X1-CAS1-4	Aug 10 2010	-105	4.4714E-05	5
Castillian Mine	STD-X1-CAS1-4	Aug 10 2010	-103	4.4823E-05	5
Castillian Mine	STD-X1-CAS1-4	Aug 10 2010	-88	4.5568E-05	5
Castillian Mine	STD-X1-CAS1-4	Aug 10 2010	-94	4.5230E-05	5

Appendix 3:

Copper Isotopic Analyses of Turquoise Provenance Samples by SIMS

Appendix 3. Copper Isotopic Analyses of Turquoise Provenance Samples by SIMS.

Turquoise Deposit	Mount No.	Date of Analysis	$\delta^{65}Cu_{NIST976}$ (‰)	$^{65}Cu/^{63}Cu$ (SIMS)	1σ (SIMS)
Sleeping Beauty, Arizona					
Sleeping Beauty	STD-X1-SB1-2	Mar 18 2009	7.0	4.4368E-01	0.4
Sleeping Beauty	STD-X1-SB1-2	Mar 18 2009	7.4	4.4384E-01	0.4
Sleeping Beauty	STD-X1-SB1-2	Mar 18 2009	7.0	4.4366E-01	0.4
Sleeping Beauty	STD-X1-SB1-2	Mar 18 2009	7.4	4.4382E-01	0.4
Sleeping Beauty	STD-X1-SB1-2	Mar 18 2009	7.7	4.4398E-01	0.4
Sleeping Beauty	STD-X1-SB1-2	Mar 19 2009	7.2	4.4381E-01	0.4
Sleeping Beauty	STD-X1-SB1-2	Mar 19 2009	7.5	4.4394E-01	0.4
Sleeping Beauty	STD-X1-SB1-2	Mar 19 2009	7.6	4.4400E-01	0.4
Sleeping Beauty	STD-X1-SB1-2	Mar 19 2009	7.1	4.4378E-01	0.4
Sleeping Beauty	STD-X1-SB1-2	Mar 19 2009	7.1	4.4376E-01	0.4
Sleeping Beauty	STD-X1-SB1-2	Mar 19 2009	7.4	4.4389E-01	0.4
Sleeping Beauty	STD-X1-SB1-2	Mar 20 2009	7.8	4.4435E-01	0.4
Sleeping Beauty	STD-X1-SB1-2	Mar 20 2009	7.3	4.4414E-01	0.4
Sleeping Beauty	STD-X1-SB1-2	Mar 20 2009	6.9	4.4397E-01	0.4
Sleeping Beauty	STD-X1-SB1-2	Mar 20 2009	7.2	4.4412E-01	0.4
Sleeping Beauty	STD-X1-SB1-1	Mar 21 2009	7.7	4.4401E-01	0.4
Sleeping Beauty	STD-X1-SB1-1	Mar 21 2009	7.4	4.4389E-01	0.4
Sleeping Beauty	STD-X1-SB1-1	Mar 21 2009	7.1	4.4378E-01	0.4
Sleeping Beauty	STD-X1-SB1-1	Mar 21 2009	7.0	4.4371E-01	0.4
Sleeping Beauty	STD-X1-SB1-1	Mar 22 2009	7.6	4.4412E-01	0.4
Sleeping Beauty	STD-X1-SB1-1	Mar 22 2009	7.2	4.4395E-01	0.4
Sleeping Beauty	STD-X1-SB1-1	Mar 22 2009	6.8	4.4376E-01	0.4
Sleeping Beauty	STD-X1-SB1-1	Mar 22 2009	6.8	4.4377E-01	0.4
Sleeping Beauty	STD-X1-SB1-1	Mar 22 2009	8.0	4.4430E-01	0.4
Sleeping Beauty	STD-X1-SB1-1	Mar 22 2009	7.3	4.4395E-01	0.4
Sleeping Beauty	STD-X1-SB1-1	Mar 23 2009	7.8	4.4397E-01	0.4
Sleeping Beauty	STD-X1-SB1-1	Mar 23 2009	7.2	4.4372E-01	0.4
Sleeping Beauty	STD-X1-SB1-1	Mar 23 2009	6.8	4.4354E-01	0.4
Sleeping Beauty	STD-X1-SB1-1	Mar 23 2009	7.3	4.4377E-01	0.4
Sleeping Beauty	STD-X1-SB1-1	Apr 2 2009	7.8	4.4407E-01	0.5
Sleeping Beauty	STD-X1-SB1-1	Apr 2 2009	6.9	4.4366E-01	0.5
Sleeping Beauty	STD-X1-SB1-1	Apr 2 2009	7.2	4.4378E-01	0.5
Sleeping Beauty	STD-X1-SB1-1	Apr 2 2009	7.4	4.4388E-01	0.5
Sleeping Beauty	STD-X1-SB1-1	Apr 3 2009	7.2	4.4357E-01	0.4
Sleeping Beauty	STD-X1-SB1-1	Apr 3 2009	6.8	4.4343E-01	0.5
Sleeping Beauty	STD-X1-SB1-1	Apr 3 2009	7.8	4.4384E-01	0.4
Sleeping Beauty	STD-X1-SB1-1	Apr 3 2009	6.9	4.4343E-01	0.5
Sleeping Beauty	STD-X1-SB1-1	Apr 3 2009	7.8	4.4384E-01	0.5
Sleeping Beauty	STD-X1-SB1-1	Apr 4 2009	7.7	4.4390E-01	0.4
Sleeping Beauty	STD-X1-SB1-1	Apr 4 2009	7.3	4.4375E-01	0.5
Sleeping Beauty	STD-X1-SB1-1	Apr 4 2009	6.7	4.4349E-01	0.4
Sleeping Beauty	STD-X1-SB1-1	Apr 4 2009	6.8	4.4355E-01	0.4
Sleeping Beauty	STD-X1-SB1-1	Apr 4 2009	7.2	4.4369E-01	0.5
Sleeping Beauty	STD-X1-SB1-1	Apr 4 2009	7.7	4.4390E-01	0.5
Sleeping Beauty	STD-X1-SB1-1	Apr 4 2009	7.7	4.4393E-01	0.4

Turquoise Deposit	Mount No.	Date of Analysis	$\delta^{65}Cu_{NIST976}$ (‰)	$^{65}Cu/^{63}Cu$ (SIMS)	1σ (SIMS)
Sleeping Beauty	STD-X1-SB1-1	Apr 6 2009	7.4	4.4402E-01	0.4
Sleeping Beauty	STD-X1-SB1-1	Apr 6 2009	7.5	4.4407E-01	0.4
Sleeping Beauty	STD-X1-SB1-1	Apr 6 2009	6.9	4.4379E-01	0.4
Sleeping Beauty	STD-X1-SB1-1	Apr 6 2009	7.5	4.4405E-01	0.4
Sleeping Beauty	STD-X1-SB1-1	Apr 6 2009	7.2	4.4393E-01	0.4
Sleeping Beauty	STD-X1-SB1-2	Jun 6 2009	7.4	4.4344E-01	0.4
Sleeping Beauty	STD-X1-SB1-2	Jun 6 2009	7.1	4.4332E-01	0.4
Sleeping Beauty	STD-X1-SB1-2	Jun 6 2009	6.8	4.4318E-01	0.4
Sleeping Beauty	STD-X1-SB1-2	Jun 6 2009	7.7	4.4358E-01	0.4
Sleeping Beauty	STD-X1-SB1-2	Jun 6 2009	7.6	4.4352E-01	0.4
Sleeping Beauty	STD-X1-SB1-2	Jun 7 2009	7.3	4.4350E-01	0.4
Sleeping Beauty	STD-X1-SB1-2	Jun 7 2009	7.2	4.4345E-01	0.4
Sleeping Beauty	STD-X1-SB1-2	Jun 7 2009	7.2	4.4346E-01	0.4
Sleeping Beauty	STD-X1-SB1-2	Jun 7 2009	7.4	4.4356E-01	0.4
Sleeping Beauty	STD-X1-SB1-2	Jun 7 2009	7.3	4.4350E-01	0.4
Sleeping Beauty	STD-X1-SB1-2	Jun 9 2009	7.4	4.4314E-01	0.4
Sleeping Beauty	STD-X1-SB1-2	Jun 9 2009	6.7	4.4284E-01	0.4
Sleeping Beauty	STD-X1-SB1-2	Jun 9 2009	7.8	4.4333E-01	0.4
Sleeping Beauty	STD-X1-SB1-2	Jun 9 2009	7.0	4.4300E-01	0.4
Sleeping Beauty	STD-X1-SB1-2	Jun 9 2009	7.7	4.4328E-01	0.4
Sleeping Beauty	STD-X1-SB1-2	Jun 10 2009	7.4	4.4286E-01	0.4
Sleeping Beauty	STD-X1-SB1-2	Jun 10 2009	7.2	4.4277E-01	0.4
Sleeping Beauty	STD-X1-SB1-2	Jun 10 2009	7.2	4.4275E-01	0.4
Sleeping Beauty	STD-X1-SB1-2	Jun 10 2009	7.4	4.4284E-01	0.4
Sleeping Beauty	STD-X1-SB1-2	Jun 11 2009	7.4	4.4317E-01	0.3
Sleeping Beauty	STD-X1-SB1-2	Jun 11 2009	7.5	4.4320E-01	0.4
Sleeping Beauty	STD-X1-SB1-2	Jun 11 2009	7.3	4.4311E-01	0.4
Sleeping Beauty	STD-X1-SB1-2	Jun 11 2009	6.9	4.4294E-01	0.4
Sleeping Beauty	STD-X1-SB1-2	Jun 13 2009	7.3	4.4302E-01	0.4
Sleeping Beauty	STD-X1-SB1-2	Jun 13 2009	7.4	4.4306E-01	0.4
Sleeping Beauty	STD-X1-SB1-2	Jun 13 2009	7.2	4.4298E-01	0.4
Sleeping Beauty	STD-X2-SB1-1	Jan 11 2010	7.7	4.4310E-01	0.4
Sleeping Beauty	STD-X2-SB1-1	Jan 11 2010	7.0	4.4278E-01	0.4
Sleeping Beauty	STD-X2-SB1-1	Jan 11 2010	6.9	4.4275E-01	0.4
Sleeping Beauty	STD-X2-SB1-2	Jan 11 2010	7.4	4.4299E-01	0.4
Sleeping Beauty	STD-X2-SB1-2	Jan 11 2010	7.5	4.4302E-01	0.5
Sleeping Beauty	STD-X2-SB1-2	Jan 12 2010	7.3	4.4280E-01	0.4
Sleeping Beauty	STD-X2-SB1-2	Jan 12 2010	7.0	4.4264E-01	0.4
Sleeping Beauty	STD-X2-SB1-2	Jan 12 2010	7.4	4.4283E-01	0.4
Sleeping Beauty	STD-X2-SB1-2	Jan 12 2010	7.6	4.4291E-01	0.4
Sleeping Beauty	STD-X2-SB1-2	Jan 12 2010	7.3	4.4278E-01	0.4
Sleeping Beauty	STD-X1-SB1-2	Jan 28 2010	7.8	4.4267E-01	0.4
Sleeping Beauty	STD-X1-SB1-2	Jan 28 2010	7.3	4.4244E-01	0.4
Sleeping Beauty	STD-X1-SB1-2	Jan 28 2010	6.8	4.4223E-01	0.4
Sleeping Beauty	STD-X1-SB1-2	Jan 28 2010	7.3	4.4243E-01	0.4
Sleeping Beauty	STD-X1-SB1-2	Jan 28 2010	7.3	4.4246E-01	0.4
Sleeping Beauty	STD-X1-SB1-2	Jan 29 2010	7.4	4.4249E-01	0.4
Sleeping Beauty	STD-X1-SB1-2	Jan 29 2010	7.0	4.4231E-01	0.4

Turquoise Deposit	Mount No.	Date of Analysis	$\delta^{65}Cu_{NIST976}$ (‰)	$^{65}Cu/^{63}Cu$ (SIMS)	1σ (SIMS)
Sleeping Beauty	STD-X1-SB1-2	Jan 29 2010	7.5	4.4252E-01	0.4
Sleeping Beauty	STD-X1-SB1-2	Jan 29 2010	7.6	4.4258E-01	0.4
Sleeping Beauty	STD-X1-SB1-2	Jan 29 2010	7.0	4.4229E-01	0.4
Sleeping Beauty	STD-X2-SB1-2	Jan 30 2010	7.7	4.4242E-01	0.4
Sleeping Beauty	STD-X2-SB1-2	Jan 30 2010	8.0	4.4258E-01	0.4
Sleeping Beauty	STD-X2-SB1-2	Jan 30 2010	6.8	4.4204E-01	0.4
Sleeping Beauty	STD-X2-SB1-2	Jan 30 2010	6.6	4.4195E-01	0.4
Sleeping Beauty	STD-X2-SB1-2	Feb 22 2010	6.9	4.4223E-01	0.4
Sleeping Beauty	STD-X2-SB1-2	Feb 22 2010	7.7	4.4255E-01	0.4
Sleeping Beauty	STD-X2-SB1-2	Feb 22 2010	7.0	4.4227E-01	0.4
Sleeping Beauty	STD-X2-SB1-2	Feb 22 2010	7.6	4.4252E-01	0.4
Sleeping Beauty	STD-X2-SB1-2	Feb 23 2010	6.9	4.4241E-01	0.4
Sleeping Beauty	STD-X2-SB1-2	Feb 23 2010	7.7	4.4272E-01	0.4
Sleeping Beauty	STD-X2-SB1-2	Feb 23 2010	7.4	4.4261E-01	0.4
Sleeping Beauty	STD-X2-SB1-2	Feb 23 2010	7.4	4.4260E-01	0.4
Sleeping Beauty	STD-X2-SB1-2	Feb 23 2010	7.6	4.4272E-01	0.4
Sleeping Beauty	STD-X2-SB1-2	Feb 23 2010	6.8	4.4237E-01	0.4
Sleeping Beauty	STD-X2-SB1-2	Feb 24 2010	7.6	4.4254E-01	0.4
Sleeping Beauty	STD-X2-SB1-2	Feb 24 2010	7.8	4.4263E-01	0.4
Sleeping Beauty	STD-X2-SB1-2	Feb 24 2010	6.8	4.4221E-01	0.4
Sleeping Beauty	STD-X2-SB1-2	Feb 24 2010	7.2	4.4239E-01	0.4
Sleeping Beauty	STD-X2-SB1-2	Feb 24 2010	7.0	4.4228E-01	0.4
Sleeping Beauty	STD-X2-SB1-2	Feb 25 2010	7.8	4.4271E-01	0.4
Sleeping Beauty	STD-X2-SB1-2	Feb 25 2010	7.0	4.4238E-01	0.4
Sleeping Beauty	STD-X2-SB1-2	Feb 25 2010	7.5	4.4257E-01	0.4
Sleeping Beauty	STD-X2-SB1-2	Feb 25 2010	6.8	4.4228E-01	0.4
Sleeping Beauty	STD-X2-SB1-2	Feb 25 2010	7.4	4.4252E-01	0.4
Sleeping Beauty	STD-X2-SB1-2	Aug 10 2010	7.3	4.4263E-01	0.4
Sleeping Beauty	STD-X2-SB1-2	Aug 10 2010	7.0	4.4251E-01	0.5
Sleeping Beauty	STD-X2-SB1-2	Aug 10 2010	7.3	4.4262E-01	0.5
Sleeping Beauty	STD-X2-SB1-2	Aug 10 2010	7.1	4.4253E-01	0.5
Sleeping Beauty	STD-X2-SB1-2	Aug 10 2010	7.8	4.4284E-01	0.5
Sleeping Beauty	STD-X2-SB1-2	Aug 11 2010	7.7	4.4276E-01	0.5
Sleeping Beauty	STD-X2-SB1-2	Aug 11 2010	6.8	4.4240E-01	0.4
Sleeping Beauty	STD-X2-SB1-2	Aug 11 2010	7.0	4.4246E-01	0.4
Sleeping Beauty	STD-X2-SB1-2	Aug 11 2010	7.5	4.4269E-01	0.5
Sleeping Beauty	STD-X2-SB1-2	Aug 11 2010	7.5	4.4269E-01	0.5
Sleeping Beauty	STD-X2-SB1-2	Aug 12 2010	7.3	4.4260E-01	0.5
Sleeping Beauty	STD-X2-SB1-2	Aug 12 2010	6.6	4.4231E-01	0.4
Sleeping Beauty	STD-X2-SB1-2	Aug 12 2010	6.9	4.4242E-01	0.4
Sleeping Beauty	STD-X2-SB1-2	Aug 12 2010	8.1	4.4295E-01	0.4
Sleeping Beauty	STD-X2-SB1-2	Aug 12 2010	7.7	4.4277E-01	0.4
Sleeping Beauty	STD-X2-SB1-2	Aug 13 2010	7.4	4.4261E-01	0.4
Sleeping Beauty	STD-X2-SB1-2	Aug 13 2010	7.3	4.4257E-01	0.4
Sleeping Beauty	STD-X2-SB1-2	Aug 13 2010	7.4	4.4261E-01	0.4
Sleeping Beauty	STD-X2-SB1-2	Aug 13 2010	7.0	4.4246E-01	0.4
Sleeping Beauty	STD-X2-SB1-2	Aug 13 2010	7.5	4.4266E-01	0.4
Sleeping Beauty	STD-X2-SB1-1	Aug 15 2010	7.2	4.4250E-01	0.4

Turquoise Deposit	Mount No.	Date of Analysis	$\delta^{65}Cu_{NIST976}$ (‰)	$^{65}Cu/^{63}Cu$ (SIMS)	1σ (SIMS)
Sleeping Beauty	STD-X2-SB1-1	Aug 15 2010	7.5	4.4266E-01	0.5
Sleeping Beauty	STD-X2-SB1-1	Aug 15 2010	6.6	4.4225E-01	0.4
Sleeping Beauty	STD-X2-SB1-1	Aug 15 2010	8.0	4.4285E-01	0.4
Sleeping Beauty	STD-X1-SB1-2	Aug 16 2010	7.6	4.4296E-01	0.4
Sleeping Beauty	STD-X1-SB1-2	Aug 16 2010	7.1	4.4276E-01	0.4
Sleeping Beauty	STD-X1-SB1-2	Aug 16 2010	6.9	4.4265E-01	0.4
Sleeping Beauty	STD-X1-SB1-2	Aug 16 2010	7.6	4.4297E-01	0.4
Sleeping Beauty	STD-X2-SB1-2	Aug 30 2010	7.3	4.4338E-01	0.5
Sleeping Beauty	STD-X2-SB1-2	Aug 30 2010	7.1	4.4331E-01	0.5
Sleeping Beauty	STD-X2-SB1-2	Aug 30 2010	6.9	4.4322E-01	0.5
Sleeping Beauty	STD-X2-SB1-2	Aug 30 2010	7.1	4.4330E-01	0.5
Sleeping Beauty	STD-X2-SB1-2	Aug 30 2010	7.7	4.4356E-01	0.4
Sleeping Beauty	STD-X2-SB1-2	Aug 30 2010	7.9	4.4363E-01	0.5
Sleeping Beauty	STD-X2-SB1-2	Aug 30 2010	7.0	4.4323E-01	0.5
Sleeping Beauty	STD-X2-SB1-2	Aug 31 2010	7.6	4.4331E-01	0.5
Sleeping Beauty	STD-X2-SB1-2	Aug 31 2010	7.0	4.4303E-01	0.5
Sleeping Beauty	STD-X2-SB1-2	Aug 31 2010	6.8	4.4297E-01	0.5
Sleeping Beauty	STD-X2-SB1-2	Aug 31 2010	7.2	4.4314E-01	0.5
Sleeping Beauty	STD-X2-SB1-2	Aug 31 2010	7.3	4.4316E-01	0.5
Sleeping Beauty	STD-X2-SB1-2	Aug 31 2010	7.9	4.4342E-01	0.5
Sleeping Beauty	STD-X2-SB1-2	Sep 3 2010	7.4	4.4319E-01	0.4
Sleeping Beauty	STD-X2-SB1-2	Sep 3 2010	7.2	4.4310E-01	0.4
Sleeping Beauty	STD-X2-SB1-2	Sep 3 2010	7.5	4.4325E-01	0.4
Sleeping Beauty	STD-X2-SB1-2	Sep 3 2010	7.1	4.4307E-01	0.4
Sleeping Beauty	STD-X2-SB1-2	Sep 4 2010	6.8	4.4303E-01	0.4
Sleeping Beauty	STD-X2-SB1-2	Sep 4 2010	7.0	4.4313E-01	0.5
Sleeping Beauty	STD-X2-SB1-2	Sep 4 2010	7.6	4.4340E-01	0.4
Sleeping Beauty	STD-X2-SB1-2	Sep 4 2010	7.8	4.4351E-01	0.4
Mineral Park, Arizona					
Kingman	AZ5.02	Mar 21 2009	5.0	4.4285E-01	0.4
Kingman	AZ5.02	Mar 21 2009	4.5	4.4262E-01	0.4
Kingman	AZ5.02	Mar 21 2009	4.6	4.4266E-01	0.4
Kingman	AZ5.02	Mar 21 2009	4.7	4.4271E-01	0.4
Kingman	AZ5.02	Mar 21 2009	4.9	4.4279E-01	0.4
Kingman	KG1.01	Aug 12 2010	5.7	4.4190E-01	0.4
Kingman	KG1.01	Aug 12 2010	5.3	4.4171E-01	0.4
Kingman	KG1.01	Aug 12 2010	4.8	4.4153E-01	0.4
Kingman	KG1.01	Aug 12 2010	4.7	4.4148E-01	0.4
Kingman	KG1.01	Aug 12 2010	5.0	4.4160E-01	0.4
Kingman	KG1.01	Aug 16 2010	4.0	4.4139E-01	0.4
Kingman	KG1.01	Aug 16 2010	4.9	4.4178E-01	0.4
Kingman	MX1.01	Sep 4 2010	4.7	4.4212E-01	0.5
Kingman	MX1.01	Sep 4 2010	5.4	4.4241E-01	0.5
Morenci, Arizona					
Morenci	AZ4.04	Mar 23 2009	1.8	4.4131E-01	0.4
Morenci	AZ4.04	Mar 23 2009	1.7	4.4130E-01	0.4
Morenci	AZ4.04	Mar 23 2009	1.6	4.4125E-01	0.4
Morenci	AZ4.04	Mar 23 2009	2.4	4.4161E-01	0.4

Turquoise Deposit	Mount No.	Date of Analysis	$\delta^{65}Cu_{NIST976}$ (‰)	$^{65}Cu/^{63}Cu$ (SIMS)	1σ (SIMS)
Morenci	AZ4.04	Mar 23 2009	1.8	4.4133E-01	0.4
Morenci	AZ4.04	Mar 23 2009	1.1	4.4104E-01	0.4
Bisbee, Arizona					
Lavender Pit	AZ4.02	Mar 23 2009	2.4	4.4159E-01	0.4
Lavender Pit	AZ4.02	Mar 23 2009	2.7	4.4171E-01	0.4
Lavender Pit	AZ4.02	Mar 23 2009	2.4	4.4161E-01	0.4
Lavender Pit	AZ4.02	Mar 23 2009	2.9	4.4183E-01	0.4
Lavender Pit	AZ4.02	Mar 23 2009	2.6	4.4169E-01	0.4
Halloran Springs, California					
Middle Camp	CA1.01	Mar 23 2009	6.3	4.4329E-01	0.4
Middle Camp	CA1.01	Mar 23 2009	5.9	4.4313E-01	0.4
Middle Camp	CA1.01	Aug 13 2010	6.1	4.4204E-01	0.4
Middle Camp	CA1.01	Aug 13 2010	6.1	4.4206E-01	0.4
East Camp	CA1.03	Mar 23 2009	7.7	4.4395E-01	0.4
East Camp	CA1.03	Mar 23 2009	6.5	4.4341E-01	0.4
East Camp	CA1.03	Mar 23 2009	6.8	4.4353E-01	0.4
East Camp	NV7.04	Aug 11 2010	6.8	4.4240E-01	0.4
East Camp	NV7.04	Aug 11 2010	5.9	4.4197E-01	0.4
East Camp	NV7.04	Aug 11 2010	7.0	4.4247E-01	0.4
East Camp	CA1.03	Aug 13 2010	7.9	4.4285E-01	0.4
East Camp	CA1.03	Aug 13 2010	6.7	4.4234E-01	0.4
East Camp	CA1.03	Aug 13 2010	8.2	4.4298E-01	0.4
East Camp	CA1.03	Aug 13 2010	7.1	4.4250E-01	0.4
Baja California, Mexico					
Evans Mine	NV7.03	Aug 11 2010	9.8	4.4372E-01	0.4
Evans Mine	NV7.03	Aug 11 2010	9.6	4.4361E-01	0.4
Evans Mine	NV7.03	Aug 11 2010	10.2	4.4388E-01	0.4
La Jara, Colorado					
King Manassa	CO2.04	Apr 2 2009	4.3	4.4251E-01	0.4
King Manassa	CO2.04	Apr 2 2009	4.3	4.4254E-01	0.4
King Manassa	CO2.04	Apr 2 2009	3.7	4.4225E-01	0.4
King Manassa	CO2.04	Feb 25 2010	3.2	4.4069E-01	0.4
King Manassa	CO2.04	Feb 25 2010	3.2	4.4067E-01	0.4
King Manassa	CO2.04	Aug 13 2010	3.8	4.4103E-01	0.4
King Manassa	CO2.04	Aug 13 2010	3.4	4.4085E-01	0.4
King Manassa	CO2.04	Aug 13 2010	3.2	4.4078E-01	0.4
King Manassa	TI.02	Aug 15 2010	4.1	4.4116E-01	0.4
King Manassa	TI.02	Aug 15 2010	3.8	4.4102E-01	0.4
King Manassa	TI.02	Aug 15 2010	4.1	4.4117E-01	0.4
Villa Grove, Colorado					
Hall Mine	CO3.02	Apr 2 2009	2.4	4.4171E-01	0.5
Hall Mine	CO3.02	Apr 2 2009	1.9	4.4148E-01	0.4
Hall Mine	CO3.02	Apr 2 2009	2.7	4.4183E-01	0.4
Hall Mine	CO3.02	Apr 2 2009	2.2	4.4161E-01	0.4
Hall Mine	AZ6.04	Feb 25 2010	1.6	4.4001E-01	0.5
Hall Mine	AZ6.04	Feb 25 2010	2.1	4.4020E-01	0.5
Hall Mine	AZ6.04	Feb 25 2010	2.5	4.4037E-01	0.5
Hall Mine	CO3.01	Aug 13 2010	2.7	4.4056E-01	0.5

Turquoise Deposit	Mount No.	Date of Analysis	$\delta^{65}Cu_{NIST976}$ (‰)	$^{65}Cu/^{63}Cu$ (SIMS)	1σ (SIMS)
Hall Mine	CO3.01	Aug 13 2010	1.7	4.4011E-01	0.5
Hall Mine	CO3.01	Aug 13 2010	3.1	4.4073E-01	0.5
Hall Mine	CO3.02	Aug 13 2010	1.3	4.3996E-01	0.5
Hall Mine	CO3.02	Aug 13 2010	2.0	4.4024E-01	0.5
Hall Mine	CO3.02	Aug 13 2010	2.2	4.4035E-01	0.5
Leadville, Colorado					
Turquoise Chief	CO2.02	Apr 2 2009	12.8	4.4627E-01	0.4
Turquoise Chief	CO2.02	Apr 2 2009	12.5	4.4616E-01	0.4
Turquoise Chief	CO2.02	Apr 2 2009	12.1	4.4597E-01	0.4
Turquoise Chief	CO2.02	Feb 25 2010	13.2	4.4508E-01	0.5
Turquoise Chief	CO2.02	Feb 25 2010	12.9	4.4495E-01	0.5
Turquoise Chief	CO2.02	Feb 25 2010	11.9	4.4449E-01	0.5
Turquoise Chief	CO2.02	Aug 13 2010	12.7	4.4494E-01	0.4
Turquoise Chief	CO2.02	Aug 13 2010	12.9	4.4506E-01	0.4
Cripple Creek, Colorado					
Cripple Creek	CO1.05	Aug 30 2010	6.7	4.4310E-01	0.4
Cripple Creek	CO1.05	Aug 30 2010	6.6	4.4308E-01	0.4
Cripple Creek	CO1.05	Aug 30 2010	6.1	4.4285E-01	0.4
Cripple Creek	CO4.02	Aug 30 2010	7.4	4.4342E-01	0.4
Crescent Peak, Nevada					
Aztec Mine	NV1.03	Mar 19 2009	4.5	4.4265E-01	0.4
Aztec Mine	NV1.03	Mar 19 2009	5.0	4.4285E-01	0.4
Aztec Mine	NV1.03	Mar 19 2009	4.3	4.4255E-01	0.4
Aztec Mine	NV1.03	Mar 19 2009	4.3	4.4253E-01	0.4
Aztec Mine	NV1.03	Mar 19 2009	4.2	4.4249E-01	0.4
Blue Point	NV1.01	Sep 3 2010	5.0	4.4216E-01	0.4
Blue Point	NV1.01	Sep 3 2010	5.4	4.4231E-01	0.4
Locality #7	NV1.04	Mar 19 2009	5.6	4.4309E-01	0.4
Locality #7	NV1.04	Sep 3 2010	5.1	4.4220E-01	0.4
Locality #7	NV1.04	Sep 3 2010	4.7	4.4200E-01	0.4
Royston, Nevada					
Royston	RY.01	Mar 19 2009	4.1	4.4245E-01	0.4
Royston	RY.01	Mar 19 2009	3.8	4.4230E-01	0.3
Royston	RY.01	Mar 19 2009	3.6	4.4222E-01	0.4
Royston	RY.01	Mar 19 2009	3.5	4.4220E-01	0.4
Royston	RY.01	Mar 19 2009	3.3	4.4210E-01	0.4
Royston	RY.01	Aug 16 2010	3.4	4.4114E-01	0.3
Royston	RY.01	Aug 16 2010	3.4	4.4110E-01	0.4
Lone Mountain, Nevada					
Lone Mountain	NV2.01	Mar 19 2009	6.7	4.4361E-01	0.5
Lone Mountain	NV2.01	Mar 19 2009	6.1	4.4335E-01	0.5
Lone Mountain	NV2.01	Mar 19 2009	6.9	4.4367E-01	0.5
Lone Mountain	NV2.01	Mar 19 2009	6.1	4.4332E-01	0.5
Lone Mountain	NV2.01	Mar 19 2009	6.4	4.4347E-01	0.5
Blue Gem, Nevada					
Blue Gem	NV5.01	Mar 20 2009	7.2	4.4411E-01	0.4
Blue Gem	NV5.01	Mar 20 2009	7.6	4.4429E-01	0.4
Blue Gem	NV5.01	Mar 20 2009	7.5	4.4423E-01	0.4

Turquoise Deposit	Mount No.	Date of Analysis	$\delta^{65}Cu_{NIST976}$ (‰)	$^{65}Cu/^{63}Cu$ (SIMS)	1σ (SIMS)
Blue Gem	NV5.01	Mar 20 2009	7.5	4.4422E-01	0.4
Blue Gem	NV5.01	Mar 20 2009	7.6	4.4428E-01	0.4
Blue Gem	NV5.01	Feb 25 2010	7.0	4.4234E-01	0.4
Blue Gem	NV5.01	Feb 25 2010	7.0	4.4234E-01	0.4
Blue Gem	STD1.04	Aug 16 2010	5.7	4.4214E-01	0.4
Blue Gem	STD1.04	Aug 16 2010	5.5	4.4205E-01	0.4
Blue Gem	NV5.01	Aug 31 2010	6.9	4.4301E-01	0.5
Blue Gem	NV5.01	Aug 31 2010	6.4	4.4275E-01	0.5
Blue Gem	NV5.01	Aug 31 2010	6.4	4.4277E-01	0.5
Green Tree, Nevada					
Green Tree	NV3.02	Mar 20 2009	15.4	4.4772E-01	0.4
Green Tree	NV3.02	Mar 20 2009	15.2	4.4765E-01	0.4
Green Tree	NV3.02	Mar 20 2009	15.0	4.4754E-01	0.4
Green Tree	NV3.02	Mar 20 2009	15.0	4.4754E-01	0.4
Green Tree	NV3.02	Mar 20 2009	15.1	4.4758E-01	0.4
Green Tree	STD1.02	Aug 16 2010	14.4	4.4596E-01	0.4
Green Tree	STD1.02	Aug 16 2010	14.8	4.4612E-01	0.4
Godber Mine, Nevada					
Godber Mine	NV4.06	Mar 21 2009	1.5	4.4129E-01	0.6
Godber Mine	NV4.06	Mar 21 2009	1.0	4.4107E-01	0.6
Godber Mine	NV4.06	Mar 21 2009	1.6	4.4132E-01	0.5
Godber Mine	NV4.06	Mar 21 2009	2.0	4.4149E-01	0.5
Godber Mine	NV4.06	Mar 21 2009	1.1	4.4110E-01	0.5
Godber Mine	NV4.06	Mar 21 2009	0.8	4.4098E-01	0.5
Black Hills, Nevada					
Black Hills	NV5.03	Feb 25 2010	-0.7	4.3898E-01	0.4
Black Hills	NV5.03	Feb 25 2010	0.0	4.3928E-01	0.4
Black Hills	NV5.03	Aug 31 2010	-0.9	4.3958E-01	0.5
Black Hills	NV5.03	Aug 31 2010	-1.3	4.3940E-01	0.5
Verde Blue, Nevada					
Verde Blue	NV5.07	Aug 31 2010	-0.7	4.3967E-01	0.6
Verde Blue	NV5.07	Aug 31 2010	0.0	4.3994E-01	0.6
Fox Mine, Nevada					
Fox Mine	NV7.01	Aug 11 2010	14.8	4.4590E-01	0.4
Fox Mine	NV7.01	Aug 11 2010	14.6	4.4581E-01	0.4
Fox Mine	NV6.03	Aug 13 2010	14.3	4.4566E-01	0.4
Fox Mine	NV6.03	Aug 13 2010	15.2	4.4606E-01	0.4
Fox Mine	NV6.03	Aug 13 2010	15.0	4.4595E-01	0.4
Old Hachita, New Mexico					
Old Hachita	NM4.04	Mar 21 2009	2.1	4.4157E-01	0.4
Old Hachita	NM4.04	Mar 21 2009	2.6	4.4179E-01	0.4
Old Hachita	NM4.04	Mar 21 2009	2.5	4.4174E-01	0.4
Old Hachita	NM4.04	Mar 21 2009	2.6	4.4176E-01	0.4
Old Hachita	NM4.04	Mar 21 2009	1.9	4.4148E-01	0.4
Old Hachita	CO3.04	Aug 13 2010	2.5	4.4045E-01	0.4
Old Hachita	CO3.04	Aug 13 2010	2.5	4.4048E-01	0.4
Cerrillos Hills, New Mexico					
Castillian Mine	STD-X1-CAS1-3	Mar 18 2009	1.3	4.4482E-01	0.3

Turquoise Deposit	Mount No.	Date of Analysis	$\delta^{65}Cu_{NIST976}$ (‰)	$^{65}Cu/^{63}Cu$ (SIMS)	1σ (SIMS)
Castillian Mine	STD-X1-CAS1-3	Mar 18 2009	1.1	4.4476E-01	0.3
Castillian Mine	STD-X1-CAS1-3	Mar 18 2009	0.9	4.4465E-01	0.3
Castillian Mine	STD-X1-CAS1-3	Mar 19 2009	1.2	4.4458E-01	0.3
Castillian Mine	STD-X1-CAS1-3	Mar 19 2009	0.9	4.4444E-01	0.3
Castillian Mine	STD-X1-CAS1-3	Mar 19 2009	0.9	4.4445E-01	0.3
Castillian Mine	STD-X1-CAS1-3	Mar 19 2009	1.0	4.4449E-01	0.3
Castillian Mine	STD-X1-CAS1-3	Mar 19 2009	1.5	4.4469E-01	0.3
Castillian Mine	STD-X1-CAS1-3	Mar 20 2009	1.3	4.4470E-01	0.3
Castillian Mine	STD-X1-CAS1-3	Mar 20 2009	1.3	4.4468E-01	0.3
Castillian Mine	STD-X1-CAS1-3	Mar 20 2009	0.9	4.4452E-01	0.3
Castillian Mine	STD-X1-CAS1-3	Mar 20 2009	1.0	4.4453E-01	0.3
Castillian Mine	STD-X1-CAS1-3	Mar 20 2009	1.1	4.4460E-01	0.3
Castillian Mine	STD-X1-CAS1-3	Mar 20 2009	1.0	4.4456E-01	0.3
Castillian Mine	STD-X1-CAS1-3	Mar 21 2009	1.3	4.4474E-01	0.3
Castillian Mine	STD-X1-CAS1-4	Mar 21 2009	0.9	4.4458E-01	0.3
Castillian Mine	STD-X1-CAS1-4	Mar 21 2009	1.3	4.4477E-01	0.3
Castillian Mine	STD-X1-CAS1-4	Mar 21 2009	1.0	4.4463E-01	0.3
Castillian Mine	STD-X1-CAS1-4	Mar 21 2009	1.1	4.4465E-01	0.3
Castillian Mine	STD-X1-CAS1-4	Mar 22 2009	0.7	4.4434E-01	0.3
Castillian Mine	STD-X1-CAS1-4	Mar 22 2009	1.3	4.4460E-01	0.3
Castillian Mine	STD-X1-CAS1-4	Mar 22 2009	0.9	4.4441E-01	0.3
Castillian Mine	STD-X1-CAS1-4	Mar 22 2009	1.5	4.4470E-01	0.3
Castillian Mine	STD-X1-CAS1-4	Mar 23 2009	1.1	4.4458E-01	0.3
Castillian Mine	STD-X1-CAS1-4	Mar 23 2009	1.6	4.4476E-01	0.3
Castillian Mine	STD-X1-CAS1-4	Mar 23 2009	1.4	4.4470E-01	0.3
Castillian Mine	STD-X1-CAS1-4	Mar 23 2009	0.3	4.4422E-01	0.3
Castillian Mine	STD-X1-CAS1-3	Apr 2 2009	1.5	4.4566E-01	0.3
Castillian Mine	STD-X1-CAS1-3	Apr 2 2009	0.9	4.4540E-01	0.3
Castillian Mine	STD-X1-CAS1-3	Apr 2 2009	1.0	4.4543E-01	0.3
Castillian Mine	STD-X1-CAS1-3	Apr 2 2009	1.2	4.4555E-01	0.3
Castillian Mine	STD-X1-CAS1-3	Apr 2 2009	0.9	4.4539E-01	0.3
Castillian Mine	STD-X1-CAS1-3	Apr 3 2009	1.7	4.4555E-01	0.3
Castillian Mine	STD-X1-CAS1-3	Apr 3 2009	1.2	4.4534E-01	0.3
Castillian Mine	STD-X1-CAS1-3	Apr 3 2009	1.6	4.4554E-01	0.3
Castillian Mine	STD-X1-CAS1-3	Apr 3 2009	0.6	4.4507E-01	0.3
Castillian Mine	STD-X1-CAS1-3	Apr 3 2009	0.8	4.4516E-01	0.3
Castillian Mine	STD-X1-CAS1-3	Apr 3 2009	0.8	4.4517E-01	0.3
Castillian Mine	STD-X1-CAS1-3	Apr 4 2009	0.9	4.4527E-01	0.3
Castillian Mine	STD-X1-CAS1-3	Apr 4 2009	1.2	4.4539E-01	0.3
Castillian Mine	STD-X1-CAS1-3	Apr 4 2009	1.0	4.4532E-01	0.3
Castillian Mine	STD-X1-CAS1-3	Apr 4 2009	1.1	4.4536E-01	0.3
Castillian Mine	STD-X1-CAS1-3	Apr 4 2009	1.2	4.4539E-01	0.3
Castillian Mine	STD-X1-CAS1-3	Apr 4 2009	1.3	4.4543E-01	0.3
Castillian Mine	STD-X1-CAS1-3	Apr 6 2009	1.1	4.4522E-01	0.3
Castillian Mine	STD-X1-CAS1-3	Apr 6 2009	0.8	4.4507E-01	0.3
Castillian Mine	STD-X1-CAS1-3	Apr 6 2009	1.4	4.4533E-01	0.3
Castillian Mine	STD-X1-CAS1-3	Apr 6 2009	1.1	4.4522E-01	0.3
Castillian Mine	STD-X1-CAS1-3	Apr 6 2009	1.2	4.4526E-01	0.3

Turquoise Deposit	Mount No.	Date of Analysis	$\delta^{65}Cu_{NIST976}$ (‰)	$^{65}Cu/^{63}Cu$ (SIMS)	1σ (SIMS)
Castillian Mine	STD-X1-CAS1-3	Jun 6 2009	1.5	4.4525E-01	0.3
Castillian Mine	STD-X1-CAS1-3	Jun 6 2009	1.8	4.4538E-01	0.3
Castillian Mine	STD-X1-CAS1-3	Jun 6 2009	0.9	4.4498E-01	0.3
Castillian Mine	STD-X1-CAS1-3	Jun 6 2009	0.5	4.4482E-01	0.3
Castillian Mine	STD-X1-CAS1-3	Jun 6 2009	0.9	4.4498E-01	0.3
Castillian Mine	STD-X1-CAS1-3	Jun 6 2009	1.2	4.4515E-01	0.3
Castillian Mine	STD-X1-CAS1-3	Jun 7 2009	1.7	4.4502E-01	0.3
Castillian Mine	STD-X1-CAS1-3	Jun 7 2009	0.8	4.4460E-01	0.3
Castillian Mine	STD-X1-CAS1-3	Jun 7 2009	1.5	4.4492E-01	0.3
Castillian Mine	STD-X1-CAS1-3	Jun 7 2009	1.3	4.4483E-01	0.3
Castillian Mine	STD-X1-CAS1-3	Jun 7 2009	1.1	4.4476E-01	0.3
Castillian Mine	STD-X1-CAS1-3	Jun 7 2009	1.1	4.4475E-01	0.3
Castillian Mine	STD-X1-CAS1-3	Jun 7 2009	0.4	4.4445E-01	0.3
Castillian Mine	STD-X1-CAS1-4	Jun 7 2009	1.0	4.4471E-01	0.3
Castillian Mine	STD-X1-CAS1-3	Jun 9 2009	1.3	4.4470E-01	0.3
Castillian Mine	STD-X1-CAS1-3	Jun 9 2009	1.4	4.4473E-01	0.3
Castillian Mine	STD-X1-CAS1-3	Jun 9 2009	1.1	4.4460E-01	0.3
Castillian Mine	STD-X1-CAS1-3	Jun 9 2009	0.9	4.4451E-01	0.3
Castillian Mine	STD-X1-CAS1-3	Jun 9 2009	0.8	4.4447E-01	0.3
Castillian Mine	STD-X1-CAS1-3	Jun 10 2009	0.4	4.4398E-01	0.3
Castillian Mine	STD-X1-CAS1-3	Jun 10 2009	1.4	4.4442E-01	0.3
Castillian Mine	STD-X1-CAS1-3	Jun 10 2009	1.1	4.4428E-01	0.3
Castillian Mine	STD-X1-CAS1-4	Jun 10 2009	1.7	4.4455E-01	0.3
Castillian Mine	STD-X1-CAS1-4	Jun 10 2009	1.0	4.4423E-01	0.3
Castillian Mine	STD-X1-CAS1-4	Jun 11 2009	0.6	4.4385E-01	0.3
Castillian Mine	STD-X1-CAS1-4	Jun 11 2009	1.7	4.4433E-01	0.3
Castillian Mine	STD-X1-CAS1-4	Jun 11 2009	1.3	4.4419E-01	0.3
Castillian Mine	STD-X1-CAS1-4	Jun 11 2009	1.3	4.4415E-01	0.3
Castillian Mine	STD-X1-CAS1-4	Jun 11 2009	0.7	4.4391E-01	0.3
Castillian Mine	STD-X1-CAS1-3	Jun 13 2009	1.5	4.4418E-01	0.3
Castillian Mine	STD-X1-CAS1-3	Jun 13 2009	0.7	4.4380E-01	0.3
Castillian Mine	STD-X1-CAS1-3	Jun 13 2009	1.3	4.4407E-01	0.3
Castillian Mine	STD-X1-CAS1-3	Jun 13 2009	1.0	4.4393E-01	0.3
Castillian Mine	STD-X2-CAS1-3	Jan 11 2010	1.2	4.3926E-01	0.3
Castillian Mine	STD-X2-CAS1-3	Jan 11 2010	0.8	4.3909E-01	0.3
Castillian Mine	STD-X2-CAS1-3	Jan 11 2010	0.8	4.3909E-01	0.3
Castillian Mine	STD-X2-CAS1-3	Jan 11 2010	1.0	4.3919E-01	0.3
Castillian Mine	STD-X2-CAS1-4	Jan 11 2010	1.8	4.3954E-01	0.3
Castillian Mine	STD-X2-CAS1-4	Jan 12 2010	0.7	4.3905E-01	0.3
Castillian Mine	STD-X2-CAS1-4	Jan 12 2010	1.9	4.3959E-01	0.3
Castillian Mine	STD-X2-CAS1-4	Jan 12 2010	1.1	4.3922E-01	0.3
Castillian Mine	STD-X2-CAS1-4	Jan 12 2010	0.8	4.3909E-01	0.3
Castillian Mine	STD-X2-CAS1-3	Jan 12 2010	1.2	4.3926E-01	0.3
Castillian Mine	STD-X1-CAS1-3	Jan 28 2010	1.5	4.3948E-01	0.3
Castillian Mine	STD-X1-CAS1-3	Jan 28 2010	1.4	4.3942E-01	0.3
Castillian Mine	STD-X1-CAS1-3	Jan 28 2010	1.5	4.3948E-01	0.3
Castillian Mine	STD-X1-CAS1-3	Jan 28 2010	1.1	4.3930E-01	0.3
Castillian Mine	STD-X1-CAS1-3	Jan 28 2010	0.1	4.3887E-01	0.3

Turquoise Deposit	**Mount No.**	**Date of Analysis**	**$\delta^{65}Cu_{NIST976}$ (‰)**	**$^{65}Cu/^{63}Cu$ (SIMS)**	**1σ (SIMS)**
Castillian Mine	STD-X1-CAS1-3	Jan 29 2010	1.5	4.3928E-01	0.3
Castillian Mine	STD-X1-CAS1-3	Jan 29 2010	1.7	4.3936E-01	0.3
Castillian Mine	STD-X1-CAS1-3	Jan 29 2010	1.1	4.3907E-01	0.3
Castillian Mine	STD-X1-CAS1-3	Jan 29 2010	0.6	4.3889E-01	0.3
Castillian Mine	STD-X1-CAS1-3	Jan 29 2010	0.6	4.3888E-01	0.3
Castillian Mine	STD-X2-CAS1-4	Jan 30 2010	1.4	4.3895E-01	0.3
Castillian Mine	STD-X2-CAS1-4	Jan 30 2010	1.0	4.3878E-01	0.3
Castillian Mine	STD-X2-CAS1-4	Jan 30 2010	1.5	4.3903E-01	0.3
Castillian Mine	STD-X2-CAS1-4	Jan 30 2010	1.4	4.3895E-01	0.3
Castillian Mine	STD-X2-CAS1-4	Jan 30 2010	0.4	4.3852E-01	0.3
Castillian Mine	STD-X2-CAS1-4	Jan 30 2010	1.1	4.3882E-01	0.3
Castillian Mine	STD-X2-CAS1-4	Feb 22 2010	1.0	4.3858E-01	0.3
Castillian Mine	STD-X2-CAS1-4	Feb 22 2010	0.9	4.3849E-01	0.3
Castillian Mine	STD-X2-CAS1-4	Feb 22 2010	1.4	4.3875E-01	0.3
Castillian Mine	STD-X2-CAS1-4	Feb 23 2010	0.5	4.3835E-01	0.3
Castillian Mine	STD-X2-CAS1-4	Feb 23 2010	0.0	4.3814E-01	0.3
Castillian Mine	STD-X2-CAS1-4	Feb 23 2010	1.3	4.3871E-01	0.3
Castillian Mine	STD-X2-CAS1-4	Feb 23 2010	1.8	4.3893E-01	0.3
Castillian Mine	STD-X2-CAS1-4	Feb 23 2010	2.0	4.3905E-01	0.3
Castillian Mine	STD-X2-CAS1-4	Feb 24 2010	1.0	4.3850E-01	0.3
Castillian Mine	STD-X2-CAS1-4	Feb 24 2010	1.1	4.3853E-01	0.3
Castillian Mine	STD-X2-CAS1-4	Feb 24 2010	1.6	4.3876E-01	0.3
Castillian Mine	STD-X2-CAS1-4	Feb 24 2010	1.1	4.3855E-01	0.3
Castillian Mine	STD-X2-CAS1-4	Feb 24 2010	0.7	4.3839E-01	0.3
Castillian Mine	STD-X2-CAS1-4	Feb 25 2010	1.3	4.3885E-01	0.3
Castillian Mine	STD-X2-CAS1-4	Feb 25 2010	1.0	4.3872E-01	0.3
Castillian Mine	STD-X2-CAS1-4	Feb 25 2010	0.9	4.3869E-01	0.3
Castillian Mine	STD-X2-CAS1-4	Feb 25 2010	1.0	4.3871E-01	0.3
Castillian Mine	STD-X2-CAS1-3	Feb 25 2010	1.3	4.3887E-01	0.3
Castillian Mine	STD-X2-CAS1-3	Aug 10 2010	0.9	4.4269E-01	0.4
Castillian Mine	STD-X2-CAS1-3	Aug 10 2010	1.8	4.4307E-01	0.3
Castillian Mine	STD-X2-CAS1-3	Aug 10 2010	0.9	4.4269E-01	0.3
Castillian Mine	STD-X2-CAS1-3	Aug 10 2010	0.9	4.4270E-01	0.3
Castillian Mine	STD-X2-CAS1-4	Aug 11 2010	0.5	4.4232E-01	0.4
Castillian Mine	STD-X2-CAS1-4	Aug 11 2010	0.6	4.4233E-01	0.3
Castillian Mine	STD-X2-CAS1-4	Aug 11 2010	1.5	4.4276E-01	0.3
Castillian Mine	STD-X2-CAS1-4	Aug 11 2010	1.7	4.4282E-01	0.3
Castillian Mine	STD-X2-CAS1-4	Aug 11 2010	1.2	4.4263E-01	0.3
Castillian Mine	STD-X2-CAS1-4	Aug 11 2010	1.2	4.4260E-01	0.3
Castillian Mine	STD-X2-CAS1-4	Aug 12 2010	0.6	4.4215E-01	0.3
Castillian Mine	STD-X2-CAS1-4	Aug 12 2010	0.6	4.4214E-01	0.3
Castillian Mine	STD-X2-CAS1-4	Aug 12 2010	1.5	4.4256E-01	0.3
Castillian Mine	STD-X2-CAS1-4	Aug 12 2010	1.8	4.4267E-01	0.3
Castillian Mine	STD-X2-CAS1-4	Aug 12 2010	1.1	4.4237E-01	0.3
Castillian Mine	STD-X2-CAS1-4	Aug 13 2010	0.4	4.4234E-01	0.3
Castillian Mine	STD-X2-CAS1-4	Aug 13 2010	1.5	4.4279E-01	0.3
Castillian Mine	STD-X2-CAS1-4	Aug 13 2010	0.9	4.4254E-01	0.3
Castillian Mine	STD-X2-CAS1-4	Aug 13 2010	1.1	4.4264E-01	0.3

Turquoise Deposit	Mount No.	Date of Analysis	$\delta^{65}Cu_{NIST976}$ (‰)	$^{65}Cu/^{63}Cu$ (SIMS)	1σ (SIMS)
Castillian Mine	STD-X2-CAS1-4	Aug 13 2010	1.3	4.4273E-01	0.3
Castillian Mine	STD-X2-CAS1-4	Aug 13 2010	1.4	4.4275E-01	0.3
Castillian Mine	STD-X2-CAS1-3	Aug 15 2010	0.4	4.4258E-01	0.3
Castillian Mine	STD-X2-CAS1-3	Aug 15 2010	1.4	4.4301E-01	0.3
Castillian Mine	STD-X2-CAS1-3	Aug 15 2010	1.3	4.4296E-01	0.3
Castillian Mine	STD-X2-CAS1-3	Aug 15 2010	1.4	4.4301E-01	0.3
Castillian Mine	STD-X1-CAS1-3	Aug 16 2010	1.0	4.4277E-01	0.3
Castillian Mine	STD-X1-CAS1-3	Aug 16 2010	1.2	4.4286E-01	0.3
Castillian Mine	STD-X1-CAS1-3	Aug 16 2010	1.0	4.4274E-01	0.3
Castillian Mine	STD-X1-CAS1-3	Aug 16 2010	1.2	4.4284E-01	0.3
Castillian Mine	STD-X2-CAS1-4	Aug 30 2010	1.6	4.4243E-01	0.4
Castillian Mine	STD-X2-CAS1-4	Aug 30 2010	1.3	4.4232E-01	0.3
Castillian Mine	STD-X2-CAS1-4	Aug 30 2010	1.2	4.4223E-01	0.4
Castillian Mine	STD-X2-CAS1-4	Aug 30 2010	1.2	4.4225E-01	0.3
Castillian Mine	STD-X2-CAS1-4	Aug 30 2010	0.6	4.4199E-01	0.3
Castillian Mine	STD-X2-CAS1-4	Aug 30 2010	1.0	4.4217E-01	0.3
Castillian Mine	STD-X2-CAS1-4	Aug 30 2010	0.8	4.4209E-01	0.3
Castillian Mine	STD-X2-CAS1-4	Aug 31 2010	1.1	4.4233E-01	0.3
Castillian Mine	STD-X2-CAS1-4	Aug 31 2010	1.4	4.4249E-01	0.3
Castillian Mine	STD-X2-CAS1-4	Aug 31 2010	0.8	4.4222E-01	0.3
Castillian Mine	STD-X2-CAS1-4	Aug 31 2010	1.2	4.4238E-01	0.3
Castillian Mine	STD-X2-CAS1-4	Sep 3 2010	1.4	4.4277E-01	0.3
Castillian Mine	STD-X2-CAS1-3	Sep 3 2010	1.8	4.4296E-01	0.3
Castillian Mine	STD-X2-CAS1-3	Sep 3 2010	0.7	4.4250E-01	0.3
Castillian Mine	STD-X2-CAS1-3	Sep 3 2010	1.1	4.4264E-01	0.3
Castillian Mine	STD-X2-CAS1-3	Sep 3 2010	0.6	4.4242E-01	0.3
Castillian Mine	STD-X2-CAS1-3	Sep 4 2010	1.2	4.4282E-01	0.3
Castillian Mine	STD-X2-CAS1-3	Sep 4 2010	1.0	4.4273E-01	0.3
Castillian Mine	STD-X2-CAS1-3	Sep 4 2010	1.5	4.4294E-01	0.3
Castillian Mine	STD-X2-CAS1-3	Sep 4 2010	0.8	4.4264E-01	0.3

Appendix 4:

Recap of Hydrogen and Copper Isotopic Analyses of Turquoise Artifact Samples by SIMS

Appendix 4. Recap of Hydrogen and Copper Isotopic Analyses of Turquoise Artifact Samples by SIMS.

Archaeological Provenance	Mount No.	Turquoise Provenance	Average δD_{VSMOW} (‰)	STD 2σ δD_{VSMOW} (‰)	Average $\delta^{65}Cu_{NIST976}$ (‰)	STD 2σ $\delta^{65}Cu_{NIST976}$ (‰)
Pueblo Bonito						
Room 26	ARF7.02	King Manassa	-83	5	2.6	0.6
Room 28	ARF16.03	Unknown	-103	4	8.4	0.5
Room 28	ARF7.03	Crescent Peak	-81	4	5.2	0.7
Room 33	ARF15.03	Castillian	-94	4	2.0	0.5
Room 33	ARF5.02	Villa Grove	-103	4	1.7	0.5
Room 33	ARF15.05	Villa Grove	-89	5	2.4	0.4
Room 33	ARF10.02	Castillian	-90	4	0.6	0.6
Room 33	ARF10.03	Unknown	-96	4	-0.2	0.6
Room 33	ARF10.04	Castillian	-95	5	0.9	0.5
Room 33	ARF10.05	Unknown	-75	5	1.4	0.5
Room 33	ARF4.03	Unknown	-64	5	5.4	0.5
Room 33	ARF13.03	Unknown	-77	4	0.0	0.5
Room 33	ARF15.01	King Manassa	-87	4	3.6	0.4
Room 33	ARF15.02	Villa Grove	-92	4	2.2	0.4
Room 33	ARF5.04	Unknown	-50	4	1.1	0.4
Room 33	ARF14.01	Unknown	-78	5	-1.9	0.5
Room 33	ARF14.02	Unknown	-61	4	-1.3	0.5
Room 33	ARF14.03	Unknown	-89	4	-0.8	0.5
Room 33	ARF14.04	Castillian	-93	5	0.3	0.4
Room 33	ARF4.04	Unknown	-90	4	-0.4	0.5
Room 33	ARF19.02	Villa Grove	-102	4	2.7	0.4
Room 33	ARF4.01	Castillian	-85	4	1.5	0.5
Room 40	ARF16.01	Castillian	-90	4	0.9	0.4
Room 85	ARF19.04	Lone Mountain	-119	5	5.5	0.5
Room 85	ARF19.03	Villa Grove	-100	4	1.8	0.5
Room 96	ARF6.01	Unknown	-84	4	-0.7	0.6
Room 127	ARF16.04	Unknown	-96	5	12.2	0.4
Room 127	ARF7.01	Castillian	-87	4	1.0	0.6
Room 173	ARF6.04	Villa Grove	-91	4	2.7	0.5

Archaeological Provenance	Mount No.	Turquoise Provenance	Average δD_{VSMOW} (‰)	STD 2σ δD_{VSMOW} (‰)	Average $\delta^{65}Cu_{NIST976}$ (‰)	STD 2σ $\delta^{65}Cu_{NIST976}$ (‰)
29SJ1360						
Trash midden, TT 1	C2.07	Unknown	-117	4	5.8	0.5
29SJ1659 Shabik'eshchee						
Pithouse Y, floor fill	C1.01	Sleeping Beauty	-76	6	6.6	0.6
29SJ423						
Pithouse A, stone bowl	C1.03	Morenci	-124	6	2.3	0.4
29SJ625 Three C site						
Room E, floor, hearth	C3.10	Unknown	-113	5	4.6	0.4
29SJ627						
Kiva G	C4.15	Royston	-114	4	4.3	0.5
Room 10, floor 2	C3.13	Royston	-122	6	3.5	0.4
Room 10, level 2	C3.14	Lone Mountain	-125	6	5.3	0.5
29SJ628						
Pithouse E	C1.04	Royston	-111	6	3.1	0.4
Pithouse A, ventilator shaft	C2.05	Unknown	-112	5	6.1	0.6
29SJ629 Spadefoot Toad						
Trash midden 59, level 2	C4.16	Royston	-113	5	2.8	0.5
29SJ633 Eleventh Hour						
Room 7, layer 8, below floor 2	C5.22	Unknown	-114	5	6.4	0.4
Room 8, layer 2, level 4	C5.24	Royston	-106	4	3.6	0.4
Aztec Ruin						
N XV 2	ARF9.04	Halloran Springs	-96	5	6.3	0.6
N XV 2	ARF12.04	Cripple Creek	-86	4	6.4	0.5
N XV 2	ARF13.01	Villa Grove	-89	5	2.2	0.5
N XV 2	ARF13.02	Unknown	-80	5	-1.6	0.4
N XV 2	ARF2.02	Unknown	-89	5	-1.9	0.6
E Room 52	ARF12.03	Unknown	-83	6	2.4	0.4
E Room 52	ARF2.01	Villa Grove	-100	6	2.5	0.6
N Room 65	ARF3.02	King Manassa	-72	5	4.4	0.7
S Room 9	ARF2.04	Unknown	-61	4	7.4	0.6
Wing N Room 111	ARF9.05	Castillian	-100	4	0.4	0.7
Wing N Room 111	ARF11.03	King Manassa	-86	5	3.1	0.5

Archaeological Provenance	**Mount No.**	**Turquoise Provenance**	**Average δD_{VSMOW} (‰)**	**STD 2σ δD_{VSMOW} (‰)**	**Average $\delta^{65}Cu_{NIST976}$ (‰)**	**STD 2σ $\delta^{65}Cu_{NIST976}$ (‰)**
Wing N Room 111	ARF11.04	Unknown	-99	4	-2.3	0.3
Wing N Room 111	ARF2.03	Unknown	-81	4	0.4	0.5
Salmon Ruin						
Room W51	ARF18.02	Unknown	-97	5	11.8	0.6
Room W51	ARF22.01	Crescent Peak	-87	4	3.5	0.6
Room W62	ARF21.01	Unknown	-110	4	0.2	0.6
West Room 0 63	ARF18.01	Unknown	-85	4	8.4	0.4
Room W91	ARF21.02	Mineral Park	-100	4	5.3	0.5
Room 98W	ARF8.02	Lone Mountain	-136	5	5.1	0.7
Room 130W	ARF8.03	Unknown	-102	6	-2.5	0.4
Room 130W	ARF8.01	Unknown	-112	6	7.3	0.4

Appendix 5:

Hydrogen Isotopic Analyses of Turquoise Artifact Samples by SIMS

Appendix 5. Hydrogen Isotopic Analyses of Turquoise Artifact Samples by SIMS.

Archaeological Site	Mount No.	Date of Analysis	δD_{VSMOW} (‰)	D/H (SIMS)	1σ (SIMS)
Pueblo Bonito					
Room 26	ARF7.02	Sep 14 2009	-80	4.4940E-05	4
Room 26	ARF7.02	Sep 14 2009	-85	4.4715E-05	4
Pueblo Bonito					
Room 28	ARF16.03	Sep 19 2009	-102	4.4017E-05	4
Room 28	ARF16.03	Sep 19 2009	-104	4.3901E-05	4
Pueblo Bonito					
Room 28	ARF7.03	Sep 14 2009	-82	4.4849E-05	4
Room 28	ARF7.03	Sep 14 2009	-80	4.4935E-05	4
Pueblo Bonito					
Room 33	ARF15.03	Sep 19 2009	-92	4.4498E-05	4
Room 33	ARF15.03	Sep 19 2009	-95	4.4317E-05	4
Pueblo Bonito					
Room 33	ARF5.02	Sep 10 2009	-104	4.2824E-05	4
Room 33	ARF5.02	Sep 10 2009	-102	4.2909E-05	4
Pueblo Bonito					
Room 33	ARF15.05	Sep 19 2009	-87	4.4748E-05	4
Room 33	ARF15.05	Sep 19 2009	-91	4.4510E-05	4
Pueblo Bonito					
Room 33	ARF10.02	Sep 16 2009	-90	4.5007E-05	4
Room 33	ARF10.02	Sep 16 2009	-90	4.4999E-05	4
Pueblo Bonito					
Room 33	ARF10.03	Sep 16 2009	-97	4.4635E-05	4
Room 33	ARF10.03	Sep 16 2009	-94	4.4784E-05	4
Pueblo Bonito					
Room 33	ARF10.04	Sep 16 2009	-97	4.4672E-05	4
Room 33	ARF10.04	Sep 16 2009	-92	4.4878E-05	4
Pueblo Bonito					
Room 33	ARF10.05	Sep 16 2009	-77	4.5629E-05	4
Room 33	ARF10.05	Sep 16 2009	-73	4.5818E-05	4
Pueblo Bonito					
Room 33	ARF4.03	Sep 10 2009	-66	4.4659E-05	4
Room 33	ARF4.03	Sep 10 2009	-62	4.4842E-05	4
Pueblo Bonito					
Room 33	ARF13.03	Sep 18 2009	-77	4.5050E-05	4
Room 33	ARF13.03	Sep 18 2009	-76	4.5065E-05	4
Pueblo Bonito					
Room 33	ARF15.01	Sep 19 2009	-88	4.4689E-05	4
Room 33	ARF15.01	Sep 19 2009	-86	4.4760E-05	4
Pueblo Bonito					
Room 33	ARF15.02	Sep 19 2009	-91	4.4524E-05	4
Room 33	ARF15.02	Sep 19 2009	-93	4.4416E-05	4
Pueblo Bonito					
Room 33	ARF5.04	Sep 11 2009	-50	4.5326E-05	4
Room 33	ARF5.04	Sep 11 2009	-49	4.5357E-05	4
Pueblo Bonito					

Archaeological Site	Mount No.	Date of Analysis	δD_{VSMOW} (‰)	D/H (SIMS)	1σ (SIMS)
Room 33	ARF14.01	Sep 18 2009	-75	4.5133E-05	4
Room 33	ARF14.01	Sep 18 2009	-80	4.4876E-05	4
Pueblo Bonito					
Room 33	ARF14.02	Sep 18 2009	-62	4.5752E-05	4
Room 33	ARF14.02	Sep 18 2009	-60	4.5858E-05	4
Pueblo Bonito					
Room 33	ARF14.03	Sep 18 2009	-88	4.4498E-05	4
Room 33	ARF14.03	Sep 18 2009	-90	4.4404E-05	4
Pueblo Bonito					
Room 33	ARF14.04	Sep 18 2009	-91	4.4330E-05	4
Room 33	ARF14.04	Sep 18 2009	-95	4.4164E-05	4
Pueblo Bonito					
Room 33	ARF4.04	Sep 10 2009	-90	4.3495E-05	4
Room 33	ARF4.04	Sep 10 2009	-89	4.3556E-05	4
Pueblo Bonito					
Room 33	ARF19.02	Sep 20 2009	-103	4.3889E-05	4
Room 33	ARF19.02	Sep 20 2009	-101	4.3979E-05	4
Pueblo Bonito					
Room 33	ARF4.01	Sep 10 2009	-84	4.3778E-05	4
Room 33	ARF4.01	Sep 10 2009	-86	4.3677E-05	4
Pueblo Bonito					
Room 40	ARF16.01	Sep 19 2009	-90	4.4605E-05	4
Room 40	ARF16.01	Sep 19 2009	-90	4.4563E-05	4
Pueblo Bonito					
Room 85	ARF19.04	Sep 20 2009	-121	4.3000E-05	4
Room 85	ARF19.04	Sep 20 2009	-117	4.3174E-05	4
Pueblo Bonito					
Room 85	ARF19.03	Sep 20 2009	-100	4.4016E-05	4
Room 85	ARF19.03	Sep 20 2009	-100	4.4035E-05	4
Pueblo Bonito					
Room 96	ARF6.01	Sep 13 2009	-85	4.4384E-05	4
Room 96	ARF6.01	Sep 13 2009	-82	4.4521E-05	4
Pueblo Bonito					
Room 127	ARF16.04	Sep 19 2009	-94	4.4405E-05	4
Room 127	ARF16.04	Sep 19 2009	-98	4.4186E-05	4
Pueblo Bonito					
Room 127	ARF7.01	Sep 14 2009	-86	4.4677E-05	4
Room 127	ARF7.01	Sep 14 2009	-87	4.4628E-05	4
Pueblo Bonito					
Room 173	ARF6.04	Sep 13 2009	-91	4.4127E-05	4
Room 173	ARF6.04	Sep 13 2009	-91	4.4131E-05	4
Chaco Canyon, 29SJ1360					
Trash midden, TT 1	C2.07	Sep 20 2009	-118	4.3155E-05	4
Trash midden, TT 1	C2.07	Sep 20 2009	-115	4.3280E-05	4
Chaco Canyon, 29SJ1659 Shabik'eshchee					
Pithouse Y, floor fill	C1.01	Apr 12 2009	-74	4.0944E-05	6
Pithouse Y, floor fill	C1.01	Apr 12 2009	-77	4.0809E-05	6
Chaco Canyon, 29SJ423					

Archaeological Site	Mount No.	Date of Analysis	δD_{VSMOW} (‰)	D/H (SIMS)	1σ (SIMS)
Pithouse A, stone bowl	C1.03	Apr 12 2009	-126	3.8651E-05	6
Pithouse A, stone bowl	C1.03	Apr 12 2009	-122	3.8832E-05	6
Chaco Canyon, 29SJ625 Three C site					
Room E, floor, hearth	C3.10	Apr 13 2009	-113	3.9405E-05	6
Room E, floor, hearth	C3.10	Apr 13 2009	-113	3.9401E-05	5
Chaco Canyon, 29SJ627					
Kiva G	C4.15	Sep 21 2009	-114	4.3444E-05	4
Kiva G	C4.15	Sep 21 2009	-113	4.3497E-05	4
Chaco Canyon, 29SJ627					
Room 10, floor 2	C3.13	Apr 13 2009	-120	3.9104E-05	6
Room 10, floor 2	C3.13	Apr 13 2009	-123	3.8952E-05	5
Chaco Canyon, 29SJ627					
Room 10, level 2	C3.14	Apr 13 2009	-123	3.8945E-05	5
Room 10, level 2	C3.14	Apr 13 2009	-127	3.8795E-05	5
Chaco Canyon, 29SJ628					
Pithouse E	C1.04	Apr 12 2009	-111	3.9294E-05	6
Pithouse E	C1.04	Apr 12 2009	-111	3.9308E-05	6
Chaco Canyon, 29SJ628					
Pithouse A, near ventilator shaft	C2.05	Sep 20 2009	-109	4.3565E-05	4
Pithouse A, near ventilator shaft	C2.05	Sep 20 2009	-114	4.3336E-05	4
Chaco Canyon, 29SJ629 Spadefoot Toad					
Trash midden 59, level 2	C4.16	Sep 21 2009	-115	4.3401E-05	4
Trash midden 59, level 2	C4.16	Sep 21 2009	-111	4.3607E-05	4
Chaco Canyon, 29SJ633 Eleventh Hour					
Room 7, layer 8, below floor 2	C5.22	Sep 21 2009	-116	4.3350E-05	4
Room 7, layer 8, below floor 2	C5.22	Sep 21 2009	-112	4.3532E-05	4
Chaco Canyon, 29SJ633 Eleventh Hour					
Room 8, layer 2, level 4	C5.24	Sep 21 2009	-107	4.3769E-05	4
Room 8, layer 2, level 4	C5.24	Sep 21 2009	-105	4.3880E-05	4
Aztec Ruin					
N XV 2	ARF9.04	Sep 16 2009	-98	4.4593E-05	4
N XV 2	ARF9.04	Sep 16 2009	-94	4.4819E-05	4
Aztec Ruin					
N XV 2	ARF12.04	Sep 17 2009	-86	4.5058E-05	4
N XV 2	ARF12.04	Sep 17 2009	-85	4.5082E-05	4
Aztec Ruin					
N XV 2	ARF13.01	Sep 18 2009	-91	4.4322E-05	4
N XV 2	ARF13.01	Sep 18 2009	-87	4.4558E-05	4
Aztec Ruin					
N XV 2	ARF13.02	Sep 18 2009	-78	4.4986E-05	4
N XV 2	ARF13.02	Sep 18 2009	-82	4.4787E-05	4
Aztec Ruin					
N XV 2	ARF2.02	Sep 9 2009	-90	4.2845E-05	4
N XV 2	ARF2.02	Sep 9 2009	-88	4.2978E-05	4

Archaeological Site	Mount No.	Date of Analysis	δD_{VSMOW} (‰)	D/H (SIMS)	1σ (SIMS)
Aztec Ruin					
E Room 52	ARF12.03	Sep 17 2009	-80	4.5315E-05	4
E Room 52	ARF12.03	Sep 17 2009	-86	4.5031E-05	4
Aztec Ruin					
E Room 52	ARF2.01	Sep 9 2009	-97	4.2514E-05	4
E Room 52	ARF2.01	Sep 9 2009	-102	4.2296E-05	4
Aztec Ruin					
N Room 65	ARF3.02	Sep 9 2009	-74	4.3637E-05	4
N Room 65	ARF3.02	Sep 9 2009	-69	4.3829E-05	4
Aztec Ruin					
S Room 9	ARF2.04	Sep 9 2009	-61	4.4209E-05	4
S Room 9	ARF2.04	Sep 9 2009	-60	4.4267E-05	4
Aztec Ruin					
Wing N Room 111	ARF9.05	Sep 16 2009	-99	4.4566E-05	4
Wing N Room 111	ARF9.05	Sep 16 2009	-100	4.4510E-05	4
Aztec Ruin					
Wing N Room 111	ARF11.03	Sep 17 2009	-84	4.5125E-05	4
Wing N Room 111	ARF11.03	Sep 17 2009	-90	4.4852E-05	4
Wing N Room 111	ARF11.03	Sep 17 2009	-85	4.5111E-05	4
Aztec Ruin					
Wing N Room 111	ARF11.04	Sep 17 2009	-99	4.4409E-05	4
Wing N Room 111	ARF11.04	Sep 17 2009	-99	4.4386E-05	4
Aztec Ruin					
Wing N Room 111	ARF2.03	Sep 9 2009	-81	4.3269E-05	4
Wing N Room 111	ARF2.03	Sep 9 2009	-80	4.3336E-05	4
Salmon Ruin					
Room W51	ARF18.02	Aug 6 2010	-99	4.7376E-05	4
Room W51	ARF18.02	Aug 6 2010	-95	4.7603E-05	4
Room W51					
Room W51	ARF22.01	Aug 9 2010	-87	4.7710E-05	4
Room W51	ARF22.01	Aug 9 2010	-84	4.7831E-05	4
Room W51	ARF22.01	Aug 9 2010	-89	4.7577E-05	4
Salmon Ruin					
Room W62	ARF21.01	Aug 10 2010	-108	4.7019E-05	4
Room W62	ARF21.01	Aug 10 2010	-112	4.6815E-05	4
Room W62	ARF21.01	Aug 7 2010	-111	4.6232E-05	4
Room W62	ARF21.01	Aug 7 2010	-107	4.6452E-05	4
Salmon Ruin					
West Room 0 63	ARF18.01	Aug 6 2010	-86	4.8072E-05	4
West Room 0 63	ARF18.01	Aug 6 2010	-84	4.8164E-05	4
Salmon Ruin					
Room W91	ARF21.02	Aug 10 2010	-98	4.7559E-05	4
Room W91	ARF21.02	Aug 10 2010	-101	4.7411E-05	4
Salmon Ruin					
Room 98W	ARF8.02	Aug 6 2010	-133	4.5603E-05	4
Room 98W	ARF8.02	Aug 6 2010	-138	4.5361E-05	4
Salmon Ruin					
Room 130W	ARF8.03	Aug 6 2010	-107	4.6976E-05	4

Archaeological Site	Mount No.	Date of Analysis	δD_{VSMOW} (‰)	D/H (SIMS)	1σ (SIMS)
Room 130W	ARF8.03	Aug 6 2010	-99	4.7395E-05	4
Room 130W	ARF8.03	Aug 6 2010	-99	4.7418E-05	4
Salmon Ruin					
Room 130W	ARF8.01	Aug 6 2010	-117	4.6467E-05	4
Room 130W	ARF8.01	Aug 6 2010	-108	4.6907E-05	4
Room 130W	ARF8.01	Aug 6 2010	-111	4.6755E-05	4

Appendix 6:

Copper Isotopic Analyses of Turquoise Artifact Samples by SIMS

Appendix 6. Copper Isotopic Analyses of Turquoise Artifact Samples by SIMS.

Archaeological Site	Mount No.	Date of Analysis	$\delta^{65}Cu_{NIST976}$ (‰)	$^{65}Cu/^{63}Cu$ (SIMS)	1σ (SIMS)
Pueblo Bonito					
Room 26	ARF7.02	Jun 13 2009	3.0	4.4113E-01	0.4
Room 26	ARF7.02	Jun 13 2009	2.9	4.4110E-01	0.4
Room 26	ARF7.02	Jan 12 2010	2.8	4.4081E-01	0.4
Room 26	ARF7.02	Jan 12 2010	2.0	4.4045E-01	0.5
Room 26	ARF7.02	Jan 12 2010	2.1	4.4052E-01	0.5
Pueblo Bonito					
Room 28	ARF16.03	Jan 30 2010	8.1	4.4260E-01	0.4
Room 28	ARF16.03	Jan 30 2010	8.6	4.4283E-01	0.4
Pueblo Bonito					
Room 28	ARF7.03	Jan 12 2010	5.5	4.4199E-01	0.5
Room 28	ARF7.03	Jan 12 2010	4.8	4.4171E-01	0.5
Pueblo Bonito					
Room 33	ARF15.03	Jan 28 2010	1.8	4.3997E-01	0.4
Room 33	ARF15.03	Jan 28 2010	2.1	4.4011E-01	0.4
Pueblo Bonito					
Room 33	ARF5.02	Jun 11 2009	1.9	4.4072E-01	0.4
Room 33	ARF5.02	Jun 11 2009	1.5	4.4056E-01	0.4
Pueblo Bonito					
Room 33	ARF15.05	Jan 28 2010	2.5	4.4029E-01	0.4
Room 33	ARF15.05	Jan 28 2010	2.4	4.4022E-01	0.4
Pueblo Bonito					
Room 33	ARF10.02	Jan 11 2010	0.7	4.4003E-01	0.5
Room 33	ARF10.02	Jan 11 2010	0.2	4.3982E-01	0.5
Room 33	ARF10.02	Jan 11 2010	1.0	4.4016E-01	0.5
Pueblo Bonito					
Room 33	ARF10.03	Jan 11 2010	0.2	4.3980E-01	0.4
Room 33	ARF10.03	Jan 11 2010	-0.5	4.3951E-01	0.4
Pueblo Bonito					
Room 33	ARF10.04	Jan 11 2010	0.9	4.4012E-01	0.5
Room 33	ARF10.04	Jan 11 2010	0.8	4.4009E-01	0.5
Pueblo Bonito					
Room 33	ARF10.05	Jan 11 2010	1.4	4.4035E-01	0.5
Room 33	ARF10.05	Jan 11 2010	1.3	4.4027E-01	0.5
Pueblo Bonito					
Room 33	ARF4.03	Jun 9 2009	5.1	4.4217E-01	0.4
Room 33	ARF4.03	Jun 9 2009	5.6	4.4236E-01	0.4
Pueblo Bonito					
Room 33	ARF13.03	Jan 29 2010	0.1	4.3930E-01	0.4
Room 33	ARF13.03	Jan 29 2010	-0.1	4.3920E-01	0.5
Pueblo Bonito					
Room 33	ARF15.01	Jan 28 2010	3.6	4.4075E-01	0.4
Room 33	ARF15.01	Jan 28 2010	3.7	4.4082E-01	0.4
Pueblo Bonito					
Room 33	ARF15.02	Jan 28 2010	2.2	4.4015E-01	0.4
Room 33	ARF15.02	Jan 28 2010	2.1	4.4011E-01	0.4

Archaeological Site	Mount No.	Date of Analysis	$\delta^{65}Cu_{NIST976}$ (‰)	$^{65}Cu/^{63}Cu$ (SIMS)	1σ (SIMS)
Pueblo Bonito					
Room 33	ARF5.04	Jun 11 2009	1.1	4.4038E-01	0.4
Room 33	ARF5.04	Jun 11 2009	1.0	4.4035E-01	0.4
Pueblo Bonito					
Room 33	ARF14.01	Jan 29 2010	-1.6	4.3853E-01	0.4
Room 33	ARF14.01	Jan 29 2010	-2.1	4.3830E-01	0.4
Pueblo Bonito					
Room 33	ARF14.02	Jan 29 2010	-1.0	4.3880E-01	0.4
Room 33	ARF14.02	Jan 29 2010	-1.5	4.3859E-01	0.4
Pueblo Bonito					
Room 33	ARF14.03	Jan 29 2010	-0.4	4.3905E-01	0.4
Room 33	ARF14.03	Jan 29 2010	-1.0	4.3881E-01	0.4
Room 33	ARF14.03	Jan 29 2010	-1.0	4.3881E-01	0.4
Pueblo Bonito					
Room 33	ARF14.04	Jan 29 2010	0.3	4.3936E-01	0.4
Room 33	ARF14.04	Jan 29 2010	0.3	4.3936E-01	0.4
Pueblo Bonito					
Room 33	ARF4.04	Jun 9 2009	-0.2	4.3982E-01	0.4
Room 33	ARF4.04	Jun 9 2009	-0.5	4.3971E-01	0.4
Pueblo Bonito					
Room 33	ARF19.02	Feb 23 2010	2.8	4.4060E-01	0.4
Room 33	ARF19.02	Feb 23 2010	2.6	4.4052E-01	0.4
Pueblo Bonito					
Room 33	ARF4.01	Jun 9 2009	1.3	4.4046E-01	0.4
Room 33	ARF4.01	Jun 9 2009	1.9	4.4072E-01	0.4
Room 33	ARF4.01	Jun 9 2009	1.3	4.4047E-01	0.4
Pueblo Bonito					
Room 40	ARF16.01	Jan 30 2010	0.8	4.3938E-01	0.4
Room 40	ARF16.01	Jan 30 2010	0.9	4.3942E-01	0.4
Pueblo Bonito					
Room 85	ARF19.04	Feb 23 2010	5.6	4.4181E-01	0.4
Room 85	ARF19.04	Feb 23 2010	5.3	4.4167E-01	0.4
Pueblo Bonito					
Room 85	ARF19.03	Feb 23 2010	1.9	4.4018E-01	0.4
Room 85	ARF19.03	Feb 23 2010	1.6	4.4006E-01	0.4
Pueblo Bonito					
Room 96	ARF6.01	Jan 12 2010	-0.9	4.3921E-01	0.4
Room 96	ARF6.01	Jan 12 2010	-0.4	4.3939E-01	0.5
Pueblo Bonito					
Room 127	ARF16.04	Jan 30 2010	12.2	4.4440E-01	0.4
Room 127	ARF16.04	Jan 30 2010	12.1	4.4435E-01	0.4
Pueblo Bonito					
Room 127	ARF7.01	Jun 13 2009	0.6	4.4113E-01	0.4
Room 127	ARF7.01	Jun 13 2009	1.6	4.4146E-01	0.4
Room 127	ARF7.01	Jun 13 2009	1.3	4.4110E-01	0.4
Room 127	ARF7.01	Jan 12 2010	1.0	4.4001E-01	0.5
Room 127	ARF7.01	Jan 12 2010	0.7	4.3991E-01	0.5
Pueblo Bonito					

Archaeological Site	Mount No.	Date of Analysis	$\delta^{65}Cu_{NIST976}$ (‰)	$^{65}Cu/^{63}Cu$ (SIMS)	1σ (SIMS)
Room 173	ARF6.04	Jun 13 2009	2.8	4.4102E-01	0.5
Room 173	ARF6.04	Jun 13 2009	2.8	4.4105E-01	0.5
Room 173	ARF6.04	Jan 12 2010	2.9	4.4084E-01	0.5
Room 173	ARF6.04	Jan 12 2010	2.5	4.4070E-01	0.5
Chaco Canyon, 29SJ1360					
Trash midden, TT 1	C2.07	Jun 6 2009	5.3	4.4251E-01	0.4
Trash midden, TT 1	C2.07	Jun 6 2009	5.7	4.4270E-01	0.4
Trash midden, TT 1	C2.07	Jun 7 2009	6.0	4.4291E-01	0.4
Trash midden, TT 1	C2.07	Jun 7 2009	6.1	4.4296E-01	0.4
Chaco Canyon, 29SJ1659 Shabik'eshchee					
Pithouse Y, floor fill	C1.01	Mar 22 2009	6.9	4.4381E-01	0.4
Pithouse Y, floor fill	C1.01	Mar 22 2009	6.9	4.4379E-01	0.4
Pithouse Y, floor fill	C1.01	Mar 22 2009	6.0	4.4342E-01	0.4
Chaco Canyon, 29SJ423					
Pithouse A, stone bowl	C1.03	Mar 22 2009	2.3	4.4176E-01	0.4
Pithouse A, stone bowl	C1.03	Mar 22 2009	2.3	4.4177E-01	0.4
Chaco Canyon, 29SJ625 Three C site					
Room E, floor, hearth	C3.10	Apr 3 2009	4.6	4.4243E-01	0.4
Room E, floor, hearth	C3.10	Apr 3 2009	4.7	4.4249E-01	0.4
Room E, floor, hearth	C3.10	Apr 3 2009	4.8	4.4251E-01	0.4
Room E, floor, hearth	C3.10	Apr 3 2009	4.4	4.4237E-01	0.4
Chaco Canyon, 29SJ627					
Kiva G	C4.15	Feb 22 2010	4.5	4.4118E-01	0.4
Kiva G	C4.15	Feb 22 2010	4.0	4.4094E-01	0.4
Chaco Canyon, 29SJ627					
Room 10, floor 2	C3.13	Apr 3 2009	3.5	4.4194E-01	0.4
Room 10, floor 2	C3.13	Apr 3 2009	3.5	4.4194E-01	0.4
Chaco Canyon, 29SJ627					
Room 10, level 2	C3.14	Apr 3 2009	5.1	4.4264E-01	0.4
Room 10, level 2	C3.14	Apr 3 2009	5.6	4.4288E-01	0.4
Room 10, level 2	C3.14	Apr 3 2009	5.3	4.4276E-01	0.4
Chaco Canyon, 29SJ628					
Pithouse E	C1.04	Mar 22 2009	3.0	4.4209E-01	0.4
Pithouse E	C1.04	Mar 22 2009	3.1	4.4213E-01	0.4
Chaco Canyon, 29SJ628					
Pithouse A, near ventilator shaft	C2.05	Jun 6 2009	6.8	4.4318E-01	0.4
Pithouse A, near ventilator shaft	C2.05	Jun 6 2009	6.0	4.4282E-01	0.4
Pithouse A, near ventilator shaft	C2.05	Jun 7 2009	5.7	4.4278E-01	0.4
Pithouse A, near ventilator shaft	C2.05	Jun 7 2009	6.2	4.4299E-01	0.4
Chaco Canyon, 29SJ629 Spadefoot Toad					
Trash midden 59, level 2	C4.16	Jun 6 2009	3.0	4.4151E-01	0.4
Trash midden 59, level 2	C4.16	Jun 6 2009	2.6	4.4134E-01	0.4
Trash midden 59, level 2	C4.16	Feb 22 2010	3.0	4.4052E-01	0.4
Trash midden 59, level 2	C4.16	Feb 22 2010	2.5	4.4027E-01	0.4

Archaeological Site	Mount No.	Date of Analysis	$\delta^{65}Cu_{NIST976}$ (‰)	$^{65}Cu/^{63}Cu$ (SIMS)	1σ (SIMS)
Chaco Canyon, 29SJ633 Eleventh Hour					
Room 7, layer 8, below floor 2	C5.22	Jun 7 2009	6.5	4.4313E-01	0.4
Room 7, layer 8, below floor 2	C5.22	Jun 7 2009	6.3	4.4304E-01	0.4
Chaco Canyon, 29SJ633 Eleventh Hour					
Room 8, layer 2, level 4	C5.24	Jun 7 2009	3.7	4.4191E-01	0.4
Room 8, layer 2, level 4	C5.24	Jun 7 2009	3.5	4.4181E-01	0.4
Aztec Ruin					
N XV 2	ARF9.04	Feb 23 2010	6.0	4.4200E-01	0.4
N XV 2	ARF9.04	Feb 23 2010	6.6	4.4225E-01	0.4
Aztec Ruin					
N XV 2	ARF12.04	Jan 29 2010	6.6	4.4213E-01	0.4
N XV 2	ARF12.04	Jan 29 2010	6.1	4.4192E-01	0.4
Aztec Ruin					
N XV 2	ARF13.01	Jan 29 2010	2.3	4.4026E-01	0.4
N XV 2	ARF13.01	Jan 29 2010	2.0	4.4010E-01	0.4
Aztec Ruin					
N XV 2	ARF13.02	Jan 29 2010	-1.5	4.3856E-01	0.4
N XV 2	ARF13.02	Jan 29 2010	-1.7	4.3850E-01	0.4
Aztec Ruin					
N XV 2	ARF2.02	Jun 9 2009	-2.2	4.3896E-01	0.4
N XV 2	ARF2.02	Jun 9 2009	-1.6	4.3920E-01	0.4
Aztec Ruin					
E Room 52	ARF12.03	Jan 29 2010	2.3	4.4025E-01	0.4
E Room 52	ARF12.03	Jan 29 2010	2.5	4.4031E-01	0.4
Aztec Ruin					
E Room 52	ARF2.01	Jun 9 2009	2.0	4.4078E-01	0.4
E Room 52	ARF2.01	Jun 9 2009	3.0	4.4124E-01	0.4
E Room 52	ARF2.01	Jun 9 2009	2.4	4.4096E-01	0.4
Aztec Ruin					
N Room 65	ARF3.02	Jun 11 2009	3.8	4.4155E-01	0.4
N Room 65	ARF3.02	Jun 11 2009	4.9	4.4204E-01	0.4
N Room 65	ARF3.02	Jun 11 2009	4.6	4.4192E-01	0.4
Aztec Ruin					
S Room 9	ARF2.04	Jun 9 2009	7.1	4.4304E-01	0.4
S Room 9	ARF2.04	Jun 9 2009	7.9	4.4336E-01	0.4
S Room 9	ARF2.04	Jun 9 2009	7.1	4.4303E-01	0.4
Aztec Ruin					
Wing N Room 111	ARF9.05	Feb 23 2010	1.0	4.3979E-01	0.4
Wing N Room 111	ARF9.05	Feb 23 2010	-0.1	4.3933E-01	0.4
Wing N Room 111	ARF9.05	Feb 23 2010	0.2	4.3946E-01	0.4
Aztec Ruin					
Wing N Room 111	ARF11.03	Jan 28 2010	3.3	4.4062E-01	0.3
Wing N Room 111	ARF11.03	Jan 28 2010	2.8	4.4040E-01	0.3
Aztec Ruin					
Wing N Room 111	ARF11.04	Jan 28 2010	-2.3	4.3815E-01	0.3
Wing N Room 111	ARF11.04	Jan 28 2010	-2.3	4.3817E-01	0.3

Archaeological Site	Mount No.	Date of Analysis	$\delta^{65}Cu_{NIST976}$ (‰)	$^{65}Cu/^{63}Cu$ (SIMS)	1σ (SIMS)
Aztec Ruin					
Wing N Room 111	ARF2.03	Jun 9 2009	0.1	4.3996E-01	0.4
Wing N Room 111	ARF2.03	Jun 9 2009	0.7	4.4022E-01	0.4
Wing N Room 111	ARF2.03	Jun 9 2009	0.5	4.4014E-01	0.4
Salmon Ruin					
Room W51	ARF18.02	Aug 15 2010	12.1	4.4470E-01	0.4
Room W51	ARF18.02	Aug 15 2010	11.5	4.4440E-01	0.4
Salmon Ruin					
Room W51	ARF22.01	Aug 12 2010	3.9	4.4113E-01	0.4
Room W51	ARF22.01	Aug 12 2010	3.7	4.4104E-01	0.4
Room W51	ARF22.01	Aug 12 2010	3.0	4.4071E-01	0.4
Salmon Ruin					
Room W62	ARF21.01	Aug 10 2010	0.0	4.3942E-01	0.5
Room W62	ARF21.01	Aug 10 2010	0.4	4.3958E-01	0.5
Salmon Ruin					
West Room 0 63	ARF18.01	Aug 15 2010	8.4	4.4304E-01	0.4
West Room 0 63	ARF18.01	Aug 15 2010	8.3	4.4298E-01	0.4
Salmon Ruin					
Room W91	ARF21.02	Aug 10 2010	5.1	4.4168E-01	0.4
Room W91	ARF21.02	Aug 10 2010	5.4	4.4180E-01	0.4
Salmon Ruin					
Room 98W	ARF8.02	Jun 10 2009	5.1	4.4186E-01	0.4
Room 98W	ARF8.02	Jun 10 2009	5.5	4.4202E-01	0.4
Room 98W	ARF8.02	Jun 10 2009	5.8	4.4216E-01	0.4
Room 98W	ARF8.02	Aug 15 2010	4.3	4.4123E-01	0.4
Room 98W	ARF8.02	Aug 15 2010	4.7	4.4142E-01	0.4
Salmon Ruin					
Room 130W	ARF8.03	Aug 15 2010	-2.5	4.3825E-01	0.4
Room 130W	ARF8.03	Aug 15 2010	-2.4	4.3830E-01	0.4
Salmon Ruin					
Room 130W	ARF8.01	Aug 15 2010	7.2	4.4250E-01	0.4
Room 130W	ARF8.01	Aug 15 2010	7.4	4.4260E-01	0.4